

HIGHLY ENANTIOSELECTIVE EPOXIDATION WITH HYDROGEN PEROXIDE AND BIOLOGICALLY INSPIRED IRON AND MANGANESE CATALYSTS

Olaf Cussó Forest

Per citar o enllaçar aquest document:

Para citar o enlazar este documento:

Use this url to cite or link to this publication:

<http://hdl.handle.net/10803/393903>

ADVERTIMENT. L'accés als continguts d'aquesta tesi doctoral i la seva utilització ha de respectar els drets de la persona autora. Pot ser utilitzada per a consulta o estudi personal, així com en activitats o materials d'investigació i docència en els termes establerts a l'art. 32 del Text Refós de la Llei de Propietat Intel·lectual (RDL 1/1996). Per altres utilitzacions es requereix l'autorització prèvia i expressa de la persona autora. En qualsevol cas, en la utilització dels seus continguts caldrà indicar de forma clara el nom i cognoms de la persona autora i el títol de la tesi doctoral. No s'autoritza la seva reproducció o altres formes d'explotació efectuades amb finalitats de lucre ni la seva comunicació pública des d'un lloc aliè al servei TDX. Tampoc s'autoritza la presentació del seu contingut en una finestra o marc aliè a TDX (framing). Aquesta reserva de drets afecta tant als continguts de la tesi com als seus resums i índexs.

ADVERTENCIA. El acceso a los contenidos de esta tesis doctoral y su utilización debe respetar los derechos de la persona autora. Puede ser utilizada para consulta o estudio personal, así como en actividades o materiales de investigación y docencia en los términos establecidos en el art. 32 del Texto Refundido de la Ley de Propiedad Intelectual (RDL 1/1996). Para otros usos se requiere la autorización previa y expresa de la persona autora. En cualquier caso, en la utilización de sus contenidos se deberá indicar de forma clara el nombre y apellidos de la persona autora y el título de la tesis doctoral. No se autoriza su reproducción u otras formas de explotación efectuadas con fines lucrativos ni su comunicación pública desde un sitio ajeno al servicio TDR. Tampoco se autoriza la presentación de su contenido en una ventana o marco ajeno a TDR (framing). Esta reserva de derechos afecta tanto al contenido de la tesis como a sus resúmenes e índices.

WARNING. Access to the contents of this doctoral thesis and its use must respect the rights of the author. It can be used for reference or private study, as well as research and learning activities or materials in the terms established by the 32nd article of the Spanish Consolidated Copyright Act (RDL 1/1996). Express and previous authorization of the author is required for any other uses. In any case, when using its content, full name of the author and title of the thesis must be clearly indicated. Reproduction or other forms of for profit use or public communication from outside TDX service is not allowed. Presentation of its content in a window or frame external to TDX (framing) is not authorized either. These rights affect both the content of the thesis and its abstracts and indexes.



Doctoral Thesis

**Highly Enantioselective Epoxidation with
Hydrogen Peroxide and Biologically
Inspired Iron and Manganese Catalysts**

OLAF CUSSÓ FOREST

2016

Doctoral programme in Chemistry

Supervised by:

Dr. Miquel Costas Salgueiro

Dr. Xavi Ribas Salamaña

Tutor:

Dr. Miquel Costas Salgueiro

Presented in partial fulfilment of the requirements for a doctoral
degree from the University of Girona



Dr. Miquel Costas Salgueiro and Dr. Xavi Ribas Salamaña of Universitat de Girona,

WE DECLARE:

That the thesis titles “Highly Enantioselective Epoxidation with Hydrogen Peroxide and Biologically Inspired Iron and Manganese Catalysts”, presented by Olaf Cussó Forest to obtain a doctoral degree, has been completed under my supervision and meets the requirements to opt for an International Doctorate.

For all intents and purposes, I hereby sign this document.

Dr. Miquel Costas Salgueiro

Dr. Xavi Ribas Salamaña

Girona, 10 de Maig del 2016

Graphical abstract

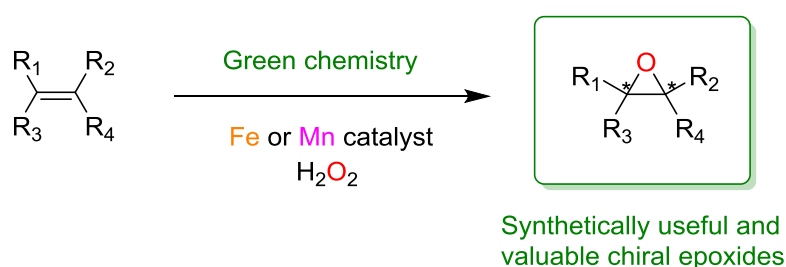
Acknowledgements

Full list of publications

Full List of Schemes, Figures and Tables

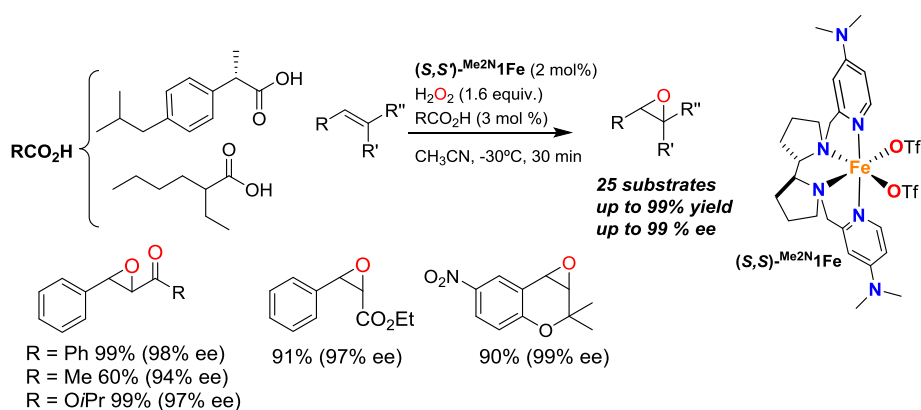
Glossary of Abbreviations

Chapter I. General Introduction (p. 29).

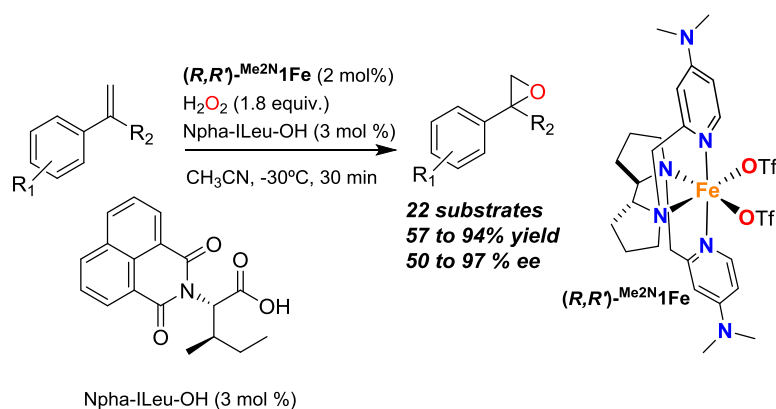


Chapter II. Main Objectives (p. 73).

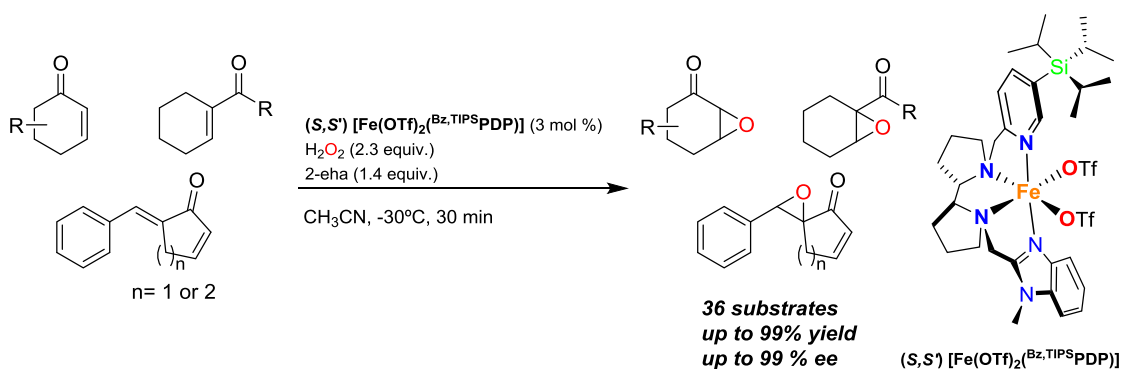
Chapter III. Asymmetric Epoxidation with H₂O₂ by Manipulating the Electronic Properties of Nonheme Iron Catalysts (p. 79).



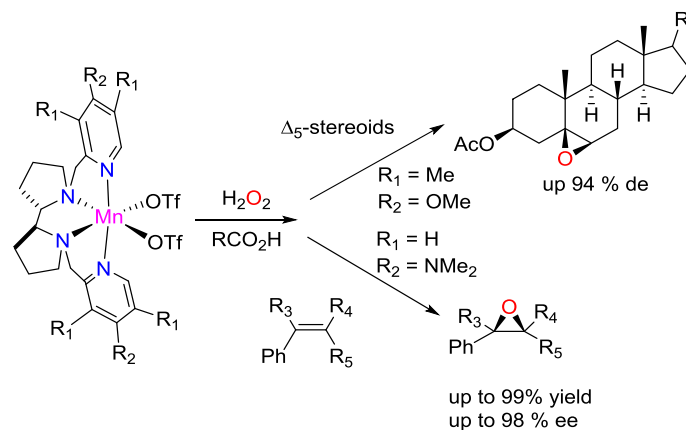
Chapter IV. Synergistic Interplay of a Nonheme Iron Catalyst and Amino acid co-ligands in H₂O₂ Activation and Asymmetric Epoxidation of α -Substituted Styrenes (p. 89).



Chapter V. Iron catalyzed highly enantioselective epoxidation of cyclic aliphatic enones with aqueous H₂O₂ (p. 97).



Chapter VI. Highly Stereoselective Epoxidation with H₂O₂ Catalyzed by Electron-Rich Aminopyridine Manganese Catalysts (p. 107).



Chapter VII. Results and Discussion (p. 113).

Chapter VIII. General conclusions (p. 149).

Experimental Section (p. 153).

ACKNOWLEDGEMENTS

Primer de tot, agrair a en Miquel Costas per oferir-me l'oportunitat de fer la tesis doctoral en el seu grup, si no fos per la seva ambició i motivació que em va traslladar en el seu moment, jo no estaria aquí fent-la. També a en Julio Lloret, que no es queda curt aportant noves idees, tot i que a vegades no es controla. A en Xavi Ribas, un altre crack indiscutible que estar conquerint els metalls de la primera serie. No podia oblidar-me de donar les gràcies a l'Isaac, el meu mestre que em va ensenyar el camí de les epoxidacions, juntament amb la Laura, "currante" al màxim i una crack sense cap dubte. La Irene i la Mercè les meves dues companyes guapes de laboratori, juntament amb la Carlota, no puc demanar res més que estar acompanyat de noies. Al meu gran company de parides de laboratori, en Zoel (l'esquerrà) que gràcies a totes les parides que diem i comentaris les hores passen volant. A en Ferran, que encara que parli de mons "imaginari" i ple de mentides teòriques en el fons se que té raó. A la Teresa, ja que per molt aviat que arribis al laboratori ella estarà allà per obrir-te. A en Diego, 100% querosè. A en Gerard, si no fos pel seus comentaris com "hola guarra" no seria el mateix. La Raquel, sense cap mena de dubte és una peça importantíssima del qbis, que ens treu feina a tots i ens la facilita a la vegada, per no parlar dels descomptes que aconsegueix, ole tu!. A la Monica que no para de saludar durant tot el dia. Al Qbis 4 colla de ... molt bona gent. Alla és on tinc les dues persones que m'han acompanyat durant 10 anys en aquesta experiència universitària, la Cristina i en Joan, un és el meu amor platònic i a l'altre li agrada Star Wars...En Marc Font per ser el Zoel del Qbis 4 i per totes les parides absurdes que diem!, l'Oriol el referent que tinc per aprendre a utilitzar el photoshop i supera'l (no passarà), la Mireia, la "pequeñaja" enrollada que sempre té alguna cosa a explicar. L'Anna Company, una perla recuperada. A l'Arnau i la Carla que ja no están al qbis, però tinc bons records d'ells. A la tribu d'italians: Giorgio, Marco i Ilaria amb els quals he passat grans moments, i sens dubte a la Michela, "la gioia della mia vita". Finalment, a tota la gent que ha passat pels Qbis en algun moment: David, Irene, Cabruja, Claudia, Margarida, Peter, Imma, Marta, Apu, Laia, etc.

Gràcies a tots per aquesta aventura única en la vida. Us desitjo el millor a tots.

This work would not have been possible without the following collaborations:

- Serveis tècnics de Recerca from Universitat de Girona for technical support.
- Prof. Scott J. Miller from Yale University (Connecticut, USA) for hosting a scientific visit and the collaborative work in the asymmetric epoxidation with iron complexes.
- LIPPSO group from Universitat de Girona for providing amino acid samples.
- Dr. Antoni Riera from Institute for Research in Biomedicine for access to a polarimeter.
- Financial support by European Research Council (ERC-2009-StG-239910), MICINN of Spain through project CTQ2009-08464/BQU and CTQ2012-37420-C02-01/BQU to M.C., and Generalitat de Catalunya for 2009SGR637 project and ICREA Acadèmia Awards to MC and XR.

FULL LIST OF PUBLICATIONS

This thesis is a compendium of research articles.

Chapter III

Asymmetric Epoxidation with H₂O₂ by Manipulating the Electronic Properties of Non-heme Iron Catalysts. Cussó O.; Garcia-Bosch, I.; Ribas, X.; Lloret-Fillol, J.; Costas, M. *J. Am. Chem. Soc.*, **2013**, *135*, 14871. (impact factor: 12.130, Q₁)

Chapter IV

Synergistic Interplay of a Non-Heme Iron Catalyst and Amino Acid Coligands in H₂O₂ Activation for Asymmetric Epoxidation of α -Alkyl-Substituted Styrenes. Cussó, O.; Ribas, X.; Lloret-Fillol, J.; Costas, M. *Angew. Chem. Int. Ed.*, **2015**, *54*, 2729. Cited in *NATURE CHEMISTRY* (RESEARCH HIGHLIGHTS). ASYMMETRIC EPOXIDATIONS, Challenging substrates. *Nat. Chem*, **2015**, *7*, 184-185. Mentioned as Very Important Paper for reviewers. (impact factor: 11.261, Q₁)

Chapter V

Iron catalyzed highly enantioselective epoxidation of cyclic aliphatic enones with aqueous H₂O₂. Cussó, O.; Cianfanelli, M.; Ribas, X.; Klein Gebbink, R. J. M.; Costas, M. *J. Am. Chem. Soc.*, **2013**, DOI: 10.1021/jacs.5b12681. (impact factor: 12.130, Q₁)

Chapter VI

Highly Stereoselective Epoxidation with H₂O₂ Catalyzed by Electron-Rich Aminopyridine Manganese Catalysts. Cussó, O.; Garcia-Bosch, I.; Font, D.; Ribas, X.; Lloret-Fillol, J.; Costas, M. *Org. Lett.* **2013**, *15*, 6158. (impact factor: 6.364, Q₁)

All these paper have been published to journals that belong to the first quartile according to JCR

Contributions in other publications not included in this thesis.

Biologically inspired non-heme iron-complexes for asymmetric epoxidation: design principles and perspectives. Cusso, O.; Ribas, X.; Costas, M. *Chem. Comm.* **2015**, 51, 14285.

Solid-Phase Synthesis of Biaryl Cyclic Peptides Containing a 3-Aryltyrosine, Afonso, A.; Cussó, O.; Feliu, L.; Planas, M. *Eur. J. Org. Chem.* **2012**, 31, 6204.

H₂ oxidation versus organic substrate oxidation in non-heme iron mediated reactions with H₂O₂. Hassanpour, A.; Acuña, F.; Luis, J. M.; Cussó, O.; de la Rosa, S. M.; Campos-Martin, J. M.; Fierro, J. L. G.; Costas, M.; Lloret-Fillol J.; Mas-Ballesté, R. *Chem. Comm.* **2015**. 14992.

Pro-oxidant activity of amine-pyridine-based iron complexes efficiently kills cancer and cancer stem-like cells. González-Bártulos, M.; Aceves-Luquero, C.; Qualai, J.; Cusso, O.; Martínez, M. A.; Fernández de Mattos, S.; Menéndez, J. A.; Villalonga, P.; Costas, M.; Ribas, X.; Massaguer, A. *Plos ONE*. **2015**, DOI:10.1371/journal.pone.0137800.

In vitro and in vivo identification of tetradentate polyamine complexes as highly efficient metallodrugs against *Trypanosoma cruzi*. Olmo, F.; Cussó, O.; Marín, C.; Rosales, M. J.; Urbanová, K.; Krauth-Siegel, L.; Costas, M.; Ribas, X.; Sánchez-Moreno, M. *Exp. Parasitol.* **2016**, DOI:10.1016/j.exppara.2016.02.004

List of schemes

Scheme 1. Schematic diagram of possible products from ring opening epoxides.....	31
Scheme 2. Established catalytic cycle for alkane hydroxylation performed by Cyt P450.	34
Scheme 3. Catalytic cycle proposed for Rieske dioxygenases.	36
Scheme 4. Some examples of evolution of biologically inspired catalysts used in oxidation processes.	38
Scheme 5. Different examples of iron porphyrins reported for asymmetric epoxidation of styrene as a model substrate. ⁴³⁻⁴⁷	39
Scheme 6. Oxidation of 1-decene catalyzed by $[\text{Fe}^{\text{II}}(\text{men})(\text{CH}_3\text{CN})_2](\text{SbF}_6)_2$	40
Scheme 7. In situ generated catalyst reported by Beller.	40
Scheme 8. Asymmetric epoxidation of olefins with the $[\text{Fe}^{\text{III}}_2(\mu\text{-O})(\text{bpp})_4(\text{H}_2\text{O})_2]^{4+}$ complex and AcOOH.	41
Scheme 9. Asymmetric epoxidation of styrenes derivatives with $[\text{Fe}^{\text{III}}_2(\mu\text{-O})(\text{Cl})_4(\text{Spp})]$, H_2O_2 and AcOH.	41
Scheme 10. Asymmetric epoxidation of <i>trans</i> -chalcones derivatives with different tetraaminodentate nonheme iron complexes , and $\text{H}_2\text{O}_2/\text{AcOH}$ as oxidant.....	43
Scheme 11. Asymmetric epoxidation of olefins with the iron complex and AcOOH reported by Yamamoto.	44
Scheme 12. Asymmetric epoxidation of olefins with the (S,S')- $[\text{Fe}(\text{OTf})_2(\text{pdp})]$ complex, H_2O_2 and AcOH or 2-eha.	45
Scheme 13. Asymmetric epoxidation of <i>trans</i> olefins with iron complex, PhIO, NaBARF SIPrAgCl reported by Nakada.	46
Scheme 14. Proposed mechanism for iron complex reported by Nakada.	46
Scheme 15. Asymmetric epoxidation of tetralone derivatives reported by Gao and co-workers.	47
Scheme 16. Proposed mechanism for epoxidation reaction via carboxylic acid assisted with tetradentate aminopyridine iron complexes and $\text{H}_2\text{O}_2/\text{AcOH}$	48
Scheme 17. Synthesis of acylperoxoiron(III) complexes from reaction of $\text{Fe}^{\text{dMM}}(\text{men})(\text{CH}_3\text{CN})_2](\text{ClO}_4)_2$, $\text{Fe}^{\text{dMM}}(\text{pdp})(\text{CH}_3\text{CN})_2](\text{ClO}_4)_2$ and $[\text{Fe}(\text{OTf})_2(\text{dMMtpa})]$ with $\text{H}_2\text{O}_2/\text{AcOH}$ or peracids.	49
Scheme 18. Asymmetric epoxidation reaction of aliphatic and aromatic olefins with the (R,R')- $[\text{Mn}(\text{OTf})_2(\text{mcp})]$ complex and AcOOH.....	53
Scheme 19. Asymmetric epoxidation reaction of aromatic olefins with the (R,R,S,S)- $[\text{Mn}(\text{OTf})_2(\text{mcpp})]$ complex and AcOOH.....	54

Scheme 20. Epoxidation reaction of different olefins with the [Mn(OTf) ₂ (Pytacn)] and [Mn(OTf) ₂ (mcp)] complexes, H ₂ O ₂ and AcOH.	55
Scheme 21. Asymmetric epoxidation reaction of aromatic olefins with the (<i>R,R,R,R'</i>)-[Mn(OTf) ₂ (bpmcp)] complex, H ₂ O ₂ and AcOH.	55
Scheme 22. Asymmetric epoxidation reaction of aromatic and aliphatic olefins with the (<i>S,S'</i>)-[Mn(OTf) ₂ (pdp)] complex, H ₂ O ₂ and AcOH.	56
Scheme 23. Asymmetric epoxidation reaction of aromatic and aliphatic olefins with (<i>R,R,R</i>)-[Mn(OTf) ₂ (pdpp)] complex, H ₂ O ₂ and AcOH.	57
Scheme 24. Asymmetric epoxidation reaction of aromatic, aliphatic and terminal olefins with (<i>S</i>)-[Mn(OTf) ₂ (peb)] complex, H ₂ O ₂ and AcOH.	58
Scheme 25. Manganese complex prepared in situ as catalyst for asymmetric epoxidation of aromatic olefins with H ₂ O ₂ and adamantane carboxylic acid.	59
Scheme 26. Asymmetric epoxidation of aromatic and aliphatic olefins with H ₂ O ₂ and AcOH with the Suresh catalyst.	59
Scheme 27. Asymmetric epoxidation reaction of aromatic olefins with the (<i>S,S'</i>)-[Mn(OTf) ₂ (^{NH₂} pdp)] complex, H ₂ O ₂ and 2-eha.	60
Scheme 28. Asymmetric epoxidations of aromatic and terminal olefins with different Mn complexes differing in the diamine backbone.	61
Scheme 29. a) Proposed active species for tetradentate amino manganese complex with hydrogen peroxide for epoxidation reaction. b) High valent manganese oxo-hydroxo and bis-hydroxo were inactive for epoxidation reaction. c) Labeling experiments demonstrated the Lewis acid activation of the iodosylbenzene, "third oxidant".	65
Scheme 30. Proposed catalytic cycle for the (<i>S,S'</i>)-[Mn(OTf) ₂ (mcp)] with ArIO and acyl or alkyl hydroperoxides	65
Scheme 31. Proposed mechanism for epoxidation of tetradentate aminopyridine manganese complexes with H ₂ O ₂ and AcOH reported by Talsi and co-workers.	67
Scheme 32. Design of different iron and manganese complexes for asymmetric epoxidation. .	76
Scheme 33. Epoxidation of terminal olefins with iron complexes and amino acids as additives.	76
Scheme 34. Synthesis of different C ₁ symmetric iron complexes for asymmetric epoxidation. .	77
Scheme 35. Competition studies between electron-rich and electron-deficient olefin.	119
Scheme 36. a) Isotopic analysis studies. b) Schematic representation of the water assisted path.	120
Scheme 37. On the left, push-pull effect in Cyt P450 and on the right the proposed push-pull effect in the system ^{Me₂N} 1Fe.	123
Scheme 38. Different products obtained from terminal chiral epoxide E13	129

Scheme 39. a) Competitive epoxidation experiment of cyclohexene **S30** and 2-cyclohexenone **S1**, c) the epoxidation of electron-deficient olefin **S31** and c) epoxidation of **S1** using H₂¹⁸O₂. 136

Scheme 40. Substrate scope of dienones in asymmetric epoxidation with **7Fe** and ^{Me2N}**1Fe** as catalyst. 136

List of figures

Figure 1. Three possible topologies for iron complexes with linear tetradentate ligands.....	42
Figure 2. Selected examples of chiral manganese porphyrins.	50
Figure 3. Selected manganese salen complexes reported by Jacobsen and Katsuki and some examples of asymmetric epoxidations.	52
Figure 4. Topology for manganese complexes with linear tetradentate ligands.	53
Figure 5. Examples of biologically inspired manganese complexes based in tetradentate aminopyridine ligands studied in asymmetric epoxidation reactions.	62
Figure 6. Schematic diagram of the iron complexes studied.	115
Figure 7. Substrate scope on the asymmetric epoxidation with the iron catalyst ^{Me2N} 1Fe . Results are shown as % isolated yield (% ee in parenthesis).....	118
Figure 8. Hammett analysis of the stereoselectivity as a function of catalyst in the epoxidation of S8 , S1 , S13 and S4 . The reaction was carried out with 1 mol % of catalyst, AcOH (1.4 equiv.), H ₂ O ₂ (1.2 equiv.) and 750 μL of acetonitrile at -30°C.....	122
Figure 9. Substrate scope on the asymmetric epoxidation with (<i>R,R</i>)- ^{Me2N} 1Fe and <i>N</i> -NPha-Ileu-OH.	129
Figure 10. Schematic diagram of different catalysts employed.....	132
Figure 11. Substrate scope of aliphatic cyclic enones in asymmetric epoxidation with 7Fe as catalyst. % yield and ee (in parenthesis) are given for each substrate.....	134
Figure 12. Substrate scope of alkyl 1-cyclohexenyl ketone derivatives in asymmetric epoxidation with 7Fe as catalyst. % yield and ee (in parenthesis) are given for each substrate.	135
Figure 13. Manganese complexes studied. On the right, an ORTEP diagram of the single crystal X-ray determined structure of (<i>R,R</i>)- ^{Me2N} 1Mn is shown. For clarity, H atoms and triflates groups, except for O atoms bound to the metal are omitted.....	139
Figure 14. Epoxidation of <i>cis</i> -β-methylstyrene as a function of AcOH loading for catalysts ^{Me2N} 1Mn , ^{dMM} 1Mn and ^H 1Mn . Reaction conditions; catalyst (0.1 mol%), <i>cis</i> -β-methylstyrene (1 equiv.), H ₂ O ₂ (1.2 equiv.) and AcOH (0.35-14 equiv.) in CH ₃ CN at - 30 °C.....	140
Figure 15. Substrate scope on the asymmetric epoxidation with manganese catalyst ^{Me2N} 1Mn	142

List of tables

Table 1. Comparison of manganese complexes in the asymmetric epoxidation of three different substrates.	63
Table 2. Screening of iron complexes on the asymmetric epoxidation of <i>cis</i> - β -methylstyrene.	116
Table 3. Screening of carboxylic acids on the asymmetric epoxidation of <i>cis</i> - β -methylstyrene with ^{Me2N} 1Fe	117
Table 4. Comparison among different oxidants in the epoxidation of S1 with (S,S') ^{Me2N} 1Fe	119
Table 5. Screening of amino acids in asymmetric epoxidation reaction	125
Table 6. Comparison with other carboxylic acids in different styrene patterns.	128
Table 7. Screening of the iron complexes in the asymmetric epoxidation reaction of 2-cyclohexenone.....	132
Table 8. Screening of manganese complexes on the asymmetric epoxidation of <i>cis</i> - β -methylstyrene.	139
Table 9. Screening of carboxylic acids on the asymmetric epoxidation of <i>cis</i> - β -methylstyrene with manganese catalyst ^{Me2N} 1Mn	140
Table 10. Epoxidation of Δ^5 -unsaturated steroids.	143

GLOSSARY OF ABBREVIATIONS

[Ox]: Oxidant.

2-eha: 2-Ethylhexanoic acid.

5-mha: 5-Methylhexanoic acid.

Aca: Adamantanecarboxylic acid.

AcOEt: Ethyl acetate.

AcOH: Acetic acid.

AcONa: Sodium acetate.

AcOOH: Peracetic acid.

mcp: *N,N'*-dimethyl-*N,N'*-bis(2-pyridylmethyl)-cyclohexane-1,2-diamine.

Bz: Benzylimidazole.

Cat: Catalyst.

CF₃SO₃: OTf: Trifluoromethanesulfonate anion.

CH₃CN: Acetonitrile.

Conv: Conversion.

Cxa: Cyclohexanecarboxylic acid.

Cyt P450: cytochrome P450.

DMF: Dimethyl formamide.

dMM: Dimethylmethoxide.

Eba: Ethylbutyric acid.

Ee: Enantiomeric excess.

Equiv.: Equivalents.

ESI: Electrospray ionization.

Et₂O: Diethyl ether.

GC: Gas chromatography.

H₂O₂: Hydrogen peroxide.

L: Ligand

LO: Lipoxygenase.

Men: *N,N'*-dimethyl-*N,N'*-bis(2-pyridylmethyl)ethane-1,2-diamine

NaBARF: Sodium tetrakis[2,5-bis(trifluoromethyl)phenyl] borate.

NDO: Naphthalene-1,2-dioxygenase.

NMR: Nuclear magnetic resonance.

OAc: Acetate group.

OPiv: Pivalate group.

pdp: *N,N'*-bis(2-pyridylmethyl)-2,2'-bipyrrolidine.

PhIO: Isodosylbenzene.

PPh₃: triphenylphosphine.

Py: Pyridine.

Pytacn: 1-(2'-pyridylmethyl)-4,7-dimethyl-1,4,7-triazacyclononane.

r.t: Room temperature.

S-2-mba: S-2-Methylbutyric acid.

S-lbp: S-Ibuprofen.

SIPrAgCl: Silver *N,N'*-bis(2,6-diisopropylphenyl)-4,5-dihydroimidazol-2-ylidene chloride.

SOD: Superoxide dismutase.

TBHP: *Tert*-butylhydroperoxide.

THF: Tetrahydrofuran.

tips: Triisopropylsilyl group.

tpa: *tris*-(2-pyridylmethyl)amine).

tpp: 5,10,15,20-tetraphenylporphyrin.

Triflate: Trifluoromethanesulfonate anion.

CONTENTS

Summary	23
Resum	24
Resumen	26
Chapter I. General introduction	31
I.1. Modern challenges in alkene epoxidation	31
I.1.1. Epoxidation of alkenes	31
I.2. Metalloenzymes as inspiration elements for catalyst development	32
I.2.1. Cytochrome P450	33
I.2.2. Rieske Oxygenases	34
I.4. Manganese in biological systems	36
I.4.1. Manganese proteins involved in oxidative reactions	36
I.5. Iron and manganese bioinspired complexes	37
I.5.1. Asymmetric epoxidation catalysis mediated by bioinspired iron systems	38
I.5.1.1. Role of acetic acid in oxidation reactions with bioinspired iron complexes	47
I.5.2. Asymmetric epoxidation catalysis mediated by Biologically inspired manganese systems	49
I.5.2.1. Proposed mechanisms for bioinspired manganese complexes	64
I.6 References	68
Chapter II. Main Objectives	75
Chapter III. Asymmetric Epoxidation with H₂O₂ by Manipulating the Electronic Properties of Non-Heme Iron Catalysts	79
Chapter IV. Synergistic Interplay of a Non-Heme Iron Catalyst and Amino acid co-ligands in H₂O₂ Activation and Asymmetric Epoxidation of α-Substituted Styrenes	89
Chapter V. Iron catalyzed highly enantioselective epoxidation of cyclic aliphatic enones with aqueous H₂O₂	97
Chapter VI. Highly Stereoselective Epoxidation with H₂O₂ Catalyzed by Electron-Rich Aminopyridine Manganese Catalysts	107
Chapter VII. Results and Discussion	115
VII.1. Asymmetric Epoxidation with H ₂ O ₂ by Manipulating the Electronic Properties of NonHeme Iron Catalysts	115
VII.2. Synergistic Interplay of a Non-Heme Iron Catalyst and Amino acid co-ligands in H ₂ O ₂ Activation and Asymmetric Epoxidation of α -Substituted Styrenes	124
VII.3. Iron catalyzed highly enantioselective epoxidation of cyclic aliphatic enones with aqueous H ₂ O ₂	131
VII.4. Highly Stereoselective Epoxidation with H ₂ O ₂ Catalyzed by Electron-Rich Aminopyridine Manganese Catalysts	138
References	144

VIII. General conclusions	149
Experimental Section	153
Experimental section: Chapter VII.1	156
Experimental section: Chapter VII.2	179
Experimental section: Chapter VII.3	200
Experimental section: Chapter VII.4	237

Supplementary Digital information

- Pdf file of the Ph.D. Dissertation
- Pdf file of the Digital Annex containing additional NMR, GC and HPLC spectra
- CIF files for each crystal structure presented in this thesis

SUMMARY

This thesis has been devoted to the discovery of new catalytic systems capable to epoxidize wide range of olefins with high efficiencies and stereoselectivities in mild conditions. The source of inspiration for these epoxidation systems are iron dependent oxygenases, such as cytochrome P450 or Rieske dioxygenase, among others. These metalloxygenases perform biological catalytic reactions with molecular oxygen as an oxidant to obtain oxidized products with high levels of selectivity. In this thesis, we focus on the synthesis of chiral manganese and iron coordination complexes that reproduce basic structural and functional aspects of metalloxygenases, and employ them as catalysts in the stereoselective epoxidation of olefins, employing hydrogen peroxide as oxidant.

In this thesis, in Chapter III, V and VI, a family of chiral manganese and iron complexes with tetradentate aminopyridine ligands is described. The electronic and steric properties of the set of ligands employed are tuned in a systematic manner, and the impact of these factors in asymmetric epoxidation reactions is studied. In addition, the positive role of a carboxylic acid additive in the efficient activation of H₂O₂ and in the stereoselectivity of the reactions is developed as a valuable tool for optimizing the catalytic reactions. Moreover, mechanistic studies have been performed to elucidate the reaction mechanism. From these studies, iron and manganese complexes with electron rich aminopyridine ligands, in combination with selected carboxylic acids have emerged as particularly efficient and stereoselective epoxidation catalysts for different classes of aromatic olefins and cyclic aliphatic enones.

Moreover, in Chapter IV, we use the more electron-rich iron and more active iron complexes described in Chapter III, in combination with different amino acids as co-ligands to carry out the asymmetric epoxidation of different classes of aromatic olefins. It is discovered that amino acids are excellent co-ligands for these catalysts that allow highly stereoselective epoxidation of *cis* aromatic olefins and very challenging substrates such as α -alkyl-styrenes. This chapter illustrates the versatility of this class of catalysts that can be readily adapted to different classes of substrates by employing different carboxylic acids, without the need of further elaboration or modification of the metal catalyst.

RESUM

Aquesta tesi ha estat dedicada al descobriment de nous sistemes capaços d'epoxidar una gran rang d'olefines amb altes eficiències i estereoselectivitats en condicions suaus. La font d'inspiració d'aquestes epoxidacions són les oxigenases de ferro, com ara el citocrom P450 o les oxigenases de Rieske, entre altres. Aquestes metal·loxigenases duen a terme reaccions biològiques i catalítiques utilitzant l'oxigen molecular com a oxidant per obtenir productes oxidats amb alts nivells de selectivitat. En aquesta tesi ens centrarem en la síntesi de complexes de manganès i de ferro quirals que reproduïxen l'estructura bàsica i funcional de les metal·loxigenases, i utilitzar-los en catàlisis d'epoxidació estereoselectiva d'olefines amb aigua oxigenada com a oxidant.

En aquesta tesi, en el Chapter III, V i VI, es descriuran una família de complexes de manganès i ferro quirals aminotetradentats. Les propietats electròniques i estèriques del lligands utilitzats seran modificades de manera sistemàtica, i l'impacte d'aquestes seran estudiades en epoxidacions asimètriques. A més a més, el rol positiu dels àcids carboxílics en l'eficient activació del H_2O_2 i en l'estereoselectivitat de les reaccions es utilitzada com a eina per optimitzar les reaccions catalítiques.. A més a més s'han fet estudis mecanístics per aclarir el mecanisme de reacció. A partir d'aquests estudis, els complexes de manganès i ferro que contenen aminopiridines riques electrònicament, juntament amb la combinació d'àcids carboxílics, s'ha demostrat que són uns catalitzadors molt efectius i estereoselectius per diferents tipus de olefines aromàtiques i enones cícliques alifàtiques

A més, en el Chapter IV utilitzem el complex de ferro més electrodonador descrit en el Chapter III, en combinació amb diferents aminoàcids com a co-lligands per dur a terme epoxidacions asimètriques de diferents classes d'olefines aromàtiques. S'ha descobert que els aminoàcids son uns excel·lents co-lligands per aquestes catàlisis, ja que donen altes estereoselectivitats per olefins *cis*-aromàtiques i fins i tot per olefines com alfa-alcà-estirens, que són molts difícils d'epoxidar. Aquest capítol mostra la versatilitat d'aquests catalitzadors, que pot ser adaptada a diferents classes de substrats en funció

dels diferents àcids carboxílics utilitzats, sense la necessitat d'elaboració o modificació del catalitzador metàl·lic

RESUMEN

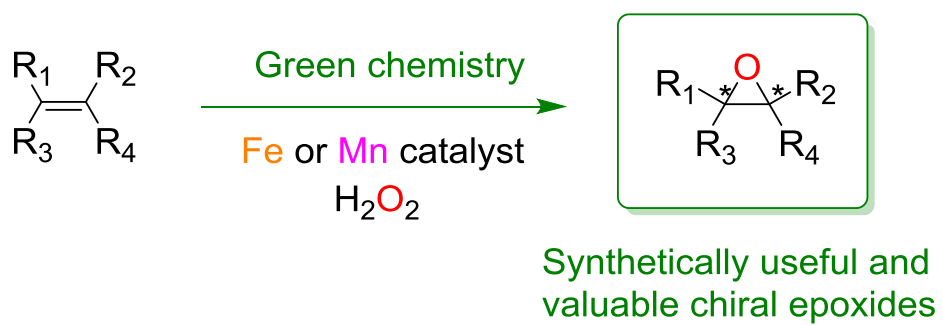
Esta tesis está dedicada al descubrimiento de nuevos sistemas capaces de epoxidar un gran rango de olefinas con altas eficiencias y estereoselectividades en condiciones suaves. La fuente de inspiración de estas epoxidaciones son las oxigenasas de hierro, como el citocromo P450 o la Rieske oxigenasa, entre otras. Estas metaloxigenasas llevan a cabo reacciones biológicas y catalíticas utilizando oxígeno molecular como oxidante para obtener productos oxidados con altos niveles de selectividad. En esta tesis nos centramos en la síntesis de complejos de manganeso y hierro quirales que reproducen la estructura básica y funcional de las metaloxigenasas, utilizándolos en catálisis de epoxidaciones estereoselectivas de olefinas con agua oxigenada como oxidante.

En esta tesis, en los Chapter III, V y VI, se describen una familia de complejos de manganeso y hierro quirales aminotetradentados. Las propiedades electrónicas y estéricas de los ligandos utilizados serán modificadas de manera sistemática, y el impacto de estas serán estudiadas en epoxidaciones asimétricas. Además, el rol positivo de los ácidos carboxílicos en la eficiencia de la activación del H_2O_2 y en la estereoselectividad de las reacciones es utilizado como herramienta para optimizar las reacciones catalíticas. También, se harán estudios mecanísticos para aclarar el mecanismo de reacción. A partir de estos estudios, los complejos de manganeso y hierro que contienen aminopiridinas ricas electrónicamente, juntamente con la combinación de los ácidos carboxílicos, se ha demostrado que son unos catalizadores muy efectivos y estereoselectivos para diferentes tipos de olefinas aromáticas y enonas cíclicas alifáticas.

Además, en el chapter IV, utilizaremos el complejo de hierro más electrófilo descrito en el Chapter III, en combinación con diferentes aminoácidos como co-ligandos para llevar a cabo epoxidaciones asimétricas de diferentes clases de olefinas aromáticas. Se ha descubierto que los aminoácidos son unos excelentes co-ligandos para estas catálisis, porque muestran altas estereoselectividades para olefinas *cis*-aromáticas, e incluso para olefinas α -alquino-estirenos, que son muy difíciles de epoxidar. Este capítulo muestra la versatilidad de estos catalizadores, que puede ser adaptada a diferentes clases

de sustratos en función de los diferentes ácidos carboxílicos utilizados, sin la necesidad de elaboración o modificación del catalizador metálico.

General Introduction

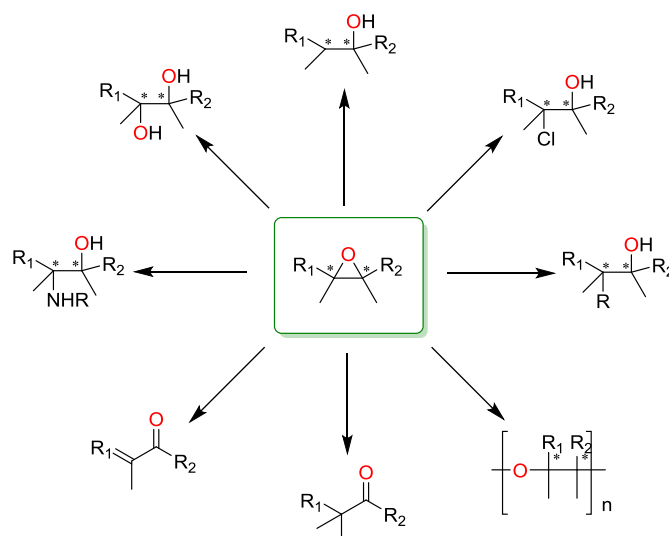


CHAPTER I. GENERAL INTRODUCTION

I.1. MODERN CHALLENGES IN ALKENE EPOXIDATION

I.1.1. EPOXIDATION OF ALKENES

Alkenes are one of the most important starting materials for organic synthesis, due to their high reactivity. Also, their possible oxidation reactions lead to different products, such as epoxides, *cis*-diols, aldehydes, allylic oxidation products, ketones and alcohols. Among these, epoxides constitute an important and extremely versatile class of intermediate organic compounds and building blocks for chemical synthesis.¹⁻⁷ For this reason, the epoxidation is an important reaction very actively studied. Most remarkably and challenging constitutes the asymmetric epoxidation of olefins, because the reaction can produce two stereogenic centers, and the chiral epoxides obtained can be readily and straightforwardly converted in other interesting chiral compounds, such as alcohols, diols, amino alcohols, chloride moieties, etc (Scheme 1). All of them have high interest in synthetic organic chemistry.



Scheme 1. Schematic diagram of possible products from ring opening epoxides.

I.2. METALLOENZYMES AS INSPIRATION ELEMENTS FOR CATALYST DEVELOPMENT

Enzymes are the catalysts responsible for most of the reactions taking place in living organisms. Those containing metal ions are known as metalloenzymes. The rich chemistry of transition metal ions, which can exist in multiple oxidation states and geometries, is crucial for the enzymes to carry out the biochemical transformations associated with their function, allowing them to participate in highly specialized biological functions, such as oxygen activation or transportation.⁸ The active centers can be monometallic or polymetallic, and all of them have in common the presence of nitrogen, oxygen or sulfur donor molecules. In most of the cases, these atoms are part of amino acids in the polypeptide chain of the protein. In a number of enzymes, non-proteinic molecules such as porphyrins can be also used as metal ligands. In specific cases, the position of the donor atoms are governed by the structure of the active site, and this causes the metal at the active site to adopt unusual coordination geometries and coordination numbers, which become essential in defining a particular chemistry. The reactivity of the metal based species is also aided by effects imposed by the active site; size, polarity, and weak interactions combine with the metal innate reactivity leading to reactions with excellent chemo-, regio- and stereoselectivities. An additional interesting aspect of the chemistry of metalloenzymes is that they operate under mild conditions, and their reactions are remarkably efficient, producing minimum, if any, waste. For example, oxidative enzymes employ O_2 or H_2O_2 to perform oxidation reactions, leaving water as the only byproduct.

Given the unique properties of enzymatic reactions, they have become a source of inspiration for the design of novel, more efficient chemical synthetic processes. This idea has a broad sense and includes multiple and different approaches. In the particular case of oxidation reactions, biological inspiration can be taken to design metal catalysts, which will be based in biologically relevant transition metals (basically iron, copper and manganese) and will contain N, O and S donor ligands. These catalysts should activate O_2 or peroxides to produce oxidizing species, finally responsible for substrate oxidation. In this thesis, we follow this basic approach to develop some iron and

manganese coordination complexes that reproduce basic structural and chemical elements of iron dependent oxygenases. Then these “biologically inspired” complexes are studied as catalysts in asymmetric epoxidation of olefins, with the aim to develop methodologies that could be suitable for preparative organic synthesis.

P450 and Rieske Oxygenases are two families of enzymes that have served as inspiration for our development of catalysts, and because of that, their structure, function and chemistry is described in the following lines.

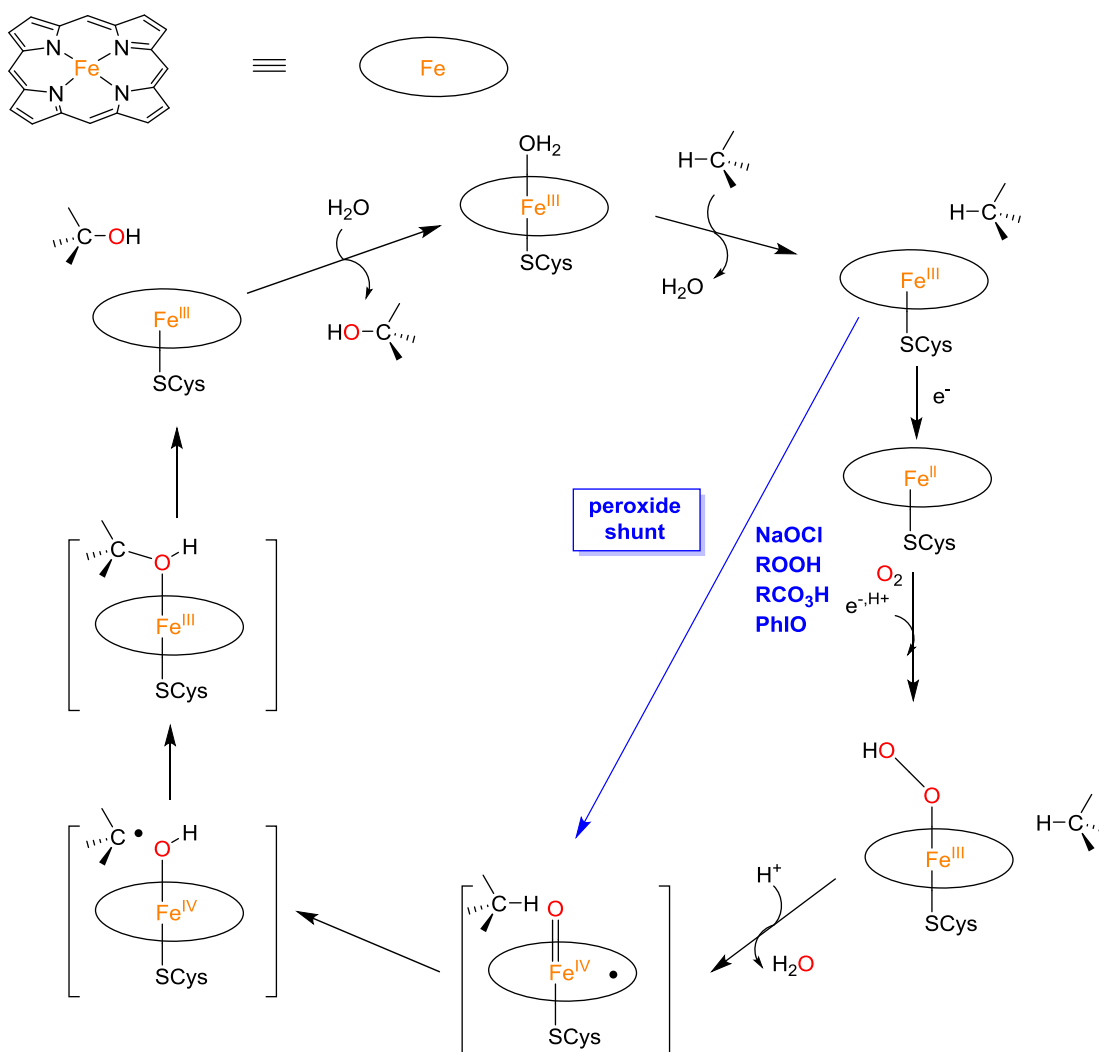
I.2.1. CYTOCHROME P450

Cytochrome P450 is a family of iron enzymes ubiquitous in life forms, from bacteria to humans.⁹⁻¹¹ These enzymes take part in a great variety of vital processes, such as drug metabolism, biosynthesis of steroids and the detoxification of xenobiotic substances. Cyt P450 catalyzes hydroxylation of aliphatic C-H bonds and the epoxidation of alkenes with high regio- and stereoselectivity. Cyt P450 is a monooxygenase; it activates molecular oxygen, inserting one oxygen atom into the substrate. Concomitantly the other oxygen atom forms a water molecule.⁸

It has been established that Cyt P450 active site consists of a single ferric heme coordinated to a cysteinate sulfur residue of the protein at one of the axial positions of the iron ion, and the sixth coordination site is occupied by either a water molecule or a hydroxide ligand. The main features of the catalytic cycle are nowadays well-defined.^{11,12} As shown in the Scheme 2, the initial step consists in the binding of the substrate at the active site, causing extrusion of the water ligand, which triggers the one-electron reduction of the Fe^{III}. The subsequent binding of O₂ to the Fe^{II} center gives a ferric Cyt P450-superoxide complex. A second electron is rapidly transferred to this complex to afford a peroxyiron(III) complex, which is further protonated to generate hydroperoxyiron(III) complex. This species undergoes proton assisted O-O heterolytic bond cleavage to generate a high-valent oxo-Fe^{IV}-porphyril radical cation and a water molecule. The oxygen atom is transferred from this oxo complex to the nearby substrate through a two-step process known as “oxygen rebound”, firstly and hydrogen atom transfer and secondly the hydroxyl

abstraction.¹³ Finally, dissociation of the product completes the catalytic cycle. Direct cycling between the resting state and the high-valent oxidant species can be performed by using oxidants such as hydro and alkylperoxides, NaOCl, PhIO or peracids. This shortcut is known as the “peroxide shunt” and it receives use in catalysis (Scheme 2).¹⁴ The intermediate species is postulated to be an iron(IV)-oxo porphyrin radical cation.¹⁵ Synthetic models of porphyrin analogs provide evidences of the active species involved in the oxidation mechanism.¹⁶⁻

19



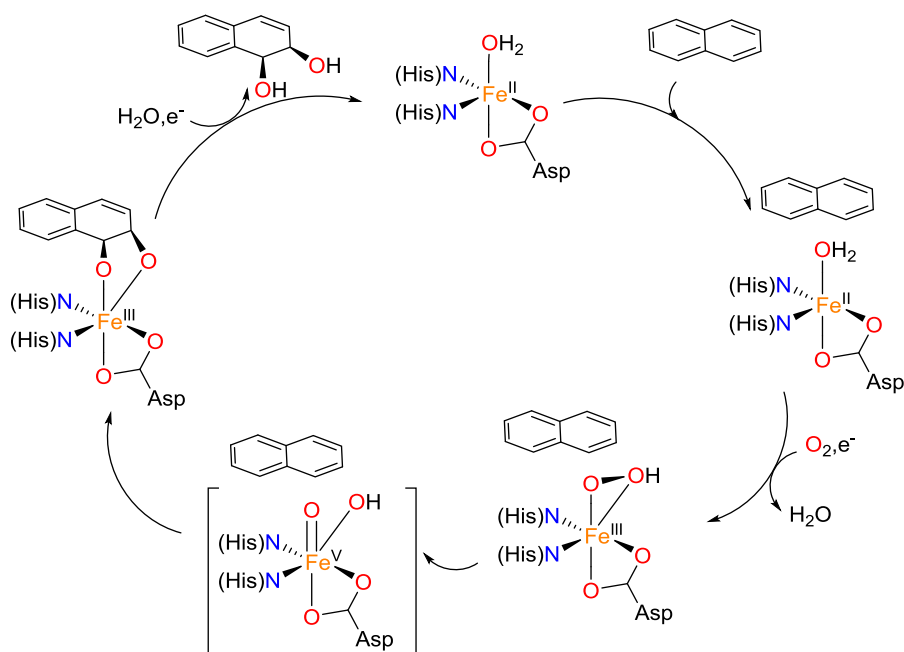
Scheme 2. Established catalytic cycle for alkane hydroxylation performed by Cyt P450.

I.2.2. RIESKE OXYGENASES

Rieske oxygenases are a family of bacterial, nonheme iron dependent oxygenases. They are less distributed among living organisms but more versatile than heme-containing Cyt P450. Rieske Oxygenase family carry out

benzylic hydroxylation, desaturation, sulfoxidation and O- and N-dealkylation.²⁰ They also perform the *syn*-hydroxylation of aromatic substrates and olefins with a high degree of stereo-, regio- and enantiospecificity. These reactions constitute the first step in the oxidative degradation of alkyl aromatic substrates.²⁰⁻²² Because of that, these enzymes have a great interest as biotechnological tools. Moreover, members of the Rieske Oxygenases contain in their active site an iron center coordinated to two histidine residues and one carboxylate residue. This basic structure is emerging as common element in a number of metalloenzymes.²³ The Rieske Oxygenases are composed of two components, a reductase and oxygenase. The reductases liberate electrons from NAD(P)H and transfer them to the oxygenase component, where molecular dioxygen is activated and oxidation of the substrate takes place. One of the most studied members of the Rieske oxygenase family of enzymes is naphthalene-1,2-dioxygenase (NDO) from the bacteria *Pseudomonas putida*, which was crystallographically characterized in 1998.²⁴ Also a catalytic cycle was proposed (Scheme 3). Time resolved cryo-crystallography on frozen crystals of NDO exposed to oxygen indicate that a side-on bound peroxo (or hydroperoxo)-iron(III) species is the last detectable intermediate before substrate oxidation, where both oxygens are incorporated to *syn*-diol product.^{23,25} Remarkably a putative Fe^V(O) species is proposed to be formed before substrate attack, because labeling studies with H₂¹⁸O show labeled oxygen incorporated into *syn*-diol product. Water incorporation is regarded as indication of the presence of a Fe=O species that can exchange its oxygen atom with water, before substrate attack.²⁶ The catalytic cycle starts when the iron center, in its reduced state binds the arene substrate. The enzyme readily reacts with O₂ and an electron (transferred from reductase component) to form an iron(III)-peroxo complex. After that, the O-O cleavage generates a presumably Fe^V(O)(OH) that attacks the substrate to form the *syn*-diol product.

In general, the evidence suggests a common mechanism of O-O activation and formation of high-valent iron-oxo species in Rieske Oxygenases and Cyt P450 systems. Moreover, NDO can carry out the oxidation reaction via a "peroxide shunt" with hydrogen peroxide as oxidant.²⁷



Scheme 3. Catalytic cycle proposed for Rieske dioxygenases.

I.4. MANGANESE IN BIOLOGICAL SYSTEMS

I.4.1. MANGANESE PROTEINS INVOLVED IN OXIDATIVE REACTIONS

It is nowadays recognized that manganese plays two key roles in biological systems. Manganese dependent oxidoreductases, transferases, hydrolases, oxygenases, lyases, isomerases, ligases and the oxygen evolving center of photosystem II take advantage of the rich chemistry of this metal.²⁸⁻³¹ Manganese participates in a number of processes of the O_2^- metabolism, both in reactions where the O_2 molecule is used as oxidant, and also in the water oxidation reaction.

One of the enzymes most studied for its relevance, is the oxygen evolving center (OEC) of photosystem II, where it has been proposed that a $Mn^V(O)$ or a $Mn^{IV}(O)$ -organic radical is the active species, oxidizing H_2O to form O_2 .^{32,33} Other studied manganese-enzymes involve in oxidation processes are manganese superoxide dismutase (Mn-SOD), manganese lipoxygenases (Mn-LO) manganese-dependent extradiol-cleaving catechol dioxygenase (MndD). Manganese dependent enzymes involved in C-H and C=C oxidation reactions are so far unknown, but there are close similarities in the chemistry of iron and manganese, suggesting that this metal can be a suitable metal for designing

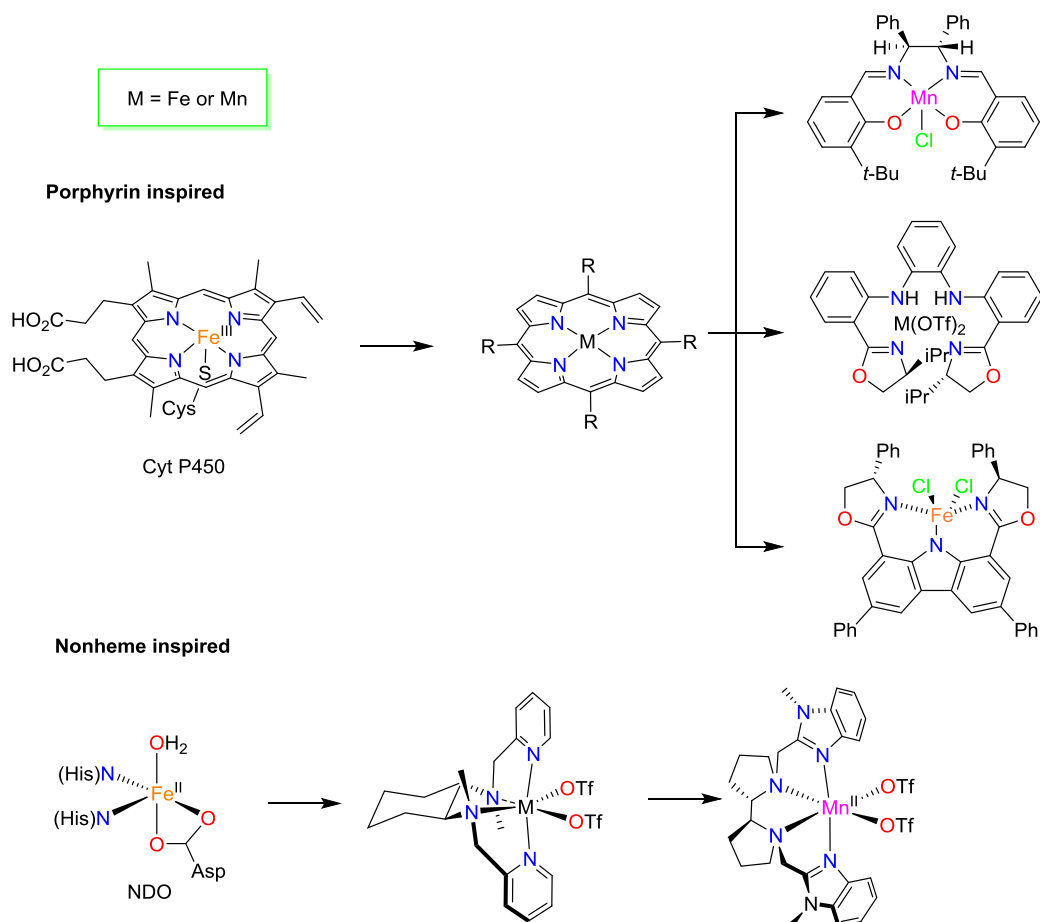
“iron-like” oxidation catalysts. Indeed, different authors have followed this approach.

I.5. IRON AND MANGANESE BIOINSPIRED COMPLEXES

From sustainability and economic points of view, nowadays the demand to employ more environmentally benign reaction conditions is increasing. This translates into an interest for the use of abundant and environmentally friendly base metals, such as Fe, Mn, Co, as catalysts, and the avoidance of oxidants that produce waste products, such as organic peracids, PhIO, TBHP. Instead there is a special interest in the use of environmentally friendly oxidants, like oxygen or hydrogen peroxide, getting water as sole subproduct.^{34,35} However, manipulation of oxygen as reagent for organic synthesis is not straightforward. Combination of O₂ and organic matter can lead to explosive mixtures. In addition, activation of O₂ is a very complex issue which often requires the use of sacrificial reducing agents. In the case of hydrogen peroxide the main problem is that in high concentrations it can be dangerous to handle. In addition, in the presence of some metals it disproportionates and generates highly reactive hydroxyl radicals that produce non-selective oxidations.³⁶⁻³⁸

Inspired by the active site of iron and manganese oxidation enzymes, chemists have designed a wide variety of complexes that functionally mimic these metalloenzymes (Scheme 4). The main goal is to create new and simpler systems that can perform the catalytic transformation as natural enzymes. This section is focused on the synthetic models described in the literature inspired in nonheme metalloenzymes. Several examples for iron and manganese bioinspired complexes are capable to epoxidizing olefins with high yields and stereoselectivities. These systems are envisioned to be valuable as environmentally friendly catalytic systems; they use hydrogen peroxide as oxidant, they are based in first row transition metals, avoid chlorinated solvents, reaction times are short, and chemistry can be readily translated into large-scale. Besides its potential applicability in organic synthesis, mechanistic insight in bioinspired catalysts will provide insight into biological pathways and new understanding of the fundamental reaction steps and reactive intermediates relevant to metalloenzymes. On the other hand, it should be recognized that the

systems are still limited in terms of substrate scope,³⁹⁻⁴¹ and that major developments in the field are needed.

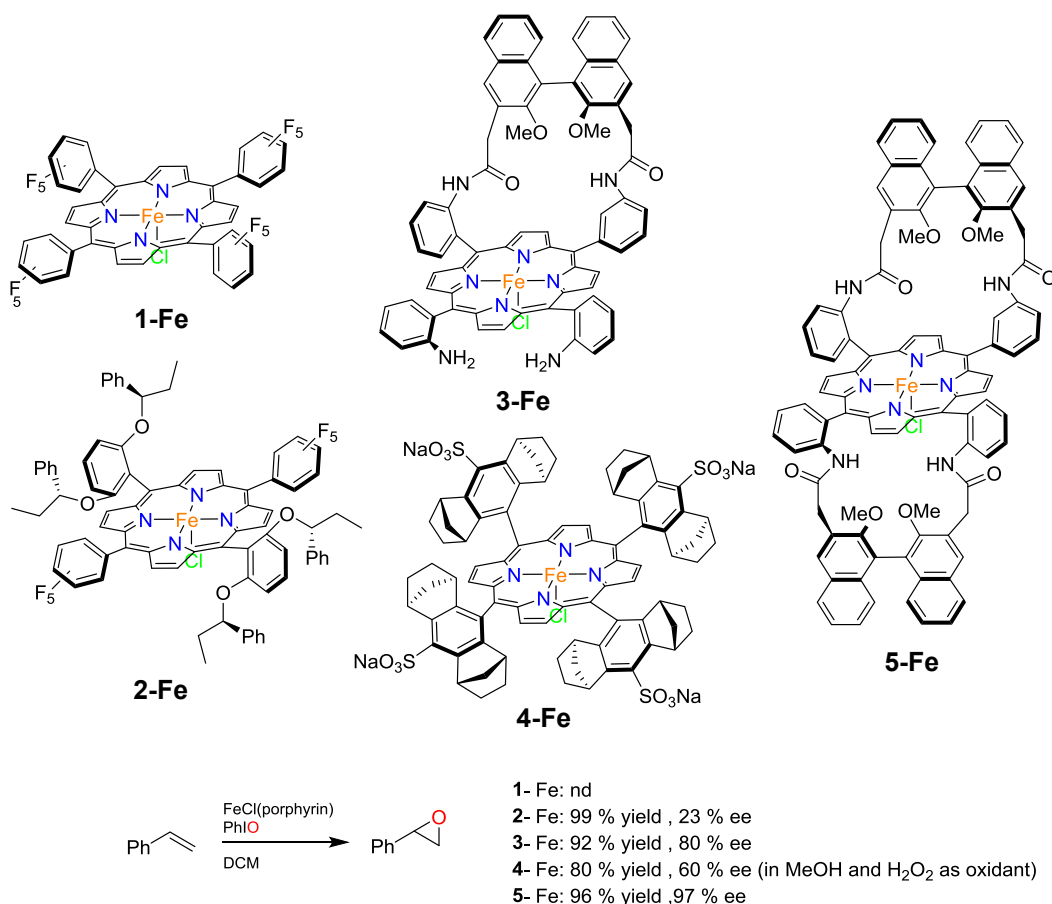


Scheme 4. Some examples of evolution of biologically inspired catalysts used in oxidation processes.

1.5.1. ASYMMETRIC EPOXIDATION CATALYSIS MEDIATED BY BIOINSPIRED IRON SYSTEMS

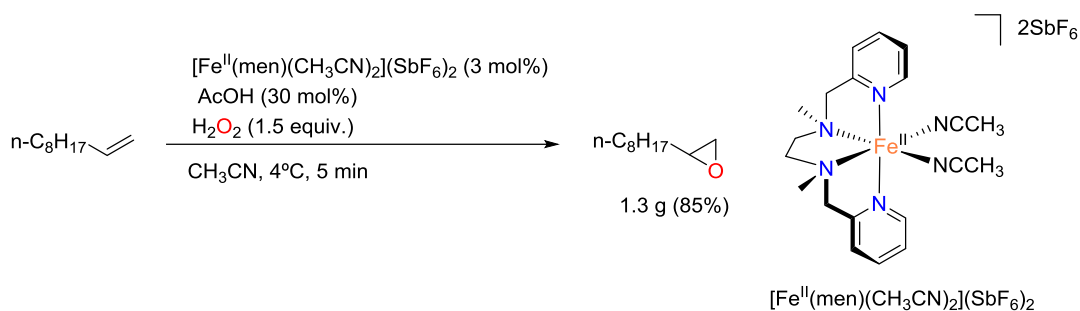
From 1976, the discovery of the peroxide shunt promoted the development of P450 biomimetic models. The first relevant example was reported by Groves and co-workers. The authors used a TPP-FeCl system (TPP = 5,10,15,20-tetraphenylporphyrin) that oxidized alkenes and alkanes through oxygen transfer from iodosylbenzene PhIO.⁴² Unfortunately, the catalyst was degraded rapidly. To avoid that, Chang added pentafluoro groups in the phenyl rings, obtaining an improvement of activity.⁴³ Numerous chiral porphyrins appeared during the last thirty-five years, but only a few provided good to excellent enantioselectivities.⁴⁴⁻⁴⁷ In Scheme 5 few reported examples are shown. One of

the main drawbacks of the use of metalloporphyrins is the use of environmentally not friendly conditions, for instance, the use of dichloromethane as solvent and iodosylbenzene as oxidant. Only few examples use hydrogen peroxide as oxidant (Scheme 5).



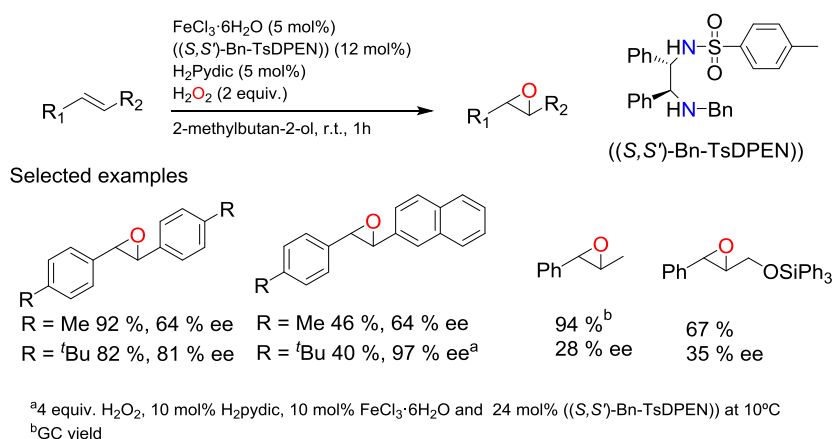
Scheme 5. Different examples of iron porphyrins reported for asymmetric epoxidation of styrene as a model substrate.⁴³⁻⁴⁷

One of the first examples in the literature describing the combination of non-porphyrinic iron catalysts and H₂O₂ to perform epoxidation reactions with potential applicability in organic synthesis was reported by Jacobsen and co-workers in 2001.⁴⁸ The nonheme iron complex was based on two pyridine and a dimethylethylenediamine [Fe^{II}(men)(CH₃CN)₂](SbF₆)₂. The epoxidation reaction was carried out with hydrogen peroxide as oxidant, acetic acid as key additive to achieve excellent activities in short reaction times in acetonitrile (in Section 1.5.1.1. we discussed the role of acetic acid). The authors obtained good to excellent yields for aliphatic alkenes and also the system was able to scale up to gram scale (Scheme 6).



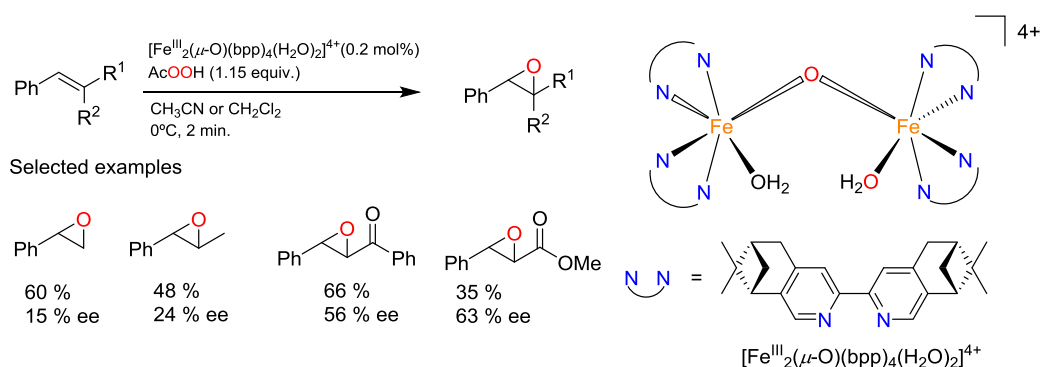
Scheme 6. Oxidation of 1-decene catalyzed by $[\text{Fe}^{\text{II}}(\text{men})(\text{CH}_3\text{CN})_2](\text{SbF}_6)_2$.

In 2007, Beller and co-workers reported the first example of highly enantioselective epoxidation with iron catalysts not based on porphyrins.⁴⁹ *In situ* generation of catalyst by combination of commercially available $\text{FeCl}_3 \cdot 6\text{H}_2\text{O}$ as iron source, pyridine-2,6-dicarboxylic acid and pyrrolidine as additives and chiral amines as ligands ((*S,S'*)-Bn-TsDPEN), H_2O_2 as oxidant to room temperature and an aerobic atmosphere provided excellent enantioselectivities for *para*-substituted *trans*-stilbenes (up to 97%, Scheme 7). However, yields and stereoselectivities showed a large variation, depending on substrate symmetry and bulkiness. In this system to identify the active species or the simple iron complex that acts as catalysts is difficult, making very difficult to propose a possible mechanism. However, the system represents an interesting biomimetic approach because of the use of carboxylic acids and amines, the basic type of ligands presents in nonheme iron oxygenases, as coordinating ligands.



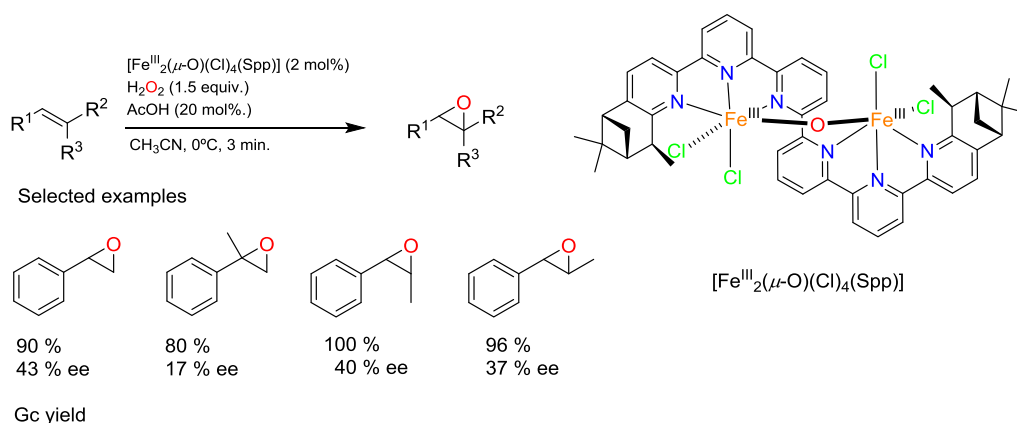
Scheme 7. In situ generated catalyst reported by Beller.

Also, in 2007, Menage and co-workers described a nonheme oxo-bridged diiron complex $[\text{Fe}^{\text{III}}_2(\mu\text{-O})(\text{bpp})_4(\text{H}_2\text{O})_2]^{4+}$ with chiral bipyridine ligands.⁵⁰ The complex oxidizes olefins with high efficiencies, up to 850 TON and moderate enantioselectivities ranging from 9–63%, the best results were obtained for electron-deficient olefins, such as *trans*-chalcones and *trans*-cinnamates with AcOOH as oxidant and CH₃CN or CH₂Cl₂ as solvents (Scheme 8).



Scheme 8. Asymmetric epoxidation of olefins with the $[\text{Fe}^{\text{III}}_2(\mu\text{-O})(\text{bpp})_4(\text{H}_2\text{O})_2]^{4+}$ complex and AcOOH.

In 2008, a better defined iron complex was reported by Kwong and co-workers based on chiral $[\text{Fe}^{\text{III}}_2(\mu\text{-O})(\text{Cl})_4(\text{Spp})]$ as an efficient catalyst for the epoxidation of alkenes with H₂O₂ in the presence of acetic acid, providing moderate enantiomeric excesses in the oxidation of aromatic olefins, up to 43 % ee (Scheme 9).⁵¹ Most remarkable, the combination of hydrogen peroxide with acetic acid didn't form AcOOH in situ, because when the reaction was performed with AcOOH as oxidant, no epoxide product was observed.



Scheme 9. Asymmetric epoxidation of styrenes derivatives with $[\text{Fe}^{\text{III}}_2(\mu\text{-O})(\text{Cl})_4(\text{Spp})]$, H₂O₂ and AcOH.

In 2011, Wei Sun and co-workers took a well-defined (*R,R'*)-[Fe(OTf)₂(mcp)] that is the chiral analogue of [Fe^{II}(men)(CH₃CN)₂](SbF₆)₂ to perform asymmetric epoxidation reactions;⁵² however, it was not the first time that this iron complex was used in asymmetric reaction, since Que and co-workers obtained modest ee for *trans*-2-heptene with hydrogen peroxide as oxidant (12 % of ee).⁵³ The catalyst is C₂ symmetric, with two pyridines *trans* to each other, and two aliphatic diamines *cis* to each other, in the so-called *cis-α* topology. The *trans*- and *cis-β* topologies, also possible for this class of catalysts are less active (Figure 1). Furthermore, Wei Sun tested the system with other kind of substrates obtaining moderated ee, for instance, *trans*-chalcone was epoxidized in a 54 % of ee with hydrogen peroxide as oxidant and acetic acid as additive in acetonitrile. Finally, Wei Sun synthesized a more robust and elaborated analogous complex by adding two chiral groups in pseudo-benzylic position in the pyridines ((*R,R,R,R'*)-[Fe(OTf)₂(bpmcp)]). Thanks to the new two chiral elements the epoxidation reaction increased in terms of activity and more importantly in terms of enantioselectivity, displaying up to 87% ee for substituted *trans*-chalcones. Unfortunately, the system was limited to substituted *trans*-chalcones with moderate to excellent yields (33-90%) (Scheme 10).

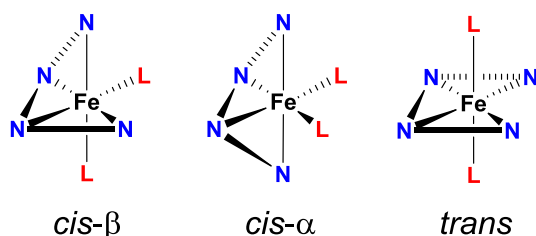
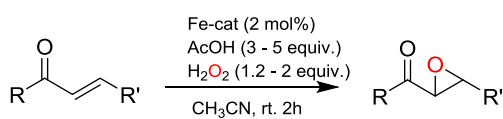


Figure 1. Three possible topologies for iron complexes with linear tetradentate ligands.

The same group developed a second catalyst (*S*)-[Fe(OTf)₂(peb)] on a more rigid chiral diamine derived from *L*-proline and two benzimidazole donor groups instead of pyridines.⁵⁴ The new catalyst showed an impressive activity up to 99% yield and 97% ee for the same kind of substrates, such as *trans-α,β*-aromatic enones and tetralone derivatives. Moreover, observing that benzimidazoles moieties gave excellent results they developed the iron complex with (*1R,2R*)-1,2-dimethylcyclohexandiamine as backbone (*R,R'*)-

[Fe(OTf)₂(mcmb)]. The results obtained for the same type of substrates were similar to those obtained with *L*-proline as a backbone (Scheme 10).⁵⁵

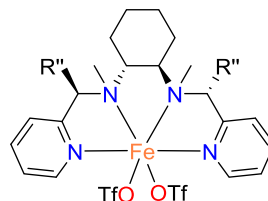


Selected examples

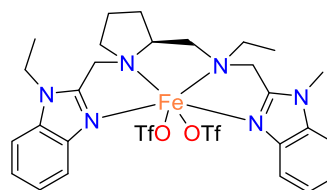
R = Ph, R' = Ph, 53 %, 77 % ee
 R = Ph, R' = *p*-Cl-Ph, 90 %, 84 % ee
 R = *p*-Me-Ph, R' = Ph, 61 %, 82 % ee
 R = Ph, R' = *p*-F-Ph, 73 %, 87 % ee

R = Ph, R' = Ph, 89 %, 92 % ee
 R = Ph, R' = *p*-Cl-Ph, 97 %, 94 % ee
 R = *p*-Me-Ph, R' = *p*-F-Ph, 93 %, 92 % ee
 R = *o*-Cl-Ph, R' = Ph, 78 %, 91 % ee

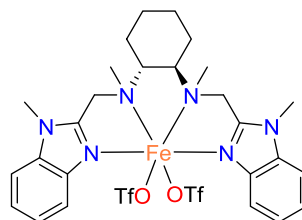
R = Ph, R' = Ph, 94 %, 93 % ee
 R = Ph, R' = *p*-Me-Ph, 71 %, 87 % ee
 R = *p*-F-Ph, R' = *p*-F-Ph, 85 %, 87 % ee
 R = Ph, R' = *o*-Cl-Ph, 76 %, 95 % ee



R'' = H (*R,R'*)-[Fe(OTf)₂(mcp)]
 R'' = Ph (*R,R,R,R'*)-[Fe(OTf)₂(pmcp)]
 R'' = 4-*t*-Bu-C₆H₄ (*R,R,R,R'*)-[Fe(OTf)₂(bpmcp)]



(*S*)-[Fe(OTf)₂(peb)]

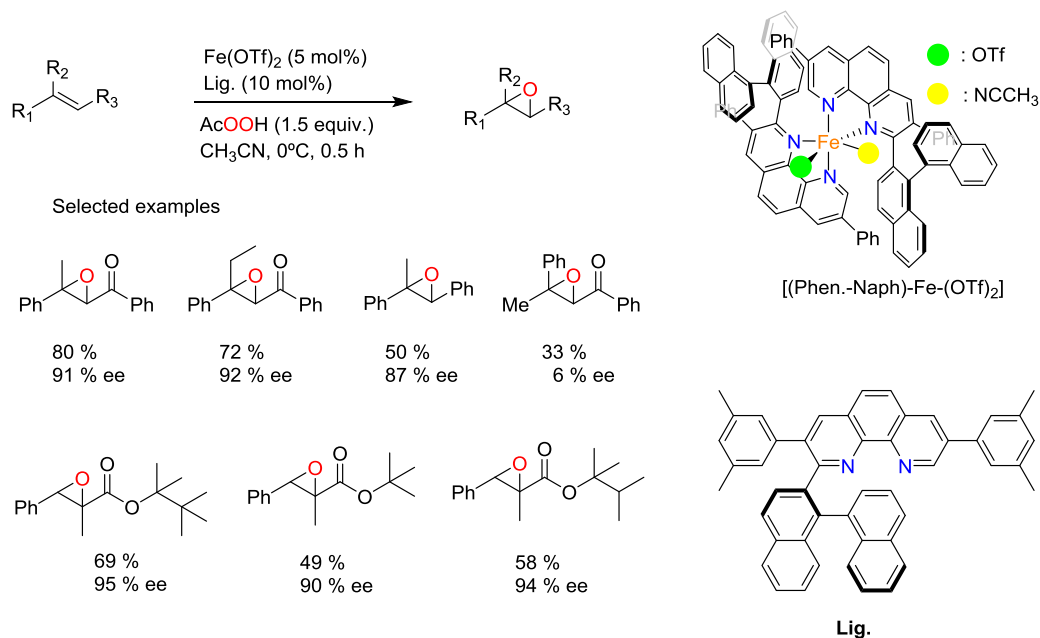


(*R,R'*)-[Fe(OTf)₂(mcmb)]

Scheme 10. Asymmetric epoxidation of *trans*-chalcones derivatives with different tetraaminodentate nonheme iron complexes, and H₂O₂/AcOH as oxidant.

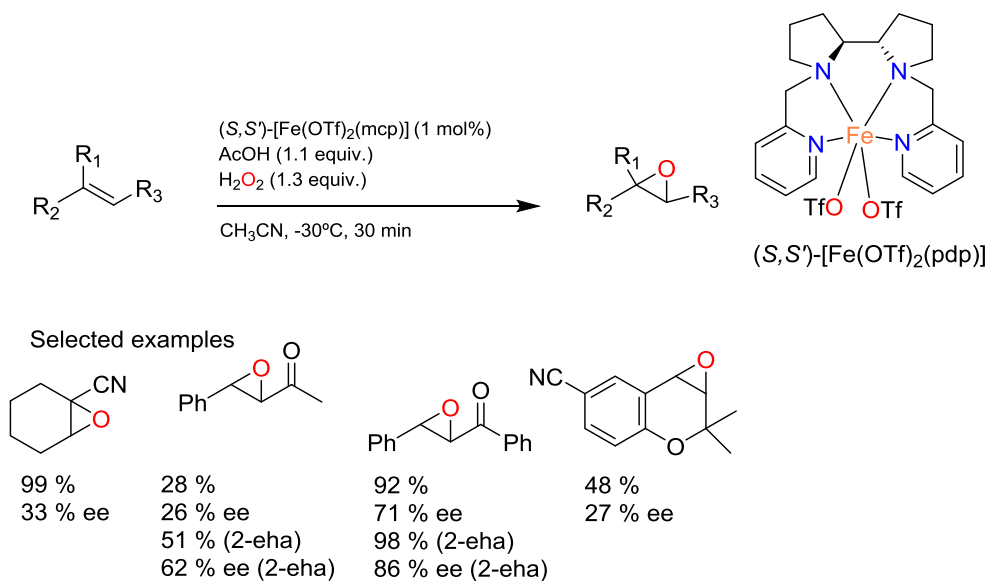
In 2011, Yamamoto and co-workers reported a new iron catalyst capable to epoxidize acyclic β,β -disubstituted enones. These represent very difficult substrates for which a stereoselective epoxidation methodology was still lacking, probably because steric congestion at the β carbon limits the Weitz-Scheffer-type epoxidation, which is the commonly employed method to access β,β disubstituted α,β -epoxy carbonyl compounds. The complex consists in an iron center (Fe(OTf)₂) with phenanthroline ligands attached to binaphthyl moieties as chiral sources (Scheme 11).⁵⁶ The epoxidation proceeds with AcOOH as oxidant or *m*CPBA with a comparable yield, but it didn't work with H₂O₂, sodium percarbonate, TBHP or cumene hydroperoxide (CHP). This system epoxidizes β,β -disubstituted enones in good yields and excellent enantioselectivities (90 - 92% ee). Also, the group achieved excellent enantioselectivities but moderate yields for α,β -unsaturated ester ranging from

16 to 69 % yield and 63 to 99 % ee.⁵⁷ Moreover, intermolecular competition between electron-rich and electron-poor alkene substrates suggest the presence of an electrophilic oxidant.



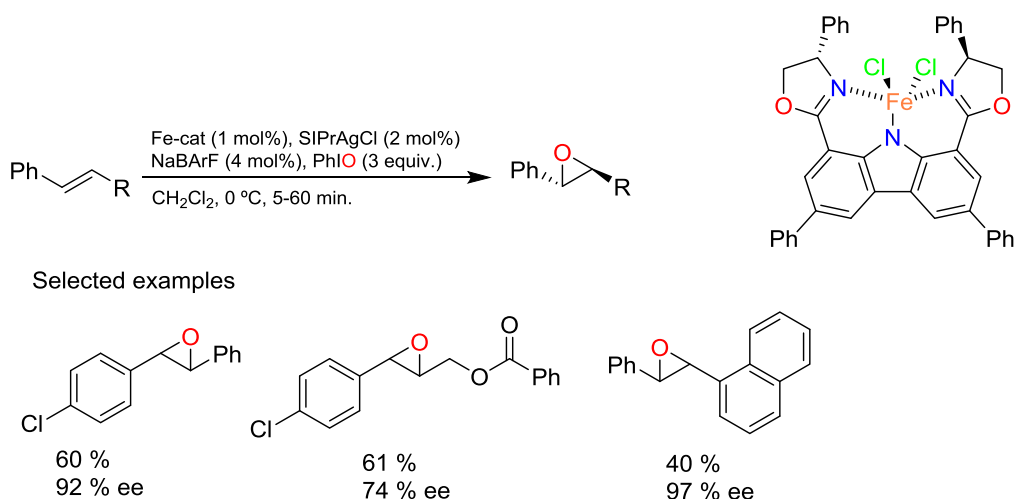
Scheme 11. Asymmetric epoxidation of olefins with the iron complex and AcOOH reported by Yamamoto.

In 2012, Talsi and co-workers used the (*S,S'*)-[Fe(OTf)₂(pdp)] reported previously by White⁵⁸ in asymmetric epoxidation reactions of different aromatic enones by using 1 mol% of catalyst, H₂O₂ as oxidant and stoichiometric amounts of acetic acid as additive. In these conditions, *trans*-chalcone was epoxidized up to 71 % of ee.⁵⁹ Most interestingly, the authors also studied different carboxylic acids as additives, observing that sterically demanding carboxylic acids favour stereoselectivities and activities in a few substrates. This study suggested that the carboxylic acid appears to affect the stereodiscrimination and is involved in defining the structure of active oxidant species. However, low conversions were obtained for strongly acid carboxylic acids. The system provided lower enantioselectivities for substrates lacking a carbonyl conjugation to the double bond, for example, 16 % ee for styrene (Scheme 12).

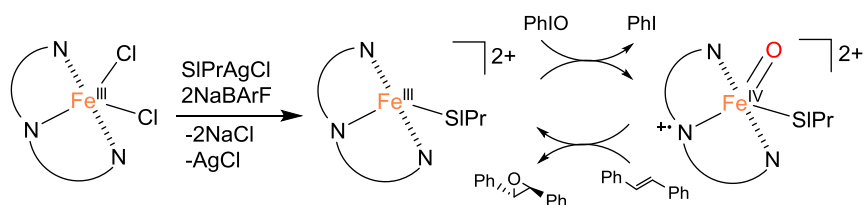


Scheme 12. Asymmetric epoxidation of olefins with the (S,S')-[Fe(OTf)₂(pdp)] complex, H₂O₂ and AcOH or 2-eha.

In 2012, Nakada and co-workers developed an iron(III) complex with a 1,8-(bisoxazolyl)-carbazole ligand for the asymmetric epoxidation of (*E*)-alkenes, such as *trans*-stilbene derivatives and cinnamyl alcohol derivatives, providing excellent yields and enantioselectivities (76- 97% of ee) in the presence of NaBARF, SIPrAgCl and PhIO as oxidant (Scheme 13).⁶⁰ Both NaBARF and SIPrAgCl were essential for the epoxidation reaction to take place. The electronic structure of the complex resembles an iron-porphyrin complex although the chiral ligand was tridentate instead of the tetradentate nature of the porphyrin core. The iron(III) complex had a five-coordinated trigonal-bipyramidal structure; three coordination sites are occupied by the carbazole moiety and the two oxazolines, and two chloride groups complete the first coordination sphere. The later groups were removed by the addition of NaBARF and SIPrAgCl, forming Fe(III)-SIPr species that react with PhIO to obtain the active oxidant, presumably a Fe^{IV}(O) cation radical (Scheme 14). The system showed remarkable analogies in oxidation chemistry with iron porphyrins, for example, the proposed oxidant active species (iron(IV)-oxo cation radical), with one of the oxidizing equivalent residing in the ligand, and the use of iodosylbenzene as oxidant.

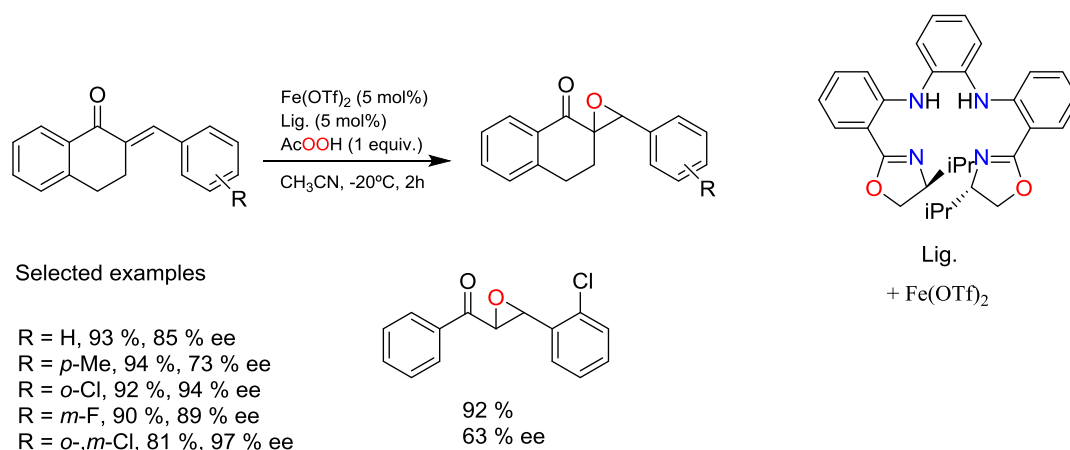


Scheme 13. Asymmetric epoxidation of *trans* olefins with iron complex, PhIO, NaBARf SIPrAgCl reported by Nakada.



Scheme 14. Proposed mechanism for iron complex reported by Nakada.

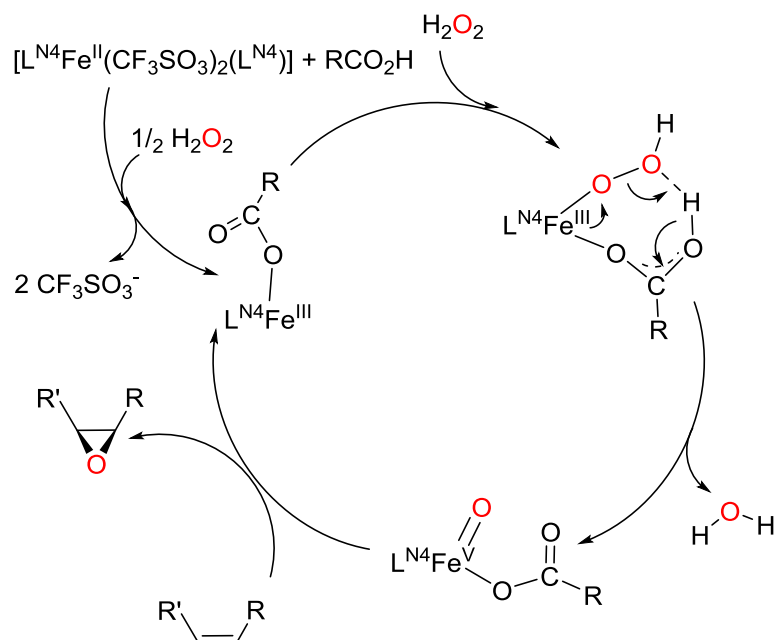
Most recently, on 2015, Gao and co-workers developed a new type of porphyrin-inspired N4 ligands bearing chiral oxazoline moieties. The main advantage of these complexes is the easily tunable ligand, due to large number of amino acid sources available that can be used to make oxazolines. Several different oxazoline derivatives of the ligand were tested in the asymmetric epoxidation reaction of tetralone derivatives with $\text{Fe}(\text{OTf})_2$ as iron source, mCPBA or AcOOH as oxidant, in acetonitrile at $-20\text{ }^\circ\text{C}$ (Scheme 15).⁶¹ The best conditions found involved the catalyst that contains isopropyl groups, and AcOOH as oxidant, obtaining a yield of 93 % and an enantioselectivity of 85 % ee for tetralone derivative. Unfortunately, the system didn't work with H_2O_2 or *t*BuOOH. With optimal conditions in hand, the authors tested substituted tetralone derivatives in asymmetric epoxidation reactions, achieving excellent yields and excellent enantioselectivities, up to 94% yield and 99% ee, respectively. The authors found a good linear correlation between $\log(k_x/k_H)$ vs σ_p^+ with negative slope ($\rho^+ = -0.52$), indicating that the active oxidant was electrophilic.



Scheme 15. Asymmetric epoxidation of tetralone derivatives reported by Gao and co-workers.

1.5.1.1. Role of acetic acid in oxidation reactions with bioinspired iron complexes

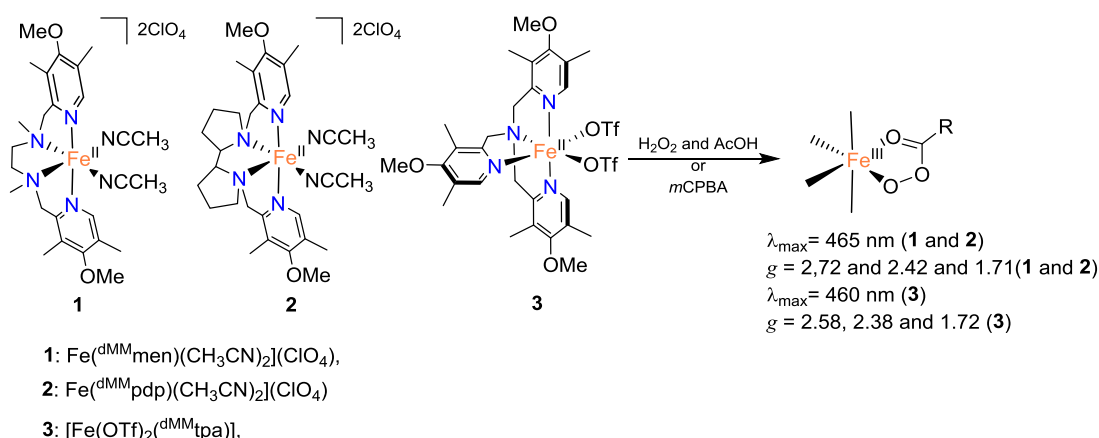
The role of carboxylic acids in the systems previously described needs to be understood. Carboxylic acids show a prominent positive role in iron catalyzed olefin epoxidation with hydrogen peroxide. Remarkably, acetic acid increases the activities and stereoselectivities of iron epoxidation catalysts.^{48,59} In addition, acetic acid inhibits iron catalyzed olefin *cis*-dihydroxylation, enhancing the chemoselectivity towards epoxidation.⁶² As Talsi, Bryliakov and co-workers first described, acetic acid can be replaced by bulkier carboxylic acids to improve the enantioselectivities and in some cases also the activities.⁵⁹ The first example employing acetic acid as additive was reported by Jacobsen and co-workers with [Fe^{II}(men)(CH₃CN)₂](SbF₆)₂ as catalyst, observing positive benefits in the activity of the system.⁴⁸ Que and co-workers studied the activity of complexes [Fe^{II}(OTf)₂(tpa)] (tpa = tris-(2-pyridylmethyl)amine) and [Fe^{II}(OTf)₂(men)], and proposed that acetic acid promotes the O-O bond cleavage in a Fe^{III}(OOH) species, presumably leading to the formation of Fe^V(O)(OAc) species, finally responsible for the epoxidation reaction (Scheme 16, carboxylic assisted mechanism).⁶³ One indirect evidence in favor of the formation of Fe^V(O)(OAc) species was the formation of *cis*-hydroxyacetoxylated product in olefin oxidations with [Fe^{II}(OTf)₂(tpa)] in the presence of acetic acid.⁶⁴



Scheme 16. Proposed mechanism for epoxidation reaction via carboxylic acid assisted with tetradentate aminopyridine iron complexes and $H_2O_2/AcOH$.

Although, observation and elucidation of intermediates are difficult due to their high reactivity and paramagnetic nature, Talsi and co-workers proposed the implication of $Fe^V(O)(OAc)$ species on the basis on EPR studies on the reaction between (S,S') - $[Fe(OTf)_2(pdp)]$, hydrogen peroxide and acetic acid. Specifically, the authors identified a rhombic $S = 1/2$ system with EPR values of $g = 2.66$, 2.42 and 1.71 in a CH_2Cl_2/CH_3CN mixture at $-70^\circ C$.⁵⁹ The decay of this species was accelerated in the presence of cyclohexene, giving cyclohexene oxide as product. However, more spectroscopic studies are necessary, because this species was formed in only 1 % yield of the total iron content in the sample. In parallel studies, Que and co-workers studied $[Fe^{(dMM)men}(CH_3CN)_2](ClO_4)_2$, $[Fe^{(dMM)pdp}(CH_3CN)_2](ClO_4)_2$ and $[Fe(OTf)_2^{(dMM)tpa}]$ complexes (Scheme 17) with electron-donating groups in the pyridine ring (dMM = Dimethylmethoxy) as catalysts, because electron-rich complexes were envisioned to stabilize high valent species. EPR studies on the reaction of the complexes with $H_2O_2/AcOH$, $AcOOH$ and $mCPBA$ showed a $S = 1/2$ system, and in the UV-Vis spectrum a band at $\lambda_{max} = 465$ nm for $[Fe^{(dMM)men}(CH_3CN)_2](ClO_4)_2$ and $Fe^{(dMM)pdp}(CH_3CN)_2](ClO_4)_2$ and $\lambda_{max} = 460$ nm for $[Fe(OTf)_2^{(dMM)tpa}]$ was observed. The authors proposed these species to be ferric acylperoxide complexes. The later complex has been studied in more detail. Its reaction with

AcOOH generates a metastable species that was well characterized by EPR ($g = 2.58, 2.38$ and 1.72), Mosbauer and ESI. The sum of the spectroscopic data suggest that the intermediate should be formulated as $[\text{tpa-Fe}^{\text{III}}(\text{OOC}(\text{O})\text{R})]$ ($\text{R} = \text{CH}_3$ or $3\text{Cl-C}_6\text{H}_4$) (Scheme 17).⁶⁴ Most interestingly, the authors observed that these species are not responsible for oxygen atom transfer to the olefin because they are not kinetically competent for reacting with olefins. However, DFT calculations suggest that these species evolve via rate determining O-O cleavage to form $\text{Fe}^{\text{V}}(\text{O})(\text{O}_2\text{C-Ar})$ or $\text{Fe}^{\text{IV}}(\text{O})(\text{O}_2\text{C-Ar})$ that act as the active oxidant.⁶⁵ Finally, Talsi and co-workers have very recently described the detection by EPR of a highly reactive intermediate formulated as a $\text{Fe}^{\text{V}}(\text{O})$ species in the reaction of dimeric iron complexes $[(\text{Fe}^{\text{II}}_2(\mu\text{-OH})_2(\text{L})_2)]^{4+}$ ($\text{L} = \text{dMM}_4\text{tpa}$ or dMM_4men) with peracids. The values observed were $g = 2.07, 2.00$ and 1.96 , characteristic of an $S = 1/2$ system. The species accumulated up to 1-2 %, and reacted with olefins at -85 °C.⁶⁶



Scheme 17. Synthesis of acylperoxyiron(III) complexes from reaction of $\text{Fe}^{\text{dMM}}(\text{men})(\text{CH}_3\text{CN})_2(\text{ClO}_4)_2$, $\text{Fe}^{\text{dMM}}(\text{pdp})(\text{CH}_3\text{CN})_2(\text{ClO}_4)_2$ and $[\text{Fe}(\text{OTf})_2(\text{dMM}_4\text{tpa})]$ with $\text{H}_2\text{O}_2/\text{AcOH}$ or peracids.

I.5.2. ASYMMETRIC EPOXIDATION CATALYSIS MEDIATED BY BIOLOGICALLY INSPIRED MANGANESE SYSTEMS

Manganese has emerged during the last three decades as a very active transition metal ion for oxidation catalysis. In 1980, Groves and co-workers pioneered the use of the first manganese metalloporphyrin as catalyst for oxidation reactions $[\text{Mn}(\text{TPP})(\text{Cl})]$ (Figure 2, left).⁶⁷ The catalysis employed

PhIO as oxidant, and reactions with *cis*-stilbene evidenced stereoscrambling, suggesting that a radical intermediate is formed that can rotate around the carbon-carbon bond. Novel examples of chiral Mn-porphyrins have been synthesized and studied as stereoselective catalysts. These include porphyrins containing electron-deficient groups,⁶⁸ “vaulted binaphthyl”,⁶⁹ D₄ symmetric porphyrins (Figure 2, center),⁷⁰ “chiral wall” (Figure 2, right),⁷¹ and chiroporphyrins.⁷² All the examples achieved moderate to excellent selectivities for styrene derivatives. Only few systems can work with H₂O₂, and in general the enantioselectivities obtained were moderate and the yields were also very poor.^{73,74}

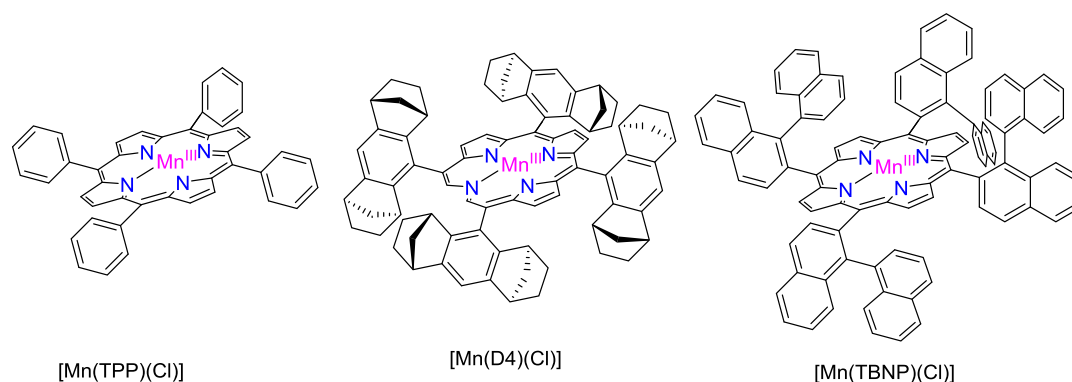


Figure 2. Selected examples of chiral manganese porphyrins.

In the 90s, Jacobsen and Katsuki synthesized Mn-salen complexes with the aim to reproduce porphyrins in a simplified manner, avoiding the hard and long synthetic pathways required for their preparation.^{75,76} Mn-salen were the first example of catalysts for highly asymmetric epoxidation of non functionalized olefins. These olefins don't have any directing group, a difference with regard to Sharpless Asymmetric Epoxidation (SAE)⁷⁷ where an alcohol group acted as a directing group to promote excellent ee's, or Juliá-Colonna epoxidation,⁷⁸ where peptide-catalyst and ketone group of the α,β , unsaturated enones interact through H-bonds. Moreover, Jacobsen and Katsuki epoxidation was very attractive due to a relatively wide substrate scope: *cis*-olefins^{79,80}, *trans*-olefins⁸¹, tri and tetrasubstituted olefins^{82,83} cyclic dienes⁸⁴ and substituted styrenes,^{85,86} were epoxidized with excellent yields and stereoselectivities. However, the system is not suitable for epoxidation of terminal and aliphatic olefins with higher enantioselectivities (Figure 3). One of the limitations is the

loss of stereochemistry in the epoxidation of *cis* conjugated olefins. Few amounts of *trans*-epoxide are obtained. A second limitation is the low enantioselectivities obtained for *trans*-olefins. Moreover, Jacobsen and co-workers found an interesting alternative, consisting in the addition of quaternary ammonium salts. These molecules can tune the lifetime and orient the sense of rotation of the substrate radicals formed in the epoxidation of *cis* olefins, providing high amounts of *trans* epoxides in higher ee's.⁸¹ Additional drawbacks are the requirement of relatively large amounts of complex, usually 10 mol%, and the need of oxidants that are not considered environmental friendly, such as *m*CPBA, PhIO and NaOCl. In parallel, Katsuki and co-workers reported that some pentadentate Mn-salen complexes are capable to oxidize olefins with H₂O₂.⁸⁷ Unfortunately the stereoselectivity was slightly lower in comparison with other Mn-Salen complexes reported before (Figure 3). For this reason, it is still necessary to develop more robust and stereoselective catalyst that could rely on the use of H₂O₂ exhibiting high activities with low catalyst loadings. Finally, the Mn-Salen system has been thoughtfully studied in order to understand the catalytic cycle. Theoretical studies have been also performed suggesting a plausible Mn^V(O) as the epoxidation agent.^{88,89}

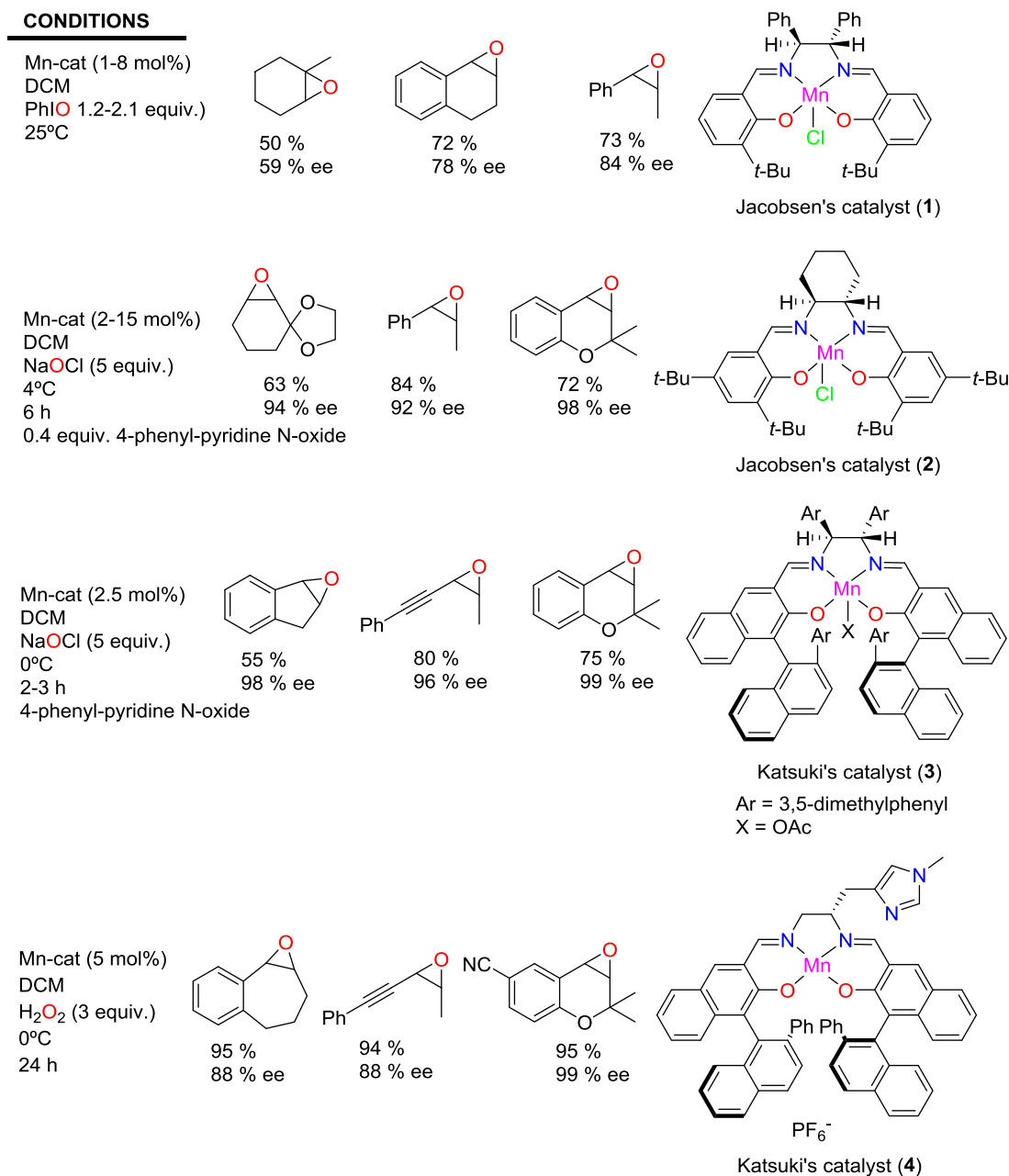


Figure 3. Selected manganese salen complexes reported by Jacobsen and Katsuki and some examples of asymmetric epoxidations.

The next generation of manganese complexes highly active in epoxidation reactions was pioneered by Stack and co-workers in 2002. The authors developed a new manganese complex based on a dimethylcyclohexanediamine backbone and two pyridine groups (*R,R'*)-[Mn(OTf)₂(mcp)] the geometry of the complex is *cis-α* coordination containing two CF₃SO₃⁻ labile anions (Figure 4). The typology is C₂ symmetric, with two aliphatic diamines *cis* to each other and the pyridine rings *trans* to each other, leaving two labile coordination sites at the

manganese center, occupied by the labile triflate groups, which could be replaced by the oxidant.

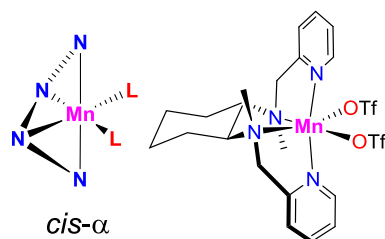
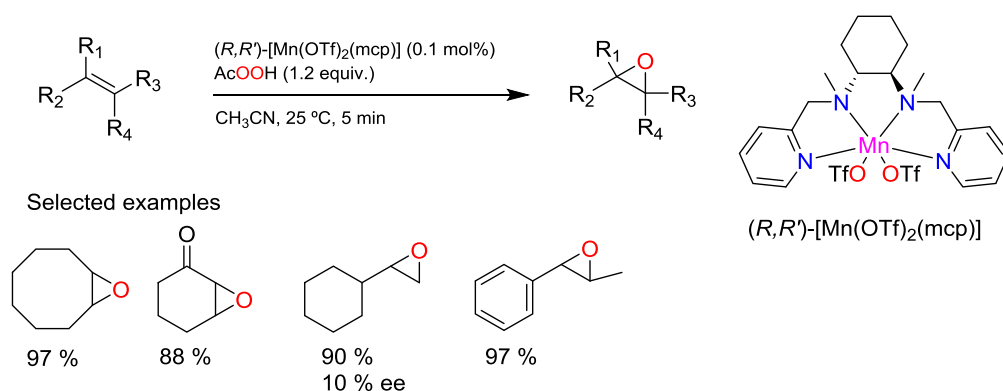


Figure 4. Topology for manganese complexes with linear tetradentate ligands.

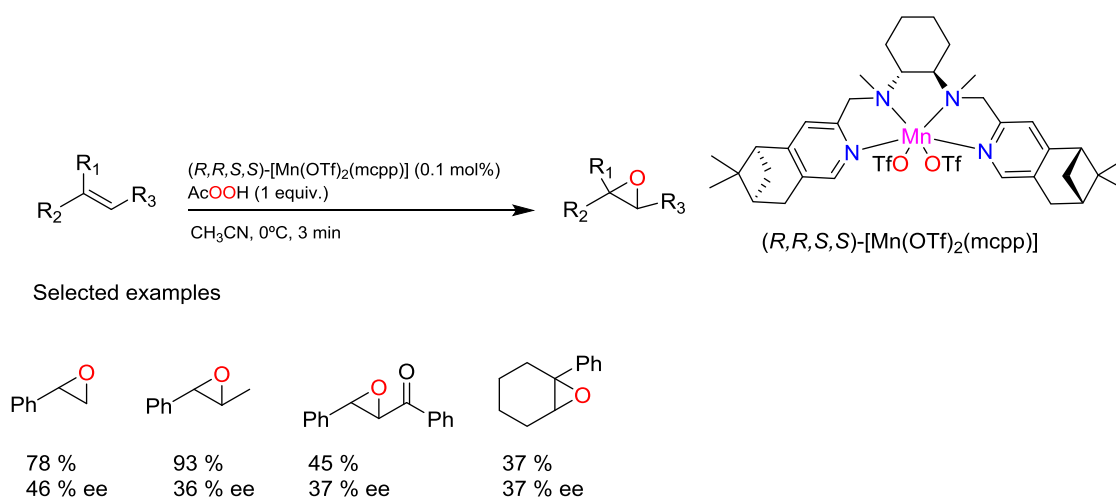
Unfortunately H_2O_2 was not a suitable oxidant for the system, and disproportionates giving water and dioxygen.⁹⁰ Fortunately, AcOOH is a valid and inexpensive alternative. The analogous iron complex reported by Que *et al.*⁹¹ provides lower activity in comparison with the manganese complex, that gave excellent yields with only 0.1 mol% and 1.2 equivalents of AcOOH in CH_3CN during five minutes. Instead, the iron analog required higher catalyst loadings, 1 mol% to elicit good activity. This methodology gave epoxide products with excellent yields for challenging olefins, such as terminal or electron-deficient olefins, otherwise, for 2-cyclohexanone and vinyl cyclohexane only poor enantioselectivities were obtained (10 % ee, for vinyl cyclohexane) (Scheme 18).



Scheme 18. Asymmetric epoxidation reaction of aliphatic and aromatic olefins with the (R,R') - $[\text{Mn}(\text{OTf})_2(\text{mcp})]$ complex and AcOOH .

In 2007, Gómez *et al.* reported a chiral manganese complex related to the one developed before by Stack and co-workers, but sterically more congested. This new complex, $((R,R,S,S)-[\text{Mn}(\text{OTf})_2(\text{mcpp})])$, bears pinene groups linked in positions 4,5 of the pyridine rings of the mcp ligand.⁹² The pinene groups define

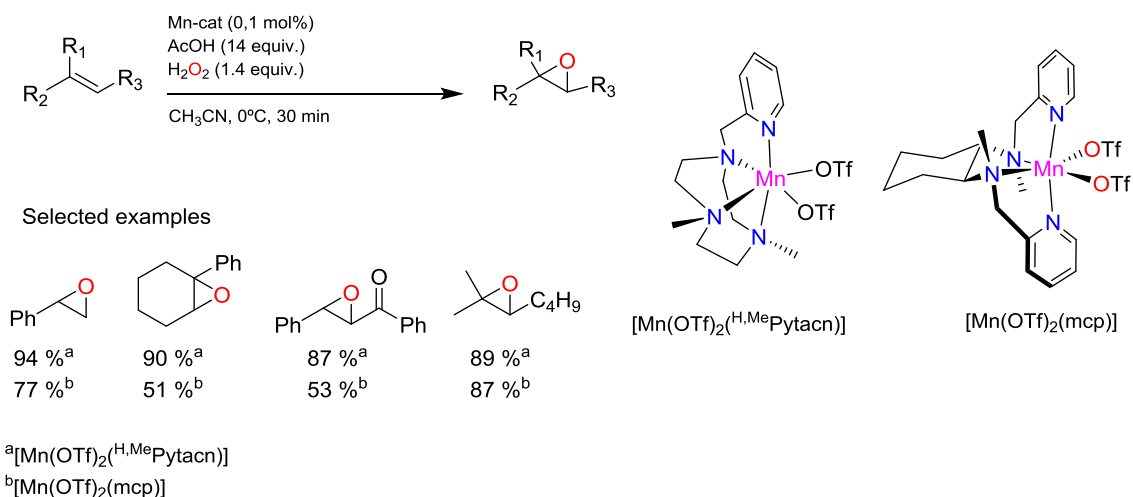
a cavity surrounding the metal, which results in an increased stereoselectivity of the system in catalytic epoxidation. The catalytic conditions were 0.5 mol% of catalyst, 1 equivalent of AcOOH in CH₃CN at 0 °C and it was tested in asymmetric epoxidation of styrene. Up to 46 % ee was achieved, which substantially improved the results with (*R,R'*)-[Mn(OTf)₂(mcp)], (15 % ee). Despite these results remained poor in comparison with Mn-salen complexes, it offered new ideas for the development of new chiral complexes and prompted the use of this kind of complexes in asymmetric epoxidation. Finally, good yields were achieved for another olefins, such as *trans*-chalcone, *trans*-cinnamates and aliphatic olefins, but the ee were still moderate up to 46 % (Scheme 19).



Scheme 19. Asymmetric epoxidation reaction of aromatic olefins with the (*R,R,S,S*)-[Mn(OTf)₂(mcpp)] complex and AcOOH.

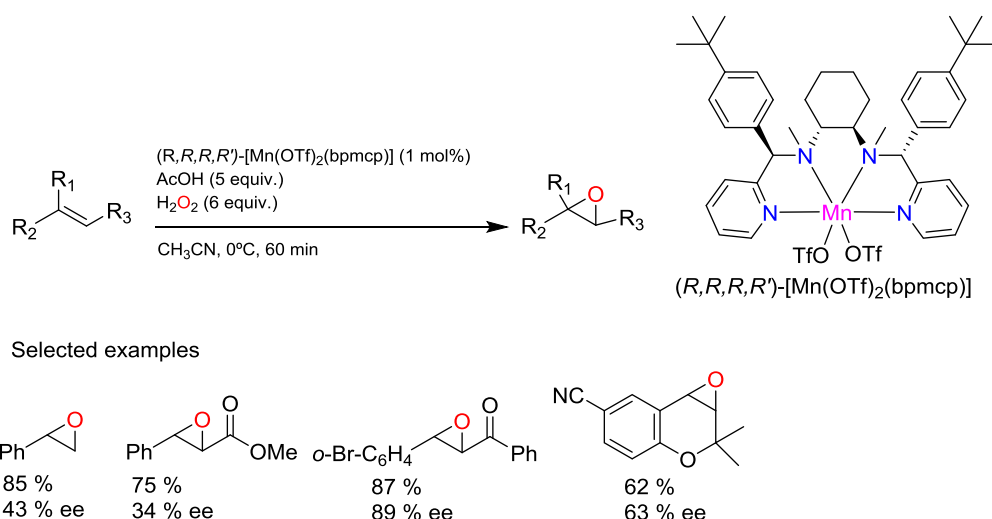
Stack and Gomez results suggested that these are interesting structures to build catalysts for asymmetric epoxidation. The main drawback is that AcOOH exhibits a poorer atom economy than H₂O₂, the cost of this oxidant when compared with H₂O₂, and the fact that commercial peracetic acid solutions are highly acidic, preventing its use in the oxidation of acid-sensitive substrates.

A methodology for using H₂O₂ as oxidant with these systems was developed by Garcia-Bosch et al. By using acetic acid as additive, oxidation of olefins with H₂O₂ catalyzed by [Mn(OTf)₂(^{H,Me}Pytacn)] and [Mn(OTf)₂(mcp)] produces the corresponding epoxides in good yields in short reaction times (Scheme 20). Interestingly, the system allows epoxidation of acid sensitive substrates.⁹³



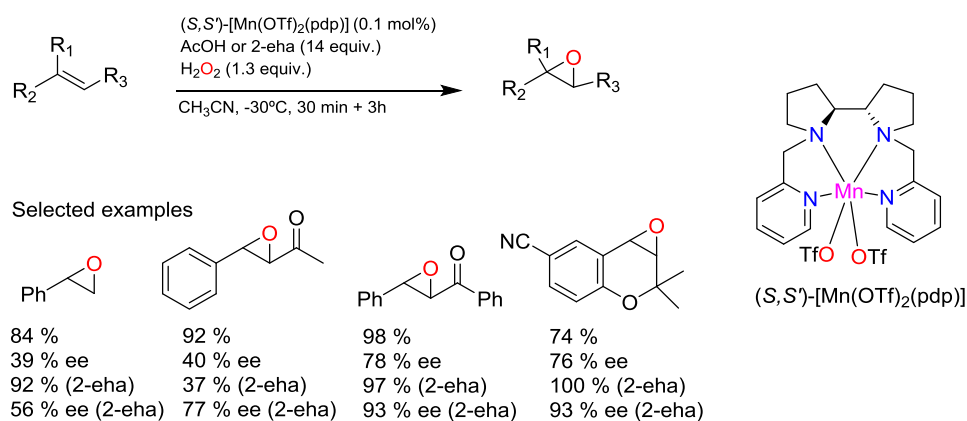
Scheme 20. Epoxidation reaction of different olefins with the [Mn(OTf)₂(Pytacn)] and [Mn(OTf)₂(mcp)] complexes, H₂O₂ and AcOH.

Wei Sun and co-workers employed the above described conditions to perform asymmetric epoxidation of olefins with H₂O₂ using a novel catalyst (*R,R,R,R'*)-[Mn(OTf)₂(bpmcp)] related to (*R,R'*)-[Mn(OTf)₂(mcp)], by introducing aromatic groups into the 2-pyridylmethyl pseudo-benzylic positions of the ligand. This modification in turn represented an extra chiral element closer to the chiral center.⁹⁴ The system epoxidizes substituted *trans*-chalcones with a maximum of 89% ee, but moderate stereoselectivities (30-50%) were accomplished for other substrates, such as styrene derivatives and *trans*-cinnamates (Scheme 21).



Scheme 21. Asymmetric epoxidation reaction of aromatic olefins with the (*R,R,R,R'*)-[Mn(OTf)₂(bpmcp)] complex, H₂O₂ and AcOH.

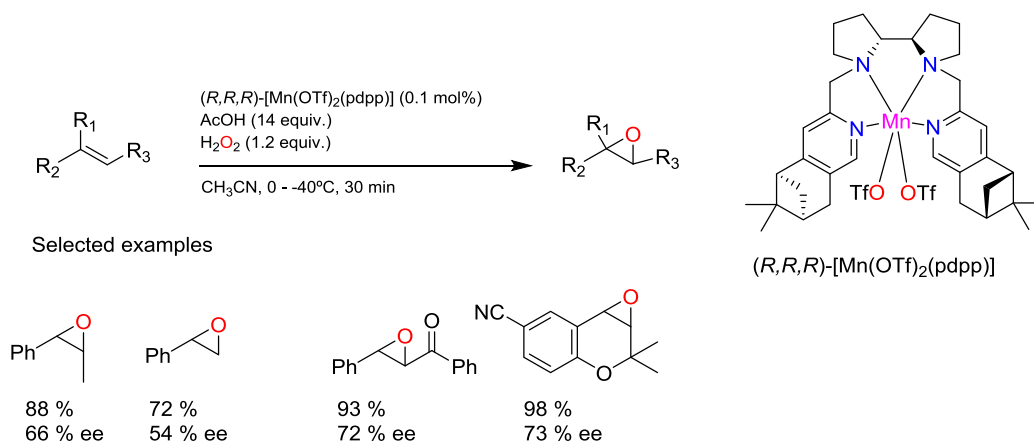
In 2011, Bryliakov and co-workers explored the activity and stereoselectivity of (S,S') -[Mn(OTf)₂(mcp)] and (S,S') -[Mn(OTf)₂(pdp)].⁹⁵ The authors showed that replacement of the cyclohexyldiamine by a bis-pyrrolidine backbone in the catalysts improved the corresponding activities and enantioselectivities in the epoxidation of most of the substrates tested. Also, two different oxidants, AcOOH and H₂O₂/AcOH were compared, observing that the activities and stereoselectivities were slightly higher in the case of AcOOH. The authors reasoned that although AcOOH seemed to perform slightly better, H₂O₂ is more attractive oxidant. In addition, different carboxylic acids were studied as potential alternatives to acetic acid in asymmetric epoxidation reactions with the (S,S') -[Mn(OTf)₂(pdp)] catalysts. In general, a remarkable improvement of stereoselectivities with regard to simple acetic acid is observed when bulky carboxylic acids are used. For instance, 2-ethylhexanoic acid gave around 37% ee improvement in the epoxidation of methyl *trans*-cinnamate and 17% ee for styrene (Scheme 22).⁵⁹ These results strongly suggest that carboxylic acids are part of the oxygen delivering species, presumably binding to the Mn center. The authors proposed these active species to be formulated as LMn^V(O)(OC(O)R), L = ligand, R = alkyl, analogous to the one proposed for iron.



Scheme 22. Asymmetric epoxidation reaction of aromatic and aliphatic olefins with the (S,S') -[Mn(OTf)₂(pdp)] complex, H₂O₂ and AcOH.

Following in the strategy initiated by Gómez et al, pinene groups were attached in positions 4 and 5 of the pyridine rings of the (S,S') -[Mn(OTf)₂(pdp)] complex to form $((R,R,R)$ -[Mn(OTf)₂(pdpp)]), and the complex was studied in asymmetric epoxidation.⁹⁶ The sum of the chirality of α -pinene groups with that of the

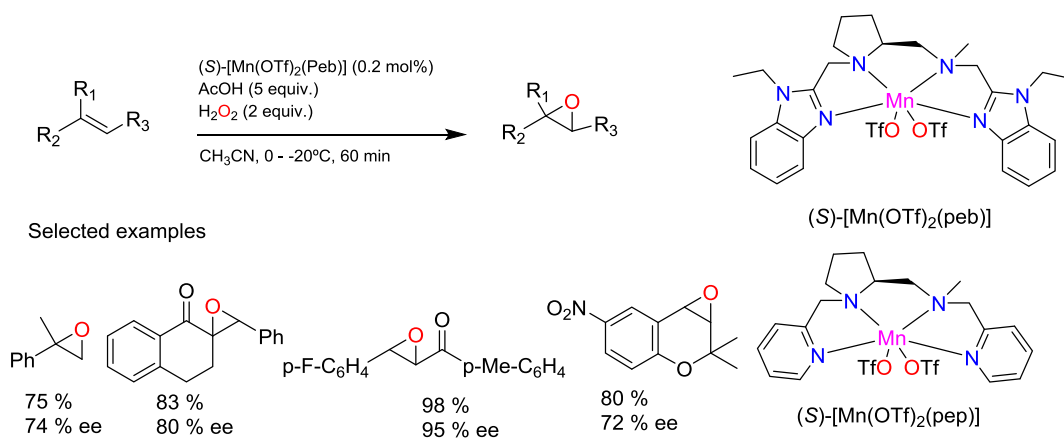
diamine backbone result in two diastereoisomeric species, that in turn give rise to chiral at the metal complexes (Λ and Δ). In the case of the Λ isomer, the CH_3 groups of the pinene rings are oriented towards the triflate groups, and in the case of Δ the opposite orientation was observed. The epoxidation was performed using H_2O_2 and acetic acid in CH_3CN at 0°C and/or -40°C . The direct comparison between the performance of the two diastereoisomeric complexes showed that Δ - (R,R,R) - $[\text{Mn}(\text{OTf})_2(\text{pdpp})]$ provided better stereoselectivities, while activities remained similar, for styrene and *cis*- β -methylstyrene epoxidation. Complex Δ - (R,R,R) - $[\text{Mn}(\text{OTf})_2(\text{pdpp})]$ was further tested in different olefins observing higher yields than the parent (R,R,R) - $[\text{Mn}(\text{OTf})_2(\text{pdp})]$ in all the cases. Different substitutions in *para*-position of styrenes such as nitro, methoxy and chloride groups were tolerated. Unfortunately, enantioselectivities were moderate (up to 54% ee, Scheme 23). Finally, the best result was obtained using electron-deficient chromenes, 98% of yield and 73 % of ee.



Scheme 23. Asymmetric epoxidation reaction of aromatic and aliphatic olefins with (R,R,R) - $[\text{Mn}(\text{OTf})_2(\text{pdpp})]$ complex, H_2O_2 and AcOH .

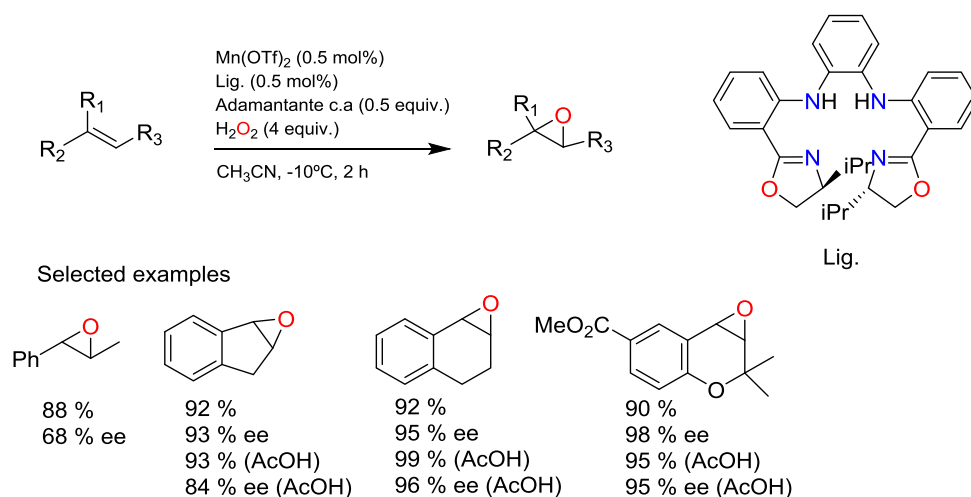
More recently, Wei Sun and co-workers developed a chiral manganese complex based on *L*-proline as ligand backbone. The backbone was attached to two pyridine groups to yield catalyst (S) - $[\text{Mn}(\text{OTf})_2(\text{pep})]$.⁹⁷ Asymmetric epoxidation was performed using H_2O_2 and acetic acid in CH_3CN at -20°C during 1 hour. Enantioselectivity for *trans*-chalcone was slightly lower in comparison with other backbones ($(1R, 2R)$ -1,2-dimethylcyclohexandiamine and $(2S,2'S)$ -2,2'-bipyrrolidine. However, in the same study Sun synthesized an analogous chiral manganese complex (S) - $[\text{Mn}(\text{OTf})_2(\text{peb})]$ where pyridine groups have been

replaced by benzoimidazole groups. Enantioselectivities for this complex increased up to 95 % ee for *trans*-chalcone and tetralone derivatives (Scheme 24).



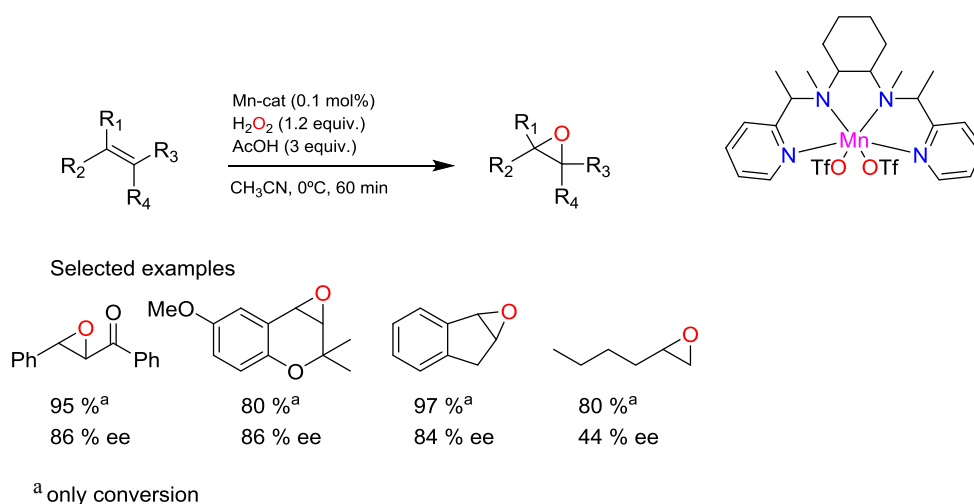
Scheme 24. Asymmetric epoxidation reaction of aromatic, aliphatic and terminal olefins with (S)-[Mn(OTf)₂(peb)] complex, H₂O₂ and AcOH.

A recent interesting discovery was reported by Gao and co-workers. They developed a set of new tetraaminodentate chiral porphyrin-inspired manganese complexes.⁹⁸ These new classes of catalysts were based in a tetradentate ligand with an aromatic 1,2-diamine site, and two oxazoline moieties as chiral source. The corresponding Mn catalysts were not isolated but generated in situ by mixing the ligand and Mn(OTf)₂ just before initiating the epoxidation reaction. The main advantages of these complex is the easily tunable ligand, due to the large number of amino acid sources available to make oxazolines. After testing a large set of ligands with different bulky groups, it was found that those containing iPr groups performed optimally. The catalytic system worked using H₂O₂ as oxidant and acetic acid as additive. After optimizing conditions, the authors obtained excellent isolated yields and enantioselectivities for electron-deficient chromenes, *trans*-stilbenes, indene and 1,2-dihydronaphthalene up to 99 % ee (Scheme 25). Moreover, competitive studies suggested the systems generate an electrophilic oxidant. Furthermore, Gao studied optimization of the reaction with different carboxylic acids and observed that adamantane-1-carboxylic acid improve the enantioselectivity.⁹⁹ Finally, this catalytic system can tolerate perfectly the presence of water, because performing the reaction in 1% of H₂O₂, activities and stereoselectivities remained unmodified. The work provided a new and interesting strategy for designing ligand-based catalysts.



Scheme 25. Manganese complex prepared in situ as catalyst for asymmetric epoxidation of aromatic olefins with H_2O_2 and adamantane carboxylic acid.

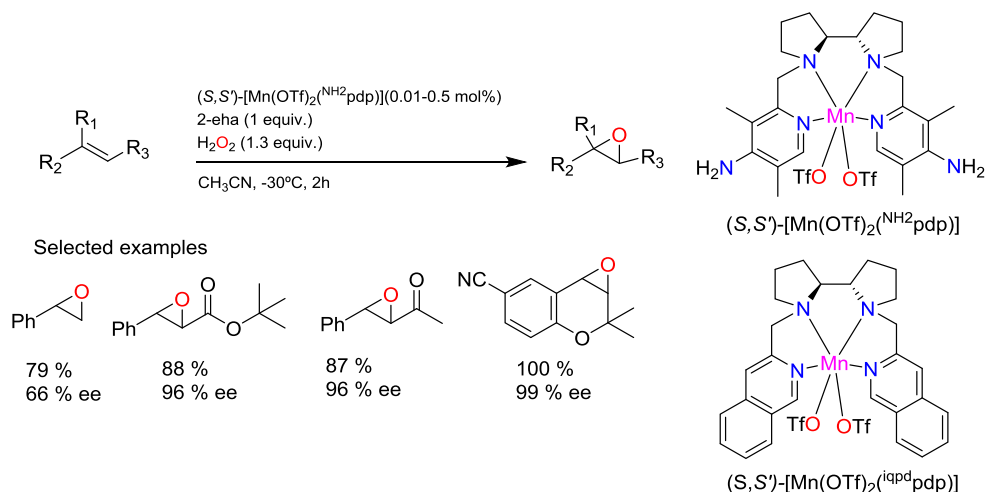
Suresh and co-workers developed a very simple, economical and recyclable manganese complex related to $[\text{Mn}(\text{OTf})_2(\text{mcp})]$ by adding methyl groups in pseudo-benzylic positions, following a similar strategy to that early reported by Sun.¹⁰⁰ The epoxidation was carried out with hydrogen peroxide and acetic acid in acetonitrile at 0°C during one hour. The outcome for *trans*-chalcones, indene and chromenes are good conversions and enantioselectivities (up to 99% and 86% ee, respectively, see Scheme 26). The relative stereochemistry of the diaminocyclohexane and pseudo-benzylic positions of the ligand was not determined by the authors.



Scheme 26. Asymmetric epoxidation of aromatic and aliphatic olefins with H_2O_2 and AcOH with the Suresh catalyst.

In 2015, Talsi and co-workers designed Mn complexes based on the (*S,S'*)- $[\text{Mn}(\text{OTf})_2(\text{pdp})]$ catalyst, where electronic and steric properties of the catalysts

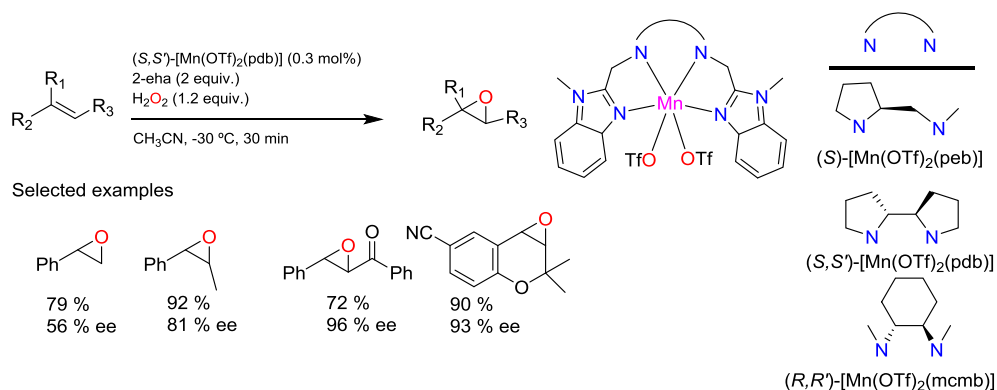
were systematically modified. This set of catalysts were very related to those previously studied by Costas and co-workers (see Chapter VI).¹⁰¹ The authors observed that the sterically demanding aromatic groups implemented in the pyridine rings of the catalysts didn't improve the performance with regard to the parent (S,S') -[Mn(OTf)₂(pdp)]. However, the complexes exhibited a systematic dependence between activity and stereoselectivity, with the electron-donating nature of the ligand, showing that electron-donating complexes achieved better activities and stereoselectivities on a broad substrate scope (Scheme 27). Additionally, the authors performed some mechanistic studies for the simple catalyst (S,S') -[Mn(OTf)₂(pdp)]; competitive oxidations of *para*-substituted *trans*-chalcones were performed, showing preferential oxidation of the more electron-rich substrate, demonstrating the electrophilic nature of the oxidant. Moreover, the authors reasoned that the transition state for the oxygen delivering step become more product-like as the ligand becomes more electron-donating. This translates into a closer substrate-catalyst interaction which justifies a more stereoselective oxygen atom transfer. Finally, the authors suggested that carbocationic intermediate is formed, because the epoxidation of *cis*-stilbene occurs with a partial erosion of stereochemistry, giving some amounts of *trans*-epoxides.



Scheme 27. Asymmetric epoxidation reaction of aromatic olefins with the (S,S') -[Mn(OTf)₂(^{NH2}pdp)] complex, H₂O₂ and 2-eha.

Most recently, Sun compared the complexes (S) -[Mn(OTf)₂(peb)] with the analogous complexes with different backbones ((1*R*,2*R*) 1,2-dimethylcyclohexandiamine and (2*S*,2*S'*)-2,2'-bipyrrolidine (Scheme 28).¹⁰² With

the optimal conditions in hand (1.2 equiv. of H_2O_2 , 2 equiv. of 2-ethylhexanoic acid), the authors tested the three catalysts using *cis*- β -methylstyrene as a model substrate, observing that the backbone (2*S*,2*S'*)-2,2'-bipyrrolidine gave better activities and stereoselectivities up to 81 %, however the best complex was limited in scope to *trans*-chalcone derivatives and electron deficient chromenes. Excellent yields and enantioselectivities were observed (up to 96 % ee, Scheme 28) for these substrates.



Scheme 28. Asymmetric epoxidations of aromatic and terminal olefins with different Mn complexes differing in the diamine backbone.

In Table 1 and Figure 5, a summary of manganese complexes used in asymmetric epoxidation is collected. Results for three different substrates are displayed, electron-deficient chromene, *trans*-chalcone and styrene.

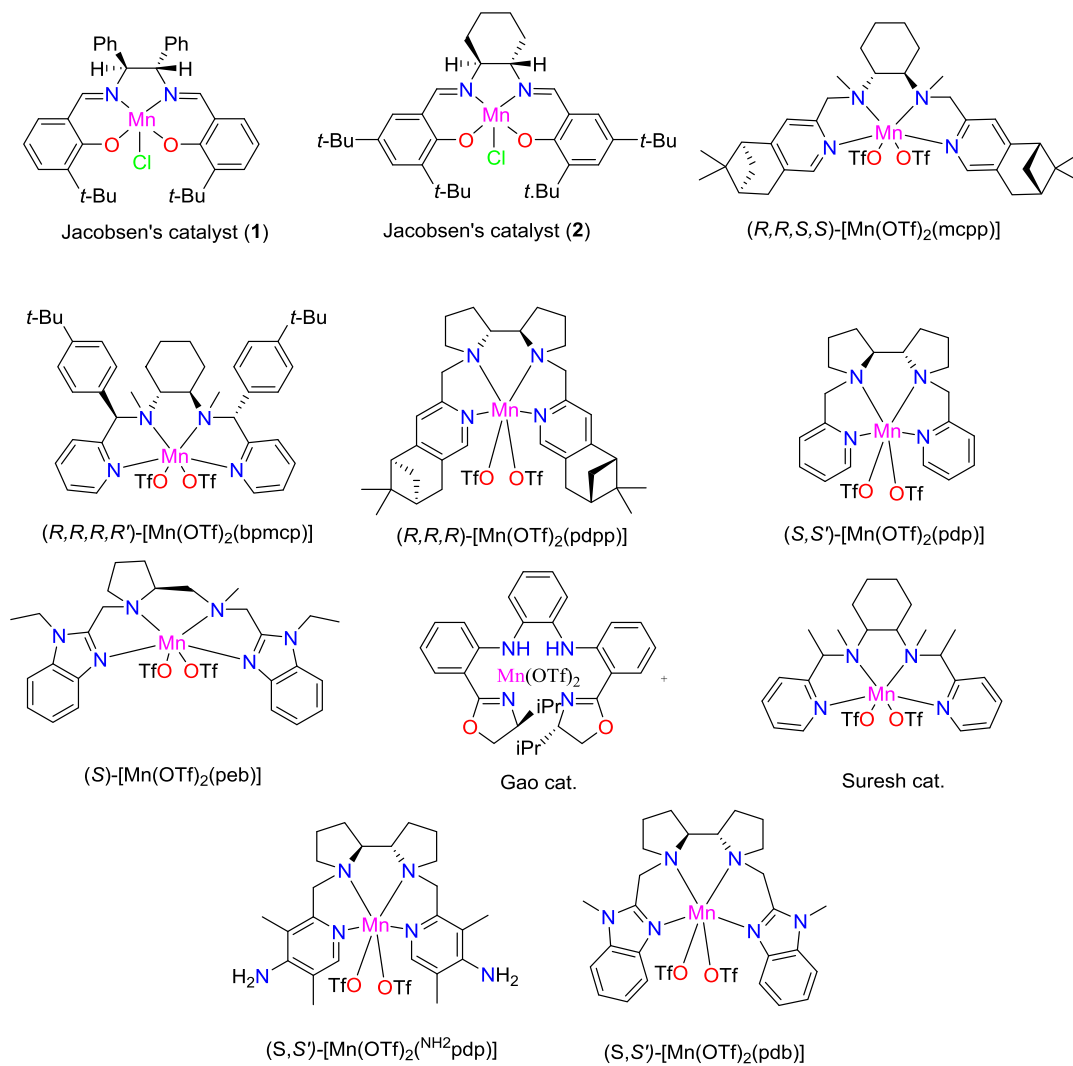
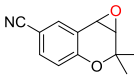
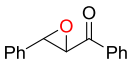
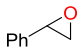


Figure 5. Examples of biologically inspired manganese complexes based in tetradentate aminopyridine ligands studied in asymmetric epoxidation reactions.

Table 1. Comparison of manganese complexes in the asymmetric epoxidation of three different substrates.

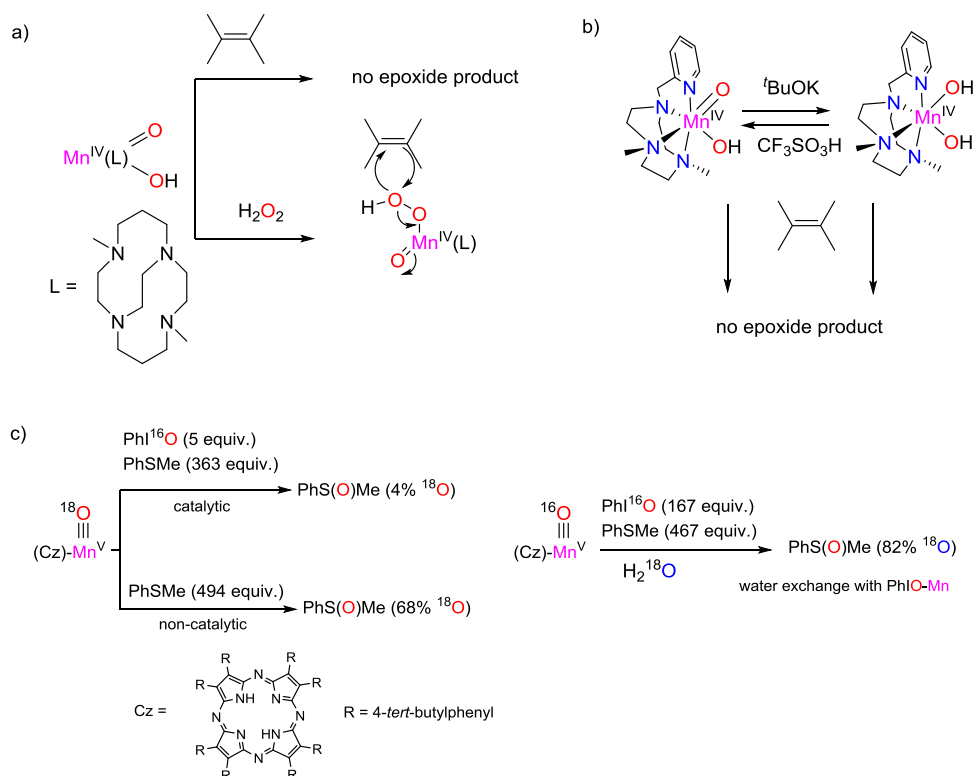
Cat.	Ox./ additive.							Ref
		yield (%)	ee (%)	yield (%)	ee (%)	yield (%)	ee (%)	
Mn-Salen (Jacobsen's cat)	NaOCl or PhIO	96 ^a	97 ^a	-	-	75 ^b	57 ^b	[75]
(<i>R,R,S,S</i>)- [Mn(OTf) ₂ (mcp)]	AcOOH/-	-	-	45	37	78	46	[92]
(<i>R,R,R,R'</i>)- [Mn(OTf) ₂ (bpmcp)]	H ₂ O ₂ / AcOH	62	63	91	78	85	43	[94]
(<i>R,R,R</i>)- [Mn(OTf) ₂ (pdpp)]	H ₂ O ₂ / AcOH	98	73	93	72	72	54	[96]
(<i>S,S'</i>)-[Mn(OTf) ₂ (pdp)]	H ₂ O ₂ / 2-eha	100	93	97	93	92	56	[95]
(<i>S</i>)-[Mn(OTf) ₂ (peb)]	H ₂ O ₂ / AcOH	80	79	93	92	-	-	[97]
Gao cat.	H ₂ O ₂ / AcOH	90 ^c	98 ^c	-	-	98	47	[98]
Suresh cat.	H ₂ O ₂ / AcOH	90	86	95	86	99	43	[100]
(<i>S,S'</i>)- Mn(OTf) ₂ (^{NH₂} pdp)]	H ₂ O ₂ / 2-eha	100	99	100	98	79	66	[101]
(<i>S,S'</i>)-[Mn(OTf) ₂ (pdb)]	H ₂ O ₂ / 2-eha	90	93	72	96	93	56	[102]

^aJacobsen catalyst (2) and NaOCl. ^bJacobsen catalyst (1) and PhIO. ^c Adamantane carboxylic acid instead of acetic acid.

I.5.2.1. Proposed mechanisms for bioinspired manganese complexes

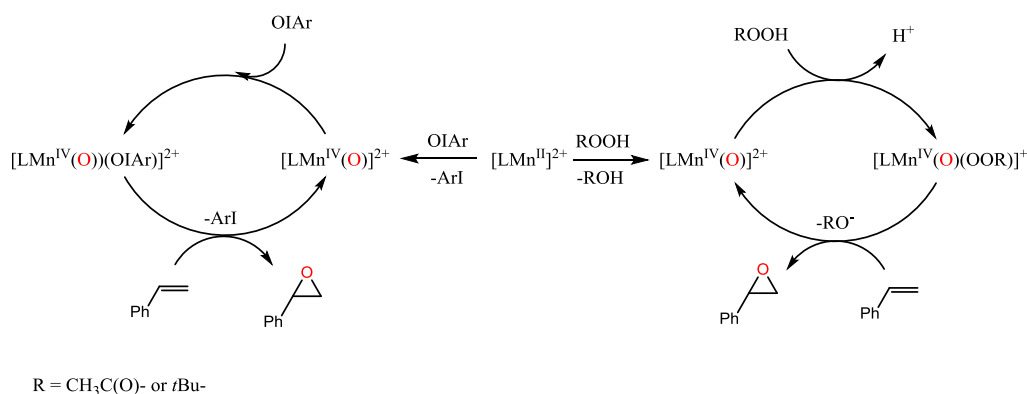
Two different possible mechanisms have been proposed for the epoxidation reactions catalyzed by mononuclear manganese complexes with tetradentate aminopyridine ligands. The first one involved Lewis acid activation of the oxidant by a manganese species. The second consider that oxygen atom transfer is performed by high valent $Mn^{IV}(O)$ or $Mn^V(O)$ species. Evidences in favor of both mechanisms are discussed in the following lines.

In first place, Busch¹⁰³ and Garcia-Bosch¹⁰⁴ demonstrated that $Mn^{IV}(O)(OH)$ complexes are not capable to transfer oxygen atoms to olefins (Scheme 29, a and b). Instead Busch proposed that a $Mn^{IV}(O)(OOH)^+$ complex is formed by exchange of a ligand between $Mn^{IV}(O)(OH)^+$ and H_2O_2 . The authors proposed that the Mn^{IV} ion activates the hydrogen peroxide, so an oxygen atom from hydrogen peroxide was transferred to the olefin. Related activation of an oxidant by a high valent Mn species was reported previously by Goldberg and co-workers who isolated $Mn^V(O)$ species with a corrazoline ligand.¹⁰⁵ This complex does not transfer the oxo group to a sulfide. However, after addition of $PhI^{16}O$ sulfoxidation reaction was observed, providing 96 % of ^{16}O -labelled product. (Scheme 29, c). This results suggests that the high valent manganese ion behaves as a Lewis acid, activating the $PhIO$ towards oxygen atom transfer to the substrate.



Scheme 29. a) Proposed active species for tetradentate amino manganese complex with hydrogen peroxide for epoxidation reaction. b) High valent manganese oxo-hydroxo and bis-hydroxo were inactive for epoxidation reaction. c) Labeling experiments demonstrated the Lewis acid activation of the iodosylbenzene, “third oxidant”.

Along the same vein, Bryliakov and co-workers suggested that similar active species are formed when acyl and alkyl hydroperoxides or iodosylarenes were used as oxidants. The proposed structures are likely $[\text{Mn}^{\text{IV}}(\text{O})(\text{OOAc})]^+$, $[\text{Mn}^{\text{IV}}(\text{O})(\text{OOAlk})]^+$ and $[\text{Mn}^{\text{IV}}(\text{O})(\text{OIAr})]^{2+}$, that transfer an oxygen atom from the oxidant, but not the oxo group, to the substrate (Scheme 30).¹⁰⁶



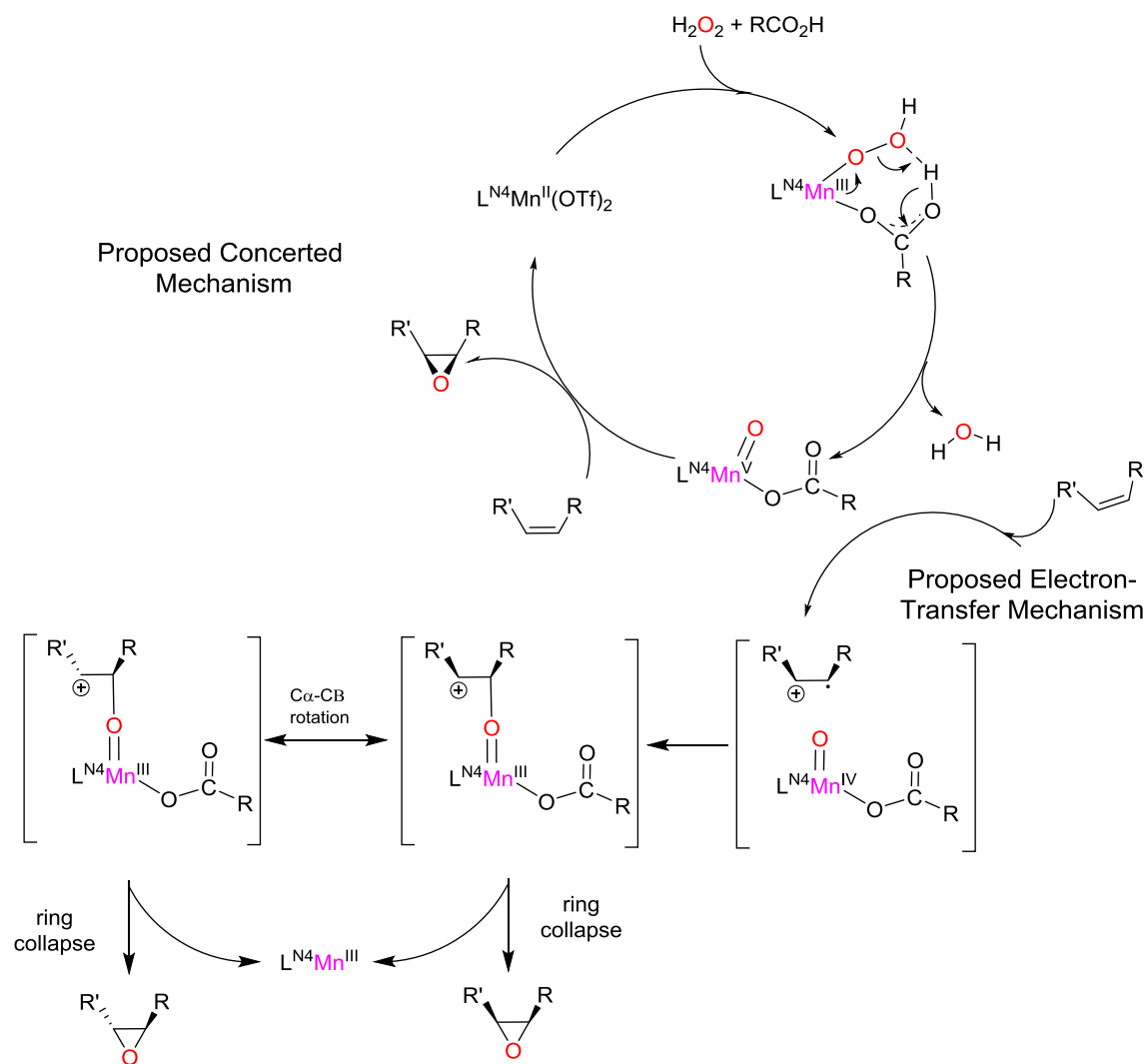
Scheme 30. Proposed catalytic cycle for the (S,S')-[Mn(OTf)₂(mcp)] with ArIO and acyl or alkyl hydroperoxides

Considering that acetic acid-assisted O-O bond lysis has also been proposed for analogous iron systems in the epoxidation reaction with H_2O_2 and acetic acid (see I.5.1.1.), Garcia-Bosch *et al.* carried out the epoxidation reaction with $[\text{Mn}(\text{OTf})_2(\text{H,MePytacn})]$ and $\text{H}_2^{18}\text{O}_2/\text{AcOH}$, showing that the peroxide is the main origin of the oxygen atoms incorporated into the products (92 % of $^{18}\text{O}_2$ incorporation).⁹³ This result is in agreement with the iron catalyzed oxidations, and suggested that either a Lewis acid activation takes place or alternatively, the Mn-oxo species, if formed, are too short-lived to exchange with water before substrate attack.

In contrast, further studies performed by Sun and co-workers suggested that high-valent manganese oxo species are a plausible active species, transferring the oxo ligand to the product.⁹⁷ For example, when catalyst $(S)\text{-}[\text{Mn}(\text{OTf})_2(\text{peb})]$ reacted with AcOOH , the corresponding epoxide showed 8.1 % incorporation of oxygen atom from labelled H_2^{18}O , suggesting the implication of a high valent Mn(O) species, that could undergo exchange of the oxygen atom with water before transferring to the substrate.

Most recently, Bryliakov and co-workers studied the mechanisms of catalyst $(S,S')\text{-}[\text{Mn}(\text{OTf})_2(\text{pdp})]$ in epoxidations with hydrogen peroxide, acetic acid and H_2^{18}O .¹⁰¹ These experiments showed that ^{18}O was not incorporated into the products. However, they observed that the catalyst with electron-donating groups ($(S,S')\text{-}[\text{Mn}(\text{OTf})_2(\text{d}^{\text{MM}}\text{pdp})]$ complex) provides oxidation products (albeit in modest yields) in the absence of a carboxylic acid. The mechanism in the absence of carboxylic acid could be then investigated. It was found that the active species originating from catalyst $(S,S')\text{-}[\text{Mn}(\text{OTf})_2(\text{d}^{\text{MM}}\text{pdp})]$ did exchange with H_2^{18}O , yielding a 35% ^{18}O -enriched styrene epoxide. The degree of ^{18}O incorporation is therefore governed by a competition between the epoxidation and the tautomeric oxo-hydroxo exchange with external water molecules. The 1,2 diol was obtained with 86 % of ^{18}O -labeled atoms (without $^{18}\text{O}^{18}\text{O}$ -diol), indicating that one of the oxygen atom comes from water rather than from H_2O_2 . Finally, with the catalyst $(S,S')\text{-}[\text{Mn}(\text{OTf})_2(\text{pdp})]$ stereoscrumbling was observed in the epoxidation of *cis*-stilbene with H_2O_2 in the presence of acetic acid, suggesting a formation of carbocationic intermediates (Scheme 31). The sum of these experimental observations lead to the proposal of the mechanism shown

in Scheme 30, where a high valent Mn-oxo species performed an electrophilic attack over the olefinic site. Then, formation of the two C-O bonds is sequential and involves an initial formation of a carbocationic intermediate.



Scheme 31. Proposed mechanism for epoxidation of tetradentate aminopyridine manganese complexes with H_2O_2 and AcOH reported by Talsi and co-workers.

I.6 REFERENCES

- (1) Katsuki, T. In *Catalytic Asymmetric Synthesis*; 2nd ed.; Ojima, I., Ed.; Wiley-VCH: New York, 2000, p 287.
- (2) De Faveri, G.; Ilyashenko, G.; Watkinson, M. *Chem. Soc. Rev.* **2011**, *40*, 1722.
- (3) Chatterjee, D. *Coord. Chem. Rev.* **2008**, *252*, 176.
- (4) Wong, O. A.; Shi, Y. *Chem. Rev.* **2008**, *108*, 3958.
- (5) David, D.; Marta, G. N.; Ana, B. A.; Garcia, P.; Moro, R. F.; Garrido, N. M.; Isidro, S. M.; Basabe, P.; Julio, G. U. *Current Organic Synthesis* **2008**, *5*, 186.
- (6) Zhu, Y.; Wang, Q.; Cornwall, R. G.; Shi, Y. *Chem. Rev.* **2014**, *114*, 8199.
- (7) Davis, R. L.; Stiller, J.; Naicker, T.; Jiang, H.; Jørgensen, K. A. *Angew. Chem. Int. Ed.* **2014**, *53*, 7406.
- (8) Bertini, I.; Gray, H. B.; Stiefel, E. I.; Valentine, S. J. *Biological inorganic Chemistry: structure & reactivity*; University Science Books: Sausalito, California, 2007.
- (9) Montellano, P. O. d. *Cytochrome P450 : Structure, Mechanism, and Biochemistry*; 3rd ed.; Springer ed.: New York, 2005.
- (10) Meunier, B.; Bernadou, J. *Struct. Bonding* **2000**, *97*, 1.
- (11) Meunier, B.; de Visser, S. P.; Shaik, S. *Chem. Rev.* **2004**, *104*, 3947.
- (12) Schlichting, I.; Berendzen, J.; Chu, K.; Stock, A. M.; Maves, S. A.; Benson, D. E.; Sweet, R. M.; Ringe, D.; Petsko, G. A.; Sligar, S. G. *Science* **2000**, *287*, 1615.
- (13) Groves, J. T.; McCluskey, G. A. *J. Am. Chem. Soc.* **1976**, *98*, 859.
- (14) Sono, M.; Roach, M. P.; Coulter, E. D.; Dawson, J. H. *Chem. Rev.* **1996**, *96*, 2841.
- (15) Rittle, J.; Green, M. T. *Science* **2010**, *330*, 933.
- (16) Ortiz de Montellano, P. R. *Chem. Rev.* **2010**, *110*, 932.
- (17) Shaik, S.; Lai, W.; Chen, H.; Wang, Y. *Acc. Chem. Res.* **2010**, *43*, 1154.
- (18) Wang, X.; Peter, S.; Kinne, M.; Hofrichter, M.; Groves, J. T. *J. Am. Chem. Soc.* **2012**, *134*, 12897.
- (19) Meunier, B.; Bernadou, J. *Topics in Catalysis* **2002**, *21*, 47.
- (20) Gibson, D. T.; Resnick, S. M.; Lee, K.; Brand, J. M.; Torok, D. S.; Wackett, L. P.; Schocken, M. J.; Haigler, B. E. *J. Bacteriol.* **1995**, *177*, 2615.
- (21) Bruijninx, P. C. A.; van Koten, G.; Klein Gebbink, R. J. M. *Chem. Soc. Rev.* **2008**, *37*, 2716.
- (22) Wolfe, M. D.; Parales, J. V.; Gibson, D. T.; Lipscomb, J. D. *J. Biol. Chem.* **2001**, *276*, 1945.
- (23) Koehntop, K., D.; Emerson, J. P.; Que Jr., L. *J. Biol. Inorg. Chem.* **2005**, *10*, 87.
- (24) Kauppi, B.; Lee, K.; Carredano, E.; Parales, R. E.; Gibson, D. T.; Eklund, H.; Ramaswamy, S. *Structure* **1998**, *6*, 571.
- (25) Karlsson, A.; Parales, J. V.; Parales, R. E.; Gibson, D. T.; Eklund, H.; Ramaswamy, S. *Science* **2003**, *299*, 1039.
- (26) Wolfe, M. D.; Altier, D. J.; Stubna, A.; Popescu, C. V.; Münck, E.; Lipscomb, J. D. *Biochemistry* **2002**, *41*, 9611.

- (27) Wolfe, M. D.; Lipscomb, J. D. *J. Biol. Chem.* **2003**, *278*, 829.
- (28) Wu, A. J.; Penner-Hahn, J. E.; Pecoraro, V. L. *Chem. Rev.* **2004**, *104*, 903.
- (29) Yachandra, V. K.; Sauer, K.; Klein, M. P. *Chem. Rev.* **1996**, *96*, 2927.
- (30) Wilcox, D. E. *Chem. Rev.* **1996**, *96*, 2435.
- (31) Cotton, F. A.; Wilkinson, G.; Murillo, C. A.; Bochmann, M. In *Adv. Inorg. Chem.* 6th ed.; John Wiley & Sons: New York, 1999.
- (32) Umena, Y.; Kawakami, K.; Shen, J.-R.; Kamiya, N. *Nature* **2011**, *473*, 55.
- (33) Yano, J.; Kern, J.; Sauer, K.; Latimer, M. J.; Pushkar, Y.; Biesiadka, J.; Loll, B.; Saenger, W.; Messinger, J.; Zouni, A.; Yachandra, V. K. *Science* **2006**, *314*, 821.
- (34) Costas, M.; Mehn, M. P.; Jensen, M. P.; Que, L., Jr. *Chem. Rev.* **2004**, *104*, 939.
- (35) Sheldon, R. A. In *Biomimetic Oxidations Catalyzed by Transition Metal Complexes*; Meunier, B., Ed.; Imperial College Press: London, 2000, p 613.
- (36) Gopalaiiah, K. *Chem. Rev.* **2013**, *113*, 3248.
- (37) Oloo, W. N.; Que, L. *Acc. Chem. Res.* **2015**, *48*, 2612.
- (38) Talsi, E. P.; Bryliakov, K. P. *Coord. Chem. Rev.* **2012**, *256*, 1418.
- (39) Gelalcha, F. G. *Adv. Synth. Catal.* **2014**, *356*, 261.
- (40) Fingerhut, A.; Serdyuk, O. V.; Tsogoeva, S. B. *Green Chem.* **2015**, *17*, 2042.
- (41) Krishnan, K. K.; Thomas, A. M.; Sindhu, K. S.; Anilkumar, G. *Tetrahedron* **2016**, *72*, 1.
- (42) Groves, J. T.; Nemo, T. E.; Myers, R. S. *J. Am. Chem. Soc.* **1979**, *101*, 1032.
- (43) Chang, C. K.; Ebina, F. *J. Chem. Soc., Chem. Comm.* **1981**, 778.
- (44) Lindsay Smith, J. R.; Reginato, G. *Org. Biomol. Chem.* **2003**, *1*, 2543.
- (45) Maux, P. L.; Srour, H. F.; Simonneaux, G. *Tetrahedron* **2012**, *68*, 5824.
- (46) Rose, E.; Ren, Q.-Z.; Andrioletti, B. *Chem.–Eur. J.* **2004**, *10*, 224.
- (47) Ren, Q.; Hou, Z.; Zhang, H.; Wang, A.; Liu, S. *J. Porphyr. and Phthalocyanines* **2009**, *13*, 1214.
- (48) White, M. C.; Doyle, A. G.; Jacobsen, E. N. *J. Am. Chem. Soc.* **2001**, *123*, 7194.
- (49) Gelalcha, F. G.; Bitterlich, B.; Schröder, K.; Copinathan, A.; Tse, M. K.; Beller, M. *Angew. Chem. Int. Ed.* **2007**, 7293.
- (50) Marchi-Delapierre, C.; Jorge-Robin, A.; Thibon, A.; Ménage, S. *Chem. Commun.* **2007**, 1166.
- (51) Yeung, H.-L.; Sham, K.-C.; Tsang, C.-S.; Lau, T.-C.; Kwong, H.-L. *Chem. Commun.* **2008**, 3801.
- (52) Wu, M.; Miao, C.-X.; Wang, S.; Hu, X.; Xia, C.; Kühn, F. E.; Sun, W. *Advanced Synthesis & Catalysis* **2011**, *353*, 3014.
- (53) Costas, M.; Tipton, A. K.; Chen, K.; Jo, D.-H.; Que, L. *J. Am. Chem. Soc.* **2001**, *123*, 6722.
- (54) Wang, B.; Wang, S.; Xia, C.; Sun, W. *Chem.–Eur. J.* **2012**, *18*, 7332.
- (55) Wang, X.; Miao, C.; Wang, S.; Xia, C.; Sun, W. *ChemCatChem* **2013**, *5*, 2489.
- (56) Nishikawa, Y.; Yamamoto, H. *J. Am. Chem. Soc.* **2011**, *133*, 8432.

- (57) Luo, L.; Yamamoto, H. *Eur. J. Org. Chem.* **2014**, 2014, 7803..
- (58) Chen, M. S.; White, M. C. *Science* **2007**, 318, 783.
- (59) Lyakin, O. Y.; Ottenbacher, R. V.; Bryliakov, K. P.; Talsi, E. P. *Acs Catal.* **2012**, 2, 1196.
- (60) Niwa, T.; Nakada, M. *J. Am. Chem. Soc.* **2012**, 134, 13538.
- (61) Dai, W.; Li, G.; Chen, B.; Wang, L.; Gao, S. *Org. Lett.* **2015**, 17, 904.
- (62) Mas-Balleste, R.; Que, L., Jr. *J. Am. Chem. Soc.* **2007**, 129, 15964.
- (63) Mas-Balleste, R.; Fujita, M.; Que, L. *Dalton Trans.* **2008**, 1828.
- (64) Oloo, W. N.; Meier, K. K.; Wang, Y.; Shaik, S.; Muenck, E.; Que, L. *Nature Commun.* **2014**, 5.
- (65) Makhlynets, O. V.; Oloo, W. N.; Moroz, Y. S.; Belaya, I. G.; Palluccio, T. D.; Filatov, A. S.; Mueller, P.; Cranswick, M. A.; Que, L., Jr.; Rybak-Akimova, E. V. *Chem. Comm.* **2014**, 50, 645.
- (66) Lyakin, O. Y.; Zima, A. M.; Samsonenko, D. G.; Bryliakov, K. P.; Talsi, E. P. *ACS Catal.* **2015**, 5, 2702.
- (67) Groves, J. T.; Kruper, W. J.; Haushalter, R. C. *J. Am. Chem. Soc.* **1980**, 102, 6375.
- (68) Gonsalves, A. M. d. A. R.; Pereira, M. M. *J. Mol. Catal. A-Chem.* **1996**, 113, 209.
- (69) Groves, J. T.; Viski, P. *J. Org. Chem.* **1990**, 55, 3628.
- (70) Halterman, R. L.; Jan, S. T. *J. Org. Chem.* **1991**, 56, 5253.
- (71) O'Malley, S.; Kodadek, T. *J. Am. Chem. Soc.* **1989**, 111, 9116.
- (72) Pérollier, C.; Pécaut, J.; Ramasseul, R.; Marchon, J.-C. *Inorg. Chem.* **1999**, 38, 3758.
- (73) Srour, H.; Maux, P. L.; Simonneaux, G. *Inorg. Chem.* **2012**, 51, 5850.
- (74) Vilain-Deshayes, S.; Robert, A.; Maillard, P.; Meunier, B.; Momenteau, M. *J. Mol. Catal. A:-Chem.* **1996**, 113, 23.
- (75) Zhang, W.; Loebach, J. L.; Wilson, S. R.; Jacobsen, E. N. *J. Am. Chem. Soc.* **1990**, 112, 2801.
- (76) Irie, R.; Noda, K.; Ito, Y.; Matsumoto, N.; Katsuki, T. *Tetrahedron: Asymmetry* **1991**, 2, 481.
- (77) Katsuki, T.; Sharpless, K. B. *J. Am. Chem. Soc.* **1980**, 102, 5974.
- (78) Juliá, S.; Masana, J.; Vega, J. C. *Angew. Chem. Int. Ed. Eng* **1980**, 19, 929.
- (79) Jacobsen, E. N.; Zhang, W.; Muci, A. R.; Ecker, J. R.; Deng, L. *J. Am. Chem. Soc.* **1991**, 113, 7063.
- (80) Jacobsen, E. N.; Deng, L.; Furukawa, Y.; Martínez, L. E. *Tetrahedron* **1994**, 50, 4323.
- (81) Chang, S.; Galvin, J. M.; Jacobsen, E. N. *J. Am. Chem. Soc.* **1994**, 116, 6937.
- (82) Brandes, B. D.; Jacobsen, E. N. *J. Org. Chem.* **1994**, 59, 4378.
- (83) Brandes, B. D.; Jacobsen, E. N. *Tetrahedron Lett.* **1995**, 36, 5123.
- (84) Chang, S.; Heid, R. M.; Jacobsen, E. N. *Tetrahedron Lett.* **1994**, 35, 669.

- (85) Palucki, M.; Pospisil, P. J.; Zhang, W.; Jacobsen, E. N. *J. Am. Chem. Soc.* **1994**, *116*, 9333.
- (86) Palucki, M.; McCormick, G. J.; Jacobsen, E. N. *Tetrahedron Lett.* **1995**, *36*, 5457.
- (87) Shitama, H.; Katsuki, T. *Tetrahedron Lett.* **2006**, *47*, 3203.
- (88) Palucki, M.; Finney, N. S.; Pospisil, O. J.; Güler, M. L.; Ishida, T. T.; Jacobsen, E. N. *J. Am. Chem. Soc.* **1998**, *120*, 948.
- (89) Cavallo, L.; Jacobsen, H. *J. Org. Chem.* **2003**, *68*, 6202.
- (90) Murphy, A.; Dubois, G.; Stack, T. D. P. *J. Am. Chem. Soc.* **2003**, *125*, 5250.
- (91) Costas, M.; Tipton, A. K.; Chen, K.; Jo, D.-H.; Que Jr., L. *J. Am. Chem. Soc.* **2001**, *123*, 6722.
- (92) Gómez, L.; Garcia-Bosch, I.; Company, A.; Sala, X.; Fontrodona, X.; Ribas, X.; Costas, M. *Dalton Trans.* **2007**, 5539.
- (93) Garcia-Bosch, I.; Ribas, X.; Costas, M. *Adv. Synth. Catal.* **2009**, *351*, 348.
- (94) Wu, M.; Wang, B.; Wang, S.; Xia, C.; Sun, W. *Org. Lett.* **2009**, *11*, 3622.
- (95) Ottenbacher, R. V.; Bryliakov, K. P.; Talsi, E. P. *Adv. Synth. Catal.* **2011**, *353*, 885.
- (96) Garcia-Bosch, I.; Gómez, L.; Polo, A.; Ribas, X.; Costas, M. *Adv. Synth. Catal.* **2012**, *354*, 65.
- (97) Wang, B.; Miao, C.; Wang, S.; Xia, C.; Sun, W. *Chem.-Eur. J.* **2012**, *18*, 6750.
- (98) Dai, W.; Li, J.; Li, G.; Yang, H.; Wang, L.; Gao, S. *Org. Lett.* **2013**, *15*, 4138.
- (99) Dai, W.; Shang, S.; Chen, B.; Li, G.; Wang, L.; Ren, L.; Gao, S. *J. Org. Chem.* **2014**, *79*, 6688.
- (100) Maity, N. C.; Kumar Bera, P.; Ghosh, D.; Abdi, S. H. R.; Kureshy, R. I.; Khan, N.-u. H.; Bajaj, H. C.; Suresh, E. *Catal. Sci. Technol.* **2014**, *4*, 208.
- (101) Ottenbacher, R. V.; Samsonenko, D. G.; Talsi, E. P.; Bryliakov, K. P. *ACS Catal.* **2014**, *4*, 1599.
- (102) Shen, D.; Miao, C.; Wang, S.; Xia, C.; Sun, W. *Eur. J. Inorg. Chem.* **2014**, *2014*, 5777.
- (103) Yin, G.; Buchalova, M.; Danby, A. M.; Perkins, C. M.; Kitko, D.; Carter, J. D.; Scheper, W. M.; Busch, D. H. *J. Am. Chem. Soc.* **2005**, *127*, 17170.
- (104) Garcia-Bosch, I.; Company, A.; Cady, C. W.; Styring, S.; Browne, W. R.; Ribas, X.; Costas, M. *Angew. Chem. Int. Ed.* **2011**, *50*, 5648.
- (105) Wang, S. H.; Mandimutsira, B. S.; Todd, R.; Ramdhanie, B.; Fox, J. P.; Goldberg, D. P. *J. Am. Chem. Soc.* **2004**, *126*, 18.
- (106) Ottenbacher, R. V.; Bryliakov, K. P.; Talsi, E. P. *Inorg. Chem.* **2010**, *4*, 8620.

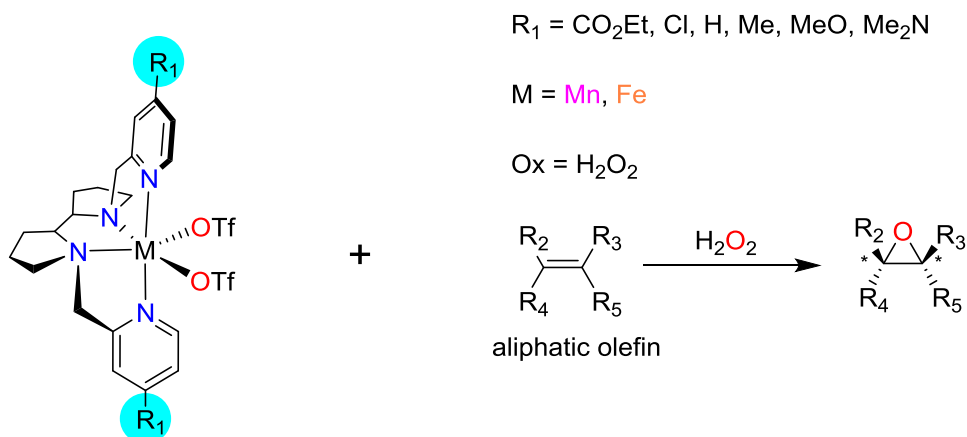
Chapter II

Main objectives

CHAPTER II. MAIN OBJECTIVES

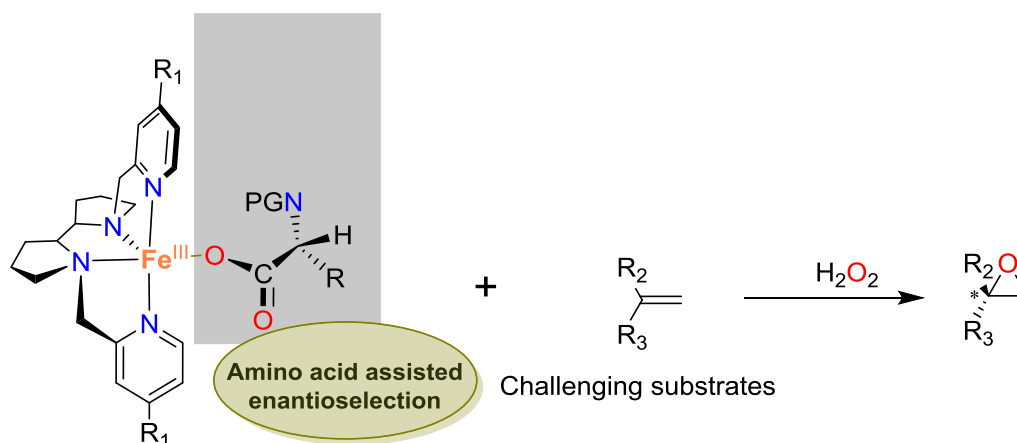
Metalloenzymes devoted to the oxidation of substances can overcome the limitations found in oxidation protocols in conventional organic synthesis, since they can perform oxidation processes in a highly effective and selective manner. For this reason, small molecule catalysts capable to operate like metalloenzymes may open novel synthetic strategies for oxidation catalysis. Inspired by the excellent efficiency, selectivity and soft conditions of oxidation reactions that take place in nature and are catalyzed by metalloenzymes, such as Cyt P450, herein we target the development of biologically inspired iron and manganese coordination complexes as oxidation catalysts. Two strategies for designing selective oxidation reactions have been pursued in this thesis.

The first strategy that we have developed consists in investigating iron and manganese chiral complexes as potential catalysts in asymmetric epoxidation reactions (Scheme 32). To design these catalysts, we take as starting point the simple tetradentate N-based ligands, whose iron and manganese complexes have been previously described in the literature. In particular, we focused in the bis-pyrrolidine based system (pdp) for which iron and manganese complexes have proven active in alkane oxidation and epoxidation reactions. The development of new catalysts is extended by tuning the electronic properties of the ligands, using different electron-withdrawing and electron-rich groups in the position 4th of the pyridine ring. The catalytic performance of the resulting iron and manganese complexes will be tested on a broad substrate scope of different olefins employing H₂O₂ as oxidant. Moreover, the mechanism of epoxidation will be examined in order to gain insight in the active species responsible for the catalysis. Finally, it was envisioned that the study will provide directions for future rational design of catalysts.



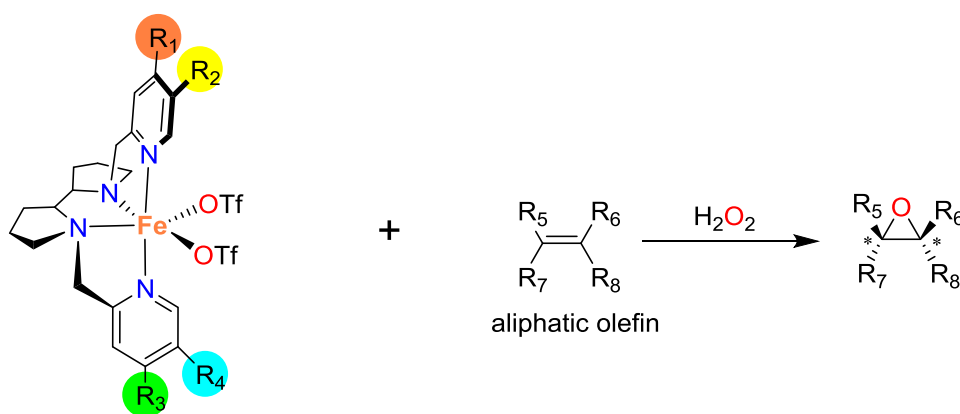
Scheme 32. Design of different iron and manganese complexes for asymmetric epoxidation.

The second strategy pursued will be to explore the possibility of controlling the stereoselectivity of the epoxidation reaction by using different amino acid moieties. This strategy, if successful, will allow improvement of the system, hopefully increasing substrate scope, but avoiding tedious modifications of the catalyst (Scheme 33). The main idea of this objective regards to mimic natural enzymes where amino acid chains play a key role in defining activity and stereoselectivity. One of the main objectives of this strategy is to epoxidize challenging olefins that to date have not given satisfactory results with other chiral epoxidizing agents.



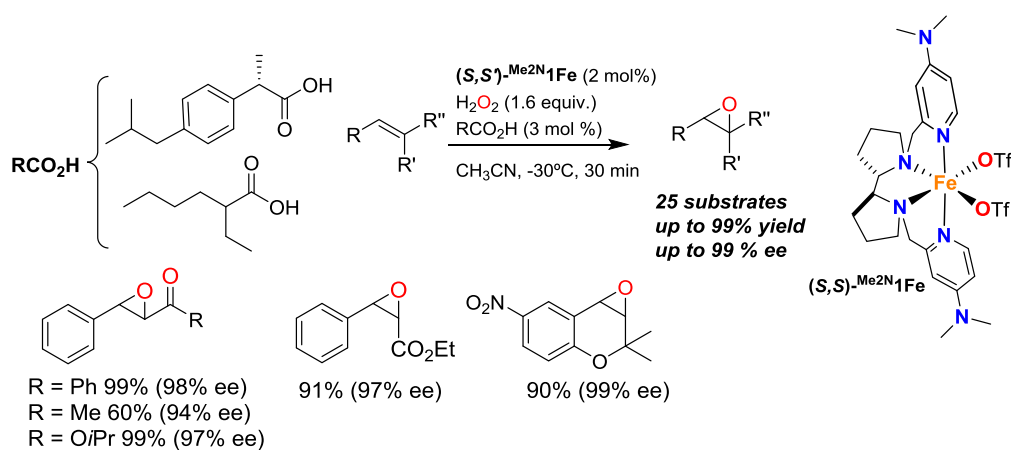
Scheme 33. Epoxidation of terminal olefins with iron complexes and amino acids as additives.

Finally, the third strategy will be to develop new tetradentate N-based C_1 symmetric iron complexes with distinct pyridines, combining different electronic and steric properties (Scheme 34). In particular, we focused in the bis-pyrrolidine based system (pdp) as first strategy. The main objective of this strategy is to epoxidize aliphatic olefins, one of the most challenging substrates in asymmetric catalysis. Also, the iron complexes will be tested in polyenes. Finally, it is envisioned that the development of C_1 -symmetric Fe complexes will provide a novel strategy in the design of stereoselective catalysts.



Scheme 34. Synthesis of different C_1 symmetric iron complexes for asymmetric epoxidation.

Asymmetric Epoxidation with H₂O₂ by Manipulating the Electronic Properties of Nonheme Iron Catalysts



This chapter corresponds to the following publication:

Cussó, O.; Garcia-Bosch, I.; Ribas, X.; Lloret-Fillol J.; Costas, M. *J. Am. Chem. Soc.*, 2013, **135**, 14871.

Reproduced with permission from Cussó O.; Garcia-Bosch, I.; Ribas, X.; Lloret-Fillol, J.; Costas, M.
“Asymmetric Epoxidation with H₂O₂ by Manipulating the Electronic Properties of Non-heme Iron Catalysts”. *Journal of American Chemical Association*, num. 135, issue 39 (2013) : 14871-14878

<http://dx.doi.org/10.1021/ja4078446>

Copyright © 2013 American Chemical Society

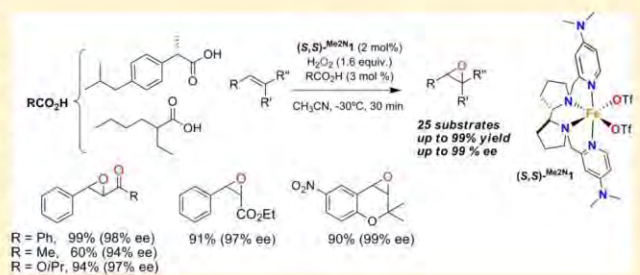
Asymmetric Epoxidation with H₂O₂ by Manipulating the Electronic Properties of Non-heme Iron Catalysts

Olaf Cussó, Isaac Garcia-Bosch, Xavi Ribas, Julio Lloret-Fillol, and Miquel Costas*

QBIS ResearchGroup, Institut de Química Computacional i Catàlisi (IQCC) and Departament de Química, Universitat de Girona, Campus Montilivi, Girona E-17071, Catalonia, Spain

S Supporting Information

ABSTRACT: A non-heme iron complex that catalyzes highly enantioselective epoxidation of olefins with H₂O₂ is described. Improvement of enantiomeric excesses is attained by the use of catalytic amounts of carboxylic acid additives. Electronic effects imposed by the ligand on the iron center are shown to synergistically cooperate with catalytic amounts of carboxylic acids in promoting efficient O–O cleavage and creating highly chemo- and enantioselective epoxidizing species which provide a broad range of epoxides in synthetically valuable yields and short reaction times.



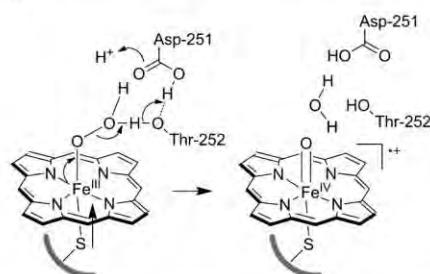
INTRODUCTION

Inspired by oxidations taking place at oxygenases, the combination of iron-based catalysts and hydrogen peroxide is an attractive approach for developing oxidation methods because of availability, low cost, and low toxicity considerations.¹ A particularly appealing transformation for this strategy is asymmetric epoxidation due to its pivotal role in modern organic synthesis.² Given its importance, asymmetric epoxidation has been actively pursued, and some excellent metal-based catalytic methods are well established.^{2a–c} However, iron-catalyzed asymmetric epoxidations that employ H₂O₂ and provide product yields and stereoselectivities amenable for preparative purposes remain scarce and limited in substrate scope, mainly because of the intrinsic complexities of Fe–H₂O₂ reactions.^{1f,g,3–5} While mononuclear iron (hydro)peroxide species are common intermediates in heme and non-heme oxygenases,^{6,7} in the absence of the elaborate machinery provided by enzymatic sites, the rich redox chemistry of iron and hydrogen peroxide poses serious problems for controlling the crucial O–O bond cleavage event. Basic concepts and strategies need to be developed for mastering this reaction such that metal-based oxidants susceptible to engage in selective oxygen atom transfer reactions are generated, thus avoiding Fenton-type processes and nonproductive peroxide disproportionation reactions. As a matter of fact, two recent reports of iron catalyzed asymmetric epoxidation bypass this problem by using peracetic acid and iododisylbenzene as alternative oxidants.⁵

Cytochromes P450 (Cyt-P450) constitute a paradigmatic example where the powerful electron-donating properties of the apical thiolate and the H-accepting character of a nearby threonine residue assist the O–O cleavage step of ferric hydroperoxide species via the so-called “push–pull” effect (Scheme 1).⁷ In addition, the dianionic and redox noninnocent

nature of the porphyrin ligand alleviates positive charge from the iron center and provides stabilization of the high valent ferryl species (compound I) responsible for substrate oxidation.

Scheme 1. Schematic Diagram of the Push–Pull Effect in Assisting O–O Breakage in P450 To Form Ferryl Species Compound I



Herein we show that electronic effects resembling those operating in Cyt-P450 can be used to design excellent non-heme iron epoxidation catalysts that make an efficient use of H₂O₂ to afford epoxides with excellent yields and enantioselectivities in short reaction times. Synergistic operation of metal, a powerful electron-donating ligand, and a carboxylic acid co-ligand allows an efficient heterolytic O–O bond cleavage and relative stabilization of the electrophilic high-valent iron–oxo species, finally leading to stereoselective oxygen atom transfer. Useful insight for further catalyst development and expansion of substrate scope is disclosed.

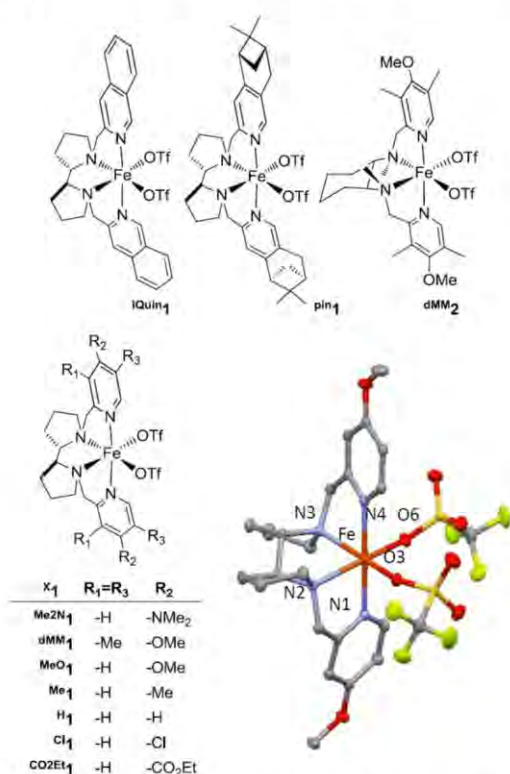
Received: July 30, 2013

Published: September 3, 2013

RESULTS AND DISCUSSION

Synthesis and Characterization of the Catalysts.

Selected iron complexes containing aminopyridine tetradentate ligands are emerging as powerful oxidation catalysts.^{8–10} Among these, the family of bipyrrolidine based complexes $[\text{Fe}^{\text{II}}(\text{CF}_3\text{SO}_3)_2(\text{X}^{\text{PDP}})](\text{X}^{\text{I}})$ ($X = \text{Me}_2\text{N}$, dMM, MeO, Me, H, Cl, CO_2Et , Scheme 2, see the Supporting Information for

Scheme 2. Schematic Diagram of the Iron Complexes Studied^a

^aThe bottom right shows an ORTEP diagram of the single-crystal X-ray determined structure of MeO₁.

experimental details), was identified as a particularly promising platform to evaluate putative electronic effects in catalytic asymmetric epoxidation, owing to the excellent performance of H₁ in C–H¹⁰ and C=C^{8e} oxidation reactions. In epoxidation reactions, H₁ in combination with H₂O₂ and acetic acid (1.1 equiv with respect to substrate) has been previously shown to elicit good yields but moderate enantioselectivities (16–62% ee).^{4e} Structurally related $[\text{Fe}^{\text{II}}(\text{CF}_3\text{SO}_3)_2(\text{iQuinPDP})]$ (iQuin₁), $[\text{Fe}^{\text{II}}(\text{CF}_3\text{SO}_3)_2(\text{pinPDP})]$ (pin₁), and $[\text{Fe}^{\text{II}}(\text{CF}_3\text{SO}_3)_2(\text{dMM}^{\text{MCP}})]$ (dMM₂) (Scheme 2) were also prepared in the present work, and their reactivity was studied and compared to X₁.

Preparation of the complexes involved straightforward reaction of the corresponding tetradentate ligand and $[\text{Fe}(\text{CF}_3\text{SO}_3)_2(\text{CH}_3\text{CN})_2]$ in acetonitrile solution. Removal of the solvent under vacuum and recrystallization by ether diffusion into CH₂Cl₂ solutions yielded the desired complexes as crystalline materials (see the Supporting Information for details). The X-ray structures of H₁ and pin₁ have been previously described.^{10a,11} An ORTEP diagram of MeO₁ is shown in Scheme 2 and serves to illustrate the basic structural

aspects of the family of complexes with general formula $[\text{Fe}^{\text{II}}(\text{CF}_3\text{SO}_3)_2(\text{X}^{\text{PDP}})](\text{X}^{\text{I}})$. Iron centers adopt a distorted octahedral coordination geometry. Four coordination sites are occupied by nitrogen atoms of the tetradentate ligand, and the two remaining sites contain oxygen atoms from the triflate groups. These are in *cis*-relative position and in the same coordination plane as the two bipyrrolidine nitrogen atoms. The two pyridine rings bind *trans* to each other. Fe–N/O distances are between 2.1 and 2.2 Å and are indicative of a high spin ferrous center.¹² When dissolved in CD₃CN or CD₂Cl₂ the full set of complexes retain a common C₂-symmetric *cis-α* topological geometry, with the iron center in the high spin state, as evidenced in their ¹H NMR spectra by the number of signals, their relative integration and the large spectral window (200 to –20 ppm) corresponding to paramagnetic molecules (see the Supporting Information for details).

Catalytic epoxidation activity. Impact of the catalyst in product yield and stereoselectivity. Epoxidation of *cis-β*-methylstyrene (S1) was taken as a model reaction. H₂O₂ (1.6 equiv) was delivered by syringe pump to an acetonitrile solution at –30 °C containing AcOH (140 mol %), catalyst (1–2 mol %) and substrate (see Table 1) under air.

Moderate yield (38%) and enantioselectivity (21% ee) is obtained with the simplest catalyst of the series, H₁ (Table 1, entry 1). When electron-withdrawing groups are introduced at the *para* position (R₂) of the pyridine (Table 1, entries 2–3), both yield and selectivity experience erosion, but they became very much improved in the presence of electron-donating

Table 1. Epoxidation of S1 Using Different Iron Complexes^a

entry	catalyst	AcOH (x mol %)	conv (yield, %)	ee (%)
1	H ₁	140	61 (38)	21
2	Cl ₁	140	57 (33)	15
3	CO ₂ Et ₁	140	44 (22)	19
4	Me ₁	140	44 (27)	31
5	MeO ₁	140	64 (37)	39
6	dMM ₁	140	97 (81)	40
7	Me ₂ N ₁	140	100 (82)	60
8 ^b	Me ₂ N ₁	140	100 (85)	61
9	pin ₁ ^c	140	89 (69)	30
10	iQuin ₁	140	80 (46)	20
11	dMM ₂	140	82 (55)	32
12	Me ₂ N ₁	3	100 (87)	62
13	Me ₂ N ₁	0	45 (20)	46
14	H ₁	3	49 (26)	19
15	Cl ₁	3	32 (15)	16
16	CO ₂ Et ₁	3	31 (13)	21
17	Me ₁	3	31 (17)	30
18	MeO ₁	3	38 (26)	38
19 ^b	dMM ₁	3	82 (67)	38
20	pin ₁ ^c	3	53 (41)	30
21	iQuin ₁	3	34 (15)	19

^aProduct yields, substrate conversions and ee's were determined by GC (see the Supporting Information for further details). Unless stated, catalysts employed have (S,S) chirality at the bipyrrolidine moiety. ^b2 mol % catalyst, H₂O₂ (1.6 equiv). ^c(R,R)-Catalyst was employed.

substituents (Table 1, entries 4–8). Among the series of catalysts tested, excellent epoxide yield and moderate enantioselectivity were obtained with complex $\text{Me}_2\text{N}1$ (82% yield and 60% ee, Table 1, entry 7), which contains strongly donating NMe_2 groups in the pyridines, and a further slight improvement in epoxide yield (85%) and enantioselectivity (61% ee) can be gained by using 2 mol % of catalyst (entry 8). On the other hand, catalysts containing more elaborate pyridine derivatives such as $^i\text{Quin}1$ and $^{\text{pin}}1$ (Scheme 2) give more modest yields (46–69%) and enantioselectivities (20–30% ee, entries 10 and 9). For comparison, catalyst $^{\text{dMM}}2$ elicits reduced ee's (entry 11); thus, the bipyrolidine backbone is better than the cyclohexyldiamine backbone for eliciting optimum stereoselectivity. Finally, control experiments showed that the $\text{Me}_2\text{N}1$ PDP ligand alone is not an epoxidation catalyst and also that the simple addition of 4-(dimethylamino)pyridine (DMAP) inhibits the epoxidation activity of $^{\text{H}}1$.

Therefore, from the results collected in Table 1 (entries 1–11), it can be concluded that yields and stereoselectivities of the epoxidation reactions appear to be strongly and systematically dependent on the electron-donating nature of the pyridine of the ligand, and $^{\text{dMM}}1$ and $\text{Me}_2\text{N}1$ are identified as the best catalysts of the series.

Impact of the Carboxylic Acid Loading Required for Efficient Catalytic Activity. Acetic acid has been previously shown to play a key positive role in enhancing yields and chemoselectivity in iron-catalyzed epoxidation reactions.^{8a} Because of that, further studies were conducted to investigate the role of carboxylic acids (CAs) in the current reactions. Most remarkably, by using $\text{Me}_2\text{N}1$ (2 mol %) the amount of acetic acid could be lowered down to only 1.5 equiv with respect to the iron catalyst, and these conditions even slightly improved yield and ee's (Table 1, compare entry 12 with entries 7 and 8). However, in the absence of acetic acid, both yields and stereoselectivities experience a substantial decrease (Table 1, entry 13). Most remarkably, a perusal of Table 1 shows that only $\text{Me}_2\text{N}1$ has the ability to efficiently operate at nearly stoichiometric acid concentration. For the rest of the catalysts (Table 1, entries 14–21), the use of 1.5 equiv of acetic acid has a small effect on ee's (<2% ee), but substrate conversions and epoxide yields were substantially smaller than in analogous reactions run with 140 equiv of acetic acid (entries 1–11).

Along the same vein, the effect of the carboxylic acid loading on the chemoselectivity toward epoxidation of the reactions is also dependent on the nature of the catalysts (Table 1). Catalysts that contain the most electron-rich pyridines within the series retain their chemoselectivity when low CA loadings are employed. These include $\text{Me}_2\text{N}1$ but also $^{\text{pin}}1$, $^{\text{dMM}}1$, and $^{\text{MeO}}1$. On the other hand, $^{\text{H}}1$, $^{\text{Me}}1$, $^{\text{Cl}}1$, $^i\text{Quin}1$, and $^{\text{CO}_2\text{Et}}1$ lose chemoselectivity at low CA loadings, even though the latter reactions proceed under a priori more favorable conditions for selectivity since lower substrate conversions are obtained. Therefore, the $\text{Me}_2\text{N}1$, $^{\text{pin}}1$, $^{\text{dMM}}1$, and $^{\text{MeO}}1$ catalysts appear to generate more selective oxidizing species.

In conclusion, $\text{Me}_2\text{N}1$ exhibits a unique ability to operate as a remarkably efficient and selective epoxidation catalyst employing H_2O_2 as oxidant and low CA concentration, reflecting an unusual ability to activate and channel H_2O_2 reactivity toward selective epoxidizing species.

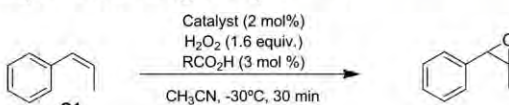
Optimization of the Catalytic Activity with Regard to Amount and Identity of the Carboxylic Acid. Further optimization took advantage of a recent report by Lyakin et al. showing an improvement in epoxidation stereoselectivities by

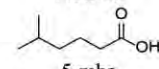
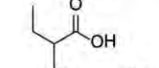
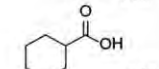
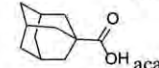
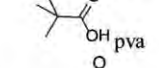
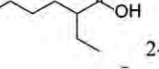
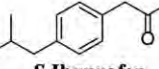
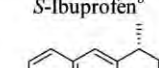
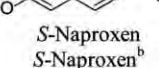
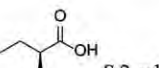
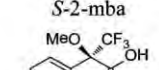
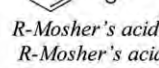
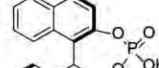
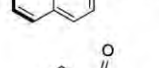
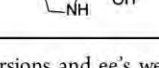
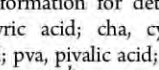
using different CA additives (up to 86% ee for chalcone).^{4c} However, the large acid loading required for efficient operation (0.5–1.4 equiv with respect to the substrate) in common iron systems limits the diversity of CAs that could be employed. Instead, since $\text{Me}_2\text{N}1$ requires only 1.5 equiv with respect to the catalyst, rapid screening of different CAs differing in the electronic and spatial properties could be tested with the aim of improving the enantioselectivity without requiring extensive catalyst preparation. This approach was then further pursued by taking the epoxidation of **S1** as a model reaction (Table 2).

We noticed that certain criteria were necessary for efficient and selective epoxidation activity. First, poor activity was observed when a strong acid such as $\text{CF}_3\text{CO}_2\text{H}$ was used (entry 1). In addition, the use of sodium acetate instead of acetic acid resulted in very small epoxide yields (entry 2). The combination of the two observations indicates that both the carboxylate moiety and the proton are important for optimized epoxidation activity. Improved performance both in terms of epoxide yield and enantioselectivity with regard to acetic acid can be gained with the use of a number of aliphatic carboxylic acids (Table 2, entries 3–8). Of these, as also shown by Lyakin et al., racemic 2-ethylhexanoic acid (2-eha) provides relatively high ee's (80% ee, entry 8). Chiral carboxylic acids could be also tested, leading to the discovery that the combination of *S*-Ibuprofen (*S*-ibp) with $\text{Me}_2\text{N}1$ affords the epoxide with high yield and good enantioselectivity (97% yield, 86% ee, entry 9). Interestingly, use of $(R,R)\text{-Me}_2\text{N}1$ in combination with *S*-ibuprofen resulted in smaller enantioselectivity (63% ee, entry 10) indicating that the high stereoselection requires proper matching of the chirality of the complex with that of the acid. Analogous results were obtained when other chiral carboxylic acids were tested (entries 11–16); for example, *S*-Naproxen provides the epoxide with 77% and 66% ee's when $^{\text{NMe}_2}1$ and $(R,R)\text{-Me}_2\text{N}1$ are employed (entries 10 and 11), respectively. Unfortunately, examples of quite versatile families of chiral carboxylic acids such as amino acids and chiral phosphoric acids (entries 17 and 18) proved incompatible with this system.

Substrate Scope. Substrate scope was then explored under optimized conditions (Table 3), using *S*-ibp and 2-eha as the carboxylic acids of choice.

For both carboxylic acids, good yields and excellent enantioselectivities were obtained with *cis*-cinnamic esters (**S2**, Table 3, entries 2 and 3), an amide derivative (**S3**, Table 3, entries 4 and 5), and with electron-deficient chromenes (Table 3, entries 6–9). We conclude that this catalyst constitutes a rare example of an iron-based system which effectively epoxidizes *cis*-aromatic substrates with high enantioselectivity.¹³ On the other hand, *trans*- β -methylstyrene (**S6**) and the terminal aromatic olefin α -methyl styrene (**S7**) were epoxidized with modest chemoselectivity and only low ee's (entries 10–13). Further scope of the catalyst includes the epoxidation of aromatic enones. Initial experiments employing *S*-ibuprofen as a coligand did elicit good stereoselectivities in the epoxidation of chalcone, but only moderate yields (entry 14). However, excellent yields (99%) and stereoselectivities (98% ee) were obtained in the epoxidation of chalcone when employing 2-eha (Table 3, entry 15, **S8**), which are the highest reported for an iron-based system.¹⁴ Introduction of electron-donating (**S9**) or electron-withdrawing (**S10** and **S11**) groups in the aromatic rings retains the excellent performance (Table 3, entries 16–18). Most interestingly, *trans*-cinnamic esters (**S13**–**S16**) are also a suitable family of substrates and are epoxidized with excellent yields and selectivities (entries 20–

Table 2. Asymmetric Epoxidation of **S1** Using Different Carboxylic Acids Using Catalyst $\text{Me}_2\text{N}1^a$


Entry	RCO ₂ H	Conv.(yield) (%)	ee (%)
1	CF ₃ CO ₂ H	37(13)	36
2	AcONa	26(6)	58
3	 5-mha	100(81)	64
4	 eba	100(88)	80
5	 cha	100(76)	67
6	 aca	100(91)	73
7	 pva	100(73)	76
8	 2-eha	100(86)	80
9	 S-Ibuprofen <i>S</i> -Ibuprofen ^b	100(97)	86
10	 <i>S</i> -Ibuprofen ^b	100(87)	63
11	 <i>S</i> -Naproxen <i>S</i> -Naproxen ^b	100(97)	77
12	 <i>S</i> -Naproxen ^b	100(87)	66
13	 <i>S</i> -2-mba ^b	100(84)	74
14	 <i>S</i> -2-mba	100(84)	76
15	 <i>R</i> -Mosher's acid ^b <i>R</i> -Mosher's acid	62(42)	58
16	 <i>R</i> -Mosher's acid ^b <i>R</i> -Mosher's acid	60(36)	63
17		-	-
18		-	-

^aYields, conversions and ee's were determined by chiral GC (see the Supporting Information for details): 5-mha, 5-methylhexanoic acid; eba, ethylbutyric acid; cha, cyclohexanoic acid; aca, adamantane carboxylic acid; pva, pivalic acid; 2-eha, 2-ethylhexanoic acid; S-2-mba, *S*-methylbutyric acid. ^bReaction with (*R,R*)- $\text{Me}_2\text{N}1$

23, ee's 91–97%), and the same applies to an alkylstyrylketone **S17** (entry 24, 94% ee). The amide derivative **S18** is epoxidized

Table 3. Substrate Scope on the Optimized Asymmetric Epoxidation^a

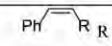
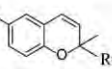
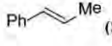

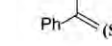
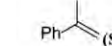
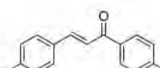
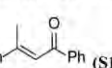
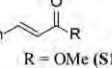
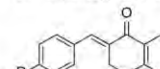
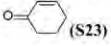
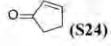
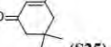
Entry	Substrate	CA	Conv.(Epoxy. Isol. Yield, %)	ee (%)
1	 R = Me (S1)	<i>S</i> -ibp	100(97) ^b	86
2 ^c	R = CO ₂ Et (S2)	<i>S</i> -ibp	91	97
3	R = CO ₂ Et (S2)	2-eha	81	95
4 ^c	R = C(O)N(OMe)(Me) (S3)	<i>S</i> -ibp	84	96
5	R = C(O)N(OMe)(Me) (S3)	2-eha	78	95
6	 R = CN (S4)	<i>S</i> -ibp	100(85) ^d	98(3 <i>R</i> ,4 <i>R</i>)
7	R = CN (S4)	2-eha	95	99(3 <i>R</i> ,4 <i>R</i>)
8	R = NO ₂ (S5)	<i>S</i> -ibp	100(90) ^d	99(3 <i>R</i> ,4 <i>R</i>)
9	R = NO ₂ (S5)	2-eha	97	99(3 <i>R</i> ,4 <i>R</i>)
10	 Me (S6)	<i>S</i> -ibp	48(21) ^b	7
11	 Me (S6)	2-eha	53(32) ^b	19
12	 (S7)	<i>S</i> -ibp	100(67) ^b	45
13	 (S7)	2-eha	82(47) ^b	31
14	 R ₁ (S8)	<i>S</i> -ibp	57(38)	90
15	R = R ₁ = H (S8)	2-eha	99	98(2 <i>R</i> ,3 <i>S</i>)
16	R = Me = R ₁ = H (S9)	2-eha	95	97(2 <i>R</i> ,3 <i>S</i>)
17	R = Cl = R ₁ = H (S10)	2-eha	97	97(2 <i>R</i> ,3 <i>S</i>)
18	R = H = R ₁ = CF ₃ (S11)	2-eha	94	97(2 <i>R</i> ,3 <i>S</i>)
19	 Ph (S12)	2-eha	69	47
20	 R (S13)	2-eha	66	91(2 <i>R</i> ,3 <i>S</i>)
21	R = OEt (S14)	2-eha	91	91
22	R = O <i>i</i> Pr (S15)	2-eha	94	97(2 <i>R</i> ,3 <i>S</i>)
23	R = OBz (S16)	2-eha	94	96
24	R = Me (S17)	2-eha	60	94
25	R = N(OMe)(Me) (S18)	2-eha	95	99
26	 R (S19)	2-eha	94	90(2 <i>R</i> ,3 <i>S</i>)

Table 3. continued

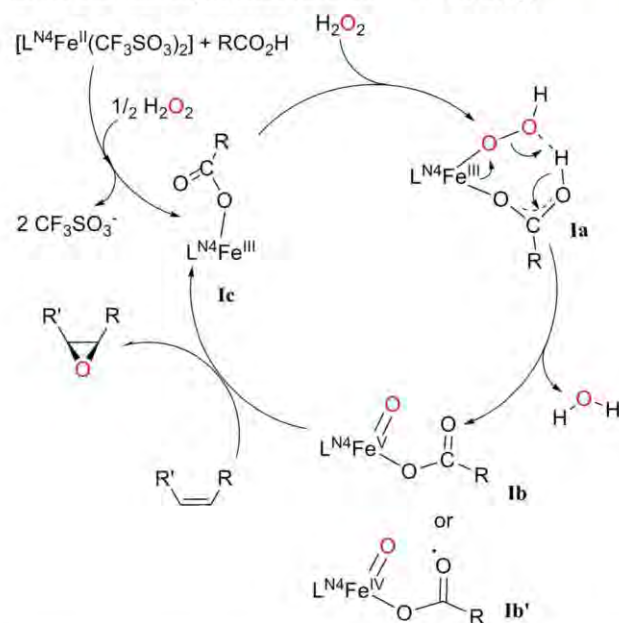
Entry	Substrate	CA	Conv.(Epoxy. Isol. Yield, %)	ee (%)
27	R = Me (S20)	2-eha	97	97(2R,3S)
28	R = F (S21)	2-eha	96	97(2R,3S)
29	R = <i>t</i> Bu (S22)	2-eha	96	95
30 ^a	 (S23)	2-eha	100(99) ^b	84 (<i>R</i>)
31 ^c	 (S24)	2-eha	92(79) ^b	87
32 ^e	 (S25)	2-eha	94(79) ^b	80

^aUnless stated, reaction conditions are as follow: **Me2N1** (2 mol %), H₂O₂ (1.6 equiv), and CA (3 mol %) in CH₃CN at -30 °C during 30 min. Yields refer to isolated yields of pure epoxide. ee's and configuration were determined by chiral GC and HPLC (see the Supporting Information for details). ^bEpoxide yields and substrate conversions determined by GC. ^c5 mol % catalyst, and 3 equiv of H₂O₂. ^dEpoxide yields and substrate conversions determined by ¹H NMR. ^eReaction conditions: **dMM1** (1 mol %), H₂O₂ (1.2 equiv), and 2-eha (140 mol %) in CH₃CN at -30 °C during 30 min.

with outstanding enantioselectivity (entry 25, 99% ee). Epoxidation of trisubstituted aromatic enones was also accomplished with varying outcomes. α -Methyl-substituted chalcone **S12** yielded moderate ee's (entry 19, 47% ee), but the cyclic enones **S19–S22** (Table 3, entries 26–29) were epoxidized with excellent yield (94–97%) and enantioselectivity (90–97% ee).

Encouraged by the results in the epoxidation of aromatic enones, we turned our attention to the challenging cyclic aliphatic enones.¹⁴ Initial epoxidation reactions using catalyst **Me2N1** provided poor yields (12%) and moderate enantioselectivity (76% ee) in the epoxidation of 2-cyclohexen-1-one (**S23**). The poor performance of **Me2N1** in the epoxidation of these cyclic enones is most likely due to the rapid deactivation of this catalyst that occurs when the substrate is not rapidly oxidized under the standard oxidation conditions. Competitive epoxidation of chalcone (**S8**) and cyclic enone (**S23**) with **Me2N1** indeed shows that the former is epoxidized preferentially (ratio of epoxides >10:1) over the later. Instead, **dMM1** is more tolerant to the oxidative conditions, giving improved yields and ee's in the epoxidation of 2-cyclohexen-1-one (**S23**), (Table 3, entry 30, 99% yield, 84% ee) and 2-cyclopenten-1-one (**S24**) (Table 3, entry 31, 79% yield, 87% ee), albeit 140 mol % of 2-eha coligand was required. Trisubstituted aliphatic cyclic enones were also convenient substrates for the system and were epoxidized with good yields and enantioselectivity (Table 3, entry 32, 79% yield, 80% ee). In conclusion, these catalysts exhibit a very remarkable broad substrate scope, which is substantially more extended than any other iron based system described so far.

Mechanistic Studies. Precedents. The positive role of acetic acid in iron-catalyzed oxidations has been documented for some years,^{8a} but mechanistic interpretation has not been provided until recently.¹⁵ The original mechanism proposed by Que and co-workers for the Fe-catalyzed AcOH-assisted epoxidation of olefins with H₂O₂ involves the intermediacy of oxocarboxylate–iron(V) species (**Ib**, Scheme 3) as the oxygen

Scheme 3. Original Mechanistic Scheme Proposed by Que et al. for the Carboxylic Acid Assisted O–O Cleavage¹⁵

atom delivering agent. Species **Ib** is formed via acid-assisted heterolytic cleavage of the O–O bond in a Fe^{III}(OOH)-(HOAc) (**Ia**) precursor.¹⁵ Experimental spectroscopic evidence in favor of this mechanistic scenario has been also recently provided by Talsi, Bryliakov, and co-workers,¹⁶ and further computational support for the formation and oxidative competence of these species has been built by Rajaraman et al. in a study of the *ortho*-hydroxylation of aromatic compounds by non-heme Fe complexes.¹⁷

On the other hand, Shaik, Que, et al. have recently proposed on the basis of DFT analyses that the carboxylate may play a role as a redox noninnocent ligand, sharing one electron with the iron site.¹⁸ The electronic structure of this intermediate (**Ib'**, Scheme 3) will bear obvious similarities with that of compound **I** in P450.⁷

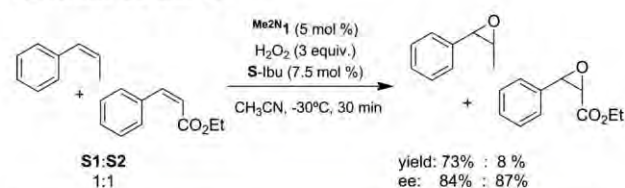
The mechanistic picture that emerges from analyzing the reactivity of **Me2N1** is in good agreement with that originally proposed by Que et al. This mechanistic scheme provides a rationale for the efficient H₂O₂ activation mediated by **Me2N1** and for the origin of the high stereoselectivity observed for this catalyst.

Mechanistic Studies into the Nature of the Oxidizing Species. Insight into the O-delivering species could be deduced by comparing the epoxidation of **S1** with catalyst **Me2N1** and acetic acid as co-ligand but employing different oxidants including H₂O₂, ^tBuOOH, and peracetic acid (Table SI.1, Supporting Information). Substrate conversion and epoxide yields are dependent on the oxidant, 32% conversion and 20% epoxide yield for ^tBuOOH and 85% conversion and 63% epoxide yield for peracetic acid, to compare with quantitative conversion and 87% epoxide yield with H₂O₂. But the most significant aspect with regard to the nature of the O-delivering species is that the enantiomeric excess in the corresponding epoxide is virtually the same (61 ± 1% ee) when any of the three different oxidants are employed. Particularly interesting is the observation that ^tBuOOH is also a competent oxidant to engage in an enantioselective epoxidation because, unlike in the

present reactions, its combination with non-heme iron complexes has been shown to produce unselective free-diffusing radical reactions initiated by homolytic O–O cleavage of $\text{Fe}^{\text{III}}(\text{OO}^t\text{Bu})$ intermediates.¹⁹ The ability of $\text{Me}_2\text{N}1$ to avoid this free-radical reactivity and engage in metal-centered stereoselective chemistry is therefore notable. Enantiomeric excesses are quite sensitive indicators of the differences in energy between the transition states associated with the oxygen atom transfer reaction, leading to the two enantiomeric epoxides, and are usually finely dependent on the nature of the reagents. Because of that, the observation of virtually identical ee's strongly suggests that oxygen atom transfer is performed by the same species, irrespective of the oxidant, discarding iron-peroxides such as **Ia** as possible oxidants. This conclusion is in agreement with recent studies by Nam et al. showing that ferric hydroperoxide and alkyl peroxide species are sluggish oxygen atom transfer agents.²⁰ Furthermore, since enantioselection is affected by both the nature and the chirality of the carboxylic acid, it could be deduced that the latter remains as a ligand in the oxygen delivering species.

Evidence in favor of the implication of an electrophilic oxidant species is derived from a competitive epoxidation of **S1** and ethyl *cis*-cinnamic ester **S2**. Epoxidation of the most electron-rich alkene **S1** (Scheme 4) is favored roughly 9 times

Scheme 4. Competitive Epoxidation Experiment of Substrates S1 and S2

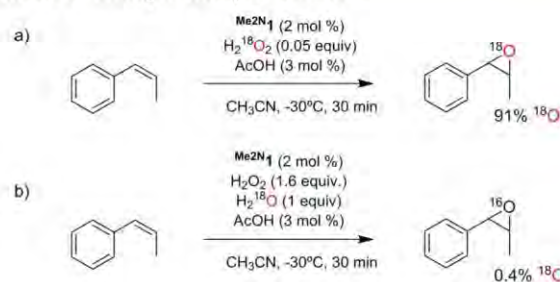


with regard to **S2**. This result is also significant because it provides solid evidence against epoxidation taking place through a nucleophilic Weitz–Scheffer-type epoxidation mechanism.^{2e,21}

The sum of these observations, namely the identical enantioselectivity irrespective of the oxidant, as well as the electrophilic character of the oxidizing species, in combination with the literature precedents for poor oxygen atom transfer reactivity of iron peroxides thus provides experimental evidence that O–O cleavage in $\text{Me}_2\text{N}1$ precedes formation of the oxidizing species. The cleavage of the O–O bond in iron peroxide species can occur through homolysis or heterolysis. Homolysis is discarded in the present case because it implies formation of poorly selective hydroxyl radicals and oxo-iron(IV) species, which are relatively modest O-atom transfer agents.²² Therefore, heterolysis must be the operating path, leading to an electrophilic $\text{Fe}^{\text{V}}(\text{O})(\text{O}_2\text{CR})$ species (**Ib**, Scheme 3), which is then responsible for the O-atom transfer.

Isotopic analyses were also employed as mechanistic tools (Scheme 5) and conform to the same mechanistic picture, providing insight into the mechanism of O–O lysis. Epoxidation of **S1** with $\text{Me}_2\text{N}1$ using $\text{H}_2^{18}\text{O}_2$ (90% ^{18}O enrichment) as oxidant provided the corresponding epoxide 91(\pm 1)% ^{18}O -labeled (Scheme 5a), and virtually no ^{18}O was incorporated (0.4(\pm 1)%) when $\text{H}_2^{16}\text{O}_2/\text{H}_2^{18}\text{O}$ was used (Scheme 5b), indicating that the oxidant is the source of oxygen atoms incorporated into the epoxide and also that oxygen from water is not incorporated. This isotopic pattern

Scheme 5. Isotopic Analysis Studies^a



^a $\text{H}_2^{18}\text{O}_2$ reagent is a 2% solution in H_2^{16}O .

argues against the implication of a water-assisted O–O lysis that results in $\text{Fe}^{\text{V}}(\text{O})(\text{OH})$ species^{8b,22} and instead points toward the carboxylic acid mediated pathway that leads to **Ib**, in line with the previous proposals.^{15,16}

On the basis of these mechanistic considerations, the ability of $\text{Me}_2\text{N}1$ to efficiently and selectively operate at low CA loadings most likely indicates that the heterolytic cleavage of the O–O bond in $\text{Fe}^{\text{III}}(\text{OOH})(\text{HOAc})$ (**Ia**) to form $\text{Fe}^{\text{V}}(\text{O})(\text{O}_2\text{CR})$ (**Ib**) is exceptionally facilitated for this catalyst. We propose that the mechanism of O–O cleavage in this case is facilitated by the assistance of a proton of the carboxylic acid (pull effect, as early proposed by Que et al.) and also by a push effect exerted by the powerful electron donating character of the dimethyl amino pyridine ligand. This synergistic operation may then provide an efficient channel for controlling the O–O cleavage event and prevent from otherwise energetically competitive alternative paths. Interestingly, this scenario bears a strong resemblance to that operating in the mechanism of formation of Cpd I in Cyt P450 (Scheme 1).⁷

Mechanistic Insights in the O-Atom Transfer Reaction. Stereospecificity and Linear Free Energy Correlation. Remarkably, epoxidation with the present iron-based catalysts is stereospecific and takes place with stereoretention even in the cases of substrates that can easily undergo epimerization during epoxidation with other reagents. For example, epoxidation of **S1** and of the sterically congested disubstituted β,β' -enone **S12** yields a single diastereomer. This indicates that oxygen atom transfer occurs through concerted formation of the two new C–O bonds, or alternatively, sequential C–O bond formation occurs very fast, without scrambling. That constitutes a difference with respect to Mn-salen systems,²⁴ and Weitz–Scheffer-type epoxidations, where some degree of epimerization takes place.^{2e,21}

Finally, this mechanistic scenario provides a rational mechanistic frame for understanding the electronic effects of the catalysts in the enantioselectivity. A plot of the log (ee) (ratio of enantiomers) corresponding to chiral induction in epoxidation of **S8** as a function of the Hammett parameter of the X group in **X1** (Figure 1) shows a linear correlation. The enantioselectivity ranges from 51% to 90% ee for epoxidation of **S8** with the series of **X1** complexes, which corresponds to a notable improvement in selectivity of $\Delta\Delta G^\ddagger \sim 1.0 \text{ kcal}\cdot\text{mol}^{-1}$. The same analysis was done for substrates **S1**, **S4**, and **S13**, showing analogous correlations. The consistent linear nature of the Hammett correlation for four different substrates strongly suggests that this linear free energy relationship is general and has mainly an electronic origin which can be straightforwardly analyzed with the previously proposed mechanistic frame (Scheme 3). As the ligand becomes more electron rich, the

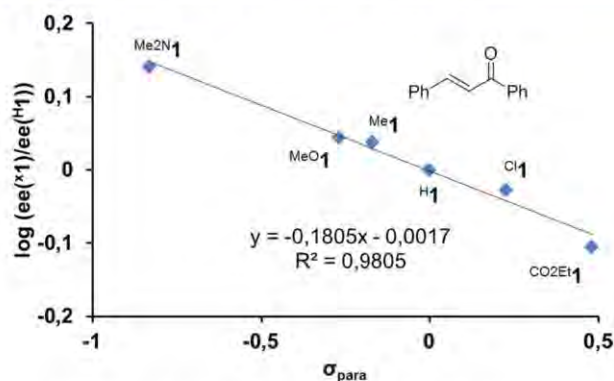


Figure 1. Hammett analysis of stereoselectivity as a function of catalyst employed in the epoxidation of **S8** (for analogous analysis with **S1**, **S4** and **S13**, see Figures S1.1 and S1.2 (Supporting Information)). Catalyst **1** (1 mol %), AcOH (140 mol %), and H₂O₂ (1.2 equiv) in CH₃CN at 0 °C. Hammett's values are taken from ref 25.

electrophilicity of the metal–oxo species is attenuated, and the transition state is displaced toward a more product-like complex, characterized by a tighter substrate/metal–oxo species, with more specific nonbonding interactions. However, electron-poorer systems result in a more electrophilic and less discriminatory oxidant, exhibiting lower stereochemical differentiation.^{27a} This scenario indeed finds precedent in Mn–salen epoxidation systems,²⁷ but its application in non-heme iron chemistry is, to the best of our knowledge, unprecedented. It is important to mention that manipulation of the electronic properties of heme ferryl species has been used to modulate the chemoselectivity of their oxidation reactions,²⁸ but translation into asymmetric oxidations has not been described so far.

CONCLUSION AND FUTURE REMARKS

In conclusion, the present work illustrates how electronic effects can be used as powerful tools for controlling the activation of H₂O₂ and O-atom transfer in non-porphyrinic iron complexes, leading to excellent catalysts for highly asymmetric epoxidation of olefins with H₂O₂. Efficient activation of H₂O₂ is proposed to occur via facile heterolytic O–O bond cleavage in electron-rich iron complexes. Although the exact details by which this reaction is exceptionally facilitated by **Me2N1** remain to be clarified, a resemblance to the so-called push–pull effect operating in P450 can be drawn.⁷ Even more exciting analogies could be also suggested between the well-established redox active non-innocent nature of porphyrins^{7,29} and dimethylamino-pyridine ligands,³⁰ and how these electronic structures may facilitate stabilization of highly electrophilic high oxidation states. From a more synthetic perspective, this work provides directions for future rational design of catalysts, fine tuning of enantioselection, and expanding substrate scope, without the need for elaborate catalyst development, but by taking advantage of cooperative catalysis effects between aminopyridine and carboxylic acid ligands. Expansion of substrate scope, extension toward other oxygen atom transfer reactions, and clarification of the reaction intermediates involved in these reactions are currently being explored.

ASSOCIATED CONTENT

Supporting Information

Experimental details for the preparation and characterization of ligands and metal complexes. Experimental details of catalytic

reactions and spectroscopic data for product characterization. X-ray data for **MeO1** (CIF). This material is available free of charge via the Internet at <http://pubs.acs.org>.

AUTHOR INFORMATION

Corresponding Author

miquel.costas@udg.edu

Notes

The authors declare no competing financial interest.

ACKNOWLEDGMENTS

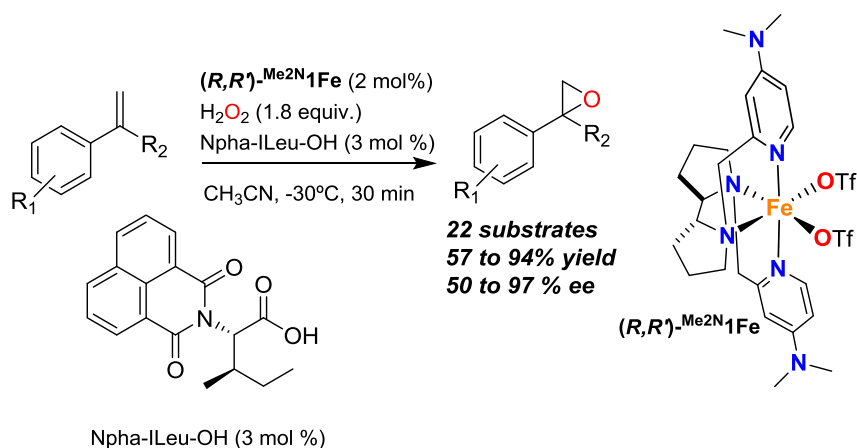
We acknowledge financial support from European Research Council (ERC-2009-StG-239910), MINECO of Spain (CTQ2012-37420-C02-01/BQU, Consolider-Ingenio CSD2010-00065), and the Catalan DIUE of the Generalitat de Catalunya (2009SGR637). J.L.L.-F. thanks MICINN for a RyC contract. X.R. and M.C. acknowledge ICREA-Academia awards. X.R. is grateful for financial support from INNPLAN-TA Project No. IPN-2011-0059-PCT-42000-ACT1. I.G.-B. thanks the European Community for an IOF Marie Curie fellowship. We acknowledge STRs from UdG for technical support.

REFERENCES

- (1) (a) Que, L.; Tolman, W. B. *Nature* **2008**, *455*, 333. (b) Enthaler, S.; Junge, K.; Beller, M. *Angew. Chem., Int. Ed.* **2008**, *47*, 3317. (c) Correa, A.; Mancheño, O. G.; Bolm, C. *Chem. Soc. Rev.* **2008**, *8*, 1108. (d) Liu, L.-X. *Curr. Org. Chem.* **2010**, *14*, 1099. (e) Chang-Liang Sun, C.-L.; Li, B.-J.; Shi, Z.-J. *Chem. Rev.* **2011**, *111*, 1293–1314. (f) Darwish, M.; Wills, M. *Catal. Sci. Technol.* **2012**, *2*, 243. (g) Gopalaiah, K. *Chem. Rev.* **2013**, *113*, 3248. (h) Bauer, E. B. *Curr. Org. Chem.* **2008**, *12*, 1341.
- (2) (a) Katsuki, T. In *Catalytic Asymmetric Synthesis*, 2nd ed.; Ojima, I., Ed.; Wiley-VCH: New York, 2000; p 287. (b) De Faveri, G.; Ilyashenko, G.; Watkinson, M. *Chem. Soc. Rev.* **2011**, *40*, 1722. (c) Chatterjee, D. *Coord. Chem. Rev.* **2008**, *252*, 176. (d) Wong, O. A.; Shi, Y. *Chem. Rev.* **2008**, *108*, 3958. (e) Diez, D.; Nunez, M. G.; Anton, A. B.; Garcia, P.; Moro, R. F.; Garrido, N. M.; Marcos, I. S.; Basabe, P.; Urones, J. G. *Curr. Org. Synth.* **2008**, *5*, 186.
- (3) Fe systems showing moderate stereoselectivity: (a) Marchi Delapierre, C.; Jorge-Robin, A.; Thibon, A.; Ménage, S. *Chem. Commun.* **2007**, *11*, 1166. (b) Yeung, H.-L.; Sham, K.-C.; Tsang, C. S.; Lau, T.-C.; Kwong, H.-L. *Chem. Commun.* **2008**, 3801. (c) Oddon, F.; Girgenti, E.; Lebrun, C.; Marchi-Delapierre, C.; Pecaut, J.; Menage, S. *Eur. J. Inorg. Chem.* **2012**, 85.
- (4) (a) Gelalcha, F. G.; Anilkumar, G.; Tse, M. K.; Brückner, A.; Beller, M. *Chem.—Eur. J.* **2008**, *14*, 7687. (b) Gelalcha, F. G.; Bitterlich, B.; Anilkumar, G.; Tse, M. K.; Beller, M. *Angew. Chem. Int. Ed.* **2007**, *46*, 7293. (c) Wu, M.; Miao, C.-X.; Wang, S.; Hu, X.; Xia, C.; Kühn, F. E.; Sun, W. *Adv. Synth. Catal.* **2011**, *353*, 3014. (d) Wang, B.; Wang, S.; Xia, C.; Sun, W. *Chem.—Eur. J.* **2012**, *18*, 7332. (e) Lyakin, O. Y.; Ottenbacher, R. V.; Bryliakov, K. P.; Talsi, E. P. *ACS Catal.* **2012**, *2*, 1196. (f) Cheng, Q. F.; Xu, X. Y.; Ma, W. X.; Yang, S. J.; You, T. P. *Chin. Chem. Lett.* **2005**, *16*, 1467.
- (5) Fe systems employing other oxidants: (a) Nishikawa, Y.; Yamamoto, H. *J. Am. Chem. Soc.* **2011**, *133*, 8432. (b) Niwa, T.; Nakada, M. *J. Am. Chem. Soc.* **2012**, *134*, 13538.
- (6) (a) Kovaleva, E. G.; Lipscomb, J. D. *Nat. Chem. Biol.* **2008**, *4*, 186. (b) Abu-Omar, M. M.; Loaiza, A.; Hontzeas, N. *Chem. Rev.* **2005**, *105*, 2227. (c) Costas, M.; Mehn, M. P.; Jensen, M. P.; Que, L., Jr. *Chem. Rev.* **2004**, *104*, 939.
- (7) (a) Shaik, S.; Cohen, S.; Wang, Y.; Chen, H.; Kumar, D.; Thiel, W. *Chem. Rev.* **2010**, *110*, 949. (b) Meunier, B.; de Visser, S. P.; Shaik, S. *Chem. Rev.* **2004**, *104*, 3947.
- (8) (a) White, M. C.; Doyle, A. G.; Jacobsen, E. N. *J. Am. Chem. Soc.* **2001**, *123*, 7194. (b) Chen, K.; Costas, M.; Kim, J.; Tipton, A. K.;

- Que, L., Jr. *J. Am. Chem. Soc.* **2002**, *124*, 3026. (c) Mikhalyova, E. A.; Makhlynets, O. V.; Palluccio, T. D.; Filatov, A. S.; Rybak-Akimova, E. V. *Chem. Commun.* **2012**, *48*, 687. (d) Wang, B.; Miao, C.-X.; Wang, S.-F.; Kuehn, F. E.; Xia, C.-G.; Sun, W. *J. Organomet. Chem.* **2012**, *715*, 9. (e) Talsi, E. P.; Bryliakov, K. P. *Coord. Chem. Rev.* **2012**, *256*, 1418. For other representative Fe-based epoxidation systems, see: (f) Dubois, G.; Murphy, A.; Stack, T. D. P. *Org. Lett.* **2003**, *5*, 2469. (g) Anilkumar, G.; Bitterlich, B.; Gelalcha, F. G.; Tse, M. K.; Beller, M. *Chem. Commun.* **2007**, *3*, 289. (h) Schroeder, K.; Enthaler, S.; Bitterlich, B.; Schulz, T.; Spannenberg, A.; Tse, M. K.; Junge, K.; Beller, M. *Chem.—Eur. J.* **2009**, *15*, 5471. (i) Schröder, K.; Join, B.; Amali, A. J.; Junge, K.; Ribas, X.; Costas, M.; Beller, M. *Angew. Chem. Int. Ed.* **2011**, *50*, 1425.
- (9) For pioneering work with Mn systems, see: (a) Murphy, A.; Dubois, G.; Stack, T. D. P. *J. Am. Chem. Soc.* **2003**, *125*, 5250. Further evolution of this type of Mn catalyst: (b) Gómez, L.; García-Bosch, I.; Company, A.; Sala, X.; Fontrodona, X.; Ribas, X.; Costas, M. *Dalton Trans.* **2007**, 5539. (c) Wu, M.; Wang, B.; Wang, S.; Xia, C.; Sun, W. *Org. Lett.* **2009**, *11*, 3622. (d) García-Bosch, I.; Gómez, L.; Polo, A.; Ribas, X.; Costas, M. *Adv. Synth. Catal.* **2012**, *354*, 65. (e) Lyakin, O. Y.; Ottenbacher, R. V.; Bryliakov, K. P.; Talsi, E. P. *ACS Catal.* **2012**, *2*, 1196. (f) Wang, B.; Miao, C.; Wang, S.; Xia, C.; Sun, W. *Chem.—Eur. J.* **2012**, *18*, 6750.
- (10) (a) Chen, M. S.; White, M. C. *Science* **2007**, *318*, 783. (b) Chen, M. S.; White, M. C. *Science* **2010**, *327*, 566. (c) Bigi, M. A.; Reed, S. A.; White, M. C. *Nat. Chem.* **2011**, *3*, 216. (d) Bigi, M. A.; Reed, S. A.; White, M. C. *J. Am. Chem. Soc.* **2012**, *134*, 9721. (e) White, M. C. *Science* **2012**, *335*, 807.
- (11) Gomez, L.; Canta, M.; Font, D.; Prat, I.; Ribas, X.; Costas, M. *J. Org. Chem.* **2013**, *78*, 1421.
- (12) (a) Diebold, A.; Hagen, K. S. *Inorg. Chem.* **1998**, *37*, 215. (b) Blakesley, D. W.; Payne, S. C.; Hagen, K. S. *Inorg. Chem.* **2000**, *39*, 1979. (c) Simaan, A. J.; Döpner, S.; Banse, F.; Bourcier, S.; Bouchoux, G.; Boussac, A.; Hildebrandt, P.; Girerd, J.-J. *Eur. J. Inorg. Chem.* **2000**, 1627. (d) Chen, K.; Que, L., Jr. *J. Am. Chem. Soc.* **2001**, *123*, 6327. (e) Britovsek, G. J. P.; England, J.; White, A. J. P. *Inorg. Chem.* **2005**, *44*, 8125. (f) Zang, Y.; Kim, J.; Dong, Y.; Wilkinson, E. C.; Appelman, E. H.; Que, L., Jr. *J. Am. Chem. Soc.* **1997**, *119*, 4197.
- (13) For a single previous precedent, see ref 4f.
- (14) (a) Lee, A.; Reisinger, C. M.; List, B. *Adv. Synth. Catal.* **2012**, *354*, 1701. (b) Wang, X.; Reisinger, C. M.; List, B. *J. Am. Chem. Soc.* **2008**, *130*, 6070. (c) Lifchits, O.; Mahlau, M.; Reisinger, C. M.; Lee, A.; Fares, C.; Polyak, I.; Gopakumar, G.; Thiel, W.; List, B. *J. Am. Chem. Soc.* **2013**, *135*, 6677.
- (15) Mas-Balleste, R.; Que, L., Jr. *J. Am. Chem. Soc.* **2007**, *129*, 15964.
- (16) (a) Lyakin, O. Y.; Bryliakov, K. P.; Britovsek, G. J. P.; Talsi, E. P. *J. Am. Chem. Soc.* **2009**, *131*, 10798. (b) Lyakin, O. Y.; Bryliakov, K. P.; Talsi, E. P. *Inorg. Chem.* **2011**, *50*, 5526.
- (17) Ansari, A.; Kaushik, A.; Rajaraman, G. *J. Am. Chem. Soc.* **2013**, *135*, 4235.
- (18) Wang, Y.; Janardanan, D.; Usharani, D.; Han, K.; Que, L.; Shaik, S. *ACS Catal.* **2013**, *3*, 1334.
- (19) (a) MacFaul, P. A.; Ingold, K. U.; Wayner, D. D. M.; Que, L. *J. Am. Chem. Soc.* **1997**, *119*, 10594. (b) Ingold, K. U.; MacFaul, P. A. In *Biomimetic Oxidations Catalyzed by Transition Metal Complexes*; Meunier, B., Ed.; Imperial College Press: London, 2000; p 45.
- (20) (a) Seo, M. S.; Kamachi, T.; Kouno, T.; Murata, K.; Park, M. J.; Yoshizawa, K.; Nam, W. *Angew. Chem., Int. Ed.* **2007**, *46*, 2291. (b) Park, M. J.; Lee, J.; Suh, Y.; Kim, J.; Nam, W. *J. Am. Chem. Soc.* **2006**, *128*, 2630.
- (21) (a) Bunton, C. A.; Minkoff, G. J. *J. Chem. Soc.* **1949**, 665. (b) Christian, C. F.; Takeya, T.; Szymanski, M. J.; Singleton, D. A. *J. Org. Chem.* **2007**, *72*, 6183. (c) House, H. O.; Ro, R. S. *J. Am. Chem. Soc.* **1958**, *80*, 2428. (d) Kelly, D. R.; Caroff, E.; Flood, R. W.; Heal, W.; Roberts, S. M. *Chem. Commun.* **2004**, 2016. (e) Kelly, D. R.; Roberts, S. M. *Pept. Sci.* **2006**, *84*, 74. (f) Meerwein, H. *J. Prakt. Chem.* **1926**, *113*, 9. (g) Weitz, E.; Scheffer, A. *Chem. Ber.* **1921**, *54*, 2344.
- (22) A single case of well-defined Fe^{IV}(O) species has been shown to be kinetically competent to mediate epoxidation of olefins, albeit at relatively low reaction rates. See: Ye, W. H.; Ho, D. M.; Friedle, S.; Palluccio, T. D.; Rybak-Akimova, E. V. *Inorg. Chem.* **2012**, *51*, 5006.
- (23) (a) Prat, I.; Mathieson, J. S.; Güell, M.; Ribas, X.; Luis, J. M.; Cronin, L.; Costas, M. *Nat. Chem.* **2011**, *3*, 788. (b) Oloo, W. N.; Fielding, A. J.; Que, L., Jr. *J. Am. Chem. Soc.* **2013**, *135*, 6438.
- (24) Jacobsen, E. N.; Zhang, W.; Muci, A. R.; Ecker, J. R.; Deng, L. *J. Am. Chem. Soc.* **1991**, *113*, 7063.
- (25) Hansch, C.; Leo, A.; Taft, R. W. *Chem. Rev.* **1991**, *91*, 165–195.
- (26) A significant deviation has only been observed for the relative enantioselectivities obtained with ¹³C¹⁸O₂Et¹ and ¹³C¹ in the epoxidation of **S1** (Figure S1, Supporting Information), showing that in specific cases other factors can alter the LFER. The importance of these deviations could be estimated by translating the corresponding ee's into differences in energy. At –30 °C, $\Delta\Delta G^\ddagger$ corresponding to ee's obtained in the epoxidation of **S1** with ¹³C¹⁸O₂Et¹ and ¹³C¹ differ by <0.07 kcal·mol⁻¹. Therefore, the significance of this deviation should be considered small.
- (27) (a) Jacobsen, E. N.; Zhang, W.; Muci, A. R.; Ecker, J. R.; Deng, L. *J. Am. Chem. Soc.* **1991**, *113*, 7063. (b) Cavallo, L.; Jacobsen, H. *J. Org. Chem.* **2003**, *68*, 6202. (c) For the opposite scenario, see: (d) Liao, S.; List, B. *Angew. Chem., Int. Ed.* **2010**, *49*, 628.
- (28) (a) Traylor, T. G.; Miksztal, A. R. *J. Am. Chem. Soc.* **1989**, *111*, 7443. (b) Groves, J. T.; Watanabe, Y. *J. Am. Chem. Soc.* **1986**, *108*, 507.
- (29) Praneeth, V. K. K.; Ringenberg, M. R.; Ward, T. R. *Angew. Chem., Int. Ed.* **2012**, *51*, 10228.
- (30) Rycke, N. D.; Couty, F.; David, O. R. P. *Chem.—Eur. J.* **2011**, *17*, 12852.

Synergistic Interplay of a Non-Heme Iron Catalyst and Amino acid co-ligands in H₂O₂ Activation and Asymmetric Epoxidation of α -Substituted Styrenes



This chapter corresponds to the following publication:

Cussó, O.; Ribas, X.; Lloret-Fillol J.; Costas, M. *Angew. Chem. Int. Ed.*, 2015, **54**, 2729.

Reproduced with permission from Cussó, O.; Ribas, X.; Lloret-Fillol, J.; Costas, M. “Synergistic Interplay of a Non-Heme Iron Catalyst and Amino Acid Coligands in H₂O₂ Activation for Asymmetric Epoxidation of α -Alkyl-Substituted Styrenes”. *Angewandte Chemie International Edition*, num. 54, issue 9 (2015) : 2729-2733

<http://dx.doi.org/10.1002/anie.201410557>

© 2015 WILEY-VCH Verlag GmbH & Co. KGaA, Weinheim

Synergistic Interplay of a Non-Heme Iron Catalyst and Amino Acid Coligands in H₂O₂ Activation for Asymmetric Epoxidation of α -Alkyl-Substituted Styrenes**

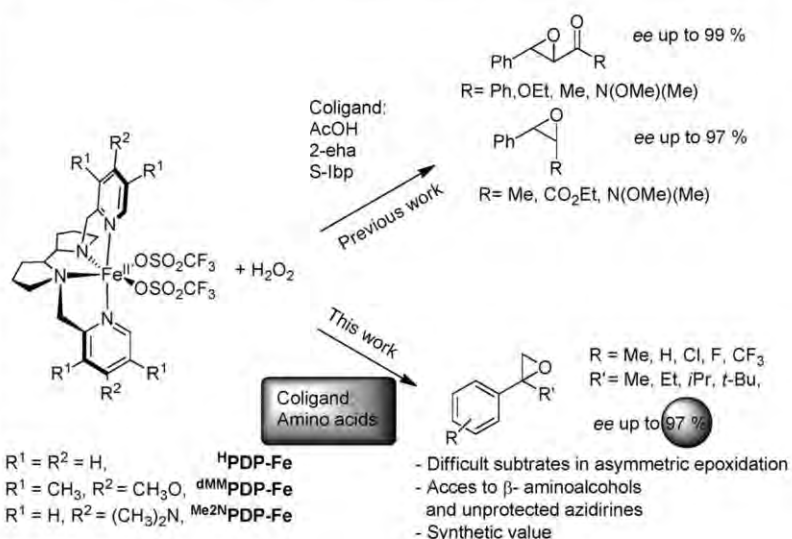
Olaf Cussó, Xavi Ribas, Julio Lloret-Fillol, and Miquel Costas*

Abstract: Highly enantioselective epoxidation of α -substituted styrenes with aqueous H₂O₂ is described by using a chiral iron complex as the catalyst and *N*-protected amino acids (AAs) as coligands. The amino acids synergistically cooperate with the iron center in promoting an efficient activation of H₂O₂ to catalyze epoxidation of this challenging class of substrates with good yields and stereoselectivities (up to 97% ee) in short reaction times.

Biolegally inspired catalysts are currently explored with the aim to produce selective oxidation reactions. The quest for catalytic methodologies that provide novel reactivities and selectivities that could complement those attained with traditional oxidants, or that could represent a more efficient alternative constitute major reasons of interest for this approach.^[1] Among oxidations, asymmetric epoxidation is a reaction of broad interest in synthetic organic chemistry because of the synthetic value of chiral epoxides.^[2] Recently we reported that iron complexes with electron-rich aminopyridine ligands catalyze highly stereoselective epoxidation of enones and *cis*- β -substituted styrenes with H₂O₂ (Scheme 1, 2-cha = 2-ethylhexanoic acid, S-Ibp = *S*-ibuprofen).^[3] In these experiments, carboxylic acids were also key elements for controlling O–O breakage and epoxidation stereoselectivity. The system could therefore be adapted to cover novel families of substrates just by employing other carboxylic acids, without requiring preparation of novel chiral iron catalysts. We reasoned that this variability could be an important aspect because the activity and reaction mechanisms of iron complexes when reacting with peroxides are very

dependent on the nature of aminopyridine ligands.^[1] With these considerations in mind, we focused our attention on amino acids (AAs) as putative coligands for the system. While their large structural diversity finds wide use in organo-catalytic epoxidation methodologies,^[2c,d,4] the compatibility of amino acids with metal-catalyzed oxidations has few but notable precedents.^[5]

Herein we show that synergistic cooperation between a non-heme iron coordination complex and amino acid coligands allows for efficient activation of hydrogen peroxide leading to highly stereoselective epoxidation reactions in short reaction times. Remarkable aspects of the current system are: a) the use of iron as the metal catalyst and aqueous H₂O₂ as oxidant, reagents that are attractive because



Scheme 1.

[*] O. Cussó, Dr. X. Ribas, Dr. J. Lloret-Fillol, Dr. M. Costas
Institut de Química Computacional i Catalisi (IQCC) and
Departament de Química
Universitat de Girona
Campus de Montilivi, 17071 Girona, Catalonia (Spain)
E-mail: miquel.costas@udg.edu

[**] We acknowledge group LIPPSO from UdG for providing amino acid samples and A. Riera (IRB) for access to a polarimeter. We acknowledge financial support from the European Research Council (ERC-2009-StG-239910), MINECO of Spain (CTQ2012-37420-C02-01/BQU, CSD2010-00065), and Generalitat de Catalunya (2009SGR637). J.L.-F. thanks MICINN for a RyC contract. X.R. and M.C. thank ICREA-Academia awards.

Supporting information for this article is available on the WWW under <http://dx.doi.org/10.1002/anie.201410557>.

of their availability and low environmental impact.^[6–8] b) The use of amino acids as a versatile source of chirality. c) The highly stereoselective epoxidation of α -substituted styrenes, a class of substrates that remain very challenging for other asymmetric epoxidation methods.^[9] Furthermore the present system can be considered a remarkable approach towards the mimicking of selective oxidation reactions taking place in non-heme iron-dependent oxygenases because a number of these enzymes rely in controlled breakage of the O–O bond, and amino acids are common biological iron ligands and provide a main element of chirality regulating stereoselectivity in the enzymatic transformations.

Initial conditions involved the epoxidation of *cis*- β -methylstyrene (**S0**) employing the electron rich catalyst

(*S,S*)-^{Me}2^NPDP-Fe (2 mol %), Scheme 1) and amino acid coligand (3 mol %) in acetonitrile solution at -30 °C, over which 1.8 equivalents of H₂O₂ were delivered by syringe pump over 30 min (Table 1). This substrate was chosen to compare the efficiency of amino acids with respect to simple organic acids as co-catalyst.^[3]

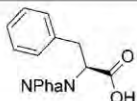
The initial screening involved the use of a range of amino acids, and also an analysis of the nature of the *N*-protecting group in reaction performance. Since both the amino acid and the iron catalyst are chiral, each amino acid was tested with both (*S,S*)-^{Me}2^NPDP-Fe (3rd–4th columns in Table 1) and (*R,R*)-^{Me}2^NPDP-Fe (5–6th columns in Table 1). The first significant observation is that proline is not a valid acid partner (Table 1, entry 1), presumably because the unprotected amine poisoned the catalyst by chelation. However, when the amine site was protected, the reaction took place with moderate to excellent yields and good enantioselectivities (entries 2–4). No major side product was detected. Boc as a protecting group provides the highest enantioselectivities of the series. Moreover, when the reaction was carried out using ^{dMM}PDP-Fe (Scheme 1), a catalyst which has less-electron-donating groups in the pyridine rings, moderate yields were obtained and the enantioselectivities decrease (Table 1 entry 6). In the same vein, the use of the simplest ^HPDP-Fe (Scheme 1) produced poor yields and stereoselectivities (Table 1, entry 7), thus illustrating the important role of the electronic properties of the aminopyridine ligand in the activation of H₂O₂ and in the O-delivering step. Then, a series of Boc-protected amino acids were tested, resulting in an improvement of the enantioselectivity up to 81 and 80% *ee* using *N*-Boc-*t*-Leu-OH (entry 8) and *N*-Boc-Ileu-OH (entry 10), respectively. Since both the iron catalyst and the amino acid coligand are chiral, matching–mismatching effects resulting from combination of the respective chiralities were also evaluated by using the two enantiomeric *R,R* and *S,S* forms of the catalyst (compare columns 4 and 6 in Table 1). Without exception when the same amino

acid was employed in combination with the two enantiomeric forms of the iron catalyst, the opposite epoxide enantiomer was obtained as major product. In addition, as a general trend, small differences in yields and stereoselectivities were observed for each of these pair of reactions. A different picture was however observed when the *N*-Npha-Ileu-OH derivative was employed (entry 13). This amino acid not only

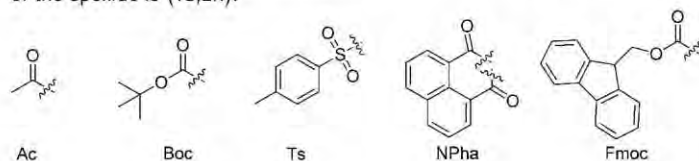
Table 1: Screening of amino acids in asymmetric epoxidation reaction (Table continued on next page).^[a]

Catalyst Entry	Amino acid	(<i>S,S</i>)- ^{Me} 2 ^N PDPFe ^[b] Conv. (Yield) [%]	(<i>S,S</i>)- ^{Me} 2 ^N PDPFe ^[b] <i>ee</i> [%]	(<i>R,R</i>)- ^{Me} 2 ^N PDPFe ^[b] Conv. (Yield) [%]	(<i>R,R</i>)- ^{Me} 2 ^N PDPFe ^[b] <i>ee</i> [%]	
1		Pro-OH	–	–	n.d.	n.d.
2		<i>N</i> -Ts-Pro-OH	47 (30)	63	87 (69)	76
3		<i>N</i> -Fmoc-Pro-OH	100 (75)	74	96 (77)	77
4		<i>N</i> -Boc-Pro-OH	100 (87)	79	95 (90)	77
5 ^[c]		<i>N</i> -Boc-Pro-OH	100 (90)	76	n.d.	n.d.
6 ^[d]		<i>N</i> -Boc-Pro-OH	50 (40)	32	n.d.	n.d.
7 ^[e]		<i>N</i> -Boc-Pro-OH	55 (27)	17	n.d.	n.d.
8		<i>N</i> -Boc- <i>t</i> -Leu-OH	100 (93)	80	100 (91)	81
9		<i>N</i> -Boc-Leu-OH	100 (89)	71	100 (89)	75
10		<i>N</i> -Boc-Ileu-OH	100 (96)	80	100 (83)	73
11		<i>N</i> -Fmoc-Ileu-OH	100 (84)	78	100 (84)	74
12		<i>N</i> -Ac-Ileu-OH	100 (89)	78	100 (82)	74
13		<i>N</i> -Npha-Ileu-OH	79 (51)	49	100 (81)	87
14		<i>N</i> -Npha- <i>t</i> -Leu-OH	72 (57)	70	100 (89)	85
15		<i>N</i> -Npha-Ala-OH	92 (74)	70	100 (87)	76

Table 1: (Continued)

Entry	Amino acid	(S,S) - Me_2N PDPFe ^[b]		(R,R) - Me_2N PDPFe ^[b]		
		Conv. (Yield) [%]	<i>ee</i> [%]	Conv. (Yield) [%]	<i>ee</i> [%]	
16		N-Npha-Phe-OH	98 (79)	68	100 (84)	74

[a] Reaction conditions are Me_2N PDP-Fe (2 mol%), H_2O_2 (1.8 equiv) and amino (3 mol%), *cis*- β -methylstyrene (**S0**, 0.11 M) in CH_3CN at $-30^\circ C$ during 30 min. [b] Conversion and yield were calculated using an internal standard. The *ee* values were determined by chiral GC. [c] 1.4 equiv of *N*-Boc-Pro-OH. [d] dMM PDP-Fe as catalyst.^[3] [e] H PDP-Fe as catalyst. n.d.: not determined. See Supporting Information for a complete list of the amino acids tested. All the amino acids have *S* configuration. The absolute configuration of the epoxide obtained with (S,S) - Me_2N PDPFe was determined as $(1R,2S)$ by comparison of optical rotation data with that from the literature,^[10] in the case of (R,R) - Me_2N PDPFe the configuration of the epoxide is $(1S,2R)$.



provides the best stereoselection among the series (up to 87% *ee*) but also a pronounced difference in epoxide yield and *ee* values responding to matching–mismatching between chiralities of *N*-Npha-Ileu-OH and of the iron complex Me_2N PDP-PFe were observed (81 vs 51% in yield and 87 vs 49% in *ee*). We interpreted this large difference as a signature that this amino acid effectively helps in defining the structure of the active site. For comparison, when the reaction is performed in the absence of amino acid, epoxide was obtained in modest 20% yield and 46% *ee*.^[3]

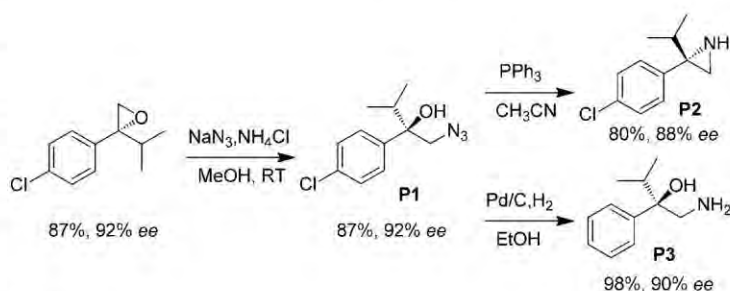
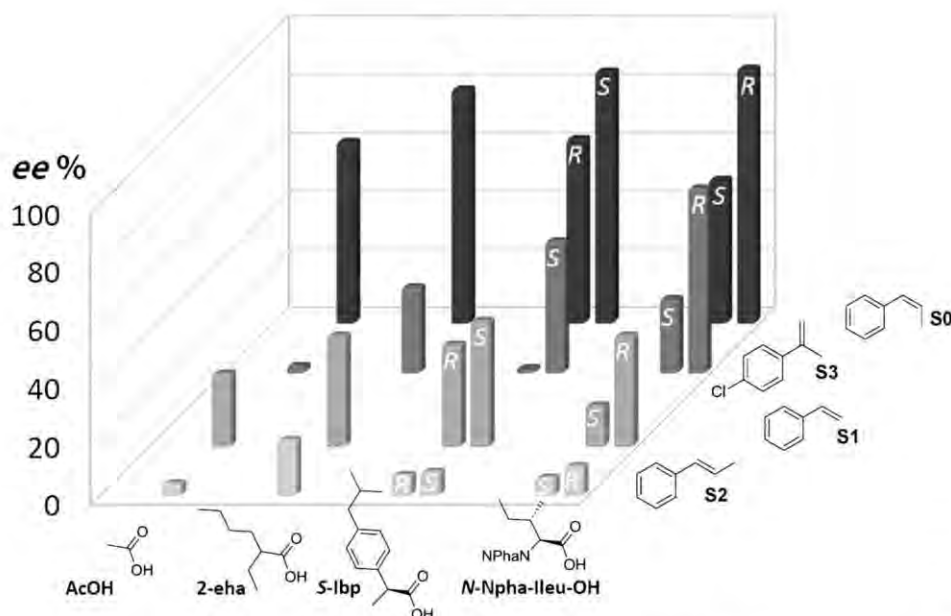

Scheme 2.


Figure 1. The stereoselectivity on epoxidation of structurally different styrenes with *R,R* and *S,S* forms of Me_2N PDP-Fe using different carboxylic acids. See supporting information for details of the reactions. *R* and *S* inside the bars refer to the chirality of Me_2N PDP-Fe. When chirality is not specified, (S,S) - Me_2N PDP-Fe was employed as the catalyst.

The benefits of using *N*-Npha-Ileu-OH and *N*-Npha-*t*-Leu-OH as acid coligand partners in asymmetric epoxidations catalyzed by Me_2N PDP-Fe was then tested against different families of substrates (Figure 1 and Table S2). Styrenes **S1–S4** differing in the substitution patterns at the olefinic site were chosen because these are recognized as a challenge for iron asymmetric epoxidation catalysis.^[6f] Furthermore results were compared with those obtained with other carboxylic acids which had previously proved to be excellent in the epoxidation of aromatic and cyclic aliphatic enones, as well as in *cis*-aromatic olefins.^[3] Most interesting from this analysis was the observa-

tion that an α -substituted styrene (**S3**) was epoxidized with values of stereoselectivity substantially better than any of the carboxylic acids previously studied. α -Alkyl substituted styrenes are particularly challenging for asymmetric catalysis because of the difficulty to differentiate between the enantiotopic faces of these substrates.^[11] To our knowledge good levels of *ee* values in their epoxidation is limited to chloroperoxidase (up to 89% *ee*)^[9a] and Shi's organocatalysts (up to 88% *ee*).^[9b] Therefore, catalytic epoxidation of a series of this class of substrates was evaluated under optimized conditions using *N*-Npha-Ileu-OH.

We examined examples of α -methylstyrene derivatives (Table 2, entries 1–3). In these cases the yields obtained were

Table 2: Substrate scope on the asymmetric epoxidation.^[a]

Entry	Substrate	Yield [%]	Npha-I-Leu-OH (ee) [%]
1		R = Cl (S3) 90	63
2		R = NO ₂ (S4) 94	66
3		R = CF ₃ (S5) 88	50
4		R = H (S6) ca. 20 (5)	84
5		R = Cl (S7) 16 (16)	87
6		R = Me (S8) 78	80
7		R = OAc (S9) 80	83
8		R = OPiv (S10) 83	81
9		R = Ph (S11) 70	80
10		R = H (S12) 60	91
11		R = Cl (S13) 87	92
12		R = F (S14) 85	91
13		R = CF ₃ (S15) 77	84
14		S16 90	97 ^[b]
15		S17 52	75
16		R = Me (S18) 79	93
17		R = H (S19) 85	91
18		R = Cl (S20) 80	94
19		R = F (S21) 85	96
20		S22 57	92
21		S23 -	-

[a] Reaction conditions are (*R,R*)-^{Me}2^NPDP-Fe (2 mol %), H₂O₂ (1.8 equiv), and *N*-Npha-I-Leu-OH (3 mol %) in CH₃CN at -30 °C during 30 min. The *ee* values and configuration are determined by chiral GC.

[b] The *ee* values are determined by ¹H NMR with europium tris [3-(heptafluoropropylhydroxymethylene)-(+)-camphorate] (see Supporting Information for details). Absolute configuration of epoxides at entries 10 and 11 are (*R*) and were determined by comparing optical rotation with that described in the literature.^[9b]

excellent (88–94 %), but enantioselectivities were moderate (50–66 % *ee*). On the other hand, replacing the α -methyl by a trifluoromethyl group (entries 4–5) the enantioselectivity increased up to 87 %, although in this case yields were small (5–16 %), presumably reflecting the poor reactivity of this electron-deficient olefin with an electrophilic reagent. Most interestingly, when the α position of styrenes was modified by sterically more demanding groups such as ethyl, isopropyl, and *tert*-butyl the enantioselectivities increased up to 97 % *ee* (entries 6–20), although the cyclohexyl derivate substrate **S17** provided a more modest *ee* value (75 %). The system tolerates *o*-, *m*- and *p*- substitutions in the aromatic ring, and also different functional groups, such as nitro, esters, and halides. On the other hand, epoxidation of α,α' -dialkyl substrates provided very low enantioselectivities (16 % *ee* for 2-methylhept-1-ene; not shown) and pyridine heterocycles inhibit the catalysis (entry 21).

To illustrate the utility of this methodology, epoxide resulting from epoxidation of **S13** (Scheme 2) was transformed into azido-alcohol **P1** with no erosion of the enantioselectivity (yield 87 %, 92 % *ee*), which can then be converted into unprotected aziridine **P2** through a Staudinger reaction (80 %, 88 % *ee*),^[12] which can be regarded as an entry into chiral amines. Alternatively, reduction of the azide using palladium under hydrogen conditions (see Scheme 2) provide the corresponding chiral 1,2-amino alcohol **P3** (yield 98 %, 90 % *ee*), which can be seen as a precursor for the synthesis of oxazolines, among other interesting products.^[13]

In summary, the present work shows the use of amino acids as suitable coligands in epoxidation reactions with aqueous H₂O₂ using bioinspired non-heme iron catalysts,^[14] extending the substrate scope of these systems to the challenging terminal olefins. The present approach is appealing as it provides proof of concept that the versatility of these systems can be extended straightforwardly towards novel classes of substrates without requiring an elaborate development of novel chiral catalysts.

Received: October 29, 2014

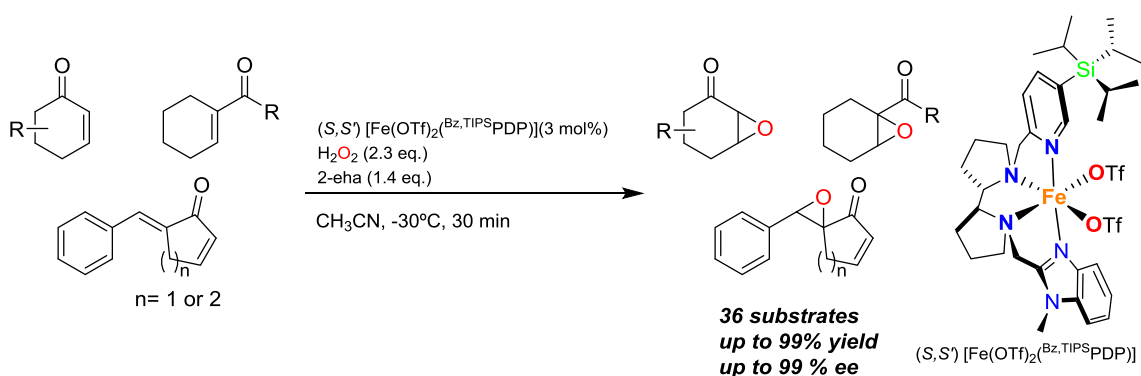
Published online: January 19, 2015

Keywords: amino acids · asymmetric catalysis · bioinspired catalysis · epoxidation · non-heme iron complexes

- [1] a) L. Que, W. B. Tolman, *Nature* **2008**, *455*, 333; b) K. P. Bryliakov, E. P. Talsi, *Coord. Chem. Rev.* **2014**, *276*, 73.
 [2] a) K. Matsumoto, T. Katsuki in *Catalytic Asymmetric Synthesis*, Wiley, Hoboken, **2010**, pp. 839; b) G. De Faveri, G. Ilyashenko, M. Watkinson, *Chem. Soc. Rev.* **2011**, *40*, 1722; c) Y. Zhu, Q. Wang, R. G. Cornwall, Y. Shi, *Chem. Rev.* **2014**, *114*, 8199; d) R. L. Davis, J. Stiller, T. Naicker, H. Jiang, K. A. Jørgensen, *Angew. Chem. Int. Ed.* **2014**, *53*, 7406–7426; *Angew. Chem.* **2014**, *126*, 7534–7556.
 [3] O. Cussó, I. Garcia-Bosch, X. Ribas, J. Lloret-Fillol, M. Costas, *J. Am. Chem. Soc.* **2013**, *135*, 14871.
 [4] Selected examples of organocatalyzed epoxidations with amino acid derivatives; a) S. Juliá, J. Masana, J. C. Vega, *Angew. Chem. Int. Ed. Engl.* **1980**, *19*, 929; *Angew. Chem.* **1980**, *92*, 968; b) S. Banfi, S. Colonna, H. Molinari, S. Juliá, J. Guixer, *Tetrahedron*

- 1984, 40, 5207; c) G. Peris, C. E. Jakobsche, S. J. Miller, *J. Am. Chem. Soc.* **2007**, 129, 8710.
- [5] a) M. B. Francis, E. N. Jacobsen, *Angew. Chem. Int. Ed.* **1999**, 38, 937; *Angew. Chem.* **1999**, 111, 987; b) N. Makita, Y. Hoshino, H. Yamamoto, *Angew. Chem. Int. Ed.* **2003**, 42, 941; *Angew. Chem.* **2003**, 115, 971; c) J. W. de Boer, W. R. Browne, S. R. Harutyunyan, L. Bini, T. D. Tiemersma-Wegman, P. L. Alsters, R. Hage, B. L. Feringa, *Chem. Commun.* **2008**, 3747; d) J. C. Lewis, *ACS Catal.* **2013**, 3, 2954.
- [6] a) S. Enthaler, K. Junge, M. Beller, *Angew. Chem. Int. Ed.* **2008**, 47, 3317; *Angew. Chem.* **2008**, 120, 3363; b) A. Correa, O. G. Mancheno, C. Bolm, *Chem. Soc. Rev.* **2008**, 37, 1108; c) C.-L. Sun, B.-J. Li, Z.-J. Shi, *Chem. Rev.* **2011**, 111, 1293; d) M. Darwish, M. Wills, *Catal. Sci. Technol.* **2012**, 2, 243; e) K. Gopalaiah, *Chem. Rev.* **2013**, 113, 3248; f) S. Rana, A. Modak, S. Maity, T. Patra, D. Maiti, *Prog. Inorg. Chem.* **2014**, 59, 1; g) F. G. Gelalcha, *Adv. Synth. Catal.* **2014**, 356, 261.
- [7] R. Noyori, M. Aoki, K. Sato, *Chem. Commun.* **2003**, 1977.
- [8] Selected examples of iron-catalyzed asymmetric epoxidations: a) Q. F. Cheng, X. Y. Xu, W. X. Ma, S. J. Yang, T. P. You, *Chin. Chem. Lett.* **2005**, 16, 1467; b) C. Marchi-Delapierre, A. Jorge-Robin, A. Thibon, S. Ménage, *Chem. Commun.* **2007**, 1166; c) F. G. Gelalcha, B. Bitterlich, G. Anilkumar, M. K. Tse, M. Beller, *Angew. Chem. Int. Ed.* **2007**, 46, 7293; *Angew. Chem.* **2007**, 119, 7431; d) F. G. Gelalcha, G. Anilkumar, M. K. Tse, A. Brückner, M. Beller, *Chem. Eur. J.* **2008**, 14, 7687; e) H.-L. Yeung, K.-C. Sham, C.-S. Tsang, T.-C. Lau, H.-L. Kwong, *Chem. Commun.* **2008**, 3801; f) M. Wu, C.-X. Miao, S. Wang, X. Hu, C. Xia, F. E. Kühn, W. Sun, *Adv. Synth. Catal.* **2011**, 353, 3014; g) Y. Nishikawa, H. Yamamoto, *J. Am. Chem. Soc.* **2011**, 133, 8432; h) F. Oddon, E. Girgenti, C. Lebrun, C. Marchi-Delapierre, J. Pecaut, S. Menage, *Eur. J. Inorg. Chem.* **2012**, 85; i) B. Wang, S. Wang, C. Xia, W. Sun, *Chem. Eur. J.* **2012**, 18, 7332; j) O. Y. Lyakin, R. V. Ottenbacher, K. P. Bryliakov, E. P. Talsi, *ACS Catal.* **2012**, 2, 1196; k) T. Niwa, M. Nakada, *J. Am. Chem. Soc.* **2012**, 134, 13538; l) V. A. Yazerski, A. Orue, T. Evers, H. Kleijn, R. J. M. K. Gebbink, *Catal. Sci. Technol.* **2013**, 3, 2810; m) L. Luo, H. Yamamoto, *Eur. J. Org. Chem.* **2014**, 35, 7803.
- [9] a) A. F. Dexter, F. J. Lakner, R. A. Campbell, L. P. Hager, *J. Am. Chem. Soc.* **1995**, 117, 6412; b) B. Wang, O. A. Wong, M.-X. Zhao, Y. Shi, *J. Org. Chem.* **2008**, 73, 9539; c) O. A. Wong, B. Wang, M.-X. Zhao, Y. Shi, *J. Org. Chem.* **2009**, 74, 6335; d) O. Boutureira, J. F. McGouran, R. L. Stafford, D. P. G. Emmerson, B. G. Davis, *Org. Biomol. Chem.* **2009**, 7, 4285; e) B. Wang, C. Miao, S. Wang, C. Xia, W. Sun, *Chem. Eur. J.* **2012**, 18, 6750.
- [10] H. Tian, X. She, H. Yu, L. Shu, Y. Shi, *J. Org. Chem.* **2002**, 67, 2435.
- [11] Representative asymmetric transformations in α -styrenes; a) H. Becker, S. B. King, M. Taniguchi, K. P. M. Vanhessche, K. B. Sharpless, *J. Org. Chem.* **1995**, 60, 3940; b) J. Mazuela, P.-O. Norrby, P. G. Andersson, O. Pàmies, M. Diéguez, *J. Am. Chem. Soc.* **2011**, 133, 13634; c) S. Monfette, Z. R. Turner, S. P. Semproni, P. J. Chirik, *J. Am. Chem. Soc.* **2012**, 134, 4561; d) E. N. Bess, M. S. Sigman, *Org. Lett.* **2013**, 15, 646; e) S. Song, S.-F. Zhu, Y.-B. Yu, Q.-L. Zhou, *Angew. Chem. Int. Ed.* **2013**, 52, 1556; *Angew. Chem.* **2013**, 125, 1596; f) L. Zhang, Z. Zuo, X. Wan, Z. Huang, *J. Am. Chem. Soc.* **2014**, 136, 15501.
- [12] C. Molinaro, A.-A. Guilbault, B. Kosjek, *Org. Lett.* **2010**, 12, 3772.
- [13] a) G. Desimoni, G. Faita, K. A. Jørgensen, *Chem. Rev.* **2006**, 106, 3561; b) G. C. Hargaden, P. J. Guiry, *Chem. Rev.* **2009**, 109, 2505.
- [14] For a discussion on the reaction mechanism and role of the carboxylic acid in H_2O_2 activation, see Ref. [3].

Iron Catalyzed Highly Enantioselective Epoxidation of Cyclic Aliphatic Enones with Aqueous H₂O₂



This chapter corresponds to the following publication:

Cussó, O.; Cianfanelli, M.; Ribas, X.; Klein Gebbink R. J. M.; Costas, M.; *J. Am. Chem. Soc.*, 2016, DOI: 10.1021/jacs.5b12681.

Reproduced with permission from Cussó, O.; Cianfanelli, M.; Ribas, X.; Klein Gebbink, R. J. M.; Costas, M. "Iron catalyzed highly enantioselective epoxidation of cyclic aliphatic enones with aqueous H₂O₂". *Journal of American Chemical Association*, num. 138, issue 8 (2016) : 2732-2738

<http://dx.doi.org/10.1021/jacs.5b12681>

Copyright © 2016 American Chemical Society

Iron Catalyzed Highly Enantioselective Epoxidation of Cyclic Aliphatic Enones with Aqueous H₂O₂

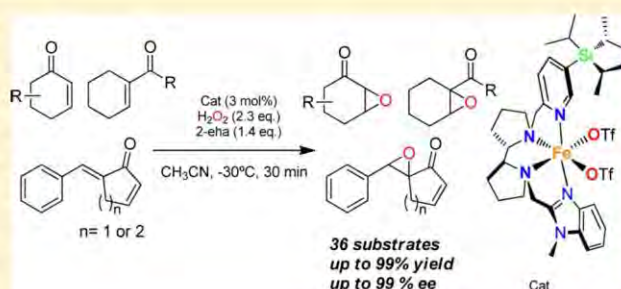
Olaf Cussó,[†] Marco Cianfanelli,[†] Xavi Ribas,[†] Robertus J. M. Klein Gebbink,^{*,‡} and Miquel Costas^{*,†}

[†]QBIS Research Group, Institut de Química Computacional i Catàlisi (IQCC) and Departament de Química, Universitat de Girona, Campus Montilivi, Girona E-17071, Catalonia Spain

[‡]Organic Chemistry & Catalysis, Debye Institute for Nanomaterials Science, Utrecht University, Universiteitsweg 99, 3584 CG Utrecht, The Netherlands

Supporting Information

ABSTRACT: An iron complex with a C₁-symmetric tetradentate N-based ligand catalyzes the asymmetric epoxidation of cyclic enones and cyclohexene ketones with aqueous hydrogen peroxide, providing the corresponding epoxides in good to excellent yields and enantioselectivities (up to 99% yield, and 95% ee), under mild conditions and in short reaction times. Evidence is provided that reactions involve an electrophilic oxidant, and this element is employed in performing site selective epoxidation of enones containing two alkene sites.



INTRODUCTION

Asymmetric epoxidation is a valuable reaction because chiral epoxides are versatile building blocks in synthetic organic chemistry.^{1–4} Catalytic epoxidation methodologies based on iron complexes and peroxides (especially H₂O₂), which can be considered as biologically inspired, are interesting because of the availability and low environmental impact of these reagents.^{5–16} Despite their appeal, the approach is challenging because it requires the design of iron coordination complexes that can activate the O—O bond of peroxides to create selective metal-based oxidants and avoid the often facile production of hydroxyl radicals via the Fenton reaction.^{10,11,17,18} Recent reports have disclosed successful examples where asymmetric epoxidation is accomplished, in some cases producing high levels of stereoselectivity (Figure 1).^{19–27} Highly enantioselective epoxidation of difficult substrates such as β,β -disubstituted aromatic enones and α -alkyl styrenes, not accessible by other methods, have also been described.^{23,24} However, a major limitation still resides in the fact that iron catalyzed asymmetric epoxidations have been limited in scope to olefins conjugated to aromatic rings^{19–35} and remains to be accomplished for aliphatic substrates. Particularly interesting are cyclic aliphatic enones. Cyclic α -epoxide enones are structures found in a number of natural products,³⁶ and are also valuable synthons that can be further elaborated into precious building blocks for organic synthesis.³⁷ However, their asymmetric epoxidation is notoriously difficult. Modest to good enantioselectivities have been obtained with chiral hydroperoxides,^{38,39} poly(amino acids) catalysts,⁴⁰ ammonium salt catalysts,^{41–43} and metal based catalysts,^{21,22,44} but excellent enantioselectivities have only been described by List^{36,45} and co-workers using cinchona alkaloid derived organocatalysts and hydrogen peroxide as oxidant. The main drawbacks of this

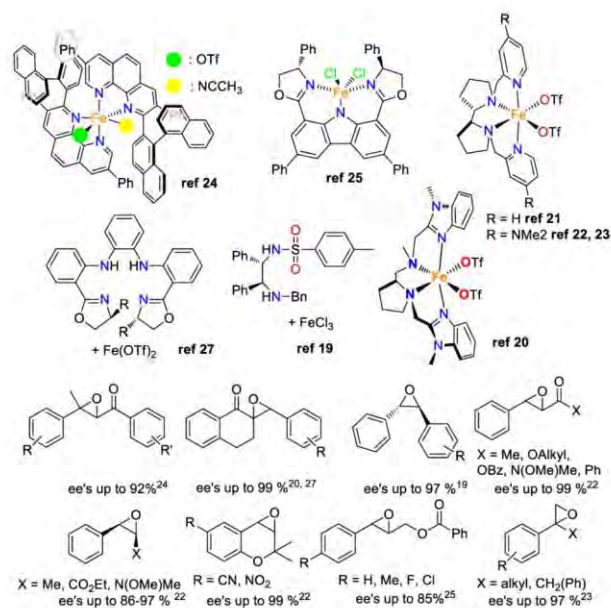


Figure 1. Representative examples of iron catalysts for asymmetric epoxidations, and current substrate scope.

system are the requirement of relatively high catalyst loadings (up to 10%) and long reaction times (from 24 to 168 h). In addition, α and α' substituted enones are not valid substrates for the system. Highly enantioselective epoxidations that could

Received: December 4, 2015

improve these aspects will be a competitive alternative. In this regard, an iron catalyzed H_2O_2 -activation methodology was envisioned as a potential option because they commonly entail powerful, fast reacting oxidants.¹² However, the high reactivity of this kind of systems can be rapidly recognized as a challenging aspect for elaborating them into highly enantioselective catalysts.

Herein, we face some of these challenges by describing the first example of an iron catalyst that epoxidizes cyclic aliphatic enones in high yields and with good to excellent stereoselectivities, employing H_2O_2 as oxidant. The optimum catalyst is C_1 -symmetric and contains a tetradentate ligand built in a modular manner by combining a bulky picoline, a benzimidazole ring, and a chiral bipyrrrolidine (catalyst 7, Figure 2). Reactions are fast (30

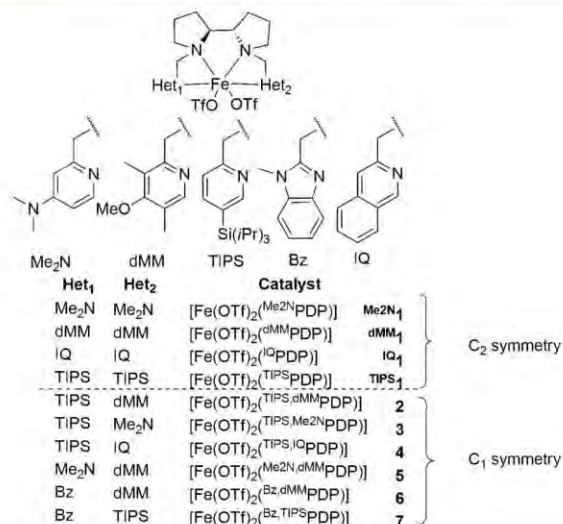


Figure 2. Schematic diagram of different catalysts employed.

min) and require relatively low catalysts loadings (1–3 mol %). Finally, it is shown that the current system operates via generation of an electrophilic oxidant, therefore differing mechanistically from asymmetric epoxidation methods described so far for this class of substrates, which operate via a Weitz–Scheffer^{45–51} mechanism where nucleophilic oxidants account for the epoxidation reaction. We show that this element represents a valuable tool for performing site selective epoxidation of enones containing two alkene sites, with orthogonal selectivity with regard to Weitz–Scheffer epoxidation agents.

RESULTS AND DISCUSSION

Catalyst Screening. Our initial screening entailed epoxidation of cyclohexenone **1**, employing different iron catalysts (details on the preparation, and characterization of the ligands and the complexes are collected in the Supporting Information, SI) with tetradentate N-based ligands (1 mol%), hydrogen peroxide as oxidant (2.3 equiv), and ethylhexanoic acid (2-eha, 1.4 equiv) as an additive necessary for helping in the controlled activation of the H_2O_2 (Table 1).^{21,22} Reactions were performed at $-30\text{ }^\circ\text{C}$ by adding H_2O_2 (during 30 min) via syringe pump to an acetonitrile solution of the substrate, the catalysts and 2-eha under air. Following H_2O_2 addition, reactions were analyzed by gas chromatography to determine conversion, epoxide yield, and stereoselectivity. Results are collected in Table 1.

Iron catalysts employed in the initial screening entailed C_2 -symmetric complexes containing tetradentate ligands based on a

Table 1. Screening of the Iron Complexes in the Asymmetric Epoxidation Reaction of 2-Cyclohexenone^a

entry	catalyst	conv (yield) % ^b	(ee)%
1	Me ₂ N ₁	85 (73)	75
2	dMM ₁	100 (94)	84
3	IQ ₁	98 (81)	72
4	TIPS ₁	87 (71)	81
5	2	100 (87)	85
6	3	90 (72)	74
7	4	100 (70)	75
8	5	99 (80)	77
9	6	73 (60)	88
10	7	67 (55)	90
11 ^c	7	100 (86)	90

^aUnless stated, reaction conditions are (*S,S'*)-catalyst (1 mol %), H_2O_2 (2.3 equiv), and 2-eha (1.4 equiv) in CH_3CN at $-30\text{ }^\circ\text{C}$ during 30 min. ^bEpoxide yields and substrate conversion determined by GC. ^c*Ee*'s determined by GC with a chiral stationary phase. The absolute configuration (2*R*,3*R*) of the epoxide was determined from its optical rotation, and by comparison from the literature.²¹ ^c3 mol % of catalyst.

bis-pyrrolidine and two-heterocyclic amine binding units (Figure 2, Me₂N₁, dMM₁, IQ₁, and TIPS₁ Table 1, entries 1–4). The heterocycles included electron-rich pyridines (entries 1–2, Me₂N₁ and dMM₁), isoquinoline (entry 3, IQ₁), and bulky pyridines (entry 4, TIPS₁). We were quite pleased to observe that the complexes provided good to excellent *ee*'s (from 72 to 84% *ee*) and good product yields (71–94%) in the epoxidation of the model substrate. C_1 -symmetric complexes (2–7) with distinct heterocyclic arms were subsequently considered (entries 5–11). Most interestingly, catalysts that combine an *N*-methylbenzimidazole ring and either an *e*-rich pyridine (6, entry 9), or a bulky pyridine (7, entries 10–11) provided the corresponding epoxide with excellent enantioselectivities (88–90 *ee*). In the case of 7, the epoxide was obtained in a modest 55% yield that could be subsequently optimized to a good yield (86%) while retaining the high level of enantioselectivity by employing 3 mol % catalyst. Replacement of 2-eha by other carboxylic acids^{22,23} did not produce an improvement in the stereoselectivity of the reaction.

Characterization of the Catalyst. Structural characterization of 7 in the solid state was accomplished by single crystal X-ray diffraction analysis (Figure 3, and SI for crystallographic details). The structure corresponds to an octahedrally coordi-

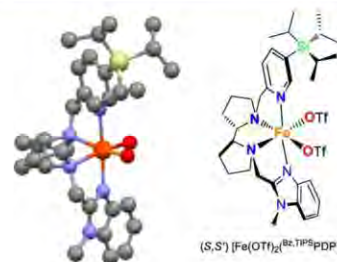


Figure 3. ORTEP diagram of the single crystal X-ray determined structure of (*S,S'*)-7 is shown. Triflate groups were omitted for clarity, except for the oxygen atoms directly bound to the iron center.

Table 2. Substrate Scope of Aliphatic Cyclic Enones in Asymmetric Epoxidation Reaction with 7 as Catalyst

Entry	Substrate	Isol. yield (%)	(ee)%	Entry	Substrate	Isol. yield (%)	(ee)%
1	(S2)	75	90	^a 13	(S13)	40(30)	66
2	(S1)	75	90	14	(S14)	63	90
3	(S3)	66	84	15	(S15)	72	92
4	(S4)	99	81	16	(S16)	78	90
^a 5	(S5)	100(84)	65	17	(S17)	65	95
^a 6	(S6)	100(82)	62	18	(S18)	74	95
7	(S7)	-	-	19	(S19)	71	89
^a 8	(S8)	92(71)	76	20	(S20)	82	85
^a 9	(S9)	100(80)	80	21	(S21)	78	91
10	(S10)	81	70	22	(S22)	73	85
11	(S11)	75	82	23	(S23)	35	92
12	(S12)	80	84				

Unless stated, reaction conditions are (*S,S'*)-7 (3 mol %), H₂O₂ (2.3 equiv) and 2-eha (1.4 equiv) in CH₃CN at -30 °C during 30 min. ^aSubstrate conversion and epoxide yields (in parentheses) determined by GC. ^b10 mol % catalyst. Ee's determined by GC with a chiral stationary phase.

nated iron center, adopting a *cis-α* topological geometry, with the two heterocycles *trans* to each other and the two labile triflate anions *cis* to each other. The binding O atoms of the triflate ligands and the iron center define a plane roughly perpendicular

to an hypothetical N_{py}—N_{BzIm} axis. Fe—N and Fe—O distances are ~2.1–2.2 Å, indicative of a high spin center. ¹H NMR analyses in CD₃CN indicate that the high spin state is retained in

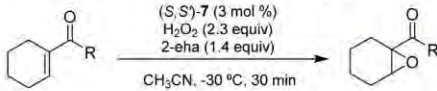
solution, being the number of signals consistent with its C_1 symmetry (see S1).

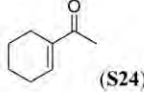
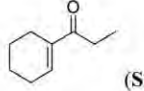
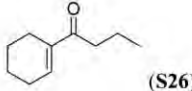
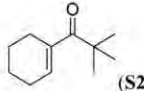
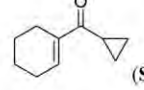
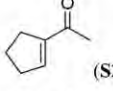
Substrate Scope. The substrate scope in the asymmetric epoxidation of a series of cyclic aliphatic enones (Table 2) catalyzed by **7** was determined using the optimized conditions. In the first place, it was observed that epoxidation of 2-cyclopentenone, a substrate that is recognized as particularly challenging,³⁶ proceeds with excellent yield and enantioselectivity (Table 2, entry 1), but a slight erosion of stereoselectivity was observed when the enone ring was enlarged up to 7 and 8 member rings (84% and 81% ee, respectively, entries 3 and 4). Substitutions in the two sides of the cyclic enone produced different effects in the level of enantioselectivity of the reactions. In general, substitutions at the olefinic side (α and β) decrease ee's, while substitutions at the opposite side (α' and β') lead to important improvement. For example, alkyl substitution at the α position of 5 and 6-member ring enones caused a significant decrease in ee's (62–65% ee, entries 5–6), that could be partially rescued by employing **2** as catalyst (for **S5** 75% yield and 76% ee, and for **S6** 81% yield and 75% ee). Also, for the *tert*-butyl group in the α position, the reaction did not take place (entry 7, **S7**). Although the current ee values leave room for improvement, it should be stated that the current catalysts constitute the first ones that provide good enantioselectivities for these substrates. β -alkylated cyclic enones also gave slightly lower enantioselectivities in comparison with the parent cyclic unsubstituted enones (see entries 8–13); isopropyl and ethyl β -substitution in 2-cyclohexenone provided more modest ee's (66 and 70% ee, entries 13 and 10, respectively) while β -alkyl substituted 2-cyclohexenones with methyl, propyl and butyl chains are epoxidized with high enantioselection (entries 9, 11 and 12, 80–84% ee). Most interestingly, the introduction of a *gem*-dimethyl group at positions α' , β' , or γ results in a very substantial improvement of the enantioselectivities. Particularly outstanding enantioselectivities were obtained for substrates with *gem*-dimethyl substitution in position α' (entries 15–18, 90–95% ee). This is a particularly relevant result since there is no alternative method for the asymmetric epoxidation of this type of substrates. Substitution at the position β' also provided high enantiomeric excesses (between 85 and 91% ee, entries 14, 19–22). Of note, natural product isophorone (entry 19) was epoxidized in 71% isolated yield and 89% ee. Substitution at position γ also enhanced enantioselectivity (92% ee, entry 23), although in this case the epoxide was obtained in a modest 35% isolated yield. The relatively modest yields of epoxides bearing bulky and rigid substituents in close proximity to the olefinic site (entries 13 and 23) suggest that steric hindrance may be limiting these reactions.

Remarkably, cyclohexene-1-kenones were also epoxidized in good yields and excellent enantioselectivities. Optimum stereoselectivities were obtained with different alkyl chains (87–92% ee, Table 3, entries 1–3). For branched groups, such as *tert*-butyl and cyclopropyl, the enantioselectivities decreased slightly (entries 4 and 5), and a significant decrease in enantioselectivity was also obtained for the 5-membered cyclopentene rings (entry 6). Of interest is the observation that the epoxidation of the cyclopropyl derived substrate produces the epoxide without detectable amounts of cyclopropane ring opening products.

The relevance of the levels of enantioselectivity obtained with **7** can be best estimated when reactions are placed into context with the methodologies reported in the literature (Scheme 1). For comparison, a single example exists in the literature where the related allylic alcohol is epoxidized with excellent ee's by

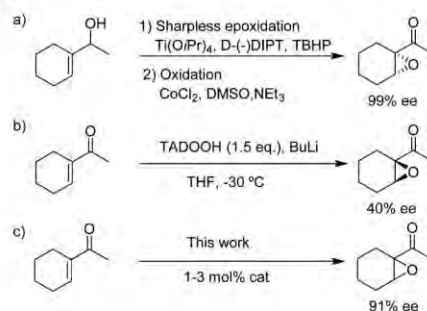
Table 3. Substrate Scope with **7** as Catalyst



Entry	Substrate	Isol. yield (%)	(ee)%
1	 (S24)	98	91
^a 2	 (S25)	77	87
^a 3	 (S26)	80	92
4	 (S27)	88	80
5	 (S28)	65	74
^b 6	 (S29)	100(74)	71

Unless stated, reaction conditions are (*S,S'*)-**7** (3 mol %), H₂O₂ (2.3 equiv) and 2-eha (1.4 equiv) in CH₃CN at -30 °C during 30 min. ^a4 mol % catalyst. ^bEpoxide yields and substrate conversion determined by GC for numbers in parentheses. Ee's determined by GC with a chiral stationary phase.

Scheme 1. Examples in the Literature for Epoxidation of 1-Acetyl-1-cyclohexene



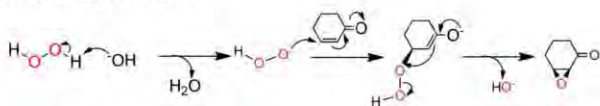
using Sharpless epoxidation, then followed by the oxidation of the alcohol to the ketone using CoCl₂ (Scheme 1a).⁵² However, direct epoxidation of the ketone has been performed with modest enantioselectivity using a chiral hydroperoxide (Scheme 1b).³⁸ To the best of our knowledge, this is the first example of a catalytic methodology that can epoxidize this kind of olefins with excellent ee's.

Mechanistic Studies. Asymmetric epoxidation of cyclic enones has been so far performed via nucleophilic attack of peroxide agents at the olefinic site, activated via formation of an

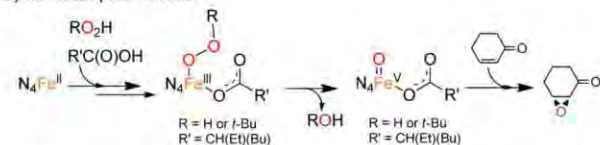
imine/iminium from reaction between the ketone moiety and a primary/secondary amine organocatalyst. This can be regarded as a variant of the Weitz–Scheffer epoxidation mechanism, where a basic peroxide is responsible for the initial attack at the β -carbon of the unsaturated carbonyl compound (Scheme 2a).^{45–51} However, activation of H_2O_2 by iron catalysts most

Scheme 2. Mechanistic Scenarios for the Asymmetric Epoxidation of a Cyclic Enone⁴⁴

a) via nucleophilic oxidant



b) via electrophilic oxidant

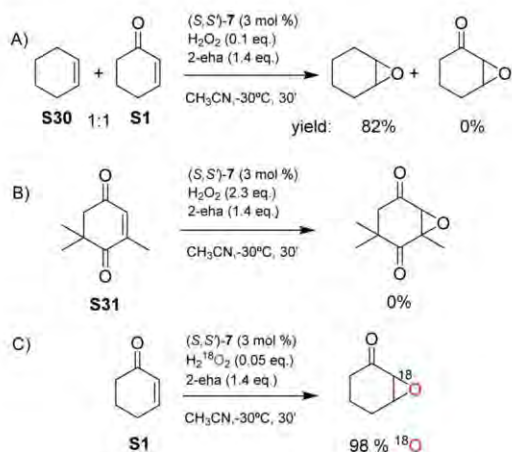


^a(A) Nucleophilic Weitz–Scheffer epoxidation mechanism and (B) electrophilic oxidation via a high valent iron oxo species.²²

commonly leads to electrophilic oxidants, and this has proven to be the case for the enantioselective epoxidation of aromatic enones with **1**.^{21,22,53–56} Nevertheless, examples for nucleophilic behavior have also been documented for related catalysts in olefin oxidation reactions.⁵⁷ Mechanistic studies were therefore performed to address this question. Evidence for the presence of an electrophilic oxidant was gathered by competitive epoxidation of a mixture of cyclohexene (**S30**) and 2-cyclohexenone (**S1**) under oxidant-limiting conditions, observing that the epoxidation only takes place at the more electron-rich olefin (Scheme 3a). Likewise, the more electron-deficient enone **S31** could not be epoxidized (Scheme 3b).

Further mechanistic studies indicate the reaction mechanism of these iron catalysts is highly reminiscent of the one operating in P450^{58,59} and in nonheme iron dependent oxygenases, such as the family of Rieske oxygenases.^{60,61} In first place, isotopic

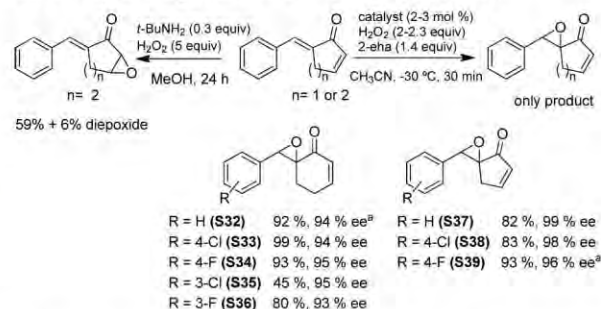
Scheme 3. (a) Competitive Epoxidation Experiment of Cyclohexene (**S30**) and 2-Cyclohexenone (**S1**), (b) the Epoxidation of Electron Deficient Olefin **S31**, and (c) Epoxidation of **S1** Using $\text{H}_2^{18}\text{O}_2$



analysis shows that hydrogen peroxide is the exclusive source of oxygen atoms that end up in the epoxide (Scheme 3c), discarding water and atmospheric O_2 as alternative sources. Indeed, reactions with O_2 as the sole oxidant do not produce the epoxide. In addition, the use of *tert*-butyl hydroperoxide instead of hydrogen peroxide in the catalytic oxidation of 2-cyclohexenone yields the epoxide in 50% of yield and 91% ee (compare with 75% yield and 90% ee with H_2O_2). The virtually common stereoselectivity irrespective of the oxidant employed constitutes strong evidence that a common oxygen atom transfer agent is formed with both oxidants. Therefore, the sum of the experimental observations are consistent with a mechanistic scheme early proposed for structurally related catalysts^{22,23} where the carboxylic acid (**2-eha**) assists the cleavage of the O—O bond, forming a carboxylate bound high valent $\text{Fe}=\text{O}$ species, which is highly electrophilic and performs the oxygen atom transfer reaction (Scheme 2b).⁶²

Regioselective Epoxidation of Diolefins. The electrophilic character of the active species can indeed find utility in the oxidation of substrates bearing olefinic moieties with distinct electronic properties. Thus, substrates **S32–S39** were subjected to oxidation under standard conditions using **Me2N1** or **7**, providing the product resulting from epoxidation at the more electron-rich site in excellent yields and stereoselectivities (Scheme 4, right),

Scheme 4. Asymmetric Epoxidation of Dienones with **Me2N1** or **7** as Catalysts (Right) and with Basic H_2O_2 (Left)



Unless stated, reaction conditions are (*S,S*)-**Me2N1** (2 mol %), H_2O_2 (2 equiv) and **2-eha** (1.4 equiv) in CH_3CN at $-30\text{ }^\circ\text{C}$ during 30 min. ^a(*S,S'*)-**7** (3 mol %), H_2O_2 (2.3 equiv), and **2-eha** (1.4 equiv) in CH_3CN at $-30\text{ }^\circ\text{C}$ during 30 min. ^bEe's determined by HPLC with a chiral stationary phase.

94–99% ee). Instead, epoxidation with basic hydrogen peroxide (*t*-Bu-NH₂ and H_2O_2) provided preferential oxidation at the cyclic aliphatic enone (59% yield, along with 6% of a diepoxide, Scheme 4 left more details SI). Therefore, asymmetric epoxidation with these iron catalysts is orthogonal with enamine catalysis.

CONCLUSIONS

In conclusion, this work describes high yield and highly enantioselective epoxidation of cyclic enones with a C_1 symmetric iron coordination complex that combines a bulky pyridine and a benzimidazole in its structure. Reactions are performed in short reaction times, employing aqueous hydrogen peroxide as oxidant. These features make this system a compelling alternative to methodologies with cinchona alkaloid organocatalysts, in some cases complementing its substrate scope. Furthermore, this work constitutes the first example where highly enantioselective (>90% ee) epoxidation of non-

aromatic substrates with iron catalysis is described, and also the first example of an enantioselective electrophilic oxidation of this challenging class of substrates. This element confers the system with an orthogonal selectivity with regard to enamine catalysis that can find use in the site selective enantioselective epoxidation of polyene substrates. Finally, the design of C_1 symmetric complexes where the electronic and steric properties of distinct heterocycles are combined constitutes a novel aspect in the design of this class of catalysts. Further studies will be devoted to extend the development of this class of catalysts in order to improve enantioselectivities and to expand their application to oxidation of other families of challenging substrates.

■ ASSOCIATED CONTENT

Supporting Information

The Supporting Information is available free of charge on the ACS Publications website at DOI: 10.1021/jacs.5b12681.

Experimental details for the preparation and characterization of ligands and metal complexes. Experimental details of catalytic reactions, and spectroscopic data for product characterization (PDF) (CIF)

■ AUTHOR INFORMATION

Corresponding Authors

*r.j.m.kleingebink@uu.nl

*miquel.costas@udg.edu

Notes

The authors declare no competing financial interest.

■ ACKNOWLEDGMENTS

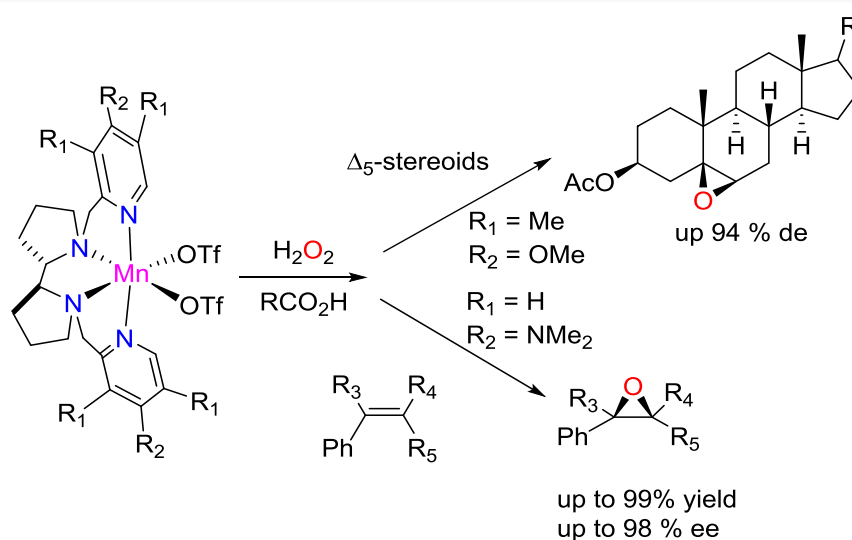
We acknowledge financial support from European Research Council (ERC-2009-StG-239910), MINECO of Spain (CTQ2012-37420-C02-01/BQU, Consolider-Ingenio CSD2010-00065), and the Catalan DIUE of the Generalitat de Catalunya (2009SGR637). X.R. and M.C. thank ICREA-Academia awards. We thank STR's from UdG for technical support.

■ REFERENCES

- (1) Matsumoto, K.; Katsuki, T. In *Catalytic Asymmetric Synthesis*, 3rd ed.; Ojima, I., Ed.; John Wiley & Sons, Inc.: Hoboken, NJ, 2010; p 839.
- (2) De Faveri, G.; Ilyashenko, G.; Watkinson, M. *Chem. Soc. Rev.* **2011**, *40*, 1722.
- (3) Zhu, Y.; Wang, Q.; Cornwall, R. G.; Shi, Y. *Chem. Rev.* **2014**, *114*, 8199.
- (4) Davis, R. L.; Stiller, J.; Naicker, T.; Jiang, H.; Jorgensen, K. A. *Angew. Chem., Int. Ed.* **2014**, *53*, 7406.
- (5) Que, L.; Tolman, W. B. *Nature* **2008**, *455*, 333.
- (6) Enthaler, S.; Junge, K.; Beller, M. *Angew. Chem., Int. Ed.* **2008**, *47*, 3317.
- (7) Correa, A.; Mancheno, O. G.; Bolm, C. *Chem. Soc. Rev.* **2008**, *37*, 1108.
- (8) Bauer, E. B. *Curr. Org. Chem.* **2008**, *12*, 1341.
- (9) Liu, L.-X. *Curr. Org. Chem.* **2010**, *14*, 1099.
- (10) Darwish, M.; Wills, M. *Catal. Sci. Technol.* **2012**, *2*, 243.
- (11) Gopalaiah, K. *Chem. Rev.* **2013**, *113*, 3248.
- (12) Cusso, O.; Ribas, X.; Costas, M. *Chem. Commun.* **2015**, *51*, 14285.
- (13) Gelalcha, F. G. *Adv. Synth. Catal.* **2014**, *356*, 261.
- (14) Wang, C.; Yamamoto, H. *Chem. - Asian J.* **2015**, *10*, 2056.
- (15) Fingerhut, A.; Serdyuk, O. V.; Tsoogoeva, S. B. *Green Chem.* **2015**, *17*, 2042.
- (16) For selected examples of Fe-catalyzed epoxidation reactions, see:
(a) White, M. C.; Doyle, A. G.; Jacobsen, E. N. *J. Am. Chem. Soc.* **2001**, *123*, 7194. (b) Chen, K.; Costas, M.; Kim, J.; Tipton, A. K.; Que, L., Jr. *J. Am. Chem. Soc.* **2002**, *124*, 3026. (c) Dubois, G.; Murphy, A.; Stack, T. D. P. *Org. Lett.* **2003**, *5*, 2469. (d) Bukowski, M. R.; Comba, P.; Lienke, A.; Limberg, C.; de Laorden, C. L.; Mas-Balleste, R.; Merz, M.; Que, L., Jr. *Angew. Chem., Int. Ed.* **2006**, *45*, 3446. (e) Anilkumar, G.; Bitterlich, B.; Gelalcha, F. G.; Tse, M. K.; Beller, M. *Chem. Commun.* **2007**, *3*, 289. (f) Liu, P.; Wong, E. L.; Yuen, A. W.; Che, C. *Org. Lett.* **2008**, *10*, 3275. (g) Company, A.; Feng, Y.; Güell, M.; Ribas, X.; Luis, J. M.; Que, L., Jr.; Costas, M. *Chem. - Eur. J.* **2009**, *15*, 3359. (h) Schröder, K.; Enthaler, S.; Join, B.; Junge, K.; Beller, M. *Adv. Synth. Catal.* **2010**, *352*, 1771. (i) Schroeder, K.; Enthaler, S.; Bitterlich, B.; Schulz, T.; Spannenberg, A.; Tse, M. K.; Junge, K.; Beller, M. *Chem. - Eur. J.* **2009**, *15*, 5471. (j) Schröder, K.; Join, B.; Amali, A. J.; Junge, K.; Ribas, X.; Costas, M.; Beller, M. *Angew. Chem., Int. Ed.* **2011**, *50*, 1425. (k) Mikhalyova, E. A.; Makhlynets, O. V.; Palluccio, T. D.; Filatov, A. S.; Rybak-Akimova, E. V. *Chem. Commun.* **2012**, *48*, 687. (l) Perandones, B. F.; Nieto, E. D.; Godard, C.; Castillon, S.; De Frutos, P.; Claver, C. *ChemCatChem* **2013**, *5*, 1092. (m) Skobeev, I. Y.; Kudrik, E. V.; Zalomaeva, O. V.; Albrieux, F.; Afanasiev, P.; Kholdeeva, O. A.; Sorokin, A. B. *Chem. Commun.* **2013**, *49*, 5577. (n) Clemente-Tejada, D.; López-Moreno, A.; Bermejo, F. A. *Tetrahedron* **2013**, *69*, 2977. (o) Kuck, J. W.; Raba, A.; Markovits, I. I. E.; Cokoja, M.; Kuhn, F. E. *ChemCatChem* **2014**, *6*, 1882. (p) Chishiro, T.; Kon, Y.; Nakashima, T.; Goto, M.; Sato, K. *Adv. Synth. Catal.* **2014**, *356*, 623. (q) Kück, J. W.; Anneser, M. R.; Hofmann, B.; Pöthig, A.; Cokoja, M.; Kühn, F. E. *ChemSusChem* **2015**, *8*, 4056.
(17) Oloo, W. N.; Que, L., Jr. *Acc. Chem. Res.* **2015**, *48*, 2612.
(18) Talsi, E. P.; Bryliakov, K. P. *Coord. Chem. Rev.* **2012**, *256*, 1418.
(19) Gelalcha, F. G.; Bitterlich, B.; Anilkumar, G.; Tse, M. K.; Beller, M. *Angew. Chem., Int. Ed.* **2007**, *46*, 7293.
(20) Wang, B.; Wang, S.; Xia, C.; Sun, W. *Chem. - Eur. J.* **2012**, *18*, 7332.
(21) Lyakin, O. Y.; Ottenbacher, R. V.; Bryliakov, K. P.; Talsi, E. P. *ACS Catal.* **2012**, *2*, 1196.
(22) Cussó, O.; Garcia-Bosch, I.; Ribas, X.; Lloret-Fillol, J.; Costas, M. *J. Am. Chem. Soc.* **2013**, *135*, 14871.
(23) Cussó, O.; Ribas, X.; Lloret-Fillol, J.; Costas, M. *Angew. Chem., Int. Ed.* **2015**, *54*, 2729.
(24) Nishikawa, Y.; Yamamoto, H. *J. Am. Chem. Soc.* **2011**, *133*, 8432.
(25) Niwa, T.; Nakada, M. *J. Am. Chem. Soc.* **2012**, *134*, 13538.
(26) Luo, L.; Yamamoto, H. *Eur. J. Org. Chem.* **2014**, *2014*, 7803.
(27) Dai, W.; Li, G.; Chen, B.; Wang, L.; Gao, S. *Org. Lett.* **2015**, *17*, 904.
(28) Kaku, Y.; Otsuka, M.; Ohno, M. *Chem. Lett.* **1989**, *18*, 611.
(29) Francis, M. B.; Jacobsen, E. N. *Angew. Chem., Int. Ed.* **1999**, *38*, 937.
(30) Cheng, Q. F.; Xu, X. Y.; Ma, W. X.; Yang, S. J.; You, T. P. *Chin. Chem. Lett.* **2005**, *16*, 1467.
(31) (a) Marchi-Delapierre, C.; Jorge-Robin, A.; Thibon, A.; Ménage, S. *Chem. Commun.* **2007**, *11*, 1166. (b) Oddon, F.; Girgenti, E.; Lebrun, C.; Marchi-Delapierre, C.; Pecaut, J.; Menage, S. *Eur. J. Inorg. Chem.* **2012**, *2012*, 85.
(32) (a) Gelalcha, F. G.; Anilkumar, G.; Tse, M. K.; Brückner, A.; Beller, M. *Chem. - Eur. J.* **2008**, *14*, 7687.
(33) Yeung, H.-L.; Sham, K.-C.; Tsang, C.-S.; Lau, T.-C.; Kwong, H.-L. *Chem. Commun.* **2008**, 3801.
(34) Wu, M.; Miao, C.-X.; Wang, S.; Hu, X.; Xia, C.; Kühn, F. E.; Sun, W. *Adv. Synth. Catal.* **2011**, *353*, 3014.
(35) Wang, B.; Lee, Y.-M.; Seo, M. S.; Nam, W. *Angew. Chem., Int. Ed.* **2015**, *54*, 11740.
(36) Lee, A.; Reisinger, C. M.; List, B. *Adv. Synth. Catal.* **2012**, *354*, 1701.
(37) Uteuliyev, M. M.; Nguyen, T. T.; Coltart, D. M. *Nat. Chem.* **2015**, *7*, 1024.
(38) Aoki, M.; Seebach, D. *Helv. Chim. Acta* **2001**, *84*, 187.
(39) Kienle, M.; Argyrakakis, W.; Baro, A.; Laschat, S. *Tetrahedron Lett.* **2008**, *49*, 1971.
(40) Julia, S.; Guixer, J.; Masana, J.; Rocas, J.; Colonna, S.; Annuziata, R.; Molinari, H. J. *Chem. Soc., Perkin Trans. 1* **1982**, 1317.
(41) Macdonald, G.; Alcaraz, L.; Lewis, N. J.; Taylor, R. J. K. *Tetrahedron Lett.* **1998**, *39*, 5433.

- (42) Barrett, A. G. M.; Blaney, F.; Campbell, A. D.; Hamprecht, D.; Meyer, T.; White, A. J. P.; Witty, D.; Williams, D. J. *J. Org. Chem.* **2002**, *67*, 2735.
- (43) Adam, W.; Rao, P. B.; Degen, H.-G.; Levai, A.; Patonay, T.; Saha-Möller, C. R. *J. Org. Chem.* **2002**, *67*, 259.
- (44) (a) Wang, B.; Miao, C.-X.; Wang, S.-F.; Kühn, F. E.; Xia, C.-G.; Sun, W. *J. Organomet. Chem.* **2012**, *715*, 9. (b) Wang, B.; Miao, C.; Wang, S.; Xia, C.; Sun, W. *Chem. - Eur. J.* **2012**, *18*, 6750.
- (45) (a) Wang, X.; Reisinger, C. M.; List, B. *J. Am. Chem. Soc.* **2008**, *130*, 6070. (b) Lifchits, O.; Mahlau, M.; Reisinger, C. M.; Lee, A.; Fares, C.; Polyak, I.; Gopakumar, G.; Thiel, W.; List, B. *J. Am. Chem. Soc.* **2013**, *135*, 6677.
- (46) Weitz, M. S. A. *Ber. Dtsch. Chem. Ges. B* **1921**, *54*, 2327.
- (47) Wang, Z. In *Comprehensive Organic Name Reactions and Reagents*; John Wiley & Sons, Inc.: Hoboken, NJ, 2010.
- (48) Bunton, C. A.; Minkoff, G. J. *J. Chem. Soc.* **1949**, 665.
- (49) House, H. O.; Ro, R. S. *J. Am. Chem. Soc.* **1958**, *80*, 2428.
- (50) Kelly, D. R.; Caroff, E.; Flood, R. W.; Heal, W.; Roberts, S. M. *Chem. Commun.* **2004**, 2016.
- (51) Kelly, D. R.; Roberts, S. M. *Biopolymers* **2006**, *84*, 74.
- (52) Nomura, K.; Matsubara, S. *Chem. - Asian J.* **2010**, *5*, 147.
- (53) Mas-Balleste, R.; Que, L., Jr. *J. Am. Chem. Soc.* **2007**, *129*, 15964.
- (54) Lyakin, O. Y.; Zima, A. M.; Samsonenko, D. G.; Bryliakov, K. P.; Talsi, E. P. *ACS Catal.* **2015**, *5*, 2702.
- (55) Wang, Y.; Janardanan, D.; Usharani, D.; Han, K.; Que, L.; Shaik, S. *ACS Catal.* **2013**, *3*, 1334.
- (56) Lyakin, O. Y.; Bryliakov, K. P.; Talsi, E. P. *Inorg. Chem.* **2011**, *50*, 5526.
- (57) Fujita, M.; Costas, M.; Que, J. L. *J. Am. Chem. Soc.* **2003**, *125*, 9912.
- (58) Shaik, S.; Cohen, S.; Wang, Y.; Chen, H.; Kumar, D.; Thiel, W. *Chem. Rev.* **2010**, *110*, 949.
- (59) Meunier, B.; de Visser, S. P.; Shaik, S. *Chem. Rev.* **2004**, *104*, 3947.
- (60) Chakrabarty, S.; Austin, R. N.; Deng, D.; Groves, J. T.; Lipscomb, J. D. *J. Am. Chem. Soc.* **2007**, *129*, 3514.
- (61) Barry, S. M.; Challis, G. L. *ACS Catal.* **2013**, *3*, 2362.
- (62) Serrano-Plana, J.; Oloo, W. N.; Acosta-Rueda, L.; Meier, K. K.; Verdejo, B.; Garcia-Espana, E.; Basallote, M. G.; Munck, E.; Que, L., Jr.; Company, A.; Costas, M. *J. Am. Chem. Soc.* **2015**, *137*, 15833.

Highly Stereoselective Epoxidation with H_2O_2 Catalyzed by
Electron-Rich Aminopyridine Manganese Catalysts



This chapter corresponds to the following publication:

Cussó, O.; Garcia-Bosch, I.; Font, D.; Ribas, X.; Lloret-Fillol J.; Costas, M. *Org. Lett.*, 2013, **15**, 6158-6161.

Reproduced with permission from Cussó, O.; Garcia-Bosch, I.; Font, D.; Ribas, X.; Lloret-Fillol, J.; Costas, M. "Highly Stereoselective Epoxidation with H₂O₂ Catalyzed by Electron-Rich Aminopyridine Manganese Catalysts". *Organic Letters*, num. 15, issue 24 (2013) : 6158-6161

<http://dx.doi.org/10.1021/ol403018x>

Copyright © 2013 American Chemical Society

Highly Stereoselective Epoxidation with H₂O₂ Catalyzed by Electron-Rich Aminopyridine Manganese Catalysts

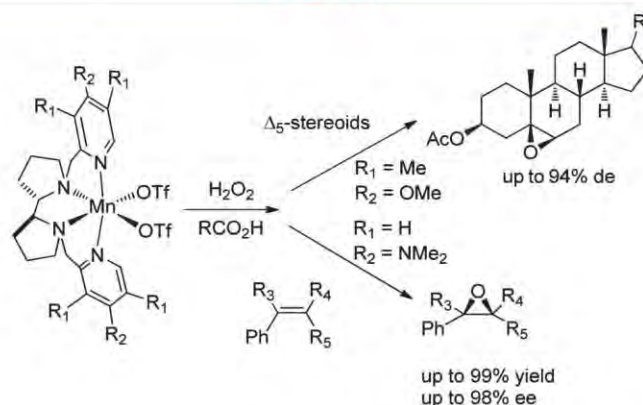
Olaf Cussó, Isaac Garcia-Bosch, David Font, Xavi Ribas, Julio Lloret-Fillol, and Miquel Costas*

Institut de Química Computacional i Catàlisi (IQCC), and Departament de Química, Universitat de Girona, Campus de Montilivi, E-17071 Girona, Catalonia, Spain

miquel.costas@udg.edu

Received October 21, 2013

ABSTRACT



Fast, efficient, and highly stereoselective epoxidation with H₂O₂ is reached by manganese coordination complexes with e-rich aminopyridine tetradentate ligands. It is shown that the electronic properties of these catalysts vary systematically with the stereoselectivity of the O-atom transfer event and exert fine control over the activation of hydrogen peroxide, reducing the amount of carboxylic acid co-catalyst necessary for efficient operation.

Asymmetric epoxidation is an important reaction in organic synthesis because of the versatility of epoxides as useful intermediates in the preparation of a diverse array of functional molecules.^{1,2} Current challenges for this reaction lay in finding environmentally more sustainable methods; for example, oxidations with catalysts based on first-row, non-toxic earth-abundant metals and oxidants exhibiting good atom economy that generate minimum waste are highly desirable. In this regard, selected manganese

coordination complexes with aminopyridine-based ligands have emerged as efficient oxidation catalysts. Seminal studies by Stack and co-workers described [Mn(CF₃SO₃)₂-(*R,R*-MCP)], MCP = *N,N'*-bis(2-pyridylmethyl)-*N,N'*-dimethyl-*trans*-1,2-diaminocyclohexane as a very active epoxidation catalyst employing peracetic acid (AcOOH) as oxidant.³ Further elaboration of the manganese complex by Sun et al. led to the development of a catalyst that showed good enantioselectivity in the epoxidation of chalcones.⁴ Hydrogen peroxide constitutes a particularly interesting oxidant, but its use in manganese-catalyzed reactions is challenging because of competing hydrogen peroxide disproportionation reactions. Garcia-Bosch et al. showed that hydrogen peroxide could be used as terminal

(1) (a) Sundermeier, U.; Döbler, C.; Beller, M. *Modern Oxidation Methods*. Wiley-VCH: Weinheim, 2004. (b) Lane, B. S.; Burgess, K. *Chem. Rev.* **2003**, *103*, 2457. (c) Saisaha, P.; de Boer, J.; Browne, W. *Chem. Soc. Rev.* **2013**, *42*, 2059.

(2) (a) Katsuki, T. In *Catalytic Asymmetric Synthesis*, 2nd ed.; Ojima, I., Ed.; Wiley-VCH: New York, 2000; p 287. (b) De Faveri, G.; Ilyashenko, G.; Watkinson, M. *Chem. Soc. Rev.* **2011**, *40*, 1722. (c) Chatterjee, D. *Coord. Chem. Rev.* **2008**, *252*, 176. (d) Wong, O. A.; Shi, Y. *Chem. Rev.* **2008**, *108*, 3958. (e) Diez, D.; Nunez, M. G.; Anton, A. B.; Garcia, P.; Moro, R. F.; Garrido, N. M.; Marcos, I. S.; Basabe, P.; Urones, J. G. *Curr. Org. Synth.* **2008**, *5*, 186. (f) Darwish, M.; Wills, M. *Catal. Sci. Technol.* **2012**, *2*, 243. (g) Gopalaiah, K. *Chem. Rev.* **2013**, *113*, 3248.

(3) Murphy, A.; Dubois, G.; Stack, T. D. P. *J. Am. Chem. Soc.* **2003**, *125*, 5250–5251.

(4) Wu, M.; Wang, B.; Wang, S.; Xia, C.; Sun, W. *Org. Lett.* **2009**, *11*, 3622.

oxidant with this type of catalysts in the presence of acetic acid (14 equiv).⁵ Subsequently, several manganese catalysts containing aminopyridine tetradentate ligands have been described to efficiently operate under these experimental conditions.⁶ Good to excellent enantioselectivities have been obtained in the epoxidation of chalcones, but rational strategies for further improvement of these catalysts allowing for extending their rather narrow substrate scope, and hopefully without requiring extensive trial and error testing, need to be developed.

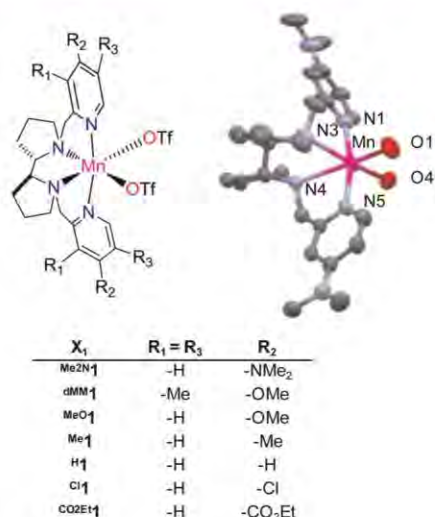


Figure 1. Manganese complexes studied and an ORTEP diagram of the X-ray-determined structure of (*R,R*)-Me₂N₁. For clarity, H atoms and triflate groups, except for O atoms bound to the metal, are omitted.

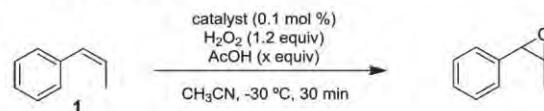
To this end, in this paper we show that the electronic properties of the manganese catalysts in the series of complexes [Mn(CF₃SO₃)₂(^HPDP)] (^HPDP = 2-[[2-(1-(pyridin-2-ylmethyl)pyrrolidin-2-yl)pyrrolidin-1-yl]methyl]pyridine, Figure 1) exert a profound and systematic impact in the activation of H₂O₂ to efficiently generate epoxidizing species and also in the stereoselectivity exhibited by these species in epoxidation reactions. This analysis has led us to the discovery of a very active Mn catalyst that requires substoichiometric amounts of a carboxylic acid for efficient H₂O₂ (1.2–2 equiv) activation, providing epoxides in short reaction times (30–60 min) with improved stereoselectivities and substrate scope in comparison with any aminopyridine–manganese system described so far.

The series of manganese complexes [Mn(CF₃SO₃)₂((*S,S*)-^XPDP)] (*S,S*)-^X**1** (Figure 1) (X = Me₂N, MeO, Me, Cl and

(5) Garcia-Bosch, I.; Ribas, X.; Costas, M. *Adv. Synth. Catal.* **2009**, *351*, 348.

(6) (a) Wu, M.; Miao, C.-X.; Wang, S.; Hu, X.; Xia, C.; Kühn, F. E.; Sun, W. *Adv. Synth. Catal.* **2011**, *353*, 3014. (b) Gomez, L.; Garcia-Bosch, I.; Company, A.; Sala, X.; Fontrodona, X.; Ribas, X.; Costas, M. *Dalton Trans.* **2007**, *0*, 5539. (c) Ottenbacher, R. V.; Bryliakov, K. P.; Talsi, E. P. *Adv. Synth. Catal.* **2011**, *353*, 885. (d) Garcia-Bosch, I.; Gómez, L.; Polo, A.; Ribas, X.; Costas, M. *Adv. Synth. Catal.* **2012**, *354*, 65. (e) Wang, B.; Miao, C.; Wang, S.; Xia, C.; Sun, W. *Chem.—Eur. J.* **2012**, *18*, 6750. (f) Dai, W.; Li, J.; Li, G.; Yang, H.; Wang, L.; Gao, S. *Org. Lett.* **2013**, *15*, 4138. (g) Lyakin, O. Y.; Ottenbacher, R. V.; Bryliakov, K. P.; Talsi, E. P. *ACS Catal.* **2012**, *2*, 1196.

Table 1. Epoxidation of *cis*- β -Methylstyrene (**1**) Using Various Manganese Complexes^a



entry	catalyst	AcOH (x equiv)	conv (yield, %)	ee (%)
1	H₁	14	61 (38)	43
2	Cl₁	14	57 (33)	40
3	CO₂Et₁	14	44 (22)	43
4	Me₂N₁	14	100 (75)	82
5	dMM₁	14	100 (86)	76
6	MeO₁	14	80 (59)	69
7	Me₁	14	100 (67)	63
8	Me₂N₁	0.35	100 (79)	73
9	dMM₁	0.35	23 (2)	55
10 ^b	Me₂N₁	14	100 (89)	90
11 ^b	Me₂N₁	0.35	100 (86)	92

^a Unless stated, reaction conditions are (*S,S*)-catalyst (0.1 mol %), H₂O₂ (1.2 equiv) and AcOH (x equiv) in CH₃CN at –30 °C. ^b 2-ethylhexanoic acid (2-cha) was used instead of AcOH.

CO₂Et) was prepared, characterized (see the Supporting Information for details), and studied as epoxidation catalysts employing H₂O₂ as oxidant. Catalysts [Mn(CF₃SO₃)₂((*S,S*)-^HPDP)], (*S,S*)-**H₁**, previously prepared and studied by Talsi and co-workers, serves as a comparative benchmark.^{6c,g} Crystallographic characterization of (*R,R*)-Me₂N₁ serves as an illustrative example of the series, showing a C₂-symmetric octahedral complex where the ligand adopts a *cis*- α topological coordination geometry.⁷ Structural and metrical parameters are very similar to those described for the Mn(mcp) catalyst,³ and **H₁**^{6g} and will not be described further (see the Supporting Information). Hydrogen peroxide (1.2 equiv) diluted in acetonitrile (1:1 v:v) was used as oxidant and delivered by syringe pump over 30 min to an acetonitrile solution of the catalyst (0.1 mol %), a substrate (*cis*- β -methylstyrene, **1**), and AcOH (14 equiv) at –30 °C. After a further 30 min of stirring, reactions were analyzed by chiral GC. Poor epoxide yield and enantioselectivity were obtained with **H₁** (Table 1, entry 1). Yield and enantioselectivity turned out to respond in a sensitive manner to the electronic properties of the pyridine rings of the ligand. When electron-withdrawing groups were introduced at the *para*-position of the pyridine (Table 1, entries 2 and 3), yields remained moderate and enantioselectivities were lower. However, we observed a very substantial improvement in both parameters in the presence of electron-donating substituents (Table 1, entries 4–7). Up to 82% ee was attained with Me₂N₁, the most e-rich catalyst of the series. The reaction was stereospecific, providing only epoxides where stereoconfiguration was retained. Good performance was also obtained with catalyst dMM₁. Therefore, we concluded that chemo- and stereoselectivity were

(7) Knof, U.; von Zelewsky, A. *Angew. Chem., Int. Ed.* **1999**, *38*, 302.

systematic and substantially improved as the ligand was more e-rich. For this reason, catalysts $\text{Me}_2\text{N}\mathbf{1}$ and $\text{dMM}\mathbf{1}$ were chosen for further investigations.

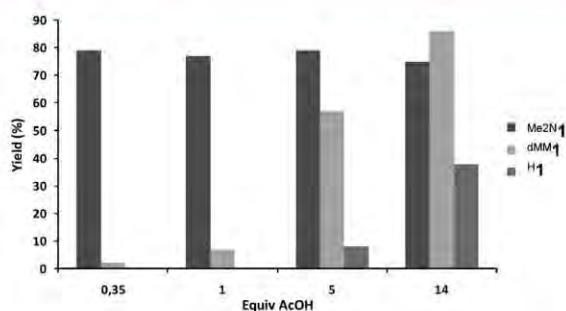


Figure 2. Epoxidation of **1** as a function of AcOH loading for catalysts (*S,S*)- $\text{Me}_2\text{N}\mathbf{1}$, (*S,S*)- $\text{dMM}\mathbf{1}$, and (*S,S*)- $\text{H}\mathbf{1}$. Reaction conditions: catalyst (0.1 mol %), H_2O_2 (1.2 equiv), and AcOH (0.35–14 equiv) in CH_3CN at -30°C .

Carboxylic acids have been previously recognized as a key additive in manganese catalyzed oxidations in order to divert H_2O_2 consumption from nonproductive peroxide disproportionation reactions toward substrate oxidation.⁸ Very interestingly, the amount of acetic acid necessary for efficient operation in the $\text{X}\mathbf{1}$ series appeared to be systematically dependent in the nature of the manganese catalyst, and more specifically in the e-releasing character of the ligand. Catalyst $\text{Me}_2\text{N}\mathbf{1}$ retained full epoxidation activity with only 0.35 equiv of AcOH, although enantioselectivity was somewhat eroded (Table 1, entry 8). A further decrease to 0.1 equiv of AcOH provided moderate epoxide yield (51%). In contrast, for $\text{dMM}\mathbf{1}$ the epoxide yield was reduced substantially as the acetic acid loading was reduced from 14 to 0.35 equiv, and a more drastic effect was observed for $\text{H}\mathbf{1}$ (see Figure 2, and entry 9 in Table 1). Therefore, the data from Table 1 and Figure 2 show that activation of H_2O_2 to form epoxidizing species is uniquely facilitated by $\text{Me}_2\text{N}\mathbf{1}$. Lyakin and co-workers have recently reported that alkyl carboxylic acids can be used instead of acetic acid, and in some specific cases this change results in improvement of the enantioselectivity.^{6g} Therefore, a range of carboxylic acids were tested in the epoxidation of **1** (see the Supporting Information, Table 1). When $\text{Me}_2\text{N}\mathbf{1}$ was used with low loadings of racemic 2-ethyl hexanoic acid (2-eha), the enantioselectivity was improved up to 90% ee, and this value was slightly improved at low carboxylic acid loading (0.35 equiv) (entries 10 and 11, respectively).

A substrate scope study is presented in Table 2. Reaction conditions involved low catalyst loadings (0.1–0.5 mol %), H_2O_2 in slight to moderate excess (1.2–2 equiv), and relatively low amounts of the carboxylic acid 2-eha (0.35 to 1 equiv). With this set of conditions in hand, the

present system provides good yields and enantioselectivity in the epoxidation of various families of olefinic substrates. In general, more e-deficient olefins such as enones required higher catalyst, H_2O_2 , and carboxylic acid loadings.

Table 2. Substrate Scope on the Asymmetric Epoxidation*

entry	substrate	isolated yield (%)	Ee (%)
1 ^a		85(63) ^b	69
2 ^a		84(64) ^b	68
3 ^c		100(88) ^c	26
4 ^c		95	97
5		77	98
6		99	96
7		65	90
8		95	96
9		93	92
10		81	96
11		99	97
12		95	57
13 ^d		67	84

* Unless stated, reaction conditions are (*S,S*)- $\text{Me}_2\text{N}\mathbf{1}$ (0.5 mol %), H_2O_2 (2 equiv) and 2-eha (1 equiv) in CH_3CN at -30°C . ^a 0.2 mol % of catalyst, H_2O_2 (2 equiv), 2-eha (0.5 equiv). ^b GC conversion and (yield). ^c 0.1 mol % of catalyst, H_2O_2 (1.5 equiv), and 2-eha (0.35 equiv). ^d Temp -10°C . ee's and configuration determined by chiral GC and HPLC (see the Supporting Information for details).

Styrenes are recognized as particularly difficult substrates for asymmetric epoxidation and are epoxidized with a remarkable 68–69% ee (entries 1 and 2). However, introduction of a methyl group in the α -olefin site results in poor stereoselection (entry 3). Excellent enantioselectivity was achieved for a substituted chromene (97% ee, entry 4) and also for *cis*-cinnamic derivatives (90–98% ee, entries 5–7). Epoxidation of aromatic enones proceeded with good to excellent yields, including not only the commonly studied *trans*-chalcone (**9**) (96% ee, entry 8) but also more challenging substrates such as *cis*-chalcone (**8**) (90% ee, entry 7), *trans*-ethyl cinnamate (**10**) (92% ee, entry 9), an alkyl styryl ketone (**11**) (96% ee, entry 10), and also an amide derivative (**12**) (97% ee, entry 11). However, as noticed for styrenes, the epoxidation of the α -methyl-substituted chalcone (**13**) proceeded with moderate enantioselectivity (57% ee, entry 12), albeit with high epoxide yield and stereospecificity. Finally, the trisubstituted tetralone-derived (**14**) epoxide was achieved with moderate yield and good enantioselectivity (84% ee, entry 13). Overall, with the single exception of the epoxidation of substrate **4**, catalyst $\text{Me}_2\text{N}\mathbf{1}$ provides improved enantioselectivities with regard to any of the Mn-based catalyst with N-based polydentate ligands described up to date⁶ and broader or complementary^{6f} substrate scope.

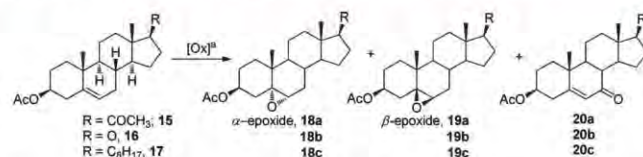
An important and interesting set of olefinic substrates is Δ^5 -unsaturated steroids. It is well established that some

(8) (a) Berkessel, A.; Sklorz, C. A. *Tetrahedron Lett.* **1999**, *40*, 7965. (b) Shul'pin, G. B.; Suss-Fink, G.; Smith, J. R. L. *Tetrahedron* **1999**, *55*, 5345. (c) de Boer, J. W.; Browne, W. R.; Brinksmas, J.; Alsters, P. L.; Hage, R.; Feringa, B. L. *Inorg. Chem.* **2007**, *46*, 6353.

β -epoxide steroids, such as withanolides, exhibit antitumor activities,⁹ and for this reason, their β -selective epoxidation is an interesting target. These natural products contain methyl groups in their β face that exert steric protection, and their epoxidation with peracids usually produces the α -epoxide as the major product.¹⁰ Reagents for selective β -epoxidation include the Parish reagent,^{10,11} structurally elaborated dioxiranes,¹² and catalytic oxidations with porphyrin ruthenium catalysts that use 2,6-Cl₂pyNO as oxidant.¹³ An attractive alternative is to employ Mn-based catalysts, making use of H₂O₂ as oxidant, but to the best of our knowledge, this approach has been described with modest selectivity.¹⁴ Considering the highly selective nature of electron-rich catalysts ^{Me}2N₁ and ^{dMM}1, their application to the oxidation of Δ^5 -unsaturated steroids was studied. Preliminary optimization experiments disclosed that pivalic acid was a more convenient coligand than 2-eha and that 15 equiv was necessary since the use of 0.35 equiv resulted in no epoxide formation (Table 3, entry 1). Using 15 equiv of pivalic acid (^{S,S}-^{Me}2N₁) provided excellent β -diastereoselectivities in the epoxidation of **15** but with poor yield and formation of 23% of allylic oxidation side product **20a** (Table 3, entry 2). Enantiomeric (^{R,R}-^{Me}2N₁) isomer retained the low product yield and modest selectivity toward the β isomer (entry 3). Fortunately, (^{S,S}-^{dMM}1) proved to be a more convenient catalyst providing improved yields, chemoselectivity, and excellent diastereoselectivity (Table 3, entry 4). On the other hand, as also observed for (^{R,R}-^{Me}2N₁) (entry 3), the enantiomer (^{R,R}-^{dMM}1) offered a more modest diastereoselectivity (Table 3, entry 5). Under optimized conditions Δ^5 -unsaturated steroids **16** and **17** were also epoxidized with moderate to good yields and excellent β -diastereoselectivities (table 3, entries 6 and 7) in short reaction times (1 h). Interestingly, oxidation of the same steroidal substrates with the analogous iron complexes¹⁵ (^{S,S}-^{dMM}1Fe and (^{S,S}-^{Me}2N₁)Fe afforded an equimolar ratio of β/α epoxides and modest selectivity toward the β epoxide, respectively.

In conclusion, the present work describes highly efficient and stereoselective manganese catalysts for the epoxidation of olefins with H₂O₂ under mild conditions and short reaction times. The work demonstrates that electronic effects can be used to improve the activation of H₂O₂ in a productive manner, as well as the stereoselectivity in

Table 3. Epoxidation of Δ^5 -Unsaturated Steroids^a



entry	substrate	catalyst	yield (%) (18 + 19)	(20) ^b ratio 19/18
1 ^c	15a	(^{S,S} - ^{Me} 2N ₁)	— (—)	—
2	15a	(^{S,S} - ^{Me} 2N ₁)	36 (23)	93:7
3	15a	(^{R,R} - ^{Me} 2N ₁)	39 ^d (20)	67:33
4	15a	(^{S,S} - ^{dMM} 1)	50 (5)	96:4
5	15a	(^{R,R} - ^{dMM} 1)	66 (4)	69:32
6	15b	(^{S,S} - ^{dMM} 1)	56 (8)	94:6
7	15c	(^{S,S} - ^{dMM} 1)	66 ^e (5) ^f	97:3
8 ^g	15b	(^{S,S} - ^{Me} 2N ₁)Fe	46 (4)	66/34
9 ^h	15b	(^{S,S} - ^{dMM} 1)Fe	60 (2)	48/52

^a Unless stated, reaction conditions are catalyst (0.25 mol %), H₂O₂ (2 equiv), and pivalic acid (15 equiv) in ACOEt/CH₃CN (4:1) at room temperature. ^b Isolated yields. ^c Pivalic acid (0.35 equiv). ^d GC yield. ^e H NMR yield. Ratio β/α determined by GC, except for entry 7 which was determined by ¹H NMR. ^f Allylic 7- β -OH alcohol. ^g Reaction catalyzed by [Fe(CF₃SO₃)₂](^{S,S}-^{Me}2N₁PDP)]. ^h Reaction catalyzed by [Fe(CF₃SO₃)₂](^{S,S}-^{dMM}1PDP)].

the oxygen atom transfer event, providing a useful guiding principle for rational design of a future generation of catalysts. Catalysts described herein complement or compare favorably in terms of enantioselectivities and substrate scope against structurally related examples described so far. When compared with the analogous iron complexes, obvious similarities arise in the electronic effects,¹⁵ but in addition the manganese catalysts require lower catalyst loadings, are more tolerant to aromatic substrates, and show enhanced β -selectivities in the epoxidation of Δ^5 -unsaturated steroids.

Acknowledgment. Financial support from ERC-2009-StG-239910, MINECO of Spain (CTQ2012-37420-C02-01/BQU and CSD2010-00065), and the Catalan DIUE (2009SGR637). J.Ll.-F. thanks MICINN for a RyC contract. X.R. and M.C. acknowledge ICREA-Academia awards. X.R. is grateful for financial support from IN-PLANTA Project No. IPN-2011-0059-PCT-42000-ACT1. I.G.-B. acknowledges an IOF Marie Curie fellowship. We acknowledge STRs from UdG for technical support.

Supporting Information Available. Experimental details for preparation of catalysts, epoxidation reactions, and product characterization. X-ray data for (^{R,R'}-^{Me}2N₁) (CIF). This material is available free of charge via the Internet at <http://pubs.acs.org>.

The authors declare no competing financial interest.

(9) Ichikawa, H.; Takada, Y.; Shishodia, S.; Jayaprakasam, B.; Nair, M. G.; Aggarwal, B. B. *Mol Cancer Ther.* **2006**, *5*, 1434.

(10) Parish, E. J.; Li, H.; Li, S. *Synth. Commun.* **1995**, *25*, 927.

(11) Baqi, Y.; Giroux, S.; Corey, E. J. *Org. Lett.* **2009**, *11*, 959.

(12) Yang, D.; Jiao, G.-S. *Chem.—Eur. J.* **2000**, *6*, 3517.

(13) Zhang, J.-L.; Che, C.-M. *Chem.—Eur. J.* **2005**, *11*, 3899.

(14) Bruyneel, F.; Letondor, C.; Bastürk, B.; Gualandi, A.; Pordea, A.; Stoeckli-Evans, H.; Neier, R. *Adv. Synth. Catal.* **2012**, *354*, 428.

(15) Cussó, O.; Garcia-Bosch, I.; Ribas, X.; Lloret-Fillol, J.; Costas, M. *J. Am. Chem. Soc.* **2013**, *135*, 14871.

Chapter VII

Results and Discussion

CHAPTER VII. RESULTS AND DISCUSSION

VII.1. Asymmetric Epoxidation with H₂O₂ by Manipulating the Electronic Properties of NonHeme Iron Catalysts

Traditionally, asymmetric epoxidation with nonheme iron catalysts is limited in substrate scope to *trans*-chalcones and *trans*-stilbenes.¹⁻⁵ For this reason, the development of new iron complexes with broader substrate scope was devised necessary. Our work focused on the design of new iron complexes based on the pdp system, where electronic properties have been systematically altered, and to study how those properties affect the activity and stereoselectivity of the corresponding catalysts. Towards this end, different electronic groups were introduced in position 4 of the pyridine rings of the pdp ligands, providing complexes (S,S')-[Fe(OTf)₂(^Rpdp)], where R = CO₂Et, Cl, H, Me, MeO and Me₂N, stands for the group introduced at position 4 (Figure 6).

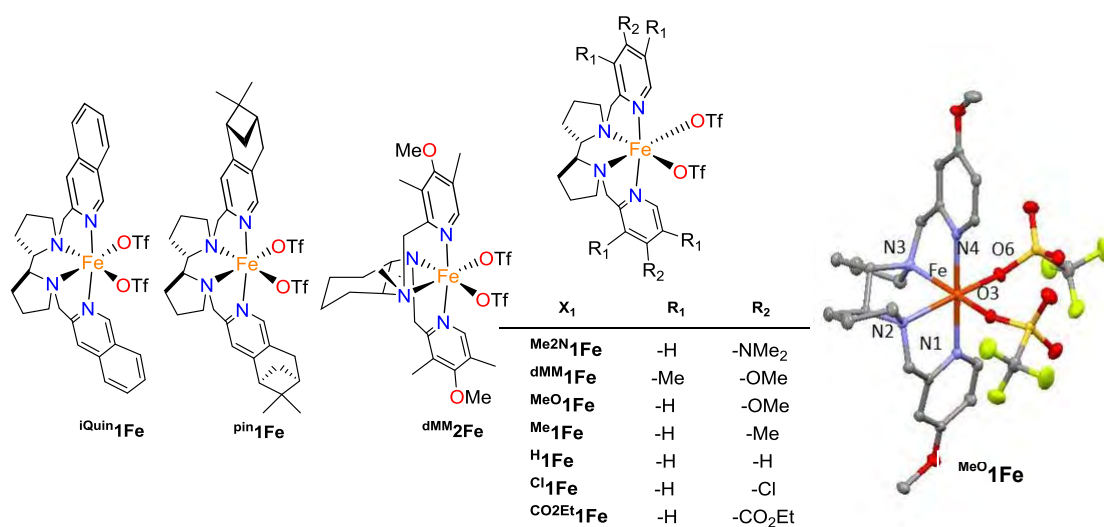
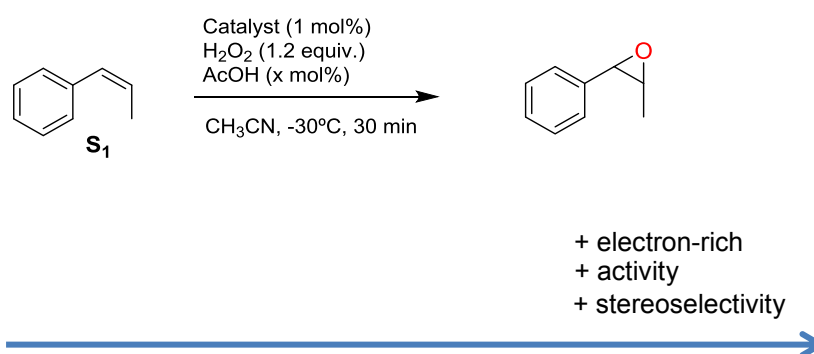


Figure 6. Schematic diagram of the iron complexes studied.

Catalytic activity of these complexes was analyzed in order to evaluate the putative electronic effects in catalytic asymmetric epoxidation reactions. We took *cis*- β -methylstyrene as model substrate, hydrogen peroxide as oxidant (1.6 equiv.) and acetic acid as additive (1.4 equiv.) in acetonitrile at -30 °C. Results show that the activities and stereoselectivities systematically increase as more electron-rich is the catalyst, up to 85 % of yield and 61 % of ee, for catalyst Me₂N₁Fe (Table 2). Also the data showed that only the most electron-rich catalyst (Me₂N₁Fe) retains intact the corresponding yields and stereoselectivities

when loading of acetic acid was decreased to catalytic levels (3 mol%, see Table 2). For all the other complexes, analogous decrease in carboxylic acid results in a substantial erosion of activity (product yields and substrate conversion). When catalyst $^{dMM}2Fe$ was used, lower activities and enantioselectivities were observed in comparison with the pdp analogous complex $^{dMM}1Fe$. Moreover, the $^{Me2N}1Fe$ tolerated other carboxylic acid additives, observing that the bulkier 2-eha gave improved enantioselectivities, up to 80 % ee and *S*-Ibuprofen (*S*-Ibp) achieved 86 % ee (Table 3).

Table 2. Screening of iron complexes on the asymmetric epoxidation of *cis*- β -methylstyrene.



Catalyst	AcOH 140 mol%							
	$^{CO_2Et}1Fe$	$^{Cl}1Fe$	H1Fe	$^{Me}1Fe$	$^{MeO}1Fe$	$^{dMM}1Fe$	$^{Me_2N}1Fe$	$^{DMM}2Fe$
Conv./ (yield) (%)	44(22)	57(33)	61(38)	44(27)	64(37)	97(81)	100(85)	82(55)
ee (%)	19	15	21	31	39	40	61	32
Catalyst	AcOH 3 mol%							
	$^{CO_2Et}1Fe$	$^{Cl}1Fe$	H1Fe	$^{Me}1Fe$	$^{MeO}1Fe$	$^{dMM}1Fe$	$^{Me_2N}1Fe$	$^{DMM}2Fe$
Conv./ yield (%)	31(13)	32(15)	49(26)	31(17)	38(26)	82(67)	100(87)	-
ee (%)	21	16	19	30	38	38	62	-

Unless stated, reaction conditions are catalyst (1 mol%), H_2O_2 (1.6 equiv) and AcOH (3-140mol %) in CH_3CN at - 30°C during 30 min. Epoxide yields and substrate conversion determined by GC. ee's and configuration determined by chiral GC.

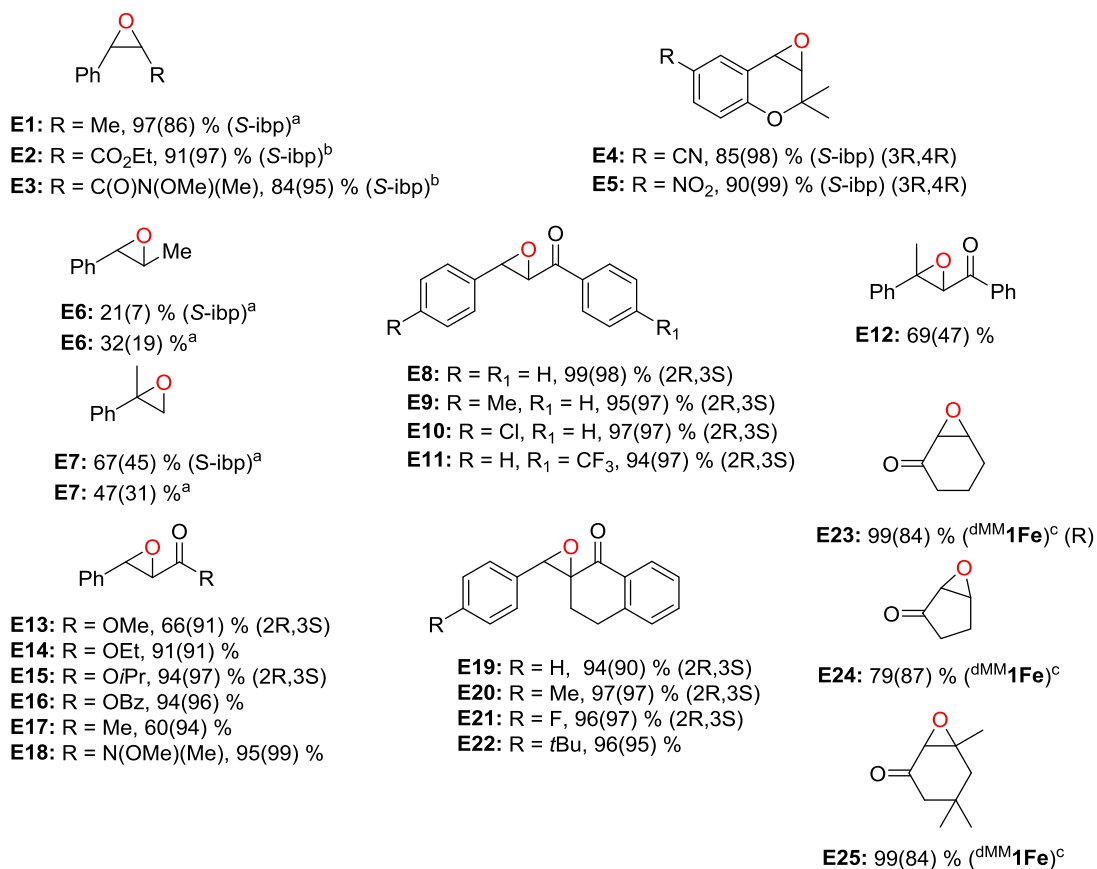
Table 3. Screening of carboxylic acids on the asymmetric epoxidation of *cis*- β -methylstyrene with $^{Me_2N}1Fe$.

RCO_2H					
Conv./yield (%)	100(87)	100(76)	100(91)	100(86)	100(97) 100(87) ^a
ee (%)	62	67	73	80	86(63) ^a

Unless stated, reaction conditions are (*S,S*)- $^{Me_2N}1Fe$ (2 mol%), H_2O_2 (1.6 equiv) and RCO_2H (3 mol %) in CH_3CN at $-30^\circ C$ during 30 min. Epoxide yields and substrate conversion determined by GC. ee's determined by chiral GC. ^a(*R,R'*)- $^{Me_2N}1Fe$ was employed.

With the optimal conditions in hand, we explored the substrate scope of the system. When *S*-Ibuprofen was used as additive we achieved good yields and excellent enantioselectivities for *cis*-aromatic olefins, *cis*-cinnamic esters, *cis*-cinnamic amides derivatives and with electron-deficient chromenes (Figure 7). In the case of using 2-eha as additive, we obtained excellent yields and enantioselectivities for *trans*-chalcone derivatives, tetralone derivatives, and *trans*-cinnamates derivatives (Figure 7). In addition, with catalyst $^{dMM}1Fe$ we obtained good yields and stereoselectivities for cyclic aliphatic enones. However, the system did not proved to be a good candidate for asymmetric epoxidation of terminal olefins, *trans*- β -methylstyrene or β,β , trisubstituted enones (Figure 7).

Figure 7. Substrate scope on the asymmetric epoxidation with the iron catalyst $\text{Me}_2\text{N}^1\text{Fe}$. Results are shown as % isolated yield (% ee in parenthesis).

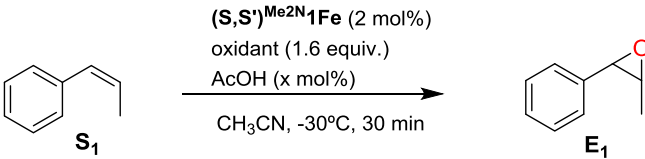


Unless stated, reaction conditions are (*S,S*)- $\text{Me}_2\text{N}^1\text{Fe}$ (2 mol%), H₂O₂ (1.6 equiv.) and 2-eha (3 mol %) in CH₃CN at -30°C during 30 min. The reactions that contain *S*-ibp between parentheses are performed with *S*-ibuprofen instead of 2-ethylhexanoic acid. ^aEpoxide yield determined by GC. ^b5 mol% catalyst, and 3 equiv. of H₂O₂. ^cReaction conditions are: (*S,S*)- $\text{d}^{\text{MM}}\text{1Fe}$ (1 mol%), H₂O₂ (1.2 equiv.) and 2-eha (140 mol%) in CH₃CN at -30°C during 30 min. ee's and configuration determined by chiral GC and HPLC.

In order to get insight into the mechanism, we performed the epoxidation of S1 using three different oxidants (Table 4). We observed the same enantioselectivities for all of them, suggesting that irrespective of the terminal oxidant, the reactions have a common transition state for the oxygen atom delivery step (Table 4). This observation strongly suggests that in the three cases a common active oxidant species is implicated, and discards iron-peroxide species as possible oxidants. The reaction with *t*BuOOH is particularly relevant because it is well known that it can readily produce tert-butoxy radicals upon reaction with iron coordination complexes, but in our reaction unselective free-diffusion radical reactions were not observed.^{6,7} Another illustrative experiment was a study on the competitive epoxidation of an electron-rich olefin (*cis*- β -methylstyrene) and an electron-deficient olefin (*cis*-cinnamic ester).

Epoxidation of the more electron-rich olefin was favored 9 times with regard to the electron deficient one, suggesting that the epoxidizing species have an electrophilic character (Scheme 35).

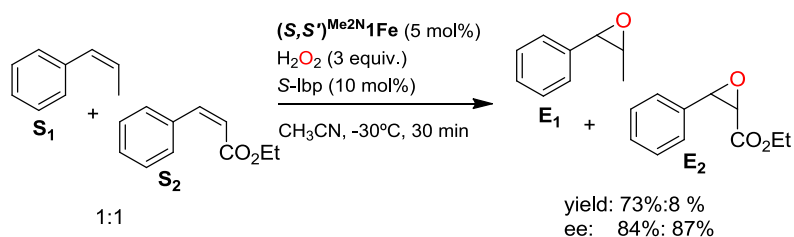
Table 4. Comparison among different oxidants in the epoxidation of **S1** with $(S,S)\text{-}^{\text{Me}2\text{N}}\mathbf{1Fe}$



Entry	Oxidant	AcOH (mol %)	Conv/yield (%)	ee (%)
1	^t BuOOH ^a	140	46(33)	61
2	^t BuOOH ^a	3	32(20)	61
3	H ₂ O ₂	3	100(87)	62
4	AcOOH ^b	-	85(63)	60

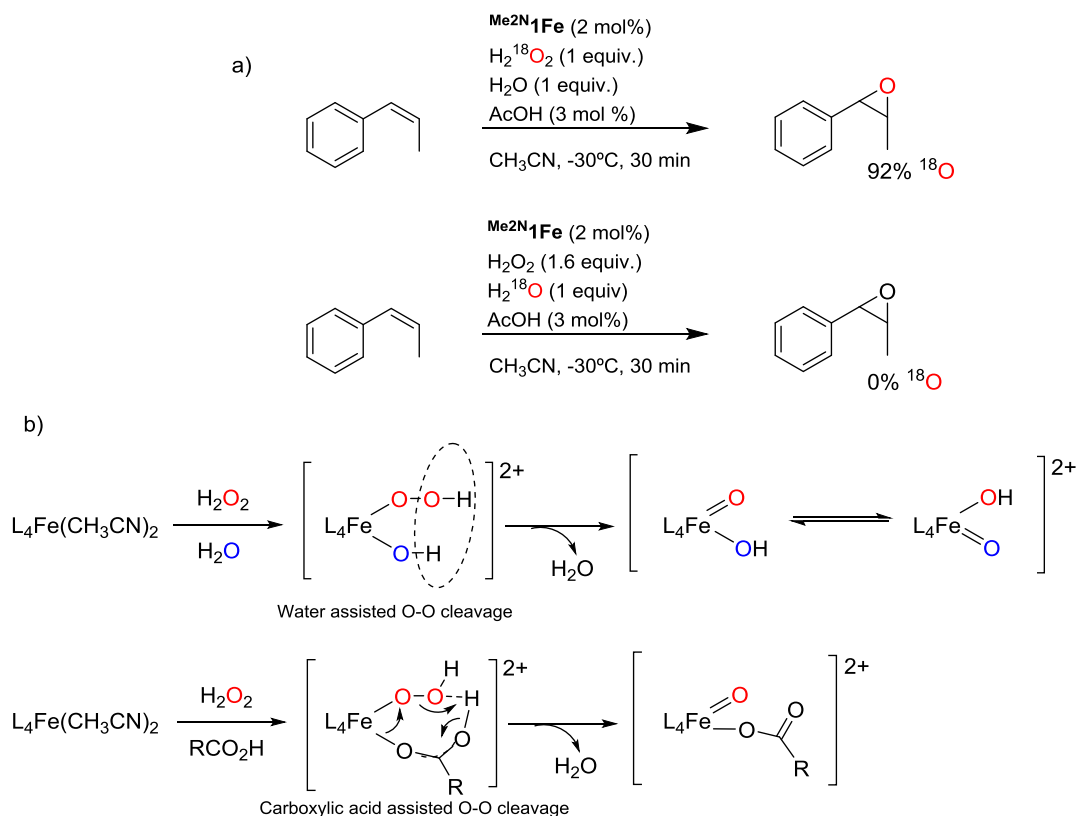
Unless stated, reaction conditions are $(S,S)\text{-}^{\text{Me}2\text{N}}\mathbf{1Fe}$ (2 mol%), oxidant (1.6 equiv) and AcOH (3 – 140 mol%) in CH₃CN at -30°C during 30 min. Epoxide yields and substrate conversion determined by GC. ^a70% in water. ^b Commercially available reagent, 32% peracetic acid content in acetic acid.

Scheme 35. Competition studies between electron-rich and electron-deficient olefin.



Moreover, labelling experiments showed that the oxygen atom incorporated in the olefin came from hydrogen peroxide and not from water, indicating that $\text{Fe}^{\text{V}}(\text{O})(\text{OH})$ (formed via a water assisted path, Scheme 36b) is not involved as active oxidant, but instead $\text{Fe}^{\text{V}}(\text{O})(\text{O}_2\text{CR})$ species were proposed to be formed via a carboxylic acid assisted O-O cleavage pathway (Scheme 36b).⁸⁻¹⁰

Scheme 36. a) Isotopic analysis studies. b) Schematic representation of the water assisted path.

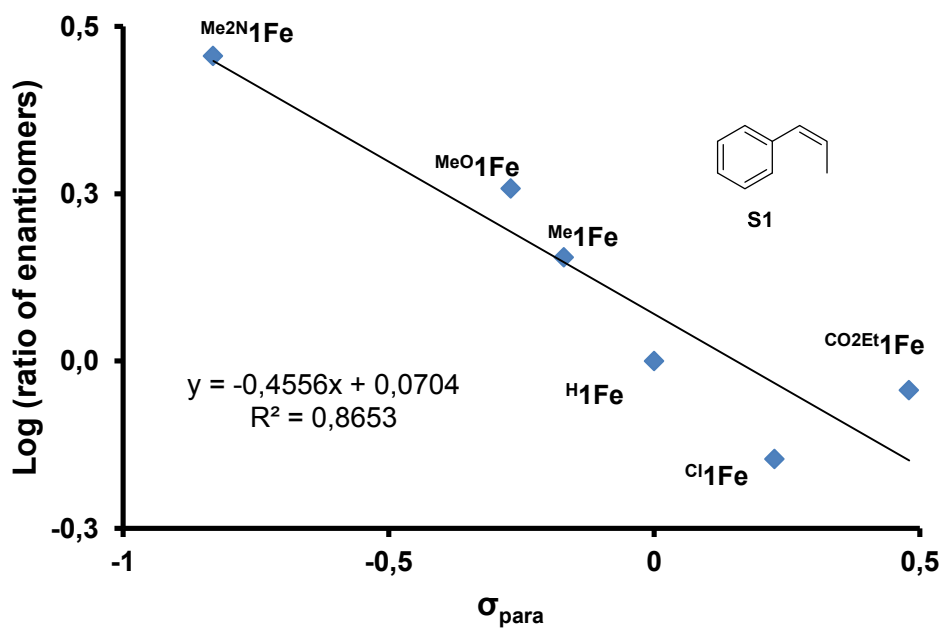
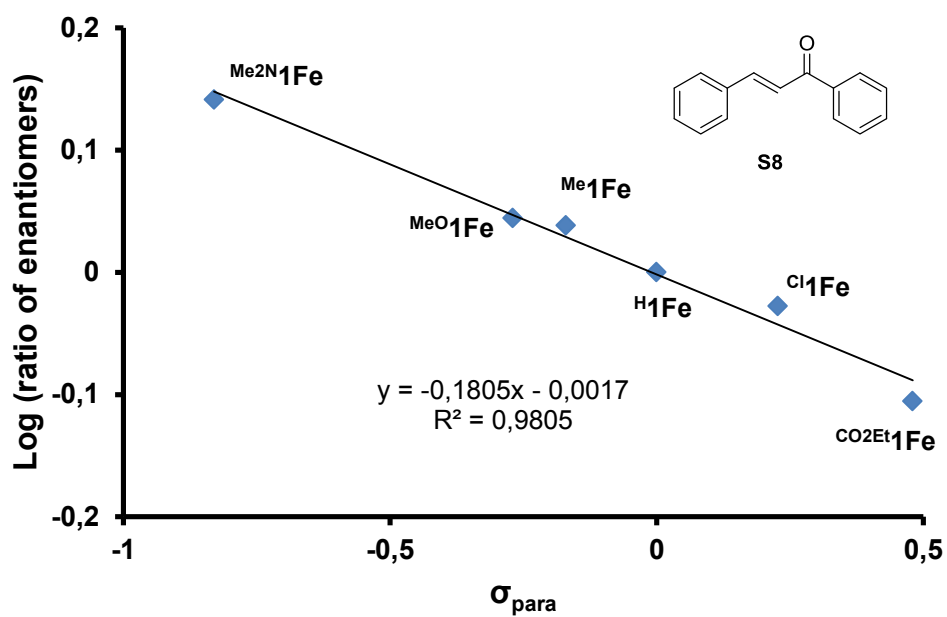


^a $\text{H}_2^{18}\text{O}_2$ reagent is a 2% solution in H_2^{16}O

The latter studies indicated that before the active oxidant is formed, lysis of the O-O bond from hydrogen peroxide is necessary, and therefore, we can suggest that $\text{Me}_2\text{N}_1\text{Fe}$ promoted and facilitated the heterolytic cleavage of $\text{Fe}^{\text{III}}(\text{OOH})(\text{HOAc})$ to form $\text{Fe}^{\text{V}}(\text{O})(\text{O}_2\text{CR})$. Homolytic cleavage was discarded because it implies formation of poorly selective hydroxyl radicals, and oxo-iron(IV) species, that are relatively modest O-atom transfer agents.¹¹

Finally, it was shown that the electronic properties of the complexes impact on the stereoselectivities found. This was shown by a Hammett plot ($\log(\text{ratio enantiomers})$ vs σ_{para} Hammett parameters of the group at position 4 of the pyridine of the ligand) for four different substrates, showing an excellent correlation and strongly suggests that this linear free energy relationship is general and has mainly an electronic origin (Figure 8). As the catalyst become more electron-rich, the electrophilicity of the metal-oxo and electrophilic character is attenuated, then less powerful and the transition state is displaced toward a more product-like complex, suggesting a closer substrate/metal-oxo

species, this fact allow to transfer better the chiral information to the substrate, showing higher enantioselectivity



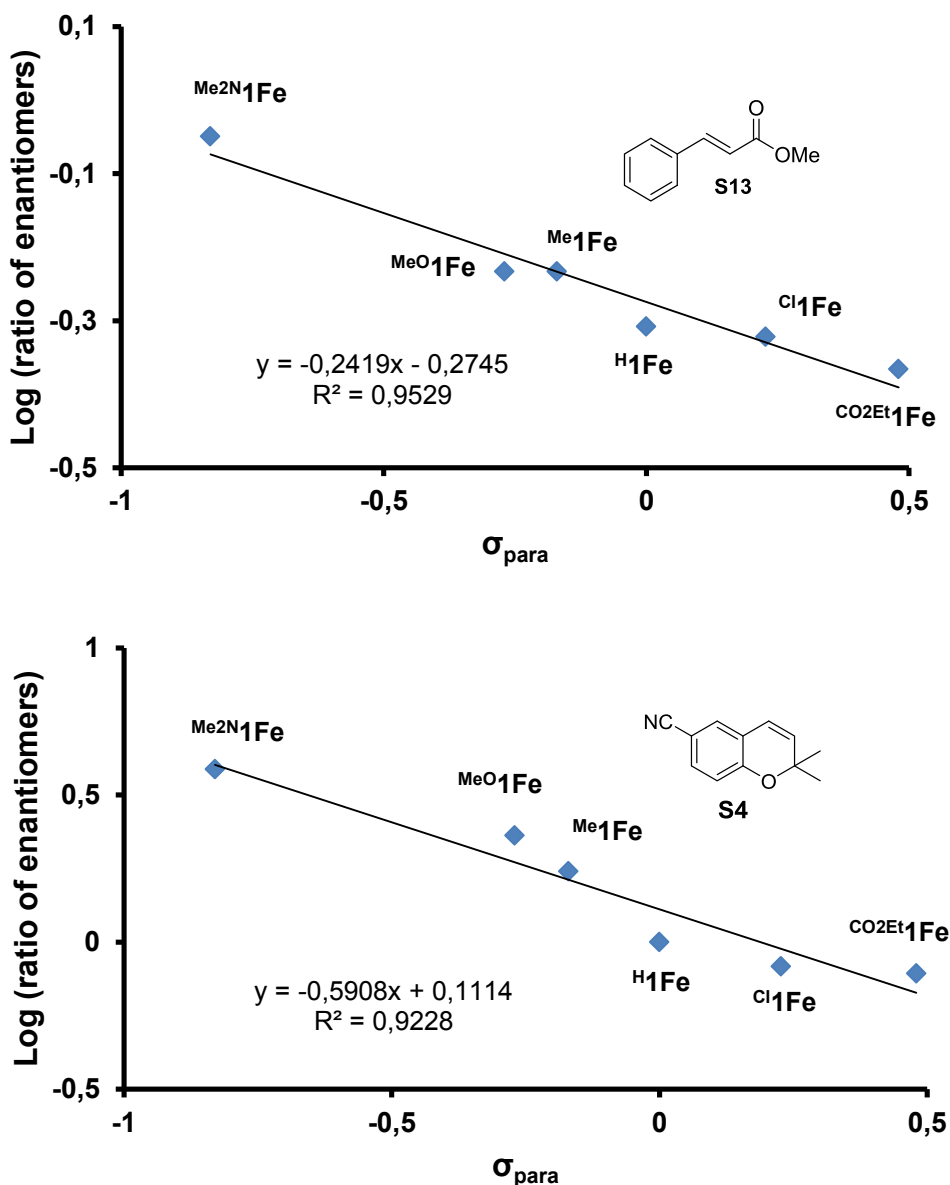
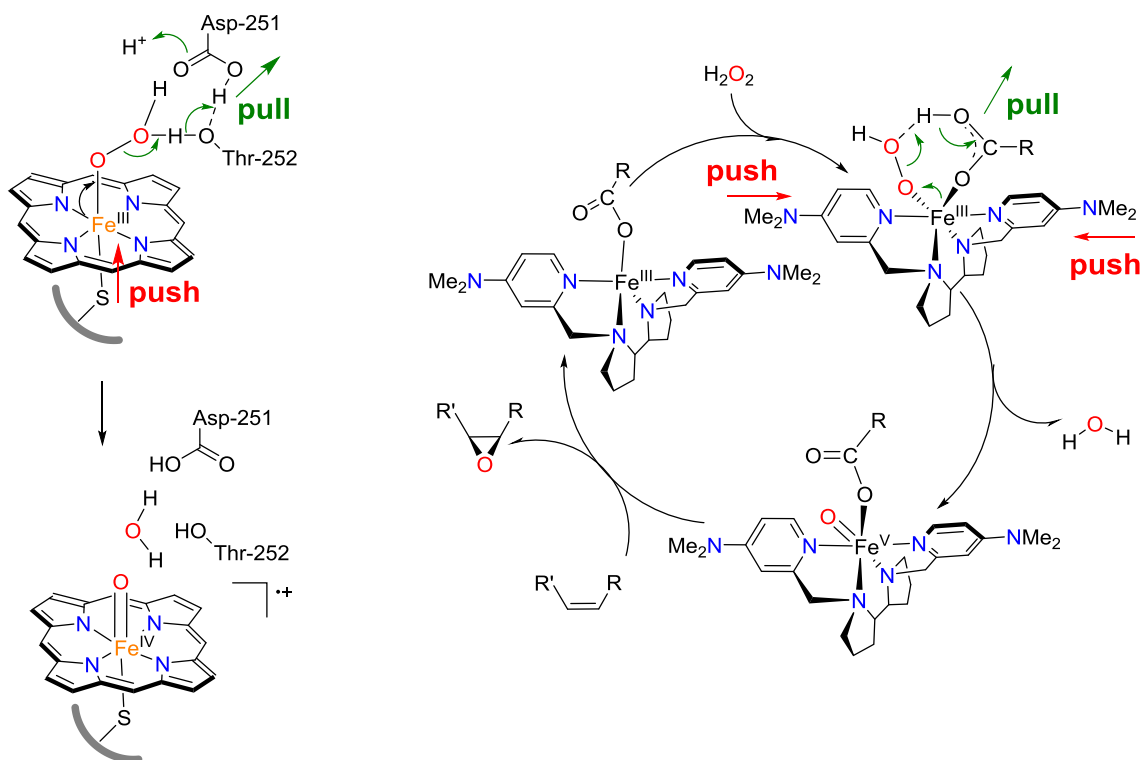


Figure 8. Hammett analysis of the stereoselectivity as a function of catalyst in the epoxidation of **S8**, **S1**, **S13** and **S4**. The reaction was carried out with 1 mol % of catalyst, AcOH (1.4 equiv.), H₂O₂ (1.2 equiv.) and 750 μ L of acetonitrile at -30°C.

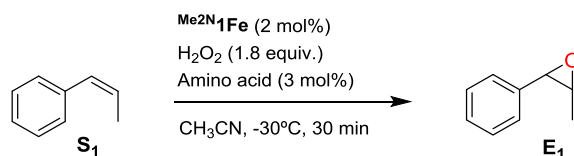
Finally, it can be seen that the operational principles of the system ^{Me}2N¹Fe/ carboxylic acid when reacting with hydrogen peroxide have a strong resemblance to the so-called push-pull effect operating in Cyt P450, assisting the O-O lysis of a Fe^{III}-OOH intermediate (Cpd 0 in Cyt P450). Electron-donating groups of the ligand exert the push effect that is played by a cysteinate residue in Cyt P450. On the other hand, the carboxylic acid facilitates liberation of a water molecule via a H-bonding interaction, analogous to the pull effect of nearby residues (Asp₂₅₁ and Thr₂₅₂ in Cyt P450) (Scheme 37).^{12,13}

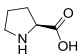
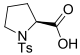
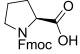
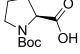
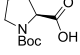
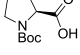
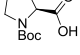
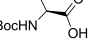
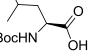
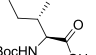
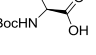
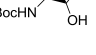
Scheme 37. On the left, push-pull effect in Cyt P450 and on the right the proposed push-pull effect in the system $^{Me_2N}1Fe$.



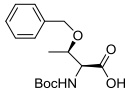
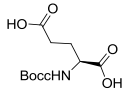
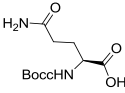
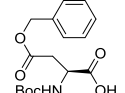
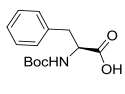
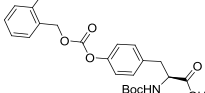
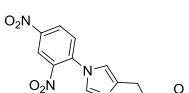
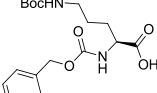
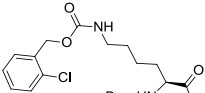
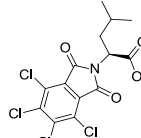
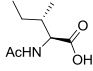
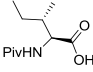
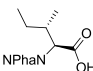
VII.2. Synergistic Interplay of a Non-Heme Iron Catalyst and Amino acid co-ligands in H₂O₂ Activation and Asymmetric Epoxidation of α -Substituted Styrenes

A standing problem in synthetic organic chemistry is to perform asymmetric epoxidation reactions of terminal olefins, because it is very difficult to distinguish the two enantiotopic faces for this class of olefins. So methods for highly enantioselective epoxidation of terminal olefins are still lacking. As we reported previously, the electron-rich complex $^{\text{Me}_2\text{N}}\mathbf{1Fe}$ facilitated the heterolytic cleavage of O-O bond and allows use of catalytic loadings of a carboxylic acid additive, that also helps in this O-O lysis event (Chapter VII.1). With both concepts in mind, we focused our attention on using amino acids as co-ligands for this system, due to the high availability and natural origin of this chiral source. It was reasoned that the combination between the catalyst and a chiral carboxylic acid source could be used to tune the structure of the active center where O-atom delivery takes place, providing asymmetric epoxidation of new kind of olefins. For this purpose, we studied the asymmetric epoxidation performance of the catalyst $(\text{S,S}')^{\text{Me}_2\text{N}}\mathbf{1Fe}$ and its enantiomer $(\text{R,R}')^{\text{Me}_2\text{N}}\mathbf{1Fe}$, using hydrogen peroxide as oxidant, different amino acids as additives and *cis*- β -methylstyrene as model substrate in acetonitrile at -30 °C (Table 5). Combination of the chirality of the amino acid with that of the catalyst was expected to lead to matching and mismatching effects, from where a synergistic combination will be identified. First, it was observed that unprotected amino acids poisoned the catalyst giving no epoxide product (Table 5, entry 1). Fortunately, protected amino acids showed epoxidation activity. Consequently, a set of amino acids was tested. After extensive optimization, the best results obtained in term of yields and stereoselectivities were obtained with the combination of $(\text{R,R}')^{\text{Me}_2\text{N}}\mathbf{1Fe}$ and *N*-NPha-ILe-OH (Table 5, entry 25).

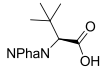
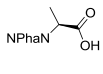
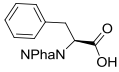
Table 5. Screening of amino acids in asymmetric epoxidation reaction

Entry	Amino acid	$(S,S)^{Me_2N_1Fe}$		$(R,R)^{Me_2N_1Fe}$	
		Conv. (Yield)%	ee(%)	Conv. (Yield)%	ee(%)
1	 <i>L</i> -Pro-OH	-	-	n.d.	n.d.
2	 <i>N</i> -Ts-Pro-OH	47(30)	63	87(69)	76
3	 <i>N</i> -Fmoc-Pro-OH	100(75)	74	96(77)	77
4	 <i>N</i> -Boc-Pro-OH	100(87)	79	95(90)	77
5	 <i>N</i> -Boc-Pro-OH	100(90)	76	n.d.	n.d.
6	 <i>N</i> -Boc-Pro-OH	50(40)	32	n.d.	n.d.
7	 <i>N</i> -Boc-Pro-OH	55(27)	17	n.d.	n.d.
8	 <i>N</i> -Boc- <i>t</i> -Leu-OH	100(93)	80	100(91)	81
9	 <i>N</i> -Boc-Leu-OH	100(89)	71	100(89)	75
10	 <i>N</i> -Boc-Ile-OH	100(96)	80	100(83)	73
11	 <i>N</i> -Boc-Ala-OH	100(88)	68	100(85)	71
12	 <i>N</i> -Boc-Val-OH	100(86)	75	100(80)	72

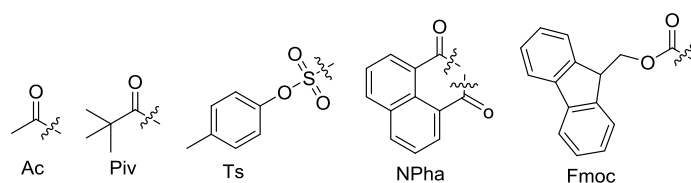
CHAPTER VII: RESULTS AND DISCUSSION

13		<i>N</i> -Boc-Thr(Bzl)-OH	92(82)	72	100(86)	71
14		<i>N</i> -Boc-Glu-OH	87(75)	65	91(86)	67
15		<i>N</i> -Boc-Gln-OH	86(69)	64	86(70)	67
16		<i>N</i> -Boc-Asp(Bzl)-OH	98(87)	58	100(90)	68
17		<i>N</i> -Boc-Phe-OH	100(88)	71	100(86)	61
18		<i>N</i> -Boc-Tyr(2Br-Z)-OH	91(83)	69	91(79)	74
19		<i>N</i> -Boc-Hys(DNP)-OH	29(14)	58	34(21)	64
20		Z-Orn(Boc)-OH	92(79)	68	90(77)	69
21		<i>N</i> -Boc-Lys(2-Cl-Z)-OH	100(88)	71	100(86)	75
22		<i>N</i> -TCP-Leu-OH	83(65)	62	100(81)	58
23		<i>N</i> -Ac-Ile-OH	100(89)	78	100(82)	74
24		<i>N</i> -Piv-Ile-OH	100(79)	81	98(80)	69
25		<i>N</i> -Npha-Ile-OH	79(51)	49	100(81)	87

CHAPTER VII: RESULTS AND DISCUSSION

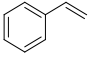
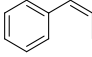
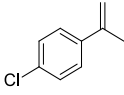
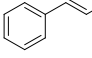
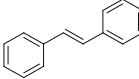
26		<i>N</i> -Npha- <i>t</i> -Leu-OH	72(57)	70	100(89)	85
27		<i>N</i> -Npha-Ala-OH	92(74)	70	100(87)	76
28		<i>N</i> -Npha-Phe-OH	98(79)	68	100(84)	74

Reaction conditions are $\text{Me}_2\text{N}^+\mathbf{1Fe}$ (2 mol%), H_2O_2 (1.8 equiv.) and amino acid (3 mol%) in CH_3CN at -30°C during 30 min. Conversion and yield were calculated using internal standard. Ee's were determined by chiral GC.



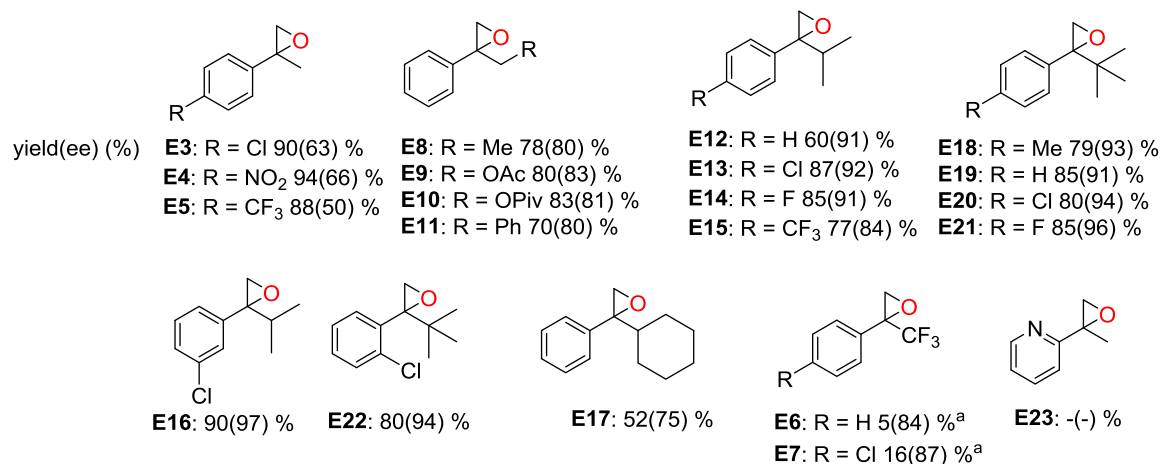
With the optimal amino acid identified, we attempted the asymmetric epoxidation of different styrene derivatives, since this is a class of substrates particularly difficult for iron oxidation catalysis. At the same time, we compared the outcomes of the use of this amino acid with the best carboxylic acids reported before (Table 6). The results showed that 4-chloro- α -methylstyrene was epoxidized with values of stereoselectivity substantially better than any of the carboxylic acids previously reported (Table 6, entry 3). Since those are particularly difficult substrates, further development of this system was pursued.

Table 6. Comparison with other carboxylic acids in different styrene patterns.

Acid	AcOH	2-eha	S-lbp	N-Npha-lLeu-OH	
Entry	Substrate	Conv/yield % (ee %)			
1	 S1	48/18 (25)	40/15 (38)	33/14 (43) 34/14 (35) ^a	39/11 (14) 53/28 (38) ^a
2	 S0	100/87 (62) ^b	100/86 (80) ^b	100/97 (86) ^b 100/87(63) ^{ab}	79/51 (49) 100/81 (87) ^a
3	 S3	98/81 (2)	100/86 (29)	100/4 (45) 72/52 (1) ^a	88/61 (25) 100/90 (63) ^a
4	 S2	67/8 (4)	53/32 (19) ^b	48/21 (7) ^b 50/8 (8) ^a	57/18 (6) 60/18 (10) ^a
5	 S24	75/62 (1)	95/87 (10)	90/82 (2) 97/91 (1) ^a	91/83 (6) 50/44 (11) ^a

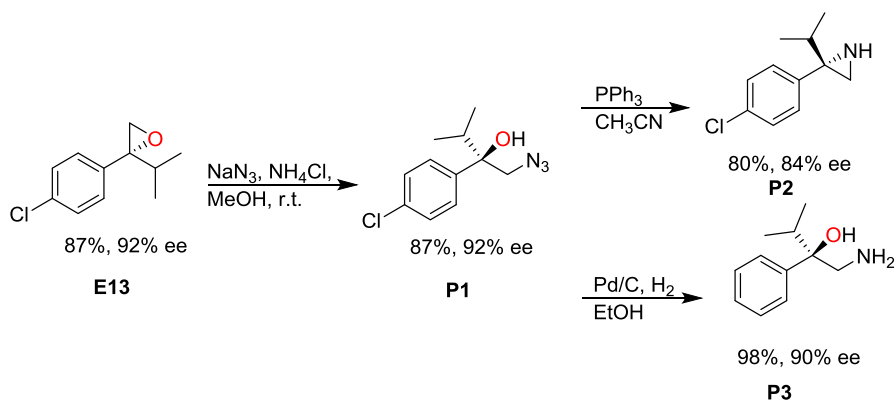
Reaction conditions are (**S,S'**)-^{Me2N}**1Fe** (2 mol%), H₂O₂ (1.8 equiv.) and Amino acid/carboxylic acid (3 mol%) in CH₃CN at -30°C during 30 min. Conversion and yield were calculated using internal standard. ee's were determined by chiral GC and HPLC CHIRALPACK IC. ^aThe reaction was carried out using (**R,R'**)-^{Me2N}**1Fe** as catalyst. ^b Data from Chapter VII.1. H-NMR yields for *trans*-stilbene (**S24**). 2-eha: 2-ethylhexanoic acid, S-lbp: S-Ibuprofen

We explored epoxidation of a series of α,α -disubstituted styrenes with different groups in the aromatic ring that could modify its electronic properties, and different bulky groups closer to the double bond. The results showed that the system tolerated different groups, including electron-withdrawing groups such as trifluoromethyl, nitro, and halogen groups and also electron-donating alkyl groups. The most interesting aspect is the systematic dependence between the enantioselectivities and the bulky nature of aliphatic groups incorporated close to the double bond, providing systematically higher enantioselectivities with increasing bulyness of the aliphatic chain of the olefins, up to 97 % of ee (Figure 9).

Figure 9. Substrate scope on the asymmetric epoxidation with (R,R) - Me_2N -**1Fe** and *N*-NPha-Ileu-OH.

Unless stated, reaction conditions are (R,R) - Me_2N -**1Fe** (2 mol%), H₂O₂ (1.6 equiv.) and *N*-NPha-Ileu-OH (3 mol %) in CH₃CN at -30°C during 30 min. Epoxide yields and substrate conversion determined by GC. Ee's determined by chiral GC, except for **E16**, that value for which was determined by ¹H-NMR with tris [3-(heptafluoropropylhydroxymethylene)-(+)-camphorate].^aEpoxide yield determined by GC.

In order to illustrate the potential utility of this methodology, the epoxide resulting from epoxidation of 4-chloro- α -methylstyrene was converted into azido-alcohol **P1** with no erosion of the enantioselectivity (yield 87%, 92% ee), which can then be converted to unprotected aziridine **P2** or alternatively, reduction of the azide using Pd/C under H₂ provides the corresponding chiral 1,2-amino alcohol **P3** (yield 98%, 90% ee), which can be seen as a precursor for the synthesis of oxazolines, among other interesting products (Scheme 38).

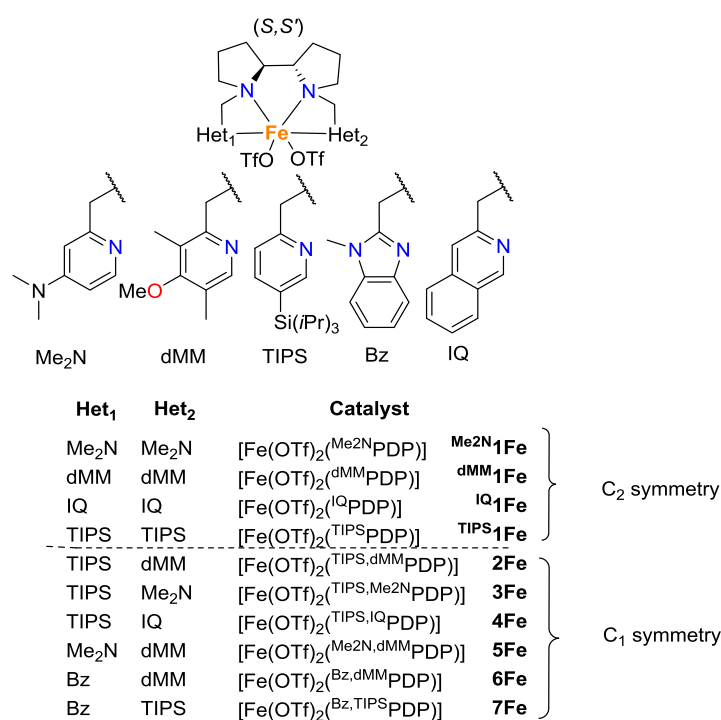
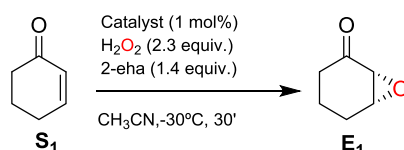
Scheme 38. Different products obtained from terminal chiral epoxide **E13**.

Finally, the present approach and the versatility of the system can be extended towards new classes of substrates without requiring the development of new chiral iron catalysts.

VII.3. Iron catalyzed highly enantioselective epoxidation of cyclic aliphatic enones with aqueous H₂O₂.

Traditionally, asymmetric epoxidation of aliphatic cyclic enones with high enantioselectivities can only be carried out with an organocatalyst and hydrogen peroxide, via formation of a nucleophilic oxidant.¹⁴⁻¹⁶ The main drawbacks were the higher catalyst loadings and long reaction times (up to 48 hours) for these reactions. However, methodologies based on metal-oxo oxidants didn't exist. For this reason, we targeted the development of new iron complexes capable to epoxidize aliphatic cyclic enones with low catalyst loadings in short reaction times with hydrogen peroxide as oxidant and carboxylic acids as additives.

First of all, we tested different C₂ symmetric complexes with different electronic and steric properties in the pyridine rings in the asymmetric epoxidation reaction (Figure 10, Table 7 entries 1-4). The reaction was carried out with hydrogen peroxide as oxidant and 2-ethylhexanoic acid as additive in CH₃CN at -30°C. The C₂ complexes provided good stereoselectivities, up to 84 % of ee, and excellent yields, up to 94 % in the epoxidation of 2-cyclohexenone. However, the stereoselectivities were lower in comparison with organocatalysts based systems. Then, we considered the development of new C₁ symmetric iron complexes with distinct heterocyclic arms (Figure 10). The iron complex that combines a 1-methylbenzimidazole ring and a bulky pyridine with triisopropylsilyl group in position 5 of the pyridine showed higher activities and higher enantioselectivities, 55 % and 90 %, respectively (Table 7, entry 10). Due **7Fe** gave lower yield, we optimized the conditions, 3 mol % of **7Fe**, 2.3 equiv. of hydrogen peroxide and 1.4 equiv. of 2-ethylhexanoic acid in CH₃CN at -30°C.

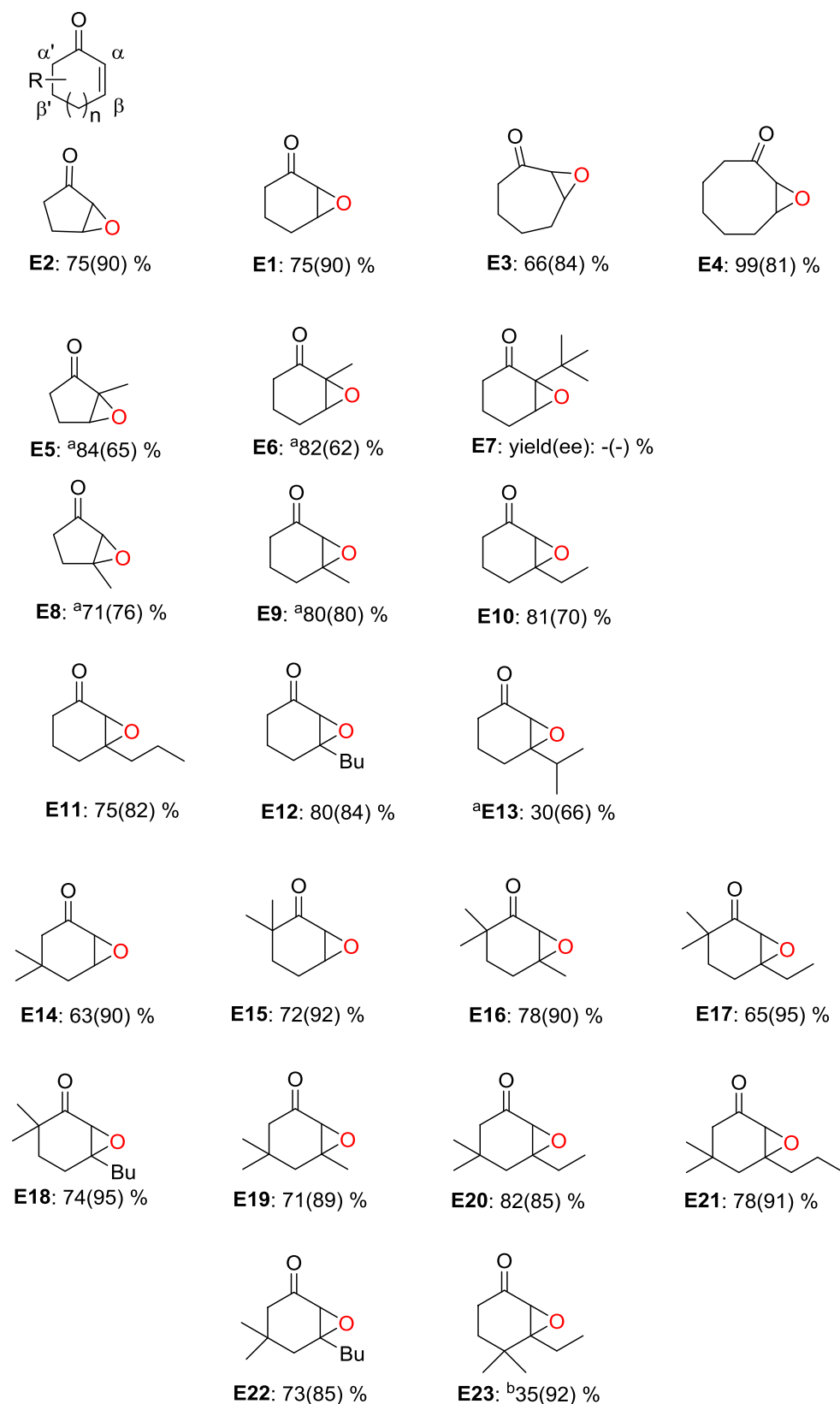
Figure 10. Schematic diagram of different catalysts employed.**Table 7.** Screening of the iron complexes in the asymmetric epoxidation reaction of 2-cyclohexenone.

C ₂ symmetric				C ₁ symmetric			
Entry	Catalyst	Conv(yield) % ^a	(ee)%	Entry	Catalyst	Conv(yield) % ^a	(ee)%
1	Me ₂ N ₁ Fe	85(73)	75	5	2Fe	100(87)	85
2	dMM ₁ Fe	100(94)	84	6	3Fe	90(72)	74
3	IQ ₁ Fe	98(81)	72	7	4Fe	100(70)	75
4	TIPS ₁ Fe	87(71)	81	8	5Fe	99(80)	77
				9	6Fe	73(60)	88
				10	7Fe	67(55)	90
				^b 11	7Fe	100(86)	90

Unless stated, reaction conditions are (S,S')-catalyst (1 mol%), H₂O₂ (2.3 equiv.) and 2-eha (1.4 equiv.) in CH₃CN at -30°C during 30 min. ^aEpoxide yields and substrate conversion determined by GC. Ee's determined by GC with a chiral stationary phase. The absolute configuration (2*R*,3*R*) of the epoxide was determined from its optical rotation, and by comparison from the literature.¹³ ^b3 mol% of catalyst

We synthesized a set of cyclic enones, which were then tested in the asymmetric epoxidation reaction (Figure 11). In first place, the enlargement of ring up to 7 and 8 membered rings provided lower enantioselectivities (84 % and 81 % ee, respectively), However, the enantioselectivity remained excellent for 5 membered ring, 90 % of ee and the yield was good, 75 %. Unfortunately, for α and β substituted enones the enantioselectivities decreased slightly (62-84 % ee, **E5-E13**). Moreover, the reaction didn't take place when bulky groups were added in α - position, such as 2-*tert*-butylcyclohex-2-one (**E7**). Of significant interest, the addition of dimethyl groups in α' and β' position of olefins leads to important improvement, up to 92 % ee (**E14-E15**); if the olefins were β -alkylated, up to 95 % ee were obtained (**E16-E22**). Also dimethylated group in γ gave excellent enantioselectivities, but the yield was poor (**E23**), suggesting that steric hindrance may be limiting these reactions; the same trend was observed for substrates **E9**, **E10**, **E13**.

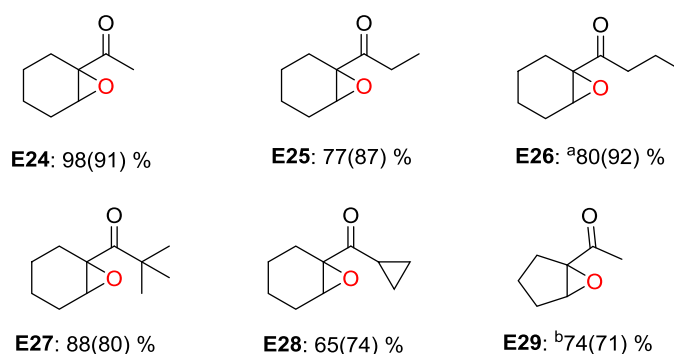
Figure 11. Substrate scope of aliphatic cyclic enones in asymmetric epoxidation with **7Fe** as catalyst. % yield and ee (in parenthesis) are given for each substrate.



Unless stated, reaction conditions are (**S,S'**)-**7Fe** (3 mol%), H₂O₂ (2.3 equiv.) and 2-eha (1.4 equiv.) in CH₃CN at -30°C during 30 min. ^a Epoxide yields determined by GC. ^b 10 mol% catalyst. Ee's determined by GC with a chiral stationary phase.

Remarkably, alkyl 1-cyclohexenyl ketone derivatives were also epoxidized in excellent yields and enantioselectivities, up to 98 and 92 %, respectively (Figure 12). For branched groups, such as tert-butyl (**E27**), the enantioselectivities decreased slightly. In the case of 5 membered ring modest ee was achieved (71 % of ee, **E29**) Most interestingly, it's known that cyclopropane rings acts as radical clocks, and the lack of formation of cyclopropane ring opening products when we performed the epoxidation of cyclopropyl derived substrate (**E28**) is very remarkable, because this fact suggested no formation of radicals in the epoxidation reaction or maybe the oxo-transfer reaction was faster than the possible radical mechanism.

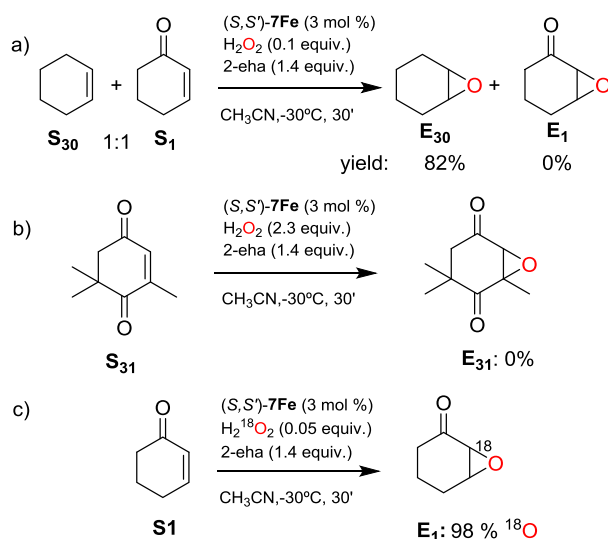
Figure 12. Substrate scope of alkyl 1-cyclohexenyl ketone derivatives in asymmetric epoxidation with **7Fe** as catalyst. % yield and ee (in parenthesis) are given for each substrate.



Unless stated, reaction conditions are (**S,S'**)-**7** (3 mol%), H₂O₂ (2.3 equiv) and 2-eha (1.4 equiv.) in CH₃CN at -30°C during 30 min. ^a4 mol % catalyst. ^b Epoxide yields determined by GC. Ee's determined by GC with a chiral stationary phase.

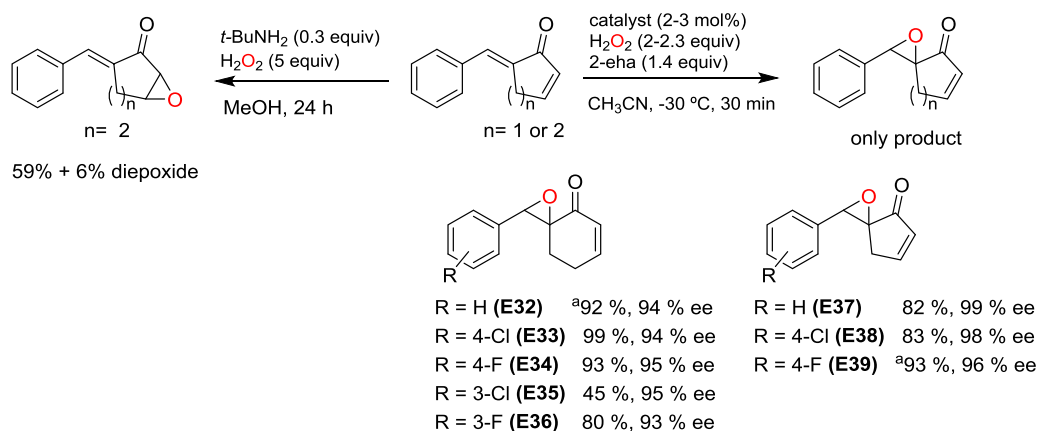
Indeed in the mechanistic scenario established earlier for this class of catalysts, we proposed the implication of an electrophilic high valent oxidant species. According to this scenario, competitive epoxidation of a mixture of cyclohexene (**S30**) and 2-cyclohexenone (**S1**), provided only the epoxide product from cyclohexene (Scheme 39, a). Moreover, a high electron deficient (**S31**) olefin could not be epoxidized (Scheme 39, b). Furthermore, isotopic labelling experiment was performed with H₂¹⁸O₂, observing that oxygen atoms came from hydrogen peroxide, discarding water and O₂ as alternative sources (Scheme 39, c).

Scheme 39. a) Competitive epoxidation experiment of cyclohexene **S30** and 2-cyclohexenone **S1**, c) the epoxidation of electron-deficient olefin **S31** and c) epoxidation of **S1** using $\text{H}_2^{18}\text{O}_2$.



The electrophilic character of the oxidant could be very useful in the oxidation of substrates bearing olefinic moieties with different electronic properties. For this purpose, different dienones were epoxidized giving only one epoxide product with excellent yields and enantioselectivities resulting from epoxidation at the more electron-rich site, for both catalyst $[\text{Fe}(\text{CF}_3\text{SO}_3)_2]^{(\text{Bz}, \text{Tips})\text{pdp}}$ (**7Fe**) and $[\text{Fe}(\text{CF}_3\text{SO}_3)_2]^{(\text{Me}_2\text{N})\text{PDP}}$ (**Me²N1Fe**) (Scheme 39). Our system is orthogonal with enamine catalysis (via nucleophilic oxidant). Consequently the epoxidation with *t*Bu-NH₂ with H₂O₂ provides preferential oxidation at the cyclic aliphatic enone (59 % yield and 6 % yield of diepoxide, Scheme 40, left)

Scheme 40. Substrate scope of dienones in asymmetric epoxidation with **7Fe** and **Me²N1Fe** as catalyst.



Unless stated, reaction conditions are (**S,S**)-**Me²N1Fe** (2 mol%), H₂O₂ (2 equiv) and 2-eha (1.4 equiv.) in CH₃CN at -30°C during 30 min. ^a (**S,S'**)-**7Fe** (3 mol%), H₂O₂ (2.3 equiv) and 2-eha (1.4 equiv.) in CH₃CN at -30°C during 30 min. Ee's determined by HPLC with a chiral stationary phase.

In conclusion, the combination of electronic and steric properties provides a novel approach towards the design of new C_1 symmetric iron complexes capable to epoxidize a new challenging family of non aromatic olefins, such as cyclic aliphatic enones and cyclohexene-1-ketone derivatives.

VII.4. Highly Stereoselective Epoxidation with H₂O₂ Catalyzed by Electron-Rich Aminopyridine Manganese Catalysts

So far, the most enantioselective manganese based systems for asymmetric epoxidation reactions were the known manganese salen complexes reported by Jacobsen and Katsuki and co-workers.^{17,18} However, these systems need large amounts of catalyst and environmentally non-friendly oxidants, such as PhIO, NaOCl and *m*CPBA. In addition, substantial epimerization products are observed in the epoxidation of *cis*-aromatic olefins.

For this reason, during the past decade new systems have been investigated and particularly interesting are novel manganese complexes with tetradentate aminopyridine ligands, that have been proven capable to epoxidize olefins using hydrogen peroxide as oxidant and acetic acid as additive.¹⁹⁻²⁴ Our goal consisted to study the impact of electronic effects in the series of complexes (S,S')[Mn(CF₃SO₃)₂(^Rpdp)] (R = CO₂Et, Cl, H, Me, MeO and Me₂N) in asymmetric epoxidation reactions with hydrogen peroxide as oxidant source (Figure 13). The simplest catalyst of the series (S,S')[Mn(CF₃SO₃)₂(^Hpdp)] (^H**1Mn**) was previously described by Talsi and co-workers¹⁷ and was devised as a good starting point for improvement by tuning its electronic properties. To this end, several groups with systematically different electronic properties were introduced in position 4 of the pyridine ring. All the new complexes developed were tested in the asymmetric epoxidation reaction taking *cis*- β -methylstyrene as model substrate, acetic acid as additive and hydrogen peroxide as oxidant in acetonitrile at -30 °C during 30 minutes (Table 8).

A systematic trend was observed, finding that the more electron-rich is the complex, the higher activity and stereoselectivity (up to 75 % yield and 82 % ee for [Mn(CF₃SO₃)₂(^{Me2N}pdp)] (^{Me2N}**1Mn**)). Also, as precedented for the iron systems, this catalyst is the only one that tolerates the use of small amounts of acetic acid without losing activity (Figure 14). Indeed, we could also observe a systematic dependence between the amount of acetic acid required for good activity and the electronic character of the ligand (Figure 14).

Figure 13. Manganese complexes studied. On the right, an ORTEP diagram of the single crystal X-ray determined structure of (R,R) - $\text{Me}_2\text{N}1\text{Mn}$ is shown. For clarity, H atoms and triflates groups, except for O atoms bound to the metal are omitted

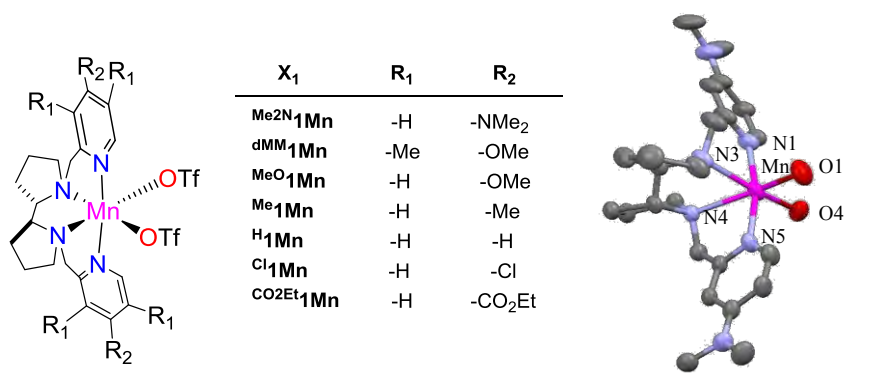
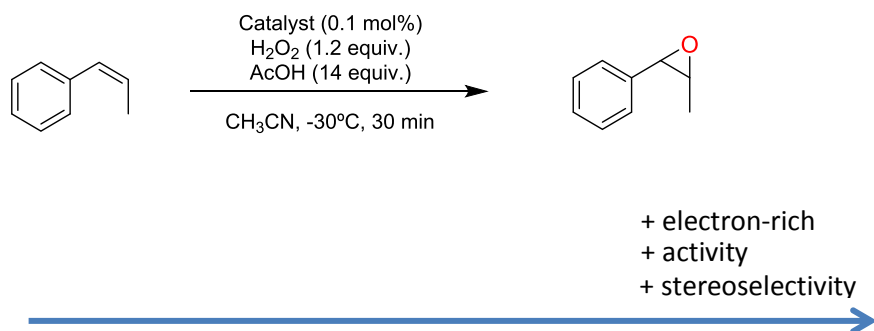


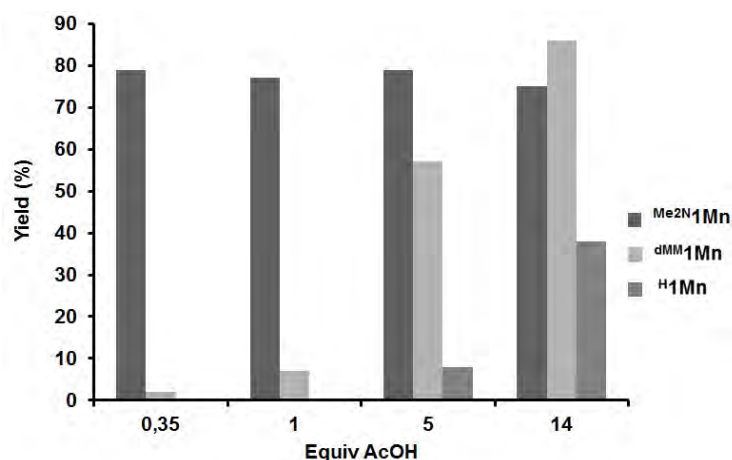
Table 8. Screening of manganese complexes on the asymmetric epoxidation of *cis*- β -methylstyrene.



Catalyst	$\text{CO}_2\text{Et}1\text{Mn}$	$\text{Cl}1\text{Mn}$	$\text{H}1\text{Mn}$	$\text{Me}1\text{Mn}$	$\text{MeO}1\text{Mn}$	$\text{dMM}1\text{Mn}$	$\text{Me}_2\text{N}1\text{Mn}$
Conv.(yield)(%)	44(22)	57(33)	61(38)	100(67)	80(59)	100(86)	100(75)
Ee (%)	43	40	43	63	69	76	82

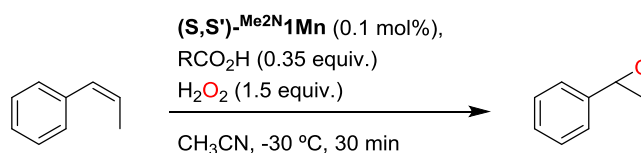
Unless stated, reaction conditions are (*S,S*)-catalyst (0.1 mol%), H₂O₂ (1.2 equiv.) and AcOH (14 equiv.) in CH₃CN at -30°C.

Figure 14. Epoxidation of *cis*- β -methylstyrene as a function of AcOH loading for catalysts $\text{Me}_2\text{N}^1\text{Mn}$, dMM^1Mn and H^1Mn . Reaction conditions; catalyst (0.1 mol%), *cis*- β -methylstyrene (1 equiv.), H_2O_2 (1.2 equiv.) and AcOH (0.35-14 equiv.) in CH_3CN at $-30\text{ }^\circ\text{C}$.



Moreover, we tested different carboxylic acids with the best catalyst $\text{Me}_2\text{N}^1\text{Mn}$ and 0.35 equiv. of carboxylic acid, because at this carboxylic acid loading the activity remained intact. The results showed a direct dependence between enantioselectivity and the size of carboxylic acids, providing the best results with 2-ethylhexanoic acid (up to 92 % ee), while retaining excellent product yields (Table 9, entry 4).

Table 9. Screening of carboxylic acids on the asymmetric epoxidation of *cis*- β -methylstyrene with manganese catalyst $\text{Me}_2\text{N}^1\text{Mn}$



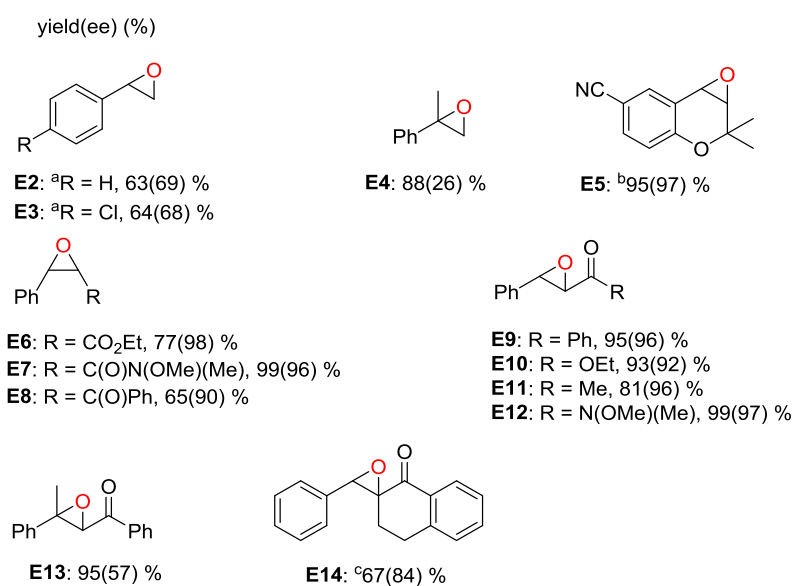
Entry	RCO_2H	Conv/yield (%)	ee (%)
1	 Eba	100(85)	90
2	 Piv	100(82)	88
3	 Aca	100(86)	87

CHAPTER VII: RESULTS AND DISCUSSION

4	2-eha	100(86)	92
^a 5	S-Ibp	100(85)	73
6	S-Ibp ^a	100(90)	86
^a 7	S-Phenylbutyric acid	100(93)	78
8	S-Phenylbutyric acid	100(87)	86
^a 9	S-2-Mba ^a	100(84)	83
10	S-2-Mba ^a	100(85)	85
^a 11	<i>R</i> -Mosher's acid ^a	100(86)	62
12	<i>R</i> -Mosher's acid ^a	100(90)	72

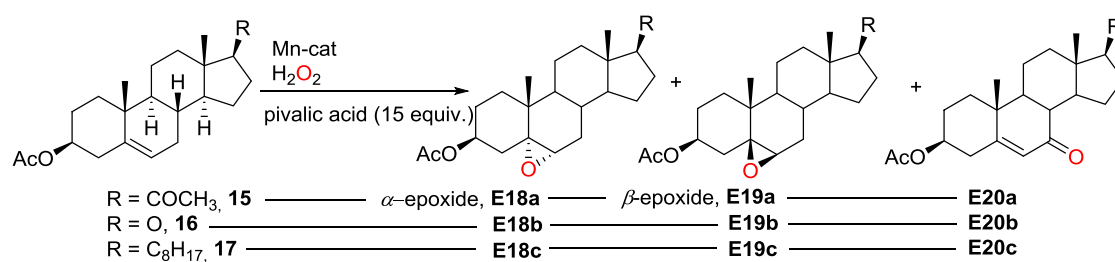
Yields, conversions and ee's were determined by GC. Eba: ethylbutyric acid, Aca: adamantane carboxylic acid and 2-eha: 2-ethylhexanoic acid, S-Ibp: S-Ibuprofen, S-2-Mba: (S)-2-methylbutyric acid. ^a Reaction with (*R,R'*)-^{Me2N}1Mn.

The substrate scope was investigated with optimal conditions in hand, and we epoxidized different families of olefins, such as styrenes with 69 % ee (**E2-E3**), electrodeficient chromenes up to 97 % ee (**E5**), *cis* aromatic olefins up to 98 % ee (**E6-E8**), *trans*-cinnamate derivatives up to 97 % of ee (**E10-E12**) and a tetralone derivative up to 84 % of ee (**E14**) (Figure 15). However, poor to moderate enantioselectivities were obtained with terminal and trisubstituted chalcones (**E4** and **E13**). In the case of electron deficient substrates it's necessary to increase from 0.1 to 0.5 mol% of catalyst (**E6-E14**) to have good results (Figure 15).

Figure 15. Substrate scope on the asymmetric epoxidation with manganese catalyst $^{Me_2N}1Mn$ 

Unless stated, reaction conditions are $(S,S)^{Me_2N}1Mn$ (0.5 mol%), H₂O₂ (2.0 equiv.) and 2-eha (1 equiv.) in CH₃CN at -30°C. ^a0.2 mol % of catalyst, H₂O₂ (2 equiv.), 2-eha (0.5 equiv.). ^b0.1 mol % of catalyst, H₂O₂ (1.5 equiv.), 2-eha (0.35 equiv.). ^cTemp -10°C. Ee's determined by chiral GC and HPLC

Most interestingly, we can also obtain good yields and excellent diastereoselectivities for the β -epoxide of Δ^5 -unsaturated steroids up to 97:3 with $(S,S)^{dMM}1Mn$ as catalyst and pivalic acid as additive (15 equiv.). To the best of our knowledge this is the first example of a first row transition metal catalyst giving high diastereoselectivity in this reaction (Table 10). When the opposite enantiomer of the catalyst was used, the diastereoselectivities decreased substantially, down to 69:32 (Entry 4, Table 10)

Table 10. Epoxidation of Δ^5 -unsaturated steroids.

Entry	Substrate	Catalyst	Yield(%) (E18 + E19) (E20) ^a	Ratio E19/E18
1	15	(<i>S,S</i>)- ^{Me2N} 1Mn	36 (23)	93:7
2	15	(<i>S,S</i>)- ^{dMM} 1Mn	50 (5)	96:4
3	15	(<i>R,R</i>)- ^{dMM} 1Mn	66 (4)	69:32
4	16	(<i>S,S</i>)- ^{dMM} 1Mn	56 (8)	94:6
5	17	(<i>S,S</i>)- ^{dMM} 1Mn	66 ^a (5) ^b	97:3

Unless stated, reaction conditions are catalyst (0.25 mol%), H₂O₂ (2.0 equiv.) and pivalic acid (15 equiv.) in AcOEt/CH₃CN (4:1) at room temperature. Isolated yields. Ratio β/α determined by GC, except for entry 3 that was determined by ¹H-NMR. ^aH-NMR yield. ^bAllylic 7-β-OH alcohol.

Finally, electronic properties in manganese complexes can be used as a powerful tool for controlling the heterolytic cleavage of O-O and O-delivering, leading to excellent catalysts for highly asymmetric epoxidation of olefins with hydrogen peroxide.

References

- (1) Gelalcha, F. G.; Bitterlich, B.; Schröder, K.; Copinathan, A.; Tse, M. K.; Beller, M. *Angew. Chem. Int. Ed.* **2007**, 7293.
- (2) Wang, B.; Wang, S.; Xia, C.; Sun, W. *Chem.-Eur. J.* **2012**, 18, 7332.
- (3) Wang, X.; Miao, C.; Wang, S.; Xia, C.; Sun, W. *ChemCatChem* **2013**, 5, 2489.
- (4) Lyakin, O. Y.; Ottenbacher, R. V.; Bryliakov, K. P.; Talsi, E. P. *Acs Catal.* **2012**, 2, 1196.
- (5) Niwa, T.; Nakada, M. *J. Am. Chem. Soc.* **2012**, 134, 13538.
- (6) MacFaul, P. A.; Ingold, K. U.; Wayner, D. D. M.; Que, L. *J. Am. Chem. Soc.* **1997**, 119, 10594.
- (7) Ingold, K. U.; MacFaul, P. A. Distinguishing Biomimetic Oxidations from Oxidations Mediated by Freely Diffusing Radicals. In *Biomimetic Oxidations Catalyzed by Transition Metal Complexes*, Meunier, B., Ed. Imperial College Press: London, 2000; pp 45.
- (8) Mas-Balleste, R.; Que, L., Jr. *J. Am. Chem. Soc.* **2007**, 129, 15964
- (9) Lyakin, O. Y.; Bryliakov, K. P.; Britovsek, G. J. P.; Talsi, E. P. *J. Am. Chem. Soc.* **2009**, 131, 10798.
- (10) Lyakin, O. Y.; Bryliakov, K. P.; Talsi, E. P. *Inorg. Chem.* **2011**, 50, 5526.
- (11) Ye, W. H.; Ho, D. M.; Friedle, S.; Palluccio, T. D.; Rybak-Akimova, E. V. *Inorg. Chem.* **2012**, 51, 5006.
- (12) Shaik, S.; Cohen, S.; Wang, Y.; Chen, H.; Kumar, D.; Thiel, W. *Chem. Rev.* **2010**, 110, 949.
- (13) Meunier, B.; de Visser, S. P.; Shaik, S. *Chem. Rev.* **2004**, 104, 3947.
- (14) Xingwang Wang, C. M. R.; List, B. *J. Am. Chem. Soc.* **2008**, 130, 6070.
- (15) Lee, A.; Reisinger, C. M.; List, B. *Adv. Synth. Catal.* **2012**, 354, 1701.
- (16) Lifchits, O.; Mahlau, M.; Reisinger, C. M.; Lee, A.; Fares, C.; Polyak, I.; Gopakumar, G.; Thiel, W.; List, B. *J. Am. Chem. Soc.* **2013**, 135, 6677
- (17) Zhang, W.; Loebach, J. L.; Wilson, S. R.; Jacobsen, E. N. *J. Am. Chem. Soc.* **1990**, 112, 2801.
- (18) Irie, R.; Noda, K.; Ito, Y.; Matsumoto, N.; Katsuki, T. *Tetrahedron: Asymmetry* **1991**, 2, 481.
- (19) Gómez, L.; Garcia-Bosch, I.; Company, A.; Sala, X.; Fontrodona, X.; Ribas, X.; Costas, M. *Dalton Trans.* **2007**, 47, 5539.
- (20) Ottenbacher, R. V.; Bryliakov, K. P.; Talsi, E. P. *Adv. Synth. Catal.* **2011**, 353, 885.
- (21) Wu, M.; Miao, C.-X.; Wang, S.; Hu, X.; Xia, C.; Kühn, F. E.; Sun, W. *Adv. Synth. & Catal.* **2011**, 353, 3014.
- (22) Wang, B.; Miao, C.; Wang, S.; Xia, C.; Sun, W., *Chem.-Eur. J.* **2012**, 18, 6750

CHAPTER VII: RESULTS AND DISCUSSION

(23) Garcia-Bosch, I.; Gómez, L.; Polo, A.; Ribas, X.; Costas, M., *Adv. Synth. Catal.* **2012**, *354*, 65.

(24) Dai, W.; Li, J.; Li, G.; Yang, H.; Wang, L.; Gao, S., *Org. Lett.* **2013**, *15*, 4138.

Chapter VIII

General Conclusions

VIII. GENERAL CONCLUSIONS

- We have developed a novel family of chiral mononuclear iron complexes based on (2*S*,2*S'*)-2,2'-bipyrrrolidine as backbone and pyridine groups with different electronic properties at position 4, such as CO₂Et, Cl, H, Me, MeO and Me₂N. These complexes contained an iron(II) center in a distorted octahedral coordination geometry with two *cis* labile sites available for the coordination of oxidant and additives.
- The efficiency of these complexes as catalysts in stereoselective epoxidation reactions was assayed. We demonstrated that the electronic properties play an important role in the activation of hydrogen peroxide and also in oxygen atom delivery to the alkene. Electron-rich complexes provide the best enantioselectivities and yields with H₂O₂ as oxidant. Moreover, it was discovered that bulky carboxylic acids, such as *S*-Ibuprofen and 2-ethylhexanoic acid also improve the enantioselectivities in comparison with acetic acid and smaller carboxylic acids. The combination of the use of electron-rich catalysts and bulky carboxylic acids results in a remarkable system for highly enantioselective epoxidation with a broad substrate scope: illustrative examples are *cis*- β -methylstyrene (86% ee), *cis*-ethylcinnamate (97% ee), electron-deficient chromenes (99% ee), *trans*-chalcone (98% ee), tetralone derivative (97% ee), *trans*-cinnamate derivatives (97% ee) and 2-cyclopentanone (87% ee).

Mechanistic studies, such as competitive oxidations of pairs of substrates and Hammett plot analyses vs enantioselectivity showed that catalysis is mediated by a high valent electrophilic oxidant and also strongly suggested that linear free energy relationships observed are general (it applies to any olefin) for this epoxidation system, and has mainly an electronic origin. Also, labelling experiments showed that the oxygen transferred came from H₂O₂ and not from scrambling with H₂O.

- We have also developed a new strategy to amplify the substrate scope for epoxidation reactions using electron-rich nonheme iron complexes in

combination with different amino acids instead of carboxylic acids. We observed that the introduction of hindered groups in alpha position of the carboxylic acid, in combination with the use of a naphthalimido *N*-protecting group, results in a system that provides high enantioselectivities for 1,1'-disubstituted styrenes (up to 97 % of ee). From a synthetic perspective, the present approach is appealing as it provides proof of concept that the versatility of these systems can be straightforwardly extended towards novel classes of substrates without requiring an elaborate catalyst development. Finally, we could obtain interesting products from these terminal epoxides as unprotected aziridines, amino alcohols and azido alcohols, without losing stereoselectivity.

- On the other hand, we have synthesized a novel C_1 symmetric iron coordination complex that combines a bulky pyridine and a benzylimidazole in its structure. We demonstrated that this iron complex epoxidized with good yields and higher enantioselectivities a set of cyclic aliphatic enones up to 95 % ee and 1-cyclohexene ketone derivatives up to 92 % ee with hydrogen peroxide as oxidant and 2-ethylhexanoic acid as additive. Moreover, the electrophilic character of the active oxidant species was used to epoxidize polyene substrates with higher regioselectivities and stereoselectivities up to 99 % ee. Moreover this element confers the system an orthogonal selectivity with regard to standard enamine catalysis. In summary, this development provides directions for future rational design of new classes of C_1 symmetric iron complexes.
- We have also developed a novel family of chiral mononuclear manganese complexes for the stereoselective epoxidation of alkenes with H_2O_2 . We demonstrated that electron-rich complexes can operate with reduced amounts of acetic acid to deliver the oxygen atom to the alkene, providing the same yields as when using high loadings of acetic acid. In addition, the electron rich complexes improve enantioselectivities and yields. Moreover, in combination with bulky carboxylic acids, such as pivalic acid and 2-ethylhexanoic acid, enantioselectivities were also

improved in comparison with acetic acid and other smaller carboxylic acids. The broad substrate scope found is truly remarkable: *cis*-beta-methylstyrene (92% ee), *cis*-ethylcinnamate (98% ee), electron-deficient chromenes (97% ee), *trans*-chalcone (96% ee), tetralone derivative (84% ee), *trans*-cinnamate derivatives (92% ee). This catalytic system is also capable of epoxidizing with high diastereoselectivities different Δ^5 -steroids, up to 94 % diastereoselectivities for β -epoxide

Experimental Section

Materials

Reagents and solvents used were of commercially available reagent quality unless stated otherwise. Solvents were purchased from SDS and Scharlab. Solvents were purified and dried by passing through an activated alumina purification system (M-Braun SPS-800) or by conventional distillation techniques.

Instrumentation

Oxidation products were identified by comparison of their GC retention times and GC/MS with those of authentic compounds, and/or by ^1H and $^{13}\text{C}\{^1\text{H}\}$ -NMR analyses. IR spectra were taken in a Mattson-Galaxy Satellite FT-IR spectrophotometer using a MKII Golden Gate single reflection ATR system. Elemental analyses were performed using a CHNS-O EA-1108 elemental analyzer from Fisons. NMR spectra were taken on BrukerDPX300 and DPX400 spectrometers using standard conditions. Electrospray ionization mass spectrometry (ESI-MS) experiments were performed on a Bruker Daltonics Esquire 3000 Spectrometer using a 1 > mM solution of the analyzed compound. High resolution mass spectra (HRMS) were recorded on a Bruker MicroTOF-Q IITM instrument with an ESI source at Serveis Tècnics of the University of Girona. Samples were introduced into the mass spectrometer ion source by direct infusion through a syringe pump and were externally calibrated using sodium formate. Chromatographic resolution of enantiomers was performed on an AgilentGC-7820-A chromatograph using a CYCLOSIL-B, Sigma-aldrich Supelco Astec CHIRALDEX G-TA column, column and HPLC 1200 series Agilent technologies using CHIRALPAK-IA and CHIRALPAK-IC columns. The configuration of the major enantiomer was determined by chemical correlation.

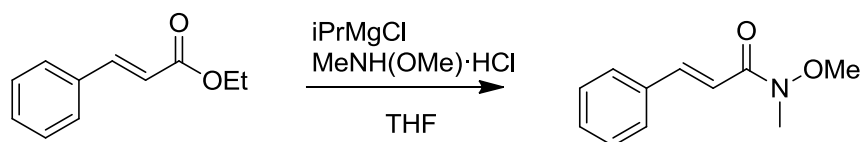
Experimental section: Chapter VII.1

Asymmetric Epoxidation with H₂O₂ by Manipulating the Electronic Properties of Non-Heme Iron Catalysts

1) Synthesis of substrates

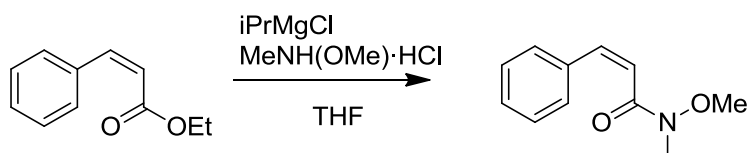
cis-ethylcinnamate (**S2**),¹ α,β -enones (**S9-S10**),² tetralone products (**S19-S22**),² nitro-chromene (**S5**)³ and α,β -trisubstituted enones (**S12**)⁴ were prepared according to the reported procedures. The substrate nomenclatures (**SX**) were exclusives for this chapter.

- Synthesis of *trans*-*N*-methoxy-*N*-methylcinnamamide (**S18**)



To a suspension of *trans*-ethylcinnamate (7.6 mmol) and *N,O*-dimethylhydroxylamine hydrochloride (19.0 mmol) in THF (15.0 mL), a solution of *i*PrMgCl in THF (2.0 M, 38.0 mmol) was added dropwise under a nitrogen atmosphere at -15 °C. After stirring the reaction for 60 min at 0 °C, it was quenched by adding saturated aq. NH₄Cl and then diluted with 20 ml of EtOAc. The organic layer was separated and washed with brine, dried over MgSO₄ and concentrated at reduced pressure. The residue was purified by silica gel column chromatography (Hexane:EtOAc= 90:10 to 70:30) to afford the corresponding *trans*-amide product as a light yellow solid (63 % yield). ¹H-NMR (CDCl₃, 300 MHz, 300K) δ , ppm: 7.74 (d, 1H, *J* = 15.8 Hz), 7.58 - 7.55 (m, 2H), 7.40 - 7.35 (m, 3H), 7.04 (d, 1H, *J* = 15.8 Hz), 3.76 (s, 3H), 3.30 (s, 3H). ¹³C-NMR 166.94, 143.43, 135.16, 129.84, 128.80, 128.04, 115.79, 61.89, 32.51 HRMS(ESI+) *m/z* calculated for C₁₁H₁₃NO₂Na [M+Na]⁺ 214.0838, found 214.0840.

- Synthesis of *cis*-*N*-methoxy-*N*-methylcinnamamide (**S3**)



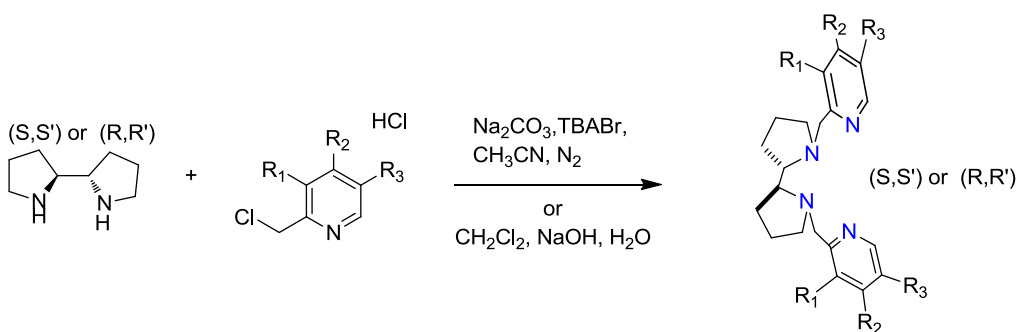
The same experimental procedure used in the preparation of **S18** was applied but in this case starting from the corresponding *cis*-ethylcinnamate. Finally, after work-up the product was analyzed by $^1\text{H-NMR}$ and GC, resulting in a mixture of 92 % of *cis*-amide, 3 % of *trans*-amide, 3 % of over-reduction and 2 % of other impurities. $^1\text{H-NMR}$ (CDCl_3 , 300 MHz, 300K) δ , ppm: 7.52-7.50 (m, 2H), 7.35 - 7.27 (m, 3H), 6.76 (d, 1H, $J = 12.8$ Hz), 6.27 (br, 1H), 3.64 (s, 3H), 3.24 (s, 3H). $^{13}\text{C}\{^1\text{H}\}$ -NMR 168.2, 137.7, 135.2, 129.1, 128.6, 128.3, 120.6, 61.7, 32.2. HRMS(ESI+) m/z calculated for $\text{C}_{11}\text{H}_{13}\text{NO}_2\text{Na}$ $[\text{M}+\text{Na}]^+$ 214.0838, found 214.0838.

2) Synthesis of complexes

2.1) Synthesis of pyridine synthons

Pyridine synthons $^{\text{dMM}}\text{PyCH}_2\text{Cl}\cdot\text{HCl}$ was purchased from Aldrich. 2-chloromethyl-4-chloropyridine, $^{\text{Cl}}\text{PyCH}_2\text{Cl}\cdot\text{HCl}$,⁵ 2-chloromethyl-4-dimethylaminopyridine, $^{\text{NMe}_2}\text{PyCH}_2\text{Cl}\cdot\text{HCl}$,⁵ 2-chloromethyl-4-ethoxycarbonilhydrochloride, $^{\text{CO}_2\text{Et}}\text{PyCH}_2\text{Cl}\cdot\text{HCl}$,⁶ $^{\text{MeO}}\text{PyCH}_2\text{Cl}\cdot\text{HCl}$,⁷ $^{\text{Me}}\text{PyCH}_2\text{Cl}\cdot\text{HCl}$ ⁸ and 3-(chloromethyl)isoquinoline $^{\text{iQuin}}\text{PyCH}_2\text{Cl}\cdot\text{HCl}$,⁹ were synthesized following previously described procedures.

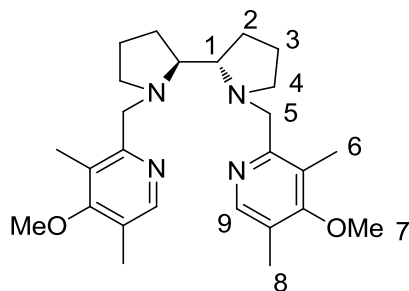
2.2) Synthesis of ligands.



$^{\text{Me}_2\text{N}}\text{PDP}$: $\text{R}_1=\text{R}_3=\text{H}$, $\text{R}_2=\text{NMe}_2$
 $^{\text{dMM}}\text{PDP}$: $\text{R}_1=\text{R}_3=\text{Me}$, $\text{R}_2=\text{OMe}$
 $^{\text{MeO}}\text{PDP}$: $\text{R}_1=\text{R}_3=\text{H}$, $\text{R}_2=\text{OMe}$
 $^{\text{Me}}\text{PDP}$: $\text{R}_1=\text{R}_3=\text{H}$, $\text{R}_2=\text{Me}$
 $^{\text{Pin}}\text{PDP}$: $\text{R}_1=\text{H}$ $\text{R}_2\text{-R}_3=\text{Pinene}$ (R,R,R)
 $^{\text{H}}\text{PDP}$: $\text{R}_1=\text{R}_3=\text{R}_2=\text{H}$
 $^{\text{iQuin}}\text{PDP}$: $\text{R}_1=\text{H}$ $\text{R}_2\text{-R}_3=\text{Ph}$
 $^{\text{Cl}}\text{PDP}$: $\text{R}_1=\text{R}_3=\text{H}$, $\text{R}_2=\text{Cl}$
 $^{\text{CO}_2\text{Et}}\text{PDP}$: $\text{R}_1=\text{R}_3=\text{H}$, $\text{R}_2=\text{CO}_2\text{Et}$

EXPERIMENTAL SECTION

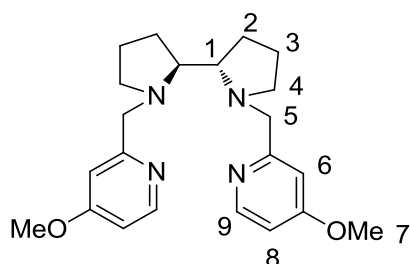
Synthesis of (S,S')-^dMM-PDP.



A solution containing (S,S')-2,2'-bipyrrrolidine *D*-tartrate (0.23 g, 0.8 mmol) and NaOH (0.25 g) in H₂O (2 mL) was added to a 10 mL round bottom flask charged with a stir bar and ^dMM-PyCH₂Cl·HCl (2-chloromethyl-4-methoxy-3,5-dimethylpyridine hydrochloride) (0.4 g, 1.7 mmol) dissolved in CH₂Cl₂ (5 mL). The combined mixture was stirred for 24 hours. At this point, the aqueous phase was extracted with CH₂Cl₂ (3 x 5 mL). The organic fractions were combined, dried over MgSO₄ and the solvent was eliminated under vacuum. The obtained brown oil that was purified by silica column (CH₂Cl₂:MeOH:NH₃ 96:3:1) and the collected fractions were removed under reduced pressure to provide 272 mg (0.62 mmol, yield 78%) of a white oil that turns solid after drying under vacuum. FT-IR (ATR) ν , cm⁻¹: 2967 – 2803 (C-H)_{sp}³, 2359, 2335, 1738, 1564, 1366, 1250, 1214, 1091, 1004, 769. ¹H-NMR (400 MHz, CDCl₃, 300 K) δ , ppm: 8.14 (s, 2H (9)), 4.05 (d, 2H, *J* = 12 Hz (5)), 3.75 (s, 6H (7)), 3.39 (d, 2H, *J* = 12 Hz (5)), 2.75 (m, 2H (4)), 2.58 (m, 2H (1)), 2.31 (s, 6H (6)), 2.24 (s, 6H (8)), 2.26 (m, 2H (4)), 1.69 - 1.53 (m, 8H (2 and 3)). ¹³C{¹H}-NMR 163.9, 157.8, 148.2, 126.0, 125.0, 65.3, 60.72, 59.8, 55.5, 26.1, 24.1, 13.3, 10.8. HRMS(ESI-MS) *m/z* calculated for C₂₆H₃₉N₄O₂[M+H]⁺ 439.3068, found 439.3060.

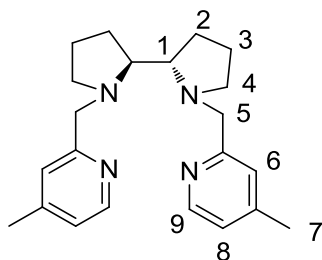
EXPERIMENTAL SECTION

Synthesis of (S,S')-^{MeO}PDP.



It was prepared in analogous manner to (S,S')-^{dMM}PDP starting from (S,S')-2,2'-bipyrrolidine and ^{MeO}PyCH₂Cl·HCl to provide 265.5 mg (0.69 mmol, yield 91 %) of a yellow oil. FT-IR (ATR) ν , cm⁻¹: 2960 – 2799 (C-H)sp³, 2359, 2341, 1737, 1591, 1565, 1418, 1297, 1153, 1036, 990, 824, 761. ¹H-NMR (400 MHz, CDCl₃, 300 K) δ , ppm: 8.31 (d, 2H, *J* = 5.8 Hz (9)), 6.97 (d, 2H, *J* = 2.6 Hz (6)), 6.64 (dd, 2H, *J* = 5.8, 2.5 Hz (8)), 4.18 (d, 2H, *J* = 14.6 Hz (5)), 3.80 (s, 6H), 3.49 (d, 2H, *J* = 14.6 Hz (5)), 3.03 (m, 2H (4)), 2.81 (m, 2H (1)), 2.25 (m, 2H (4)), 1.85 – 1.68 (m, 8H (2 and 3)) ¹³C{¹H}-NMR 166.2, 162.4, 150.0, 108.1, 108.0, 65.6, 61.2, 55.3, 54.9, 26.2, 23.7. HRMS(ESI-MS) *m/z* calculated for C₂₂H₃₀N₄O₂ [M+H]⁺ 384.2442, found 384.2449.

Synthesis of (S,S')-^{Me}PDP.

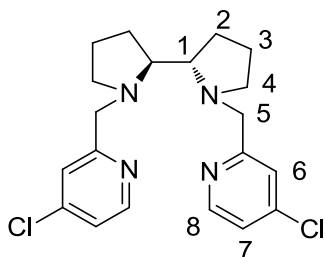


It was prepared in analogous manner to (S,S')-^{dMM}PDP starting from (S,S')-2,2'-bipyrrolidine and ^{Me}PyCH₂Cl·HCl to provide 242.3 mg (0.69 mmol, yield 96%) of a yellow solid FT-IR (ATR) ν , cm⁻¹: 2952 – 2791 (C-H)sp³, 2359, 2341, 1602, 1560, 1435, 1376, 1124, 988, 892, 820. ¹H-NMR (400 MHz, CDCl₃, 300 K) δ , ppm: 8.36 (d, 2H, *J* = 5.0 Hz (9)), 7.42 (s, 2H, (6)), 7.12 (d, 2H, *J* = 5.0(8)), 4.17 (d, 2H, *J* = 14.1 Hz (5)), 3.45 (d, 2H, *J* = 14.1 Hz (5)), 3.00 (m, 2H (4)), 2.79 (m, 2H (1)), 2.30 (s, 6H (7)), 2.24 (m, 2H (4)), 1.87 – 1.68 (m, 8H (2 and 3)) ¹³C{¹H}-NMR 160.1, 148.6, 147.3, 123.5, 122.7, 65.5, 61.2, 55.3, 25.9, 23.5,

EXPERIMENTAL SECTION

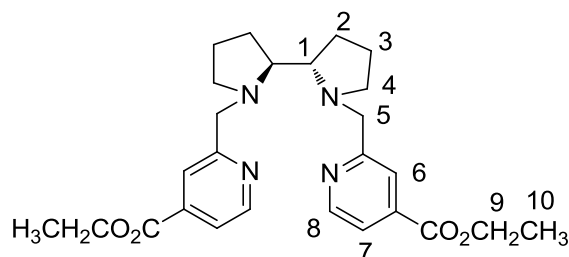
21.1. HRMS(ESI-MS) m/z calculated for $C_{22}H_{30}N_4$ $[M+H]^+$ 351.2549, found 351.2543.

Synthesis of (S,S') - Cl PDP.



It was prepared in analogous manner to (S,S') - dMM PDP starting from (S,S') -2,2'-bipyrrrolidine and $^{Cl}PyCH_2Cl \cdot HCl$ to obtain a yellow oil that was purified over a silica column ($CH_2Cl_2:MeOH:NH_3$ 96:3:1) and the collected fractions were dried under reduced pressure to provide 231 mg (0.59 mmol, yield 63%) of a yellow oil. FT-IR (ATR) ν , cm^{-1} : 2961 – 2798 (C-H) sp^3 , 2359, 2341, 1737, 1572, 1553, 1215, 1120, 882, 705. 1H -NMR (400 MHz, $CDCl_3$, 300 K) δ , ppm: 8.38 (d, 2H, $J = 5.4$ Hz (8)), 7.42 (d, 2H, $J = 1.9$ Hz (6)), 7.12 (dd, 2H, $J = 5.4, 1.9$ Hz (7)), 4.19 (d, 2H, $J = 14.9$ Hz (5)), 3.54 (d, 2H, $J = 14.9$ Hz (5)), 3.03 (m, 2H (4)), 2.81 (m, 2H (1)), 2.49 (m, 2H (4)), 1.85 – 1.72 (m, 8H (2 and 3)) $^{13}C\{^1H\}$ -NMR 162.5, 149.7, 144.5, 122.7, 122.1, 65.8, 60.8, 55.3, 26.2, 23.7. HRMS(ESI-MS) m/z calculated for $C_{20}H_{25}N_4Cl_2[M+H]^+$ 391.1451, found 391.1451.

Synthesis of (S,S') - CO_2Et PDP

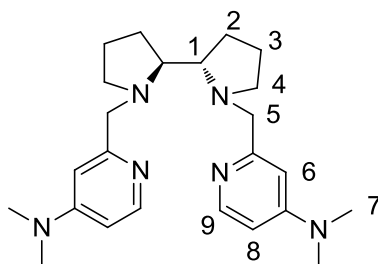


It was prepared in analogous manner to (S,S') - dMM PDP starting from (S,S) -2,2'-bipyrrrolidine and $^{CO_2Et}PyCH_2Cl \cdot HCl$ to obtain a green oil that was used without further purification. (320 mg, 0.68 mmol, yield 88%). FT-IR (ATR) ν , cm^{-1} : 2962 – 2803 (C-H) sp^3 , 2360, 2334, 1725, 1561, 1404, 1366, 1285, 1202, 1104, 763, 629. 1H -NMR (400 MHz, $CDCl_3$, 300 K) δ , ppm: 8.64 (d, 2H, $J = 5.1$ Hz (8)), 7.93

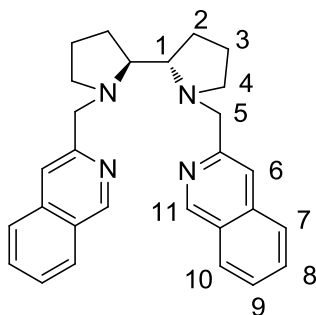
EXPERIMENTAL SECTION

(s, 2H, (6)), 7.67 (d, 2H, $J = 5.1$ Hz (7)), 4.40 (q, 4H (9)), 4.24 (d, 2H, $J = 14.6$ Hz (5)), 3.61 (d, 2H, $J = 14.6$ Hz (5)), 3.01 (m, 2H (4)), 2.84 (m, 2H (1)), 2.27 (m, 2H (4)), 1.85 – 1.73 (m, 8H (2 and 3)) 1.40 (t, 6H (10)) $^{13}\text{C}\{^1\text{H}\}$ -NMR 165.5, 161.7, 149.6, 138.1, 122.0, 120.8, 65.6, 61.7, 61.0, 55.3, 26.0, 23.7, 14.2. HRMS(ESI-MS) m/z calculated for $\text{C}_{26}\text{H}_{35}\text{N}_4\text{O}_4[\text{M}+\text{H}]^+$ 467.2653, found 467.2668.

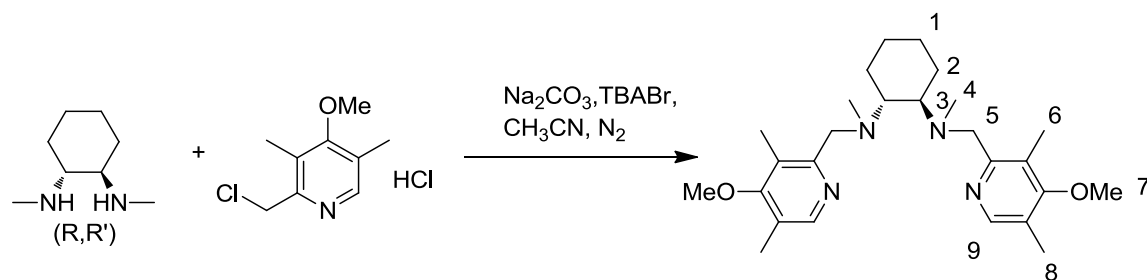
Synthesis of (S,S')-^{Me}2N PDP



2-Chloromethyl-4-dimethylaminopyridine hydrochloride (0.40 g, 1.93 mmol), (S,S')-2,2'-bipyrrrolidine (124 mg, 0.88 mmol) and anhydrous acetonitrile (12 mL) were mixed in a 25 mL flask. Na_2CO_3 (0.74 g) and tetra-butylammonium bromide, TBABr (4 mg) were added directly as solids and the resulting mixture was heated at reflux under N_2 for 15 hours. After cooling to room temperature, the resulting brown mixture was filtered and the filter cake was washed with CH_2Cl_2 . The combined filtrates were evaporated under reduced pressure. To the resulting residue, 1N NaOH (10 mL) was added and the mixture was extracted with CH_2Cl_2 (3 x 10 mL). The combined organic layers were dried over anhydrous MgSO_4 and the solvent was removed under reduced pressure. After, the residue was solved in *n*-hexane and stirred overnight. Finally, the solvent was decanted and removed under reduced temperature to yield 307 mg of yellow oil (0.75 mmol, yield 85 %). FT-IR (ATR) ν , cm^{-1} : 2955 – 2804 (C-H) sp^3 , 2357, 1737, 1596, 1542, 1375, 1218, 1001, 804. ^1H -NMR (CDCl_3 , 400 MHz, 300K) δ , ppm: 8.15 (d, 2H, $J = 6.0$ Hz (9)), 6.69 (d, 2H, $J = 2.7$ Hz (6)), 6.37 (dd, 2H, $J = 6.0, 2.7$ Hz (8)), 4.14 (d, 2H, $J = 14.2$ Hz (5)), 3.43 (d, 2H, $J = 14.2$ Hz (5)), 3.08 (m, 2H (4)), 2.97 (s, 12H, (7)), 2.83 (m, 2H (1)), 2.28 (m, 2H (4)), 1.86 – 1.69 (m, 8H (2 and 3)). $^{13}\text{C}\{^1\text{H}\}$ -NMR 160.15, 154.91, 148.88, 105.22, 105.03, 65.58, 61.58, 55.31, 39.09, 39.01, 26.22, 23.70. HRMS(ESI-MS) m/z calculated for $\text{C}_{24}\text{H}_{37}\text{N}_6[\text{M}+\text{H}]^+$ 409.3074, found 409.3065.

Synthesis of (S,S') -ⁱQuinPDP

It was prepared in analogous manner to (S,S') -^{Me2N}PDP starting from (S,S') -2,2'-bipyrrolidine and ⁱQuinCH₂Cl·HCl to obtain a yellow oil that was purified over silica column (CH₂Cl₂:MeOH:NH₃ 85:10:5) and the collected fractions were removed under reduced pressure to provide 117 mg (0.28 mmol, 53%) of a yellow oil. FT-IR (ATR) ν , cm⁻¹: 2958 – 2791 (C-H)sp³, 2360, 2341, 1737, 1627, 1589, 1366, 1136, 1137, 953, 885, 743. ¹H-NMR (CDCl₃, 400 MHz, 300K) δ , ppm: 9.12 (s, 2H (11)), 7.88 (dd, 2H, *J* = 8.2, 0.8 Hz (10)), 7.74 (dd, 2H, *J* = 8.2, 0.8 Hz (7)), 7.69 (s, 2H, (6)), 7.62 (m, 2H, (9)), 7.51 (m, 2H (8)), 4.42 (d, 2H, *J* = 14.7 Hz (5)), 3.71 (d, 2H, *J* = 14.7 Hz (5)), 3.13 (m, 2H (4)), 2.94 (m, 2H (1)) 2.32 (m, 2H (4)), 1.90 – 1.75 (m, 8H (2 and 3)). ¹³C{¹H}-NMR 153.7, 151.8, 136.4, 130.1, 127.5, 127.4, 126.5, 126.4, 118.3, 65.9, 61.2, 55.4, 26.3, 23.6. HRMS(ESI-MS) *m/z* calculated for C₂₈H₃₁N₄[M+H]⁺ 423.2543, found 423.2542.

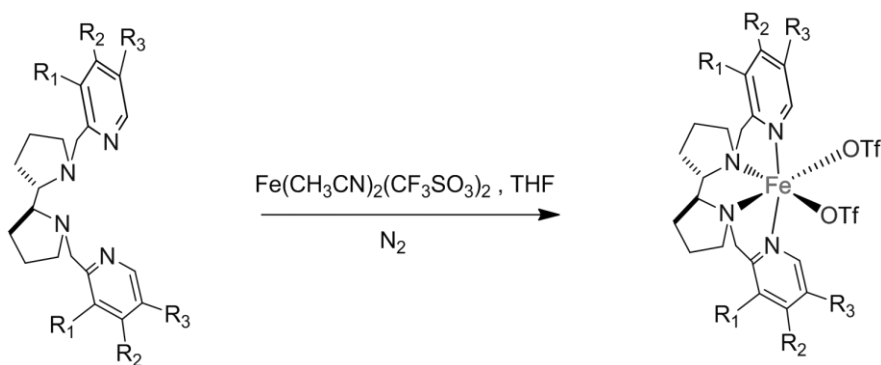
Synthesis of (R,R') -^{dMM}MCP

It was prepared in analogous manner to (S,S') -^{dMM}PDP starting from (R,R) -*N,N'*-dimethylcyclohexane-1,2-diamine (304.1 mg, 2.14) and ^{dMM}PyCH₂Cl·HCl (970.7 mg, 4.37 mmols) to obtain an orange oil that was purified over a silica column (CH₂Cl₂:MeOH:NH₃ 96:3:1) and the collected fractions were removed under reduced pressure to provide 803 mg (1.82 mmol, 85%) of a pale yellow solid. FT-IR (ATR) ν , cm⁻¹: 2990 – 2788 (C-H)sp³, 1560, 1452, 1249, 1082, 1002, 985,

874, 797, 602, 525. $^1\text{H-NMR}$ (400 MHz, CDCl_3 , 300 K) δ , ppm: 8.12 (s, 2H (9)), 3.76 (d, 2H, $J = 12.2$ Hz (5)), 3.69 (s, 6H (7)), 3.69 (d, 2H, $J = 12.2$ Hz (5)), 2.50 (m, 2H (3)), 2.32 (s, 6H (6)), 2.22 (s, 6H (8)), 2.00 - 1.96 and 1.73 - 1.71 (m, 4H (2)), 1.96 (s, 6H (4)), 1.17 - 1.08 (m, 4H, (1)) $^{13}\text{C}\{^1\text{H}\}\text{-NMR}$ 163.9, 158.3, 147.9, 126.7, 124.8, 61.7, 59.9, 59.6, 35.2, 25.8, 23.9, 13.2, 10.8. HRMS(ESI-MS) m/z calculated for $\text{C}_{26}\text{H}_{41}\text{O}_2\text{N}_4[\text{M}+\text{H}]^+$ 441.3224, found 441.3221.

(S,S) - $^{\text{H}}$ PDP and (R,R,R) - $^{\text{Pin}}$ PDP were prepared following reported procedures by C. White *et al.*,¹⁰ and L. Gomez *et al.*¹¹

2.3) Synthesis of iron complexes



(S,S) - $[\text{Fe}(\text{OTf})_2]^{\text{Me}_2\text{N}}\text{PDP}]$: $R_1=R_3=\text{H}$, $R_2=\text{NMe}_2$

(S,S) - $[\text{Fe}(\text{OTf})_2]^{\text{dMM}}\text{PDP}]$: $R_1=R_3=\text{Me}$, $R_2=\text{OMe}$

(S,S) - $[\text{Fe}(\text{OTf})_2]^{\text{MeO}}\text{PDP}]$: $R_1=R_3=\text{H}$, $R_2=\text{OMe}$

(S,S) - $[\text{Fe}(\text{OTf})_2]^{\text{Me}}\text{PDP}]$: $R_1=R_3=\text{H}$, $R_2=\text{Me}$

(R,R,R) - $[\text{Fe}(\text{OTf})_2]^{\text{Pin}}\text{PDP}]$: $R_1=\text{H}$, $R_2=R_3=\text{Pinene (R,R,R)}$

(S,S) - $[\text{Fe}(\text{OTf})_2]^{\text{H}}\text{PDP}]$: $R_1=R_3=R_2=\text{H}$

(S,S) - $[\text{Fe}(\text{OTf})_2]^{\text{iQuin}}\text{PDP}]$: $R_1=\text{H}$, $R_2=R_3=\text{Ph}$

(S,S) - $[\text{Fe}(\text{OTf})_2]^{\text{Cl}}\text{PDP}]$: $R_1=R_3=\text{H}$, $R_2=\text{Cl}$

(S,S) - $[\text{Fe}(\text{OTf})_2]^{\text{CO}_2\text{Et}}\text{PDP}]$: $R_1=R_3=\text{H}$, $R_2=\text{CO}_2\text{Et}$

(S,S) - $[\text{Fe}(\text{OTf})_2]^{\text{dMM}}\text{PDP}]$, $((S,S)^{\text{dMM}}\text{1Fe})$: A suspension of $\text{Fe}(\text{OTf})_2(\text{CH}_3\text{CN})_2$ (192.5 mg, 0.44 mmol) in anhydrous THF (1 mL) was added drop-wise to a vigorously stirred solution of $(S,S)^{\text{dMM}}\text{PDP}$ (198.4 mg, 0.44 mmol) in THF (1 mL). After a few seconds the solution became cloudy and a yellow precipitate appeared. After stirring for 1 hour the solution was filtered off and the resultant yellow solid dried under vacuum. This solid was solved in CH_2Cl_2 (3 mL) and the solution filtered off through celite®. Slow diethyl ether diffusion over the resultant solution afforded, in a few days, 250 mg of yellow crystals (0.31 mmol, yield 70 %). Anal. Calcd for $\text{C}_{28}\text{H}_{38}\text{F}_6\text{FeN}_4\text{O}_6\text{S}_2$: C, 42.43; H, 4.83; N, 7.07; S,

EXPERIMENTAL SECTION

8.09 %. Found: C, 42.68; H, 4.62; N, 7.35; S, 8.31 %. FT-IR (ATR) ν , cm^{-1} : 3001 – 2944 (C-H) sp^3 , 2360, 2334, 1738, 1303, 1233, 1216, 1161, 1029, 996, 633. $^1\text{H-NMR}$ (CD_2Cl_2 , 400 MHz, 300K) δ , ppm: 169 (s), 76 (s), 35 (s), 31 (s), 16.6 (s), -7.3 (s), -22.5 (s). ESI-HRMS calcd. for $\text{C}_{27}\text{H}_{38}\text{F}_3\text{FeN}_4\text{O}_5\text{S}$ [M-OTf] $^+$: 643.1859, found: 643.1881

(S,S')-[Fe(OTf) $_2$ (^{MeO}PDP)], **((S,S')-^{MeO}1Fe)** was prepared in analogous manner to **(S,S')-[Fe(OTf) $_2$ (^{dMM}PDP)]**, starting from **((S,S')-^{MeO}PDP)** and $\text{Fe}(\text{OTf})_2(\text{CH}_3\text{CN})_2$ to obtain the product as a yellow solid. (85.0 mg, 0.15 mmol, yield 72 %). Anal. Calcd for $\text{C}_{24}\text{H}_{30}\text{F}_6\text{FeN}_4\text{O}_8\text{S}_2$: C, 39.14; H, 4.11; N, 7.61 %. Found: C, 39.05; H, 3.84; N, 7.63%. FT-IR (ATR) ν , cm^{-1} : 2976 – 2958 (C-H) sp^3 , 2360, 2334, 1614, 1499, 1301, 1235, 1155, 1025, 897, 830, 625. $^1\text{H-NMR}$ (CD_2Cl_2 , 400 MHz, 300 K) δ , ppm: 174.6 (s), 115.5 (s), 81.6 (s), 48.0 (s), 44.9 (s), 35.3 (s), 30.1 (s), 11.7 (s), -7.6 (s), -19.5 (s). (s)ESI-HRMS calcd. for $\text{C}_{23}\text{H}_{30}\text{F}_3\text{FeN}_4\text{O}_5\text{S}$ [M-OTf] $^+$: 587.1233, found: 587.1233

(S,S')-[Fe(OTf) $_2$ (^{Me}PDP)], **((S,S')-^{Me}1Fe)** was prepared in analogous manner to **(S,S')-[Fe(OTf) $_2$ (^{dMM}PDP)]**, starting from **((S,S')-^{Me}PDP)** and $\text{Fe}(\text{CF}_3\text{SO}_3)_2(\text{CH}_3\text{CN})_2$ to obtain the product as a yellow solid. (94.0 mg, 0.13 mmol, yield 83 %). Anal. Calcd for $\text{C}_{24}\text{H}_{30}\text{F}_6\text{FeN}_4\text{O}_6\text{S}_2$: C, 40.92; H, 4.29; N, 7.95 %. Found: C, 40.88; H, 4.16; N, 8.02 %. FT-IR (ATR) ν , cm^{-1} : 2964 – 2900 (C-H) sp^3 , 2360, 2334, 1621, 1300, 1236, 1216, 1161, 1035, 925, 635. $^1\text{H-NMR}$ (CD_2Cl_2 , 400 MHz, 300 K) δ , ppm: 177.6 (s), 124 (s), 80 (s), 84.9 (s), 53.3 (s), 48.8 (s), 31.5 (s), 27.9 (s), 15.2 (s), -3.4 (s), -9.2 (s), -18.4 (s). ESI-HRMS calcd. for $\text{C}_{23}\text{H}_{30}\text{F}_3\text{FeN}_4\text{O}_3\text{S}$ [M-OTf] $^+$: 555.1335, found: 555.1337

(S,S')-[Fe(OTf) $_2$ (^{NMe2}PDP)], **((S,S')-^{Me2N}1Fe)** was prepared in analogous manner to **(S,S')-[Fe(OTf) $_2$ (^{dMM}PDP)]**, starting from **((S,S')-^{NMe2}PDP)** and $\text{Fe}(\text{OTf})_2(\text{CH}_3\text{CN})_2$ to obtain the product as a yellow solid (145.0 mg, 1.9 mmol, yield 59%). Anal. Calcd for $\text{C}_{28}\text{H}_{38}\text{F}_6\text{FeN}_4\text{O}_8\text{S}_2 \cdot 1/2 \text{CH}_2\text{Cl}_2$: C, 39.54; H, 4.63; N, 10.44 %. Found: C, 39.56; H, 4.65; N, 10.08 %. FT-IR (ATR) ν , cm^{-1} : 2968 – 2934 (C-H) sp^3 , 2360, 2334, 1617, 1526, 1297, 1221, 1155, 1039, 1010, 825, 634. $^1\text{H-NMR}$ (CD_2Cl_2 , 400 MHz, 300K) δ , ppm: 169 (s), 89.5 (s), 84.9 (s), 43.4 (s), 39.9 (s), 39 (s), 36.3 (s), 8.9 (s), -2.6 (s), -18.7 (s). ESI-HRMS calcd. for $\text{C}_{25}\text{H}_{36}\text{F}_3\text{FeN}_6\text{O}_3\text{S}$ [M-OTf] $^+$: 613.1866, found: 613.1882

(S,S')-[Fe(OTf)₂(ⁱQuinPDP)], ((S,S')-ⁱQuin1Fe) was prepared in analogous manner to **(S,S')-[Fe(OTf)₂(^dMM PDP)],** starting from (S,S')-ⁱQuinPDP and Fe(OTf)₂(CH₃CN)₂ to obtain the product as a yellow solid (59.1 mg, 0.076 mmol, yield 84%). Anal. Calcd for C₃₀H₃₀F₆FeN₄O₆S₂ · 1/2 H₂O · 1/2 CH₂Cl₂: C, 44.25; H, 3.89; N, 6.76; S, 7.74 %. Found: C, 43.95; H, 3.60; N, 6.81; S, 8.1 %. FT-IR (ATR) ν , cm⁻¹: 2970 – 2941 (C-H)sp³, 2357, 2341, 1737, 1635, 1298, 1225, 1161, 1029, 967, 754, 631. ¹H-NMR (CD₂Cl₂, 400 MHz, 300K) δ , ppm: 191.2 (s), 148.5 (s), 81.5 (s), 47.7 (s), 31.3 (s), 26.4 (s), 20.6 (s), 14.2 (s), 11.6 (s), -4.2 (s), -10.3 (s), -19.5 (s). ESI-HRMS calcd. for C₂₉H₃₀F₃FeN₄O₃S [M-OTf]⁺: 627.1335, found: 627.1342

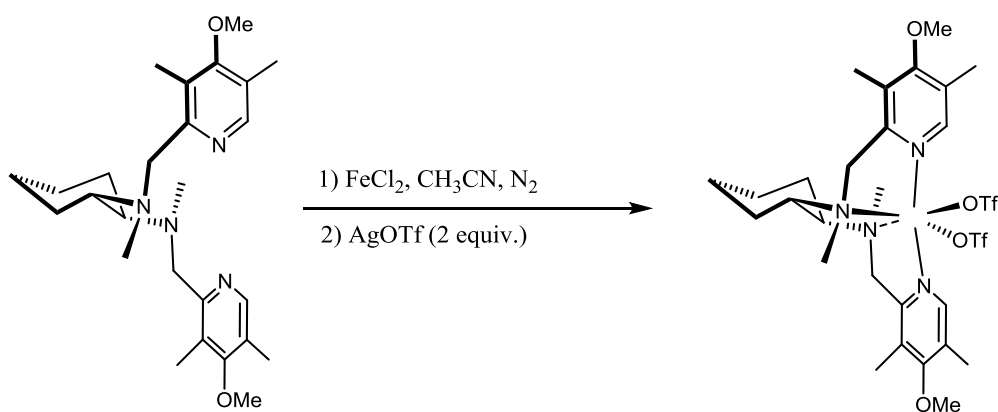
(S,S')-[Fe(OTf)₂(^{Cl}PDP)], ((S,S')-^{Cl}1Fe) was prepared in analogous manner to **(S,S')-[Fe(OTf)₂(^dMM PDP)],** starting from (S,S')-^{Cl}PDP and Fe(OTf)₂(CH₃CN)₂. (161.4 mg, 0.22 mmol, yield 75%). Anal. Calcd for C₂₂H₂₄Cl₂F₆FeN₄O₆S₂: C, 35.45; H, 3.25; N, 7.52; S, 8.60 %. Found: C, 35.73; H, 3.23; N, 7.79; S, 8.58 %. FT-IR (ATR) ν , cm⁻¹: 2971 – 2956 (C-H)sp³, 2362, 2339, 1737, 1595, 1312, 1235, 1215, 1159, 1027, 630. ¹H-NMR (CD₂Cl₂, 400 MHz, 300K) δ , ppm: 176.6 (s), 135.5 (s), 80.7 (s), 54 (s), 49.3 (s), 28.9 (s), 25.9 (s), 11.5 (s), -6.5 (s), -10.8 (s), -18.3 (s). ESI-HRMS calcd. for C₂₁H₂₄Cl₂F₃FeN₄O₃S [M-OTf]⁺: 595.0243, found: 595.0266

(S,S')-[Fe(OTf)₂(^{CO2Et}PDP)], ((S,S')-^{CO2Et}1Fe) was prepared in analogous manner to **(S,S')-[Fe(OTf)₂(^dMM PDP)],** starting from (S,S')-^{CO2Et}PDP and Fe(OTf)₂(CH₃CN)₂. to obtain the product as a orange solid. (231 mg, 0.59 mmol, yield 63%). Anal. Calcd for C₂₈H₃₄F₆FeN₄O₁₀S₂: C, 40.98; H, 4.18; N, 6.83 %. Found: C, 40.97; H, 3.96; N, 6.87 FT-IR (ATR) ν , cm⁻¹: 2981 (C-H)sp³, 1724, 1285, 1236, 1223, 1207, 1160, 1027, 635. ¹H-NMR (CD₂Cl₂, 400 MHz, 300K) δ , ppm: 179.6 (s), 139.5 (s), 79.9 (s), 57.4 (s), 52.7 (s), 26.6 (s), 24.4 (s), 13.8 (s), -8.5 (s), -11.6 (s), -16.4 (s), -18.3 (s). ESI-HRMS calcd. for C₂₇H₃₄F₃FeN₄O₇S [M-OTf]⁺: 671.1445, found: 671.1463

(S,S')-[Fe(OTf)₂(^HPDP)], ((S,S')-^H1Fe) and **(R,R,R)-[Fe(OTf)₂(^PinPDP)], ((R,R,R)-^Pin1Fe)** were prepared following reported procedures by C. White¹⁰ and L. Gomez *et al*,¹¹ respectively.

EXPERIMENTAL SECTION

Synthesis of (R,R') - $[\text{Fe}(\text{OTf})_2(\text{dMM}^{\text{MCP}})]$, $((R,R')$ - $\text{dMM}^{\text{MCP}}_2\text{Fe}$).



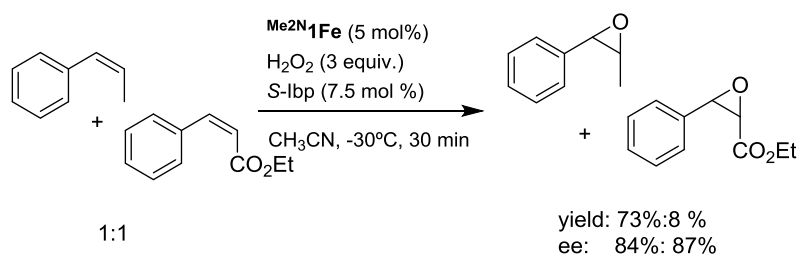
A suspension of FeCl_2 (26.4 mg, 0.21mmol) in anhydrous acetonitrile (1 mL) was added drop-wise to a vigorously stirred solution of (R,R') - dMM^{MCP} (92 mg, 0.21mmol) in acetonitrile (1 mL). After a few minutes the solution became cloudy and a yellow precipitate appeared. After stirring for 1 hour, to the solution was added 2 equiv. of $\text{Ag}(\text{OTf})$. After 1 hour of vigorous stirring, the solution was filtered off through celite©. Slow diethyl ether diffusion over the resultant solution afforded, in a few days, 122 mg of yellow crystals (0.15 mmols, 77 %). Anal. Calcd for $\text{C}_{28}\text{H}_{40}\text{F}_6\text{FeN}_4\text{O}_8\text{S}_2$: C, 42.3; H, 5.07; N, 7.05 %. Found: C, 42.68; H, 4.97; N, 7.14 %. FT-IR (ATR) ν , cm^{-1} : 2934 – 2904 (C-H) sp^3 , 1498, 1732, 1303, 1233, 1214, 1157, 1082, 1014, 994, 633, 511. $^1\text{H-NMR}$ (CD_2Cl_2 , 400 MHz, 300K) δ , ppm: 158 (s), 110 (s), 66(s), 27 (s), 19 (s), 16.6 (s), 5.3 (s), 4.1 (s). ESI-HRMS calcd. for $\text{C}_{27}\text{H}_{40}\text{F}_3\text{FeN}_4\text{O}_5\text{S}$ $[\text{M-OTf}]^+$: 645.2016, found: 645.203

3) Catalytic studies

3.1) General Procedure for epoxide isolation (Figure 7)

An acetonitrile solution (3.75 mL) of an specific olefin (0.415 mmol, final reaction concentration 0.11 M) and $\text{Me}_2\text{N}1\text{Fe}$ (6.3 mg, 8.33 μmol , final reaction concentration 2.2 mM) was prepared in a vial (10 mL) equipped with a stir bar and cooled in an acetonitrile frozen bath. 62.5 μL (solution 0.2 M) of carboxylic acid (12.5 μmol , 3 mol %) was added directly to the solution. Then, 125 μL of 1:1 v:v acetonitrile:hydrogen peroxide solution 32% (1.5 equiv.) was added by syringe pump over a period of 30 min. The solution was further stirred at $-30\text{ }^\circ\text{C}$ for 30 minutes. At this point, 15 mL of an aqueous NaHCO_3 saturated solution were added to the mixture. The resultant solution was extracted with CH_2Cl_2 (3 x 10 mL). Organic fractions were combined, dried over MgSO_4 , filtered through a silica gel plug, and the solvent was removed under reduced pressure to afford the epoxide product. This residue was filtered by silica gel column to obtain the pure epoxide (Hexane/ AcOEt : 98/2).

4) Competition studies (Scheme 35)



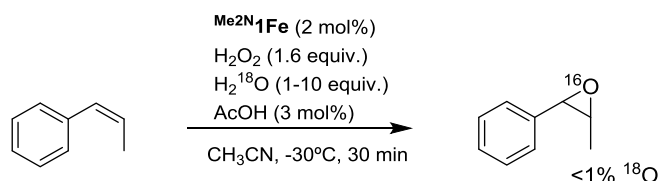
An acetonitrile solution (1.5 mL) of *cis*- β -methylstyrene (0.041 mmol), *cis*-ethylcinnamate (0.041 mmol) and $\text{Me}_2\text{N}1\text{Fe}$ (3.15 mg, 4.14 μmol , final reaction concentration 2.8 mM) was prepared in a vial (10 mL) equipped with a stir bar and cooled in an acetonitrile frozen bath. 62 μL (solution 0.1 M) of *S*-Ibuprofen (7.5 mol %) in acetonitrile was added directly to the solution. Then, 53 μL of 1:1 v:v acetonitrile:hydrogen peroxide solution 32% (3 equiv.) was added by syringe pump over a period of 30 min. The solution was further stirred at $-30\text{ }^\circ\text{C}$ for 30 minutes. At this point, an internal standard (biphenyl) was added and the solution was quickly filtered through a basic alumina plug, which was subsequently rinsed with 2 x 1 mL AcOEt . GC analysis of the solution provided

EXPERIMENTAL SECTION

substrate conversions and product yields relative to the internal standard integration. Products were identified by comparison to the GC retention time of authentic samples, and by their GC-MS spectrum.

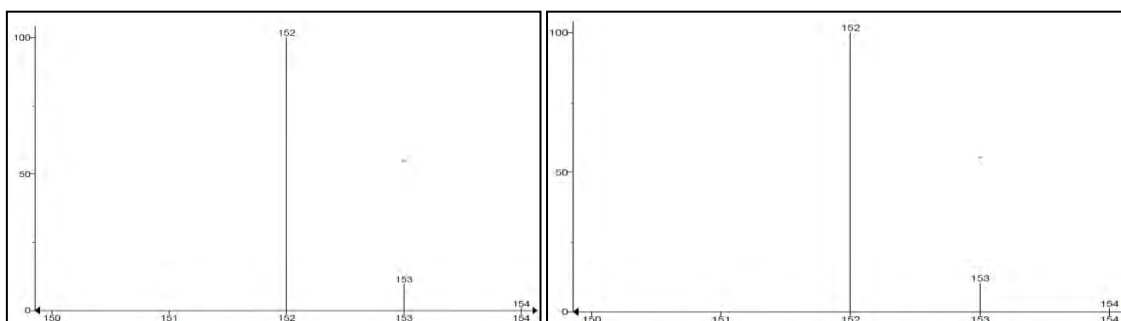
5) ^{18}O labeling studies (Scheme 36)

a) $\text{H}_2^{18}\text{O}/\text{H}_2^{16}\text{O}_2$ labeling experiment



Regular epoxide
experiment

Epoxide obtained from the H_2^{18}O



m/z	%
152	90.6051008
153	8.70284379
154	0.69205543

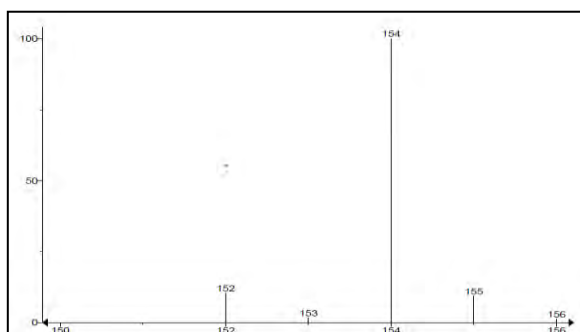
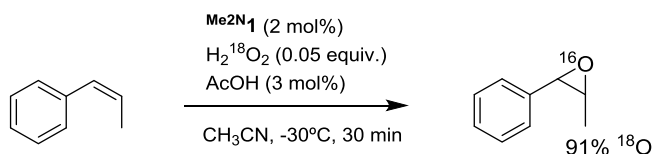
m/z	%
152	89.9223731
153	8.91495723
154	1.1626697

An acetonitrile solution (750 μL) of an *cis*- β -methylstyrene (0.083 mmol, final reaction concentration 0.11 M) and $\text{Me}_2\text{N}_1\text{Fe}$ (1.26 mg, 1.66 μmol , final reaction concentration 2.2 mM) was prepared in a vial (10 mL) equipped with a stir bar and cooled in an acetonitrile/ $\text{N}_2(\text{liq})$ bath. 12 μL (solution 0.2 M) of acetic acid (3 mol %) in acetonitrile was added directly to the solution. Also, 1.6-16 μL of H_2^{18}O (98% ^{18}O -isotopic content) was added. Then, 25 μL of 1:1 v:v

EXPERIMENTAL SECTION

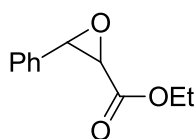
acetonitrile:hydrogen peroxide solution 32% (1.5 equiv.) was added by syringe pump over a period of 30 min. The solution was further stirred at -30 °C for 30 minutes. At this point, the epoxide product was analyzed by GC-MS-Cl using ammonia as the ionization gas. Simulation of the isotopic pattern yields 0.4% ^{18}O -incorporation into the epoxide product.

b) $\text{H}_2^{16}\text{O}/\text{H}_2^{18}\text{O}_2$ labeling experiment

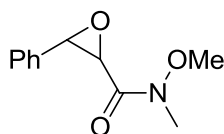


m/z	%
152	8.27538351
153	0.87670335
154	82.6247961
155	7.33574927
156	0.88736781

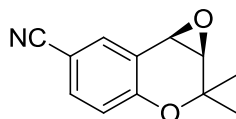
An acetonitrile solution (750 μL) of *cis*- β -methylstyrene (0.083 mmol, final reaction concentration 0.11 M) and $\text{Me}_2\text{N}_1\text{Fe}$ (0.06 mg, 0.08 μmol , final reaction concentration 0.11 mM) was prepared in a vial (10 mL) equipped with a stir bar and cooled in an acetonitrile frozen bath. 2.4 μL (solution 0.05 M) of acetic acid (3 mol %) in acetonitrile was added directly to the solution. Then, 16 μL of 1:1 v:v acetonitrile:hydrogen peroxide solution 2% H_2O_2 (90% ^{18}O -isotopic content) in water (0.05 equiv.) was added by syringe pump over a period of 30 min. The solution was further stirred at 0 °C for 30 minutes. At this point, the epoxide product was analyzed by GC-MS-Cl using ammonia as the ionization gas. Simulation of the isotopic pattern yields 91% ^{18}O -incorporation into the epoxide product.

6) Characterization of isolated epoxide products*cis*-Ethyl-3-phenyloxirane-2-carboxylate

E2, white solid; (91% yield, 97 %ee); $^1\text{H-NMR}$ (CDCl_3 , 300 MHz, 300K) δ , ppm: 7.42-7.39 (m, 2H), 7.36 - 7.29 (m, 3H), 4.26 (d, 1H, $J = 4.7$ Hz), 4.05 - 3.95 (m, 2H), 3.82 (d, 1H, $J = 4.7$ Hz), 1.01 (t, 3H, $J = 7.1$). $^{13}\text{C}\{^1\text{H}\}$ -NMR 166.6, 132.9, 128.4, 128.0, 126.6, 61.2, 57.4, 55.7, 13.9. HRMS(ESI+) m/z calculated for $\text{C}_{11}\text{H}_{12}\text{O}_3\text{Na}$ $[\text{M}+\text{Na}]^+$ 215.0679, found 215.0663. Chiral GC analysis with CYCLOSIL-B

cis-*N*-methoxy-*N*-methyl-3-phenyloxirane-2-carboxamide

E3, Yellowish oil; (84 % yield, 96 %ee); $^1\text{H-NMR}$ (CDCl_3 , 300 MHz, 300K) δ , ppm: 7.42-7.39 (m, 2H), 7.32 - 7.30 (m, 3H), 4.29 (d, 1H, $J = 4.7$ Hz), 4.14 (br, 2H), 3.56 (s, 3H), 3.04 (s, 3H). $^{13}\text{C}\{^1\text{H}\}$ -NMR 166.4, 133.7, 128.4, 128.2, 126.6, 61.8, 57.7, 55.6, 32.3. HRMS(ESI+) m/z calculated for $\text{C}_{11}\text{H}_{13}\text{NO}_3\text{Na}$ $[\text{M}+\text{Na}]^+$ 230.0788, found 230.0803. Chiral HPLC analysis (Chiralpack IC, *n*-Hex:*i*PrOH = 82/18, 25 °C, 1.0ml/min, $\lambda = 220$ nm), $t_{\text{minor}} = 38.9$ min, $t_{\text{major}} = 43.1$ min.

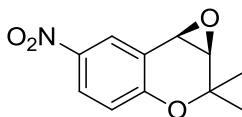
(R,R)-2,2-dimethyl-2,7b-dihydro-1aH-oxireno[2,3-c]chromene-6-carbonitrile.¹²

E4, White solid; (95 % yield, 99 %ee); $^1\text{H-NMR}$ (CDCl_3 , 300 MHz, 300K) δ , ppm: 7.66 (d, 1H, $J = 2.1$ Hz), 7.53-7.51 (dd, 1H, $J = 6.4, 2.10$ Hz), 6.86 (d, 1H, $J = 8.5$ Hz), 3.91 (d, 1H, $J = 4.4$ Hz), 3.54 (d, 1H, $J = 4.4$ Hz), 1.60 (s, 3H), 1.30 (s, 3H). $^{13}\text{C}\{^1\text{H}\}$ -NMR 156.5, 134.4, 133.8, 121.1, 119.0, 118.7, 104.3, 74.7, 62.3, 49.9, 25.5, 23.0. HRMS(ESI+) m/z calculated for $\text{C}_{12}\text{H}_{11}\text{NO}_2\text{Na}$ $[\text{M}+\text{Na}]^+$

EXPERIMENTAL SECTION

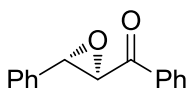
224.0682, found 224.0673. Chiral HPLC analysis (Chiralpack IA, *n*-Hex:*i*PrOH = 90/10, 25 °C, flow rate = 1.5 mL/min, λ = 254nm), t_{minor} = 5.66 min, t_{major} = 6.00 min.

(*R,R*)-2,2-dimethyl-6-nitro-2,7b-dihydro-1aH-oxireno[2,3 c]chromene.¹³



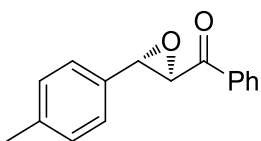
E5, Yellow solid; (97 % yield, 99 % ee); ¹H-NMR (CDCl₃, 300 MHz, 300K) δ , ppm: 8.30 (d, 1H, J = 2.6Hz), 8.16-8.12 (dd, 1H, J = 9.0, 2.72 Hz), 6.88 (d, 1H, J = 8.9 Hz), 3.99 (d, 1H, J = 4.3 Hz), 3.57 (d, 1H, J = 4.3 Hz), 1.62 (s, 3H), 1.32 (s, 3H). ¹³C{¹H}-NMR 158.3, 141.4, 126.3, 125.8, 120.3, 118.5, 75.21, 62.1, 50.0, 25.5, 23.1. HRMS(ESI+) m/z calculated for C₁₁H₁₁NO₄Na [M+Na]⁺ 244.0580, found 244.0577. Chiral HPLC analysis (Chiralpack IC, *n*-Hex:*i*PrOH = 9/1, 25 °C, flow rate = 1.0 mL/min, λ = 220nm), t_{minor} = 16.2 min, t_{major} = 31.4 min.

trans-(2*R*,3*S*)-Epoxy-1,3-diphenyl-propan-1-one.¹²



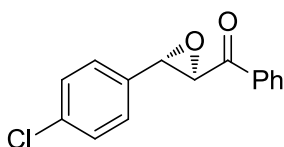
E8, White solid; (99 % yield, 98 % ee); ¹H-NMR (CDCl₃, 300 MHz, 300K) δ , ppm: 8.01 (d, 2H, J = 8.5 Hz), 7.62 (t 1H, J = 7.6 Hz), 7.49 (t, 2H, J = 7.7 Hz), 7.42-7.35 (m, 5H), 4.30 (d, 1H, J = 1.8 Hz), 4.08 (d, 1H, J = 1.8 Hz). ¹³C{¹H}-NMR 193.1, 135.5, 135.5, 134.0, 129.1, 128.9, 128.8, 128.4, 125.8, 61.0, 59.41. HRMS(ESI+) m/z calculated for C₁₅H₁₂O₂Na [M+Na]⁺ 247.0730, found 247.0721. Chiral HPLC analysis (Chiralpack IA, *n*-Hex:*i*PrOH = 98/2, 25 °C, flow rate = 1.0 mL/min, λ = 254 nm), t_{major} = 20.3 min, t_{minor} = 21.7 min.

trans-(2*R*,3*S*)-Epoxy-3-(4-methylphenyl)-1-phenyl-propan-1-one.¹³



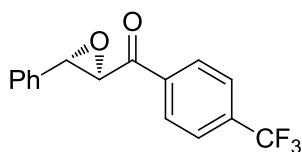
E9, Orange solid; (95% yield, 97 %ee); ¹H-NMR (CDCl₃, 300 MHz, 300K) δ, ppm: 8.00 (d, 2H, *J* = 7.4 Hz), 7.61 (tt, 1H, *J* = 7.4, 1.3 Hz), 7.48 (t, 2H, *J* = 7.42 Hz), 7.28 - 7.20 (m, 4H), 4.29 (d, 1H, *J* = 1.9 Hz), 4.04 (d, 1H, *J* = 1.9 Hz), 2.38 (s, 3H). ¹³C-NMR 193.2, 139.1, 135.5, 134.0, 132.4, 129.5, 128.9, 128.3, 125.8, 61.1, 59.5, 21.3. HRMS(ESI+) *m/z* calculated for C₁₆H₁₄O₂Na [M+Na]⁺ 261.0886, found 261.0871. Chiral HPLC analysis (Chiralpack IC, *n*-Hex:*i*PrOH = 98/2, 25 °C, flow rate = 1.0 mL/min, λ = 254nm), *t*_{minor} = 37.6 min, *t*_{major} = 38.8 min.

trans-(2*R*,3*S*)-Epoxy-3-(4-chlorophenyl)-1-phenyl-propan-1-one.¹³



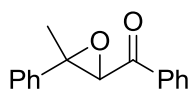
E10, Yellowish solid; (97 % yield, 97 %ee); ¹H-NMR (CDCl₃, 300 MHz, 300K) δ, ppm: 8.00 (d, 2H, *J* = 7.7 Hz), 7.63 (tt, 1H, *J* = 7.5, 1.34 Hz), 7.49 (t, 2H, *J* = 7.8 Hz), 7.37 (d, 2H, *J* = 8.6Hz), 7.30 (d, 2H, *J* = 8.7 Hz), 4.25 (d, 1H, *J* = 1.9), 4.06 (d, 1H, *J* = 1.9). ¹³C{¹H}-NMR 192.7, 135.4, 135.0, 134.1, 134.1, 129.0, 128.9, 128.4, 127.1, 60.9, 58.7. HRMS(ESI+) *m/z* calculated for C₁₅H₁₁ClO₂Na [M+Na]⁺ 281.0340, found 281.0335. Chiral HPLC analysis (Chiralpack IC, *n*-Hex:*i*PrOH = 98/2, 25 °C, flow rate = 1.0 mL/min, λ = 254nm), *t*_{major} = 29.0 min, *t*_{minor} = 31.3 min.

trans-((2*R*,3*S*)-3-Phenyloxiran-2-yl)(4-(trifluoromethyl)phenyl)methanone.¹³



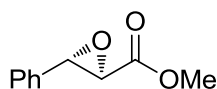
E11, White solid; (94 % yield, 97 %ee); ¹H-NMR (CDCl₃, 300 MHz, 300K) δ, ppm: 8.13 (d, 2H, *J* = 8.1 Hz), 7.75 (d, 2H, *J* = 8.2 Hz), 7.42 – 7.35 (m, 5H), 4.27 (d, 1H, *J* = 1.9 Hz), 4.09 (d, 1H, *J* = 1.9). ¹³C{¹H}-NMR 192.6, 138.0, 135.0, 129.3, 128.9, 126.0, 126.0, 125.9, 125.9, 125.9, 61.3, 59.0. HRMS(ESI+) *m/z* calculated for C₁₆H₁₁F₃O₂Na [M+Na]⁺ 315.0590, found 315.0603. Chiral HPLC analysis (Chiralpack IA, *n*-Hex:*i*PrOH = 9/1, 25 °C, flow rate = 1.0 mL/min, λ = 254nm), *t*_{major} = 9.4 min, *t*_{minor} = 10.4 min.

(3-Methyl-3-phenyloxiran-2-yl)(phenyl)methanone



E12, White solid; (69 % yield, 47 % ee); ¹H-NMR (CDCl₃, 300 MHz, 300K) δ, ppm: 7.96 (d, 2H, *J* = 8.1 Hz), 7.62 (t, 1H, *J* = 7.5 Hz), 7.52 – 7.47 (m, 4H), 7.43 (t, 2H, *J* = 7.2Hz), 7.37 (t, 1H, *J* = 7.2Hz), 4.16 (s, 1H), 1.64 (s, 3H). ¹³C{¹H}-NMR 193.0, 140.4, 135.6, 134.0, 128.9, 128.8, 128.3, 125.1, 66.0, 62.8, 16.0. HRMS(ESI+) *m/z* calculated for C₁₆H₁₄O₂Na [M+Na]⁺ 261.0886, found 261.0881. Chiral HPLC analysis (Chiralpack IA, *n*-Hex:*i*PrOH = 98/2, 25 °C, flow rate = 1.0 mL/min, λ = 254nm), *t*_{major} = 10.82 min, *t*_{minor} = 11.83 min.

(2*R*,3*S*)-Methyl-3-phenyloxirane-2-carboxylate.¹²

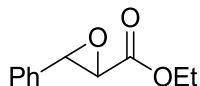


E13, Colorless oil; (66 % yield, 91 %ee); ¹H-NMR (CDCl₃, 300 MHz, 300K) δ, ppm: 7.37 – 7.33 (m, 3H), 7.31-7.27 (m, 2H), 4.10 (d, 1H, *J* = 1.8 Hz), 3.82 (s, 3H), 3.51 (d, 1H, *J* = 1.8 Hz). ¹³C{¹H}-NMR 168.6, 134.9, 129.0, 128.7, 125.8, 58.0, 56.6, 52.6. HRMS(ESI+) *m/z* calculated for C₁₀H₁₀O₃Na [M+Na]⁺ 201.0522, found 201.0518. Chiral HPLC analysis (Chiralpack IC, *n*-Hex:*i*PrOH =

EXPERIMENTAL SECTION

85/15, 25 °C, flow rate = 1.0 mL/min, λ = 220nm), t_{major} = 8.0 min, t_{minor} = 8.7 min.

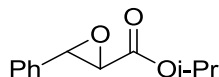
trans-Ethyl-3-phenyloxirane-2-carboxylate



This substrate has been tested with catalyst (*R,R*')-^{Me}₂NPDP-Fe-(OTf)₂

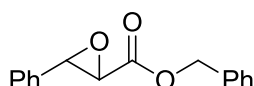
E14, Colorless oil; (91 % yield, 91 % ee); ¹H-NMR (CDCl₃, 300 MHz, 300K) δ , ppm: 7.40 – 7.33 (m, 3H), 7.32-7.27 (m, 2H), 4.34 - 4.23 (qd, 2H, J = 14.4, 7.2 Hz), 4.09 (d, 1H, J = 1.7 Hz), 3.50 (d, 1H, J = 1.7), 1.33 (t, 3H, J = 7.2 Hz). ¹³C-NMR 168.2, 135.0, 129.0, 128.7, 125.8, 61.8, 57.9, 56.8, 14.1. HRMS(ESI+) m/z calculated for C₁₁H₁₂O₃Na [M+Na]⁺ 215.0679, found 215.0677. Chiral HPLC analysis (Chiralpack IC, *n*-Hex:*i*PrOH = 85/15, 25 °C, flow rate = 1.0 mL/min, λ = 220nm), t_{major} = 7.5 min, t_{minor} = 8.4 min.

trans-Isopropyl-3-phenyloxirane-2-carboxylate



E15, Colorless oil; (94 % yield, 97 % ee); ¹H-NMR (CDCl₃, 300 MHz, 300K) δ , ppm: 7.40 – 7.33 (m, 3H), 7.32-7.27 (m, 2H), 5.20 - 5.08 (m, 1H), 4.07 (d, 1H, J = 1.7 Hz), 3.48 (d, 1H, J = 1.7 Hz), 1.30 (t, 6H, J = 5.9 Hz). ¹³C{¹H}-NMR 167.7, 135.1, 129.0, 128.6, 125.9, 69.6, 57.8, 57.0, 21.8, 21.7. HRMS(ESI+) m/z calculated for C₁₂H₁₄NO₃Na [M+Na]⁺ 229.0835, found 229.0835. Chiral HPLC analysis (Chiralpack IC, *n*-Hex:*i*PrOH = 85/15, 25 °C, flow rate = 1.0 mL/min, λ = 220nm), t_{major} = 6.7 min, t_{minor} = 7.6 min.

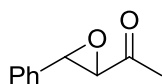
trans-Benzyl-3-phenyloxirane-2-carboxylate



E16, White solid; (94 % yield, 96 % ee); ¹H-NMR (CDCl₃, 300 MHz, 300K) δ , ppm: 7.40 - 7.25 (m, 10H), 5.20 - 5.25 (m, 2H), 4.11 (d, 1H, J = 1.7 Hz), 3.55 (d, 1H, J = 1.7 Hz). ¹³C-NMR 168.1, 135.0, 134.9, 129.1, 128.7, 128.7, 128.5,

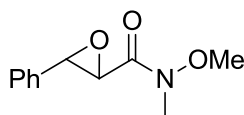
125.9, 67.5, 58.1, 56.8. HRMS(ESI+) m/z calculated for $C_{16}H_{14}O_3Na(M+Na^+)$ 277.0835, found 277.0827. Chiral HPLC analysis (Chiralpack IC, *n*-Hex:*i*PrOH = 85/15, 25 °C, flow rate = 1.0 mL/min, λ = 220nm), t_{minor} = 8.16 min, t_{major} = 8.7 min.

trans-1-(3-Phenyloxiran-2-yl)ethanone



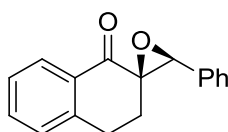
E17, Yellow oil; (60 % yield, 94 % ee); 1H -NMR ($CDCl_3$, 300 MHz, 300K) δ , ppm: 7.47 - 7.34 (m, 5H), 7.29 - 7.26 (m, 2H), 4.00 (d, 1H, J = 1.8 Hz), 3.49 (d, 1H, J = 1.8 Hz), 2.18(s, 3H). $^{13}C\{^1H\}$ -NMR 204.2, 135.0, 129.0, 128.7, 125.7, 63.5, 57.8, 24.8. HRMS(ESI+) m/z calculated for $C_{10}H_{10}O_2Na [M+Na]^+$ 185.0573, found 185.0588. Chiral HPLC analysis (Chiralpack IC, *n*-Hex:*i*PrOH = 98/2, 25 °C, flow rate = 1.0 mL/min, λ = 220nm), t_{minor} = 14.3 min, t_{major} = 15.4 min.

trans-*N*-Methoxy-*N*-methyl-3-phenyloxirane-2-carboxamide



E18, Yellow oil; (95 % yield, 99 % ee); 1H -NMR ($CDCl_3$, 300 MHz, 300K) δ , ppm: 7.41 - 7.31 (m, 5H), 4.10 (d, 1H, J = 1.9 Hz), 3.94 (br.s, 1H), 3.72 (s, 3H), 3.28 (s, 3H). $^{13}C\{^1H\}$ -NMR 167.5, 135.6, 128.8, 128.6, 125.8, 62.1, 57.7, 55.6, 32.6. HRMS(ESI+) m/z calculated for $C_{11}H_{13}NO_3Na [M+Na]^+$ 230.0788, found 230.0780. Chiral HPLC analysis (Chiralpack IC, *n*-Hex:*i*PrOH = 9/1, 25 °C, flow rate = 1.5 mL/min, λ = 220nm), t_{minor} = 35.9 min, t_{major} = 40.3 min.

(2*R*,3'*S*)-3'-Phenyl-3,4-dihydro-1*H*-spiro[naphthalene-2,2'-oxiran]-1-one.¹³

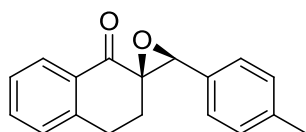


E19, Yellow solid; (94 % yield, 90 % ee); 1H -NMR ($CDCl_3$, 300 MHz, 300K) δ , ppm: 8.14 – 8.10 (m, 1H), 7.55 - 7.50 (m, 1H), 7.43 – 7.33 (m, 6H), 7.23 (d,

EXPERIMENTAL SECTION

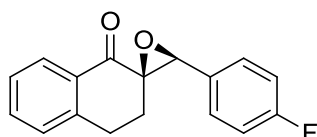
1H, $J = 7.6$ Hz), 4.36 (s, 1H), 2.85 – 2.81 (dd, 2H, $J = 8.5, 4.2$ Hz), 2.50 – 2.39 (dt, 1H, $J = 13.4, 8.7$ Hz), 1.89 – 1.82 (dt, 1H, $J = 13.5, 4.2$ Hz). $^{13}\text{C}\{^1\text{H}\}$ -NMR 193.6, 143.37, 134.3, 134.1, 132.7, 128.8, 128.4, 128.3, 127.7, 127.0, 126.6, 64.3, 64.1, 27.3, 25.3. HRMS(ESI+) m/z calculated for $\text{C}_{17}\text{H}_{14}\text{O}_2\text{Na}$ $[\text{M}+\text{Na}]^+$ 273.0886, found 273.0902. Chiral HPLC analysis (Chiralpack IA, *n*-Hex:*i*PrOH = 98/2, 25 °C, flow rate = 1.0 mL/min, $\lambda = 254$ nm), $t_{\text{minor}} = 24.6$ min, $t_{\text{major}} = 30.1$ min.

(2*R*,3'*S*)-3'-*p*-Tolyl-3,4-dihydro-1*H*-spiro[naphthalene-2,2'-oxiran]-1-one.¹³



E20, Orange solid; (97 % yield, 97 % ee); ^1H -NMR (CDCl_3 , 300 MHz, 300K) δ , ppm: 8.11 (dd, 1H, $J = 7.8, 1.1$ Hz), 7.54 - 7.49 (td, 1H, $J = 7.5, 1.5$), 7.39 – 7.33 (t, 1H, $J = 7.6$ Hz), 7.27 – 7.18 (m, 5H), 4.31 (s, 1H), 2.84 – 2.80 (dd, 2H, $J = 8.5, 4.1$ Hz), 2.49 – 2.42 (m, 1H), 2.37 (s, 3H), 1.90 – 1.82 (dt, 1H, $J = 13.5, 4.1$ Hz). $^{13}\text{C}\{^1\text{H}\}$ -NMR 193.8, 143.4, 138.2, 134.2, 132.7, 131.1, 129.0, 128.8, 127.6, 127.0, 126.6, 64.4, 64.2, 27.4, 25.3, 21.3. HRMS(ESI+) m/z calculated for $\text{C}_{18}\text{H}_{16}\text{O}_2\text{Na}$ $[\text{M}+\text{Na}]^+$ 287.1043, found 287.1034. Chiral HPLC analysis (Chiralpack IC, *n*-Hex:*i*PrOH = 9/1, 25 °C, flow rate = 1.0 mL/min, $\lambda = 254$ nm), $t_{\text{minor}} = 22.7$ min, $t_{\text{major}} = 33.1$ min.

(2*R*,3'*S*)-3'-(4-Fluorophenyl)-3,4-dihydro-1*H*-spiro[naphthalene-2,2'-oxiran]-1-one.¹³

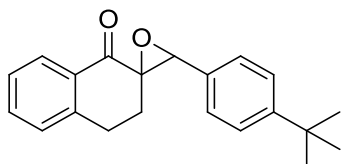


E21, Yellow solid; (96 % yield, 97 % ee); ^1H -NMR (CDCl_3 , 300 MHz, 300K) δ , ppm: 8.11 (dd, 1H, $J = 7.9, 1.5$ Hz), 7.56 - 7.50 (td, 1H, $J = 7.5, 1.5$), 7.39 – 7.33 (m, 3H), 7.24 (d, 1H, $J = 7.6$ Hz), 7.12 - 7.06 (t, 2H, $J = 8.7$ Hz), 4.33 (s, 1H), 2.86 – 2.81 (m, 2H), 2.49 – 2.39 (m, 1H), 1.85 – 1.78 (dt, 1H, $J = 13.5, 4.3$ Hz). $^{13}\text{C}\{^1\text{H}\}$ -NMR 193.4, 143.2, 134.3, 132.6, 129.9, 129.9, 128.8, 128.4, 128.3, 127.7, 127.1, 115.6, 115.3, 64.32, 63.5, 27.3, 25.2. HRMS(ESI+) m/z calculated

EXPERIMENTAL SECTION

for $C_{17}H_{13}FO_2Na$ $[M+Na]^+$ 291.0792, found 291.0784. Chiral HPLC analysis (Chiralpack IC, *n*-Hex:*i*PrOH = 9/11, 25 °C, flow rate = 1.0 mL/min, λ = 254nm), t_{minor} = 21.4 min, t_{major} = 26.8 min.

3'-(4-(tert-Butyl)phenyl)-3,4-dihydro-1*H*-spiro[naphthalene-2,2'-oxiran]-1-one



E22, Yellow solid; (96 % yield, 95 % ee); 1H -NMR ($CDCl_3$, 300 MHz, 300K) δ , ppm: 8.12 (dd, 1H, J = 7.9, 1.5 Hz), 7.54 - 7.48 (td, 1H, J = 7.5, 1.5), 7.41 - 7.35 (t, 3H, J = 8.5 Hz), 7.33 - 7.28 (t, 2H, J = 8.2 Hz), 7.22 (d, 1H, J = 7.5 Hz), 4.32 (s, 1H), 2.86 - 2.82 (dd, 2H, J = 8.2, 3.8 Hz), 2.50 - 2.39 (m, 1H), 1.92 - 1.85 (dt, 1H, J = 13.5, 4.1 Hz) 1.36 (s, 9H). $^{13}C\{^1H\}$ -NMR 193.8, 151.4, 143.4, 134.2, 132.7, 131.0, 128.8, 127.6, 127.0, 126.4, 125.3, 64.4, 64.2, 34.7, 31.3, 27.5, 25.34. HRMS(ESI+) m/z calculated for $C_{21}H_{22}O_2Na$ $[M+Na]^+$ 329.1512, found 329.1506. Chiral HPLC analysis (Chiralpack IC, *n*-Hex:*i*PrOH = 95/5, 25 °C, flow rate = 1.0 mL/min, λ = 254nm), t_{minor} = 10.0 min, t_{major} = 13.9 min.

References

- (1) Jacobsen, E. N.; Deng, L.; Furukawa, Y.; Martínez, L. E. *Tetrahedron* **1994**, *50*, 4323.
- (2) Vogel's Textbook of Practical Organic Chemistry (ELBS) *Longman Group, UK* **1989**, 1034.
- (3) Godfrey Jr, J. D.; Mueller, R. H.; Sedergran, T. C.; Soundararajan, N.; Colandrea, V. J. *Tetrahedron Letters* **1994**, *35*, 6405.
- (4) Nishikawa, Y.; Yamamoto, H. *J. Am. Chem. Soc.* **2011**, *133*, 8432.
- (5) Zhang, C. X.; Kaderli, S.; Costas, M.; Kim, E.-i.; Neuhold, Y.-M.; Karlin, K. D.; Zuberbuehler, A. D. *Inorg. Chem.* **2003**, *42*, 1807.
- (6) Kojima, T.; Hayashi, K.; Lizuka, S.; Tani, F.; Naruta, Y.; Kawano, M.; Ohashi, Y.; Hirai, Y.; Ohkubo, K.; Matsuda, Y.; Fukuzumi, S. *Chem. Eur. J.* **2007**, *13*, 8212.
- (7) Tamura, M.; Urano, Y.; Kikuchi, K.; Higuchi, T.; Hirobe, M.; Nagano, T. *Chem. Pharm. Bull. (Tokyo)* **2000**, *48*, 1514.
- (8) Prat, I.; Font, D.; Company, A.; Junge, K.; Ribas, X.; Beller, M.; Costas, M. *Adv. Synth. Catal.* **2013**, *355*, 947.
- (9) Bazzini, C.; Brovelli, S.; Caronna, T.; Gambarotti, C.; Giannone, M.; Macchi, P.; Meinardi, F.; Mele, A.; Panzeri, W.; Recupero, F.; Sironi, A.; Tubino, R. *Eur. J. Org. Chem.* **2005**, *2005*, 1247.
- (10) Chen, M. S. White, M. C. *Science* **2007**, *318*, 783.
- (11) Gomez, L.; Garcia-Bosch, I.; Company, A.; J., B.-B.; Polo, A.; Sala, X.; Ribas, X.; Costas, M. *Angew. Chem. Int. Ed. Engl.* **2009**, *48*, 5720.
- (12) Lyakin, O. Y.; Ottenbacher, R. V.; Bryliakov, K. P.; Talsi, E. P. *ACS Catal.* **2012**, *2*, 1196.
- (13) Wang, B.; Miao, C.; Wang, S.; Xia, C.; Sun, W. *Chem.– Eur. J.* **2012**, *18*, 6750.

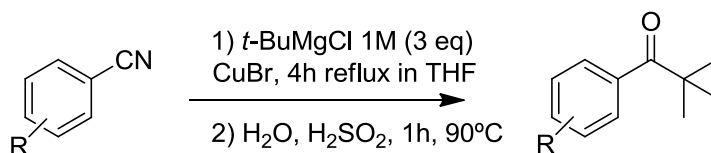
Experimental section: Chapter VII.2

Synergistic Interplay of a Non-Heme Iron Catalyst and Amino Acid co-Ligands in H₂O₂ Activation for Asymmetric Epoxidation of α -Alkyl Substituted Styrenes

1) Synthesis of substrates

Synthesis of **S8**¹, **S9**², **S12**³, **S14**⁴, **S15**⁴, **S17**⁴, **S19**³, was performed as reported in the literature. The substrate nomenclatures (**SX**) were exclusives for this chapter.

- Synthesis of ketones derivatives (**S20**, **S21** and **S22**)



R = *p*-F, *p*-Cl and *o*-Cl

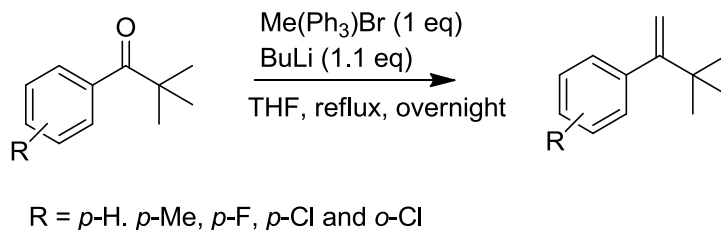
A representative procedure

A brownish solution of tert-butyl magnesium chloride (21.5 mL, 1 M in 2-methyl THF, 7.2 mmol) was added into a 0°C solution of substituted benzonitrile (1g, 14.3 mmol) dissolved in 30 mL of THF. Afterwards, copper bromide (15 mg) was added under N₂ and the resulting solution was refluxed for 5 hours. The solution was then cooled to 0°C and water (7.5 mL) was added slowly. When the vigorous reaction ceased, a H₂SO₄ 1N solution (25 mL) was added and was refluxed during 1 hour, after that it was cooled to room temperature, basified with 2M NaOH and extracted with ethyl acetate (3 × 50 mL), dried over MgSO₄ and the solvent was removed under reduced pressure to obtain a pale yellow liquid that was taken to the next step without further purification.

Synthesis of ketones precursor of substrates **S13** - **S16**, was done following the same procedure described above, but using isopropylmagnesium bromide 3M in 2-methyl-THF.

With the exception of precursor ketones of substrates **S9**² and **S10**, the rest of ketones were available from commercial sources.

- Synthesis of alkenes from ketones

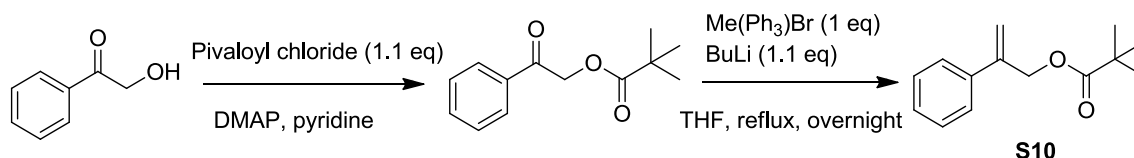


Representative procedure.

To a suspension of 2.32 g of methyltriphenylphosphonium bromide (6.34 mmol) in THF (30 mL) was added dropwise a solution of BuLi (4.4 mL, 1.6 M in hexane, 6.9 mmol) at 0°C during 30 minutes. The white suspension changed to a red solution and was stirred at 0°C for 90 min. The ketone (1.22 g, 6.22 mmol) was then added and the solution was stirred for 20 min at this temperature and then warmed to 70°C and stirred overnight. Afterwards, the reaction was quenched with water and the organic layer separated using a separatory funnel. The aqueous layer was extracted with diethyl ether (3 × 50 mL), dried over MgSO₄, and the solvent was removed under reduced pressure. Finally, purification by flash chromatography over silica (hexane/ethyl acetate 98/2) was performed.

Substrates **S3** - **S8**, **S11** - **S18**, and **S23** were prepared following an analogous procedure.

- Synthesis of 2-phenylallyl pivalate (**S10**)



2-oxo-2-phenylethyl pivalate. 2-hydroxy-1-phenylethanone (1.0 g, 7.2 mmol) and 4-(dimethylamino)pyridine (84 mg) were dissolved in pyridine (12 mL). The resulting mixture was cooled in an ice bath, and a solution of pivaloyl chloride (0.96 mL, 7.9 mmol) in pyridine (7 mL) was added dropwise. After the mixture

EXPERIMENTAL SECTION

was stirred for 24 h, the solvent was removed under reduced pressure and the resulting residue was treated with CHCl_3 (50 mL) and washed with water (25 mL), a saturated NaHCO_3 aqueous solution (25 mL), and a saturated NaCl aqueous solution (25 mL). The organic phase was dried over MgSO_4 and filtered, and the solvent was removed under reduced pressure to yield a colorless liquid. Purification by flash chromatography over silica (hexane/ethyl acetate 85/15) yielded 1.2 g of the product as a white solid (74% yield).

Further elaboration of this ketone to prepare olefin substrate **S10** was done using the same procedure as described before (33 % yield).

2) Synthesis of amino acids

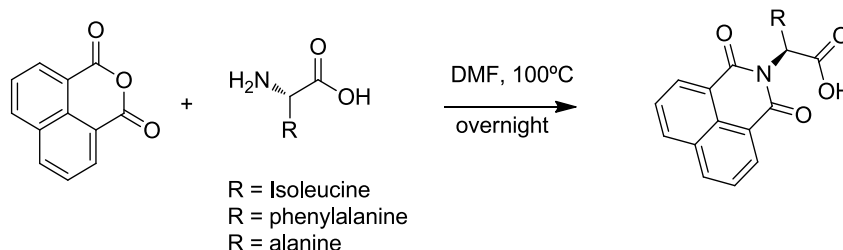
- Synthesis of Ac-Ileu-OH, Piv-Ileu-OH

General procedure for preparation of N-protected amino acid

L-Isoleucine was solved in 4 mL of NaOH 1M and stirred at 0°C . Then acetyl or pivaloyl chloride (1.1 eq.) was added slowly during 15 minutes and the solution was warmed up to room temperature and left stirring overnight. The crude was extracted 2 times with diethyl ether and the aqueous phase was acidified with HCl at pH 1 and extracted 3 times with dichloromethane. The organic phase was dried over MgSO_4 and filtered, and the solvent was removed under reduced pressure to yield the product as a white solid.

- Synthesis of Npha-Ileu-OH, Npha-Ala-OH and Npha-Phe-OH

General procedure for preparation of N-dicarbonylamino acid



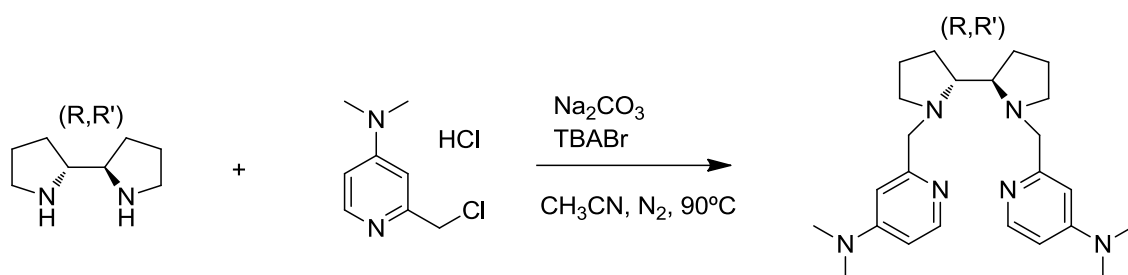
1,8-Naphthalic anhydride, amino acid and 2 mL DMF were placed in a flask and the mixture warmed to 100°C overnight. Afterwards the mixture was cooled to room temperature, diluted with ethyl acetate and washed three times with aqueous solutions of NaHCO_3 , and brine, and finally with water. The organic

phase was dried over MgSO_4 and filtered, and the solvent was removed under reduced pressure to yield a white solid. Then the crude was purified by silica column chromatography (AcOEt/Hexane 1:2) to obtain the desired amino acid derivative as a white solid.

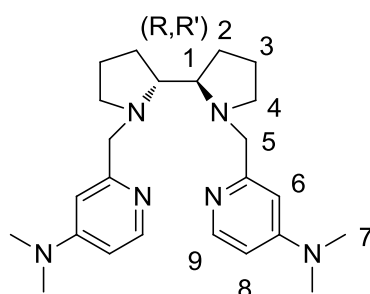
N-Npha-*t*-Leu-OH was reported previously by Yamamoto et.al⁵

3) Synthesis of complexes

3.1) Synthesis of ligands



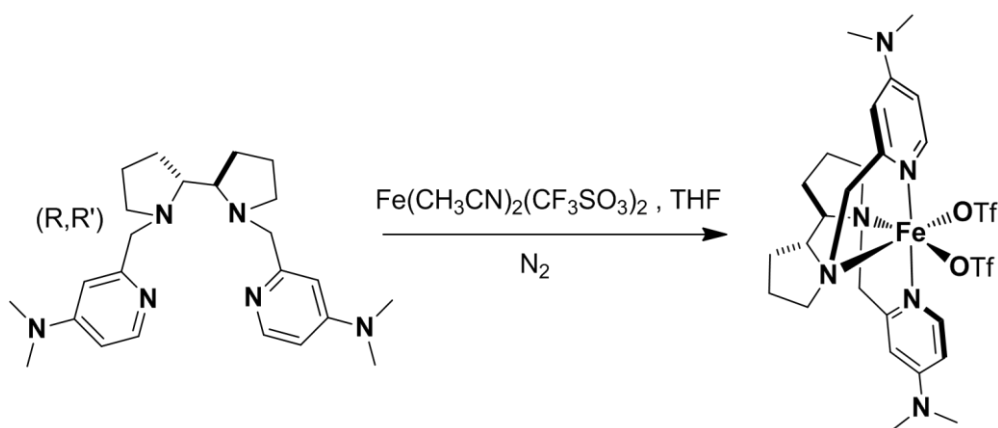
Synthesis of (R,R') - Me_2N PDP



2-Chloromethyl-4-dimethylaminopyridine hydrochloride (0.50 g, 2.42 mmol), (R,R')-2,2'-bipyrrolidine (177.5 mg, 1.26 mmol) and anhydrous acetonitrile (30 mL) were mixed in a 50 mL flask. Na_2CO_3 (1.08 g) and tetra-butylammonium bromide, TBABr (4 mg) were added directly as solids and the resulting mixture was heated at reflux under N_2 for 15 hours. After cooling to room temperature, the resulting brown mixture was filtered and the filter cake was washed with CH_2Cl_2 . The combined filtrates were evaporated under reduced pressure. To the resulting residue, 1N NaOH (20 mL) was added and the mixture was extracted with CH_2Cl_2 (3 x 20 mL). The combined organic layers were dried over anhydrous MgSO_4 and the solvent was removed under reduced pressure. After, the residue was solved in *n*-hexane and stirred overnight. Finally, the

solvent was decanted and removed under reduced temperature to yield 351 mg of yellow oil (0.86 mmol, yield 68 %). The full characterization is the same described in the literature for (*S,S'*)-^{Me2N}PDP.

3.2) Synthesis of iron complexes



(*R,R'*)-[Fe(CF₃SO₃)₂(^{Me2N}PDP)], ((*R,R'*)-^{Me2N}1Fe): A suspension of Fe(CF₃SO₃)₂(CH₃CN)₂ (130.5 mg, 0.3 mmol) in anhydrous THF (1 mL) was added drop-wise to a vigorously stirred solution of (*R,R'*)-^{Me2N}PDP (122.1 mg, 0.3 mmol) in THF (1 mL). After a few seconds the solution became cloudy and a yellow precipitate appeared. After stirring for 1 hour the solution was filtered off and the resultant yellow solid dried under vacuum. This solid was solved in CH₂Cl₂ (3 mL) and the solution filtered off through celite®. Slow diethyl ether diffusion over the resultant solution afforded, in a few days, 159.6 mg of yellow crystals (0.2 mmol, yield 70%). Anal. Calcd for C₂₈H₃₈F₆FeN₄O₈S₂·1/2 CH₂Cl₂: C, 39.54; H, 4.63; N, 10.44 %. Found: C, 39.44; H, 4.75; N, 10.10 %. FT-IR (ATR) ν , cm⁻¹: 2968 – 2934 (C-H)sp³, 2362, 2330, 1615, 1526, 1297, 1215, 1155, 1039, 1010, 825, 634. ¹H-NMR (CD₂Cl₂, 400 MHz, 300K) δ , ppm: 169 (s), 89.5 (s), 84.9 (s), 43.4 (s), 39.9 (s), 39 (s), 36.3 (s), 8.9 (s), -2.6 (s), -18.7 (s). ESI-HRMS calcd. for C₂₅H₃₆F₃FeN₆O₃S [M-OTf]⁺: 613.1866, found: 613.1880.

4) Catalytic studies

4.1) General procedure for epoxide isolation (Figure 9)

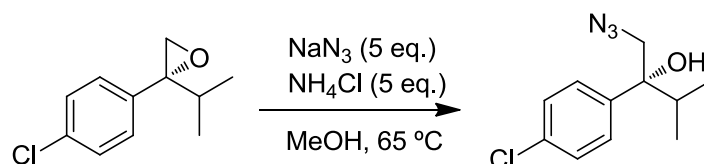
An acetonitrile solution (3.75 mL) of a given olefin (0.415 mmol, final reaction concentration 0.11 M) and iron catalyst (6.3 mg, 8.33 μ mol, final reaction concentration 2.2 mM) was prepared in a vial (10 mL) equipped with a stir bar

EXPERIMENTAL SECTION

and cooled in an acetonitrile frozen bath. 62.5 μL (solution 0.2 M) of carboxylic acid (12.5 μmol , 3 mol %) was added directly to the solution. Then, 168 μL of 1:1 v:v acetonitrile:hydrogen peroxide solution 30% (1.8 equiv.) was added by syringe pump over a period of 30 min. The solution was further stirred at $-30\text{ }^\circ\text{C}$ for 30 minutes. At this point, 15 mL of an aqueous NaHCO_3 saturated solution was added to the mixture. The resultant solution was extracted with CH_2Cl_2 (3 x 10 mL). Organic fractions were combined, dried over MgSO_4 , filtered through a silica gel plug, and the solvent was removed under reduced pressure to afford the epoxide product. This residue was purified by flash column chromatography over silica gel to obtain the pure epoxide (Hexane/ AcOEt : 98/2).

5) Reactions for Scheme 38

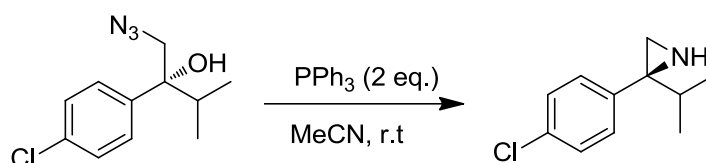
Procedure for azide product



P1. To a mixture of epoxide (170.6 mg, 0.87 mmols) and sodium azide (285.07 mg, 4.36 mmol, 5 equiv.) in 3 mL of MeOH was added NH_4Cl (238.1 mg, 4.36 mmol, 5 equiv.). The mixture was stirred overnight at $65\text{ }^\circ\text{C}$. The residue was rotavaporated and solved with dichloromethane (2 mL). A brine solution (2 mL) was added and then the resultant solution was extracted with CH_2Cl_2 (3 x 3 mL). Organic fractions were combined, dried over MgSO_4 , and the solvent was removed under reduced pressure to afford the azido-alcohol product as an orange oil (180 mg, 0.75 mmols, 87% yield, 92% ee). This product was used in the next step without further purification.

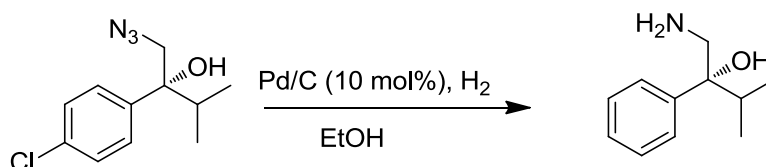
EXPERIMENTAL SECTION

Procedure for aziridine product



P2. A solution of azido-alcohol (64 mg, 0.27 mmol) in acetonitrile (2 mL) was stirred at room temperature overnight. After reaction, the residue was rotavaporated and purified by column chromatography on silica gel with Hexane/Ethyl acetate (2:1) to provide the aziridine compound as a yellow oil (41.5 mg, 0.21 mmols, 80% yield, 88% ee).

Procedure for amino alcohol product

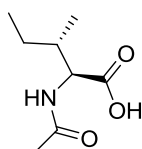


P3. To a stirred solution of azido-alcohol (84 mg, 0.35 mmol) in ethanol (2 mL) at room temperature was added 10% palladium on carbon (9 mg). The solution was placed under a H₂ atmosphere overnight. The reaction mixture was filtered through Celite® plug and concentrated under reduced pressure to provide the amino-alcohol as a white solid (62.1 mg, 0.35 mmols, 98% yield, 90% ee).

6) Characterization of all compounds

6.1) Characterization of synthesized amino acids

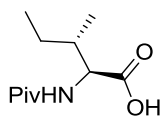
N-Ac-Ileu-OH



White solid (55 % yield); ¹H-NMR (CDCl₃, 300 MHz, 300K) δ, ppm: 6.12 (d, 1H, J = 8.0 Hz), 4.61 – 4.57 (q, 1H, J = 5.1 Hz), 2.05 (s, 3H), 1.93 (m, 1H), 1.51 – 1.45 (m, 1H), 1.28 – 1.15 (s, 1H), 0.96 – 0.93 (m, 6H). ¹³C{¹H}-NMR 175.2, 170.9, 56.6, 37.5, 25.1, 23.2, 15.4, 11.6. HRMS(ESI+) m/z calculated for C₈H₁₅NO₃Na [M+Na]⁺ 196.0944, found 196.0941.

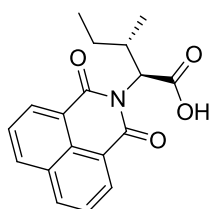
EXPERIMENTAL SECTION

N-Piv-Ileu-OH



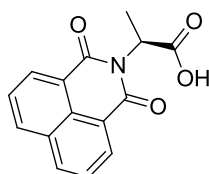
White solid (26 % yield); ¹H-NMR (CDCl₃, 300 MHz, 300K) δ, ppm: 9.71(br, 1H), 6.26 (d, 1H, J = 7.9 Hz), 4.63 – 4.59 (t, 2H, J = 8.2, 4.6 Hz), 2.00 – 1.93 (m, 1H, J = 9.3 Hz), 1.55 – 1.44 (m, 1H), 1.23 (s, 9H), 0.97 – 0.93 (m, 6H) ¹³C{¹H}-NMR 178.9, 175.9, 56.3, 38.8, 37.6, 27.4, 25.1, 15.4, 11.5. HRMS(ESI+) m/z calculated for C₁₁H₂₁NO₃Na [M+Na]⁺ 238.1414, found 238.1411.

N-NPha-Ileu-OH



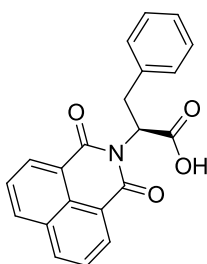
White solid (54 % yield); ¹H-NMR (CDCl₃, 300 MHz, 300K) δ, ppm: 8.60 (d, 2H, J = 7.3 Hz), 8.24 (d, 2H, J = 8.3 Hz), 7.76 (t, 2H, J = 7.6 Hz), 5.47 (d, 1H, J = 9.3 Hz), 2.65 – 2.58 (m, 1H), 1.33 – 1.29 (m, 1H), 1.26 (d, 3H, J = 6.4 Hz), 1.06 – 0.94 (m, 1H), 0.80 (t, J = 7.3 Hz) ¹³C{¹H}-NMR 175.5, 164.0, 134.4, 131.9, 131.6, 128.3, 127.0, 122.0, 58.0, 33.3, 25.1, 17.9, 11.0 HRMS(ESI+) m/z calculated for C₁₈H₁₇NO₄ [M+H]⁺ 334.1050, found 334.1034.

N-NPha-Ala-OH



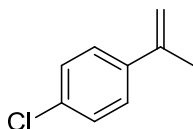
White solid (42 % yield); ¹H-NMR (DMSO-d₆, 300 MHz, 300K) δ, ppm: 8.45 (t, 4H, J = 9.2 Hz), 7.83 (t, 2H, J = 8.0 Hz), 7.76 (t, 2H, J = 7.6 Hz), 5.58 – 5.50 (q, 1H, J = 6.9 Hz), 1.49 (d, 3H, J = 7.0 Hz). ¹³C{¹H}-NMR 171.7, 163.3, 135.1, 131.7, 131.6, 127.8, 127.7, 122.1, 48.8, 14.8. HRMS(ESI+) m/z calculated for C₁₅H₁₁NO₄Na [M+Na]⁺ 292.0580, found 292.0578.

N-NPha-Phe-OH

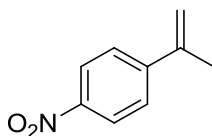


White solid (39 % yield); $^1\text{H-NMR}$ (CDCl_3 , 300 MHz, 300K) δ , ppm: 8.53 – 8.50 (dd, 2H, $J = 7.3, 0.9$ Hz), 8.20 – 8.17 (d, 2H, $J = 0.9, 8.3$ Hz), 7.74 – 7.69 (t, 2H, $J = 7.8$ Hz), 7.21 – 7.19 (m, 2H), 7.15 – 7.06 (m, 3H), 6.11 – 6.06 (m, 1H), 3.74 – 3.67 (dd, 1H, $J = 14.0, 5.6$ Hz), 3.52 – 3.45 (dd, 1H, $J = 14.4, 9.5$ Hz) $^{13}\text{C}\{^1\text{H}\}$ -NMR 175.1, 163.6, 137.2, 134.3, 131.7, 131.5, 129.2, 129.2, 128.3, 128.2, 126.9, 126.6, 121.9, 54.1, 34.8. HRMS(ESI+) m/z calculated for $\text{C}_{21}\text{H}_{15}\text{NO}_4\text{Na}$ $[\text{M}+\text{Na}]^+$ 368.0893, found 368.0868.

6.2) Characterization of synthesized substrates

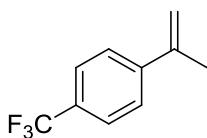


S3, Colorless oil (76 % yield); $^1\text{H-NMR}$ (CDCl_3 , 300 MHz, 300K) δ , ppm: 7.41 – 7.37 (dt, 2H, $J = 8.7, 2.5$ Hz), 7.31 – 7.26 (dt, 2H, $J = 8.7, 2.4$ Hz), 5.35 (s, 1H), 5.09 (m, 1H), 2.13 (m, 3H). $^{13}\text{C}\{^1\text{H}\}$ -NMR 142.1, 139.6, 133.2, 128.3, 126.8, 114.1, 113.0, 111.9, 21.8 HRMS(ESI+) m/z calculated for $\text{C}_9\text{H}_9\text{Cl}$ $[\text{M}+\text{H}]^+$ 153.0466, found 153.0457.

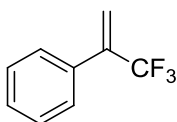


S4, Yellow solid (67 % yield); $^1\text{H-NMR}$ (CDCl_3 , 300 MHz, 300K) δ , ppm: 8.21 – 8.17 (dt, 2H, $J = 9.0, 2.4$ Hz), 7.62 – 7.57 (dt, 2H, $J = 9.0, 2.4$ Hz), 5.53 (m, 1H), 5.29 (m, 1H), 2.19 (m, 3H). $^{13}\text{C}\{^1\text{H}\}$ -NMR 147.6, 141.6, 126.3, 123.6, 116.4, 21.6 HRMS(ESI+) m/z calculated for $\text{C}_9\text{H}_9\text{NO}_2$ $[\text{M}+\text{H}]^+$ 164.0706, found 164.0698.

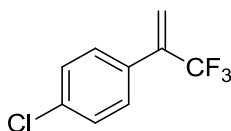
EXPERIMENTAL SECTION



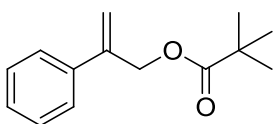
S5, Yellow oil (84 % yield); $^1\text{H-NMR}$ (CDCl_3 , 300 MHz, 300K) δ , ppm: 7.60 – 7.53 (m, 4H), 5.43 (s, 1H), 5.19 (m, 1H), 2.17 (m, 3H). $^{13}\text{C}\{^1\text{H}\}$ -NMR 144.8, 142.2, 129.3 (q, $J = 33.4$ Hz), 125.8, 125.2 (q, $J = 3.7$ Hz), 124.1 (q, $J = 271$ Hz), 21.7. HRMS(ESI+) m/z calculated for $\text{C}_{10}\text{H}_9\text{F}_3$ $[\text{M}+\text{H}]^+$ 187.0729, found 187.0719.



S6, Yellow oil (24 % yield); $^1\text{H-NMR}$ (CDCl_3 , 300 MHz, 300K) δ , ppm: 7.48 – 7.44 (m, 2H) 7.40 – 7.36 (m, 3H), 5.95 – 5.94 (q, 1H, $J = 1.32$ Hz), 5.76 – 5.75 (q, 1H, $J = 1.62$ Hz), $^{13}\text{C}\{^1\text{H}\}$ -NMR 139.0 (q, $J = 29$ Hz), 133.6, 128.9, 128.6, 127.4, 123.4 (q, $J = 276$ Hz), 120.4 (q, $J = 5.4$ Hz). GC-MS m/z for $\text{C}_9\text{H}_7\text{F}_3$ 172.0.

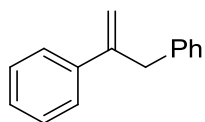


S7, Yellow oil (55 % yield); $^1\text{H-NMR}$ (CDCl_3 , 300 MHz, 300K) δ , ppm: 7.40 – 7.33 (m, 4H), 5.97 – 5.96 (q, 1H, $J = 1.35$ Hz), 5.77 – 5.75 (q, 1H, $J = 1.69$ Hz), $^{13}\text{C}\{^1\text{H}\}$ -NMR 137.9 (q, $J = 31$ Hz), 135.1, 132.0, 128.8, 128.7, 123.1 (q, $J = 273$ Hz), 120.9 (q, $J = 5.6$ Hz). GC-MS m/z for $\text{C}_9\text{H}_6\text{ClF}_3$ 206.0.

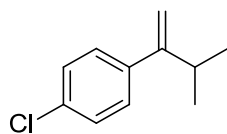


S10, Yellow oil (33 % yield); $^1\text{H-NMR}$ (CDCl_3 , 300 MHz, 300K) δ , ppm: 7.43 – 7.25 (m, 5H), 5.52 (s, 1H), 5.34 (q, 1H, $J = 2.51, 1.32$ Hz), 4.97 (m, 2H), $^{13}\text{C}\{^1\text{H}\}$ -NMR 178.2, 143.0, 138.2, 128.4, 127.9, 126.1, 114.5, 65.6, 38.8, 27.1, 27.1, 27.1. HRMS(ESI+) m/z calculated for $\text{C}_{14}\text{H}_{19}\text{O}_2$ $[\text{M}+\text{H}]^+$ 219.1380, found 219.1379.

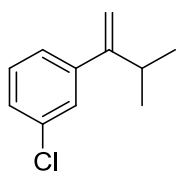
EXPERIMENTAL SECTION



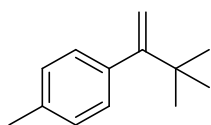
S11, Colorless oil (80 % yield); $^1\text{H-NMR}$ (CDCl_3 , 300 MHz, 300K) δ , ppm: 7.44 – 7.41 (m, 2H), 7.62 – 7.30 – 7.15 (m, 8H), 5.49 (m, 1H), 5.01 (m, 1H), 3.83 (s, 2H). $^{13}\text{C}\{^1\text{H}\}$ -NMR 146.9, 140.8, 139.5, 128.9, 128.4, 128.3, 127.5, 126.1, 126.1, 114.6, 41.6 HRMS(ESI+) m/z calculated for $\text{C}_{15}\text{H}_{14}\text{Na}$ $[\text{M}+\text{Na}]^+$ 217.0988, found 217.0973.



S13, Yellow oil (83 % yield); $^1\text{H-NMR}$ (CDCl_3 , 300 MHz, 300K) δ , ppm: 7.27 (m, 4H), 5.12 (s, 1H), 5.04 (s, 1H), 2.82 – 2.73 (m, 1H), 1.08 (d, 6H, $J = 6.8$ Hz). $^{13}\text{C}\{^1\text{H}\}$ -NMR 154.6, 141.2, 132.8, 128.2, 127.9, 110.5, 32.2, 32.2, 21.9. HRMS(ESI+) m/z calculated for $\text{C}_9\text{H}_9\text{OCl}$ $[\text{M}+\text{H}]^+$ 181.0779, found 181.0762.

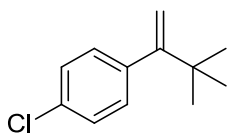


S16, Colorless oil (50 % yield); $^1\text{H-NMR}$ (CDCl_3 , 300 MHz, 300K) δ , ppm: 7.33 – 7.25 (m, 1H), 7.24 – 7.22 (m, 3H), 5.14 (m, 1H), 5.06 (m, 1H), 2.83 – 2.73 (m, 1H), 1.09 (d, 6H, $J = 6.8$ Hz). $^{13}\text{C}\{^1\text{H}\}$ -NMR 154.5, 144.7, 134.0, 129.4, 127.1, 126.8, 124.8, 111.1, 32.3, 21.9. HRMS(ESI+) m/z calculated for $\text{C}_9\text{H}_9\text{OCl}$ $[\text{M}+\text{H}]^+$ 181.0779, found 181.0768.

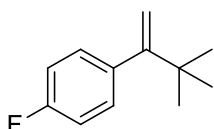


S18, Yellow oil (61 % yield); $^1\text{H-NMR}$ (CDCl_3 , 300 MHz, 300K) δ , ppm: 7.11 – 7.08 (m, 2H), 7.04 – 7.01 (m, 2H), 5.15 (d, 1H, $J = 1.9$ Hz), 4.74 (d, 1H, $J = 1.9$ Hz), 2.34 (s, 3H), 1.10 (s, 9H). $^{13}\text{C}\{^1\text{H}\}$ -NMR 159.7, 140.5, 135.7, 128.9, 128.0, 111.4, 36.1, 29.6, 21.1. HRMS(ESI+) m/z calculated for $\text{C}_{13}\text{H}_{18}$ $[\text{M}+\text{H}]^+$ 175.1481, found 175.1459.

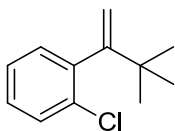
EXPERIMENTAL SECTION



S20, Yellow oil (83 % yield); $^1\text{H-NMR}$ (CDCl_3 , 300 MHz, 300K) δ , ppm: 7.26 – 7.24 (m, 2H), 7.08 – 7.05 (m, 2H), 5.18 (d, 1H, $J = 1.6$ Hz), 4.75 (d, 1H, $J = 1.6$ Hz), 1.10 (s, 9H). $^{13}\text{C}\{^1\text{H}\}$ -NMR 158.6, 141.8, 132.2, 130.3, 127.4, 112.1, 36.1, 29.5 HRMS(ESI+) m/z calculated for $\text{C}_{12}\text{H}_{15}\text{Cl}$ $[\text{M}+\text{H}]^+$ 195.0935, found 195.0915.



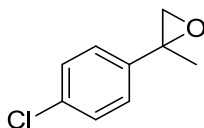
S21, Yellow oil (64 % yield); $^1\text{H-NMR}$ (CDCl_3 , 300 MHz, 300K) δ , ppm: 7.11 – 7.06 (m, 2H), 7.00 – 6.93 (m, 2H), 5.17 (d, 1H, $J = 1.7$ Hz), 4.75 (d, 1H, $J = 1.7$ Hz), 1.10 (s, 9H). $^{13}\text{C}\{^1\text{H}\}$ -NMR 161.5 (d, $J = 244$ Hz), 158.8, 139.2 (d, $J = 3.6$ Hz), 130.4 (d, $J = 7.8$ Hz), 114.2, 113.9, 112.1, 36.1, 29.5. HRMS(ESI+) m/z calculated for $\text{C}_{12}\text{H}_{15}\text{F}$ $[\text{M}+\text{H}]^+$ 179.1231, found 179.1231.



S22, Yellow oil (42 % yield); $^1\text{H-NMR}$ (CDCl_3 , 300 MHz, 300K) δ , ppm: 7.28 – 7.26 (m, 2H), 7.25 – 7.12 (m, 2H), 5.17 (d, 1H, $J = 1.7$ Hz), 4.76 (d, 1H, $J = 1.7$ Hz), 1.10 (s, 9H). $^{13}\text{C}\{^1\text{H}\}$ -NMR 159.8, 143.5, 129.0, 127.3, 126.2, 111.5, 36.1, 29.7. HRMS(ESI+) m/z calculated for $\text{C}_{12}\text{H}_{15}\text{Cl}$ $[\text{M}+\text{H}]^+$ 195.0935, found 195.0915.

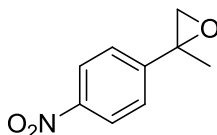
6.3) Characterization of isolated epoxide products

2-(4-chlorophenyl)-2-methyloxirane



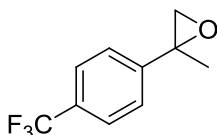
E3, yellow oil; (90 % yield, 63 % ee); $^1\text{H-NMR}$ (CDCl_3 , 300 MHz, 300K) δ , ppm: 7.30 (s, 4H), 2.98 (d, 1H, $J = 5.3$ Hz), 2.76 (dd, 1H, $J = 5.4, 0.7$ Hz), 1.70 (s, 3H). $^{13}\text{C}\{^1\text{H}\}$ -NMR 139.7, 133.3, 128.5, 126.8, 57.1, 56.3, 21.7. HRMS(ESI+) m/z calculated for $\text{C}_9\text{H}_9\text{OCl}$ $[\text{M}+\text{H}]^+$ 169.0415, found 169.0421. Chiral GC analysis with CYCLOSIL-B.

2-(4-nitrophenyl)-2-methyloxirane



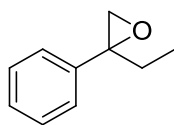
E4, colorless oil; (94 % yield, 66 % ee); $^1\text{H-NMR}$ (CDCl_3 , 300 MHz, 300K) δ , ppm: 8.22 – 8.18 (dt, 2H, $J = 9.1, 2.3$ Hz), 7.56 – 7.51 (dt, 2H, $J = 9.1, 2.4$ Hz), 2.76 (d, 1H, $J = 5.3$ Hz), 2.80 – 2.77 (dq, 1H, $J = 5.3, 0.8$ Hz), 1.77 (s, 3H). $^{13}\text{C}\{^1\text{H}\}$ -NMR 148.6, 126.3, 123.5, 57.2, 56.2, 21.3. HRMS(ESI+) m/z calculated for $\text{C}_9\text{H}_9\text{NO}_3$ $[\text{M}+\text{H}]^+$ 180.0655, found 180.0670. Chiral GC analysis with CYCLOSIL-B.

2-methyl-2-(4-(trifluoromethyl)phenyl)oxirane



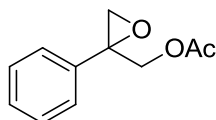
E5, yellow oil; (88 % yield, 50 % ee); $^1\text{H-NMR}$ (CDCl_3 , 300 MHz, 300K) δ , ppm: 7.61 – 7.58 (m, 2H), 7.50 – 7.47 (m, 2H), 3.02 (d, 1H, $J = 5.4$, Hz), 2.78 – 2.76 (dq, 1H, $J = 5.4, 0.7$ Hz), 1.74 (s, 3H). $^{13}\text{C}\{^1\text{H}\}$ -NMR 145.2, 129.7 (q, $J = 32.5$ Hz), 125.7, 125.3 (q, $J = 3.7$ Hz), 124.0 (q, $J = 272$ Hz), 57.1, 56.4, 21.5. HRMS(ESI+) m/z calculated for $\text{C}_{10}\text{H}_9\text{OF}_3$ $[\text{M}+\text{H}]^+$ 203.0678, found 203.0680. Chiral GC analysis with CYCLOSIL-B.

2-ethyl-2-phenyloxirane



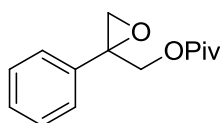
E8, yellow oil; (78 % yield, 80 % ee); $^1\text{H-NMR}$ (CDCl_3 , 300 MHz, 300K) δ , ppm: 7.40 – 7.26 (m, 5H), 2.99 (d, 1H, $J = 5.4$ Hz), 2.75 (d, 1H, $J = 5.4$ Hz), 2.26 – 2.15 (m, 1H), 1.88 – 1.76 (m, 1H), 0.97 – 0.92 (t, 3H). $^{13}\text{C}\{^1\text{H}\}$ -NMR 140.0, 128.3, 127.4, 126.0, 60.1, 55.4, 28.3, 9.0. HRMS(ESI+) m/z calculated for $\text{C}_{10}\text{H}_{12}\text{O}$ $[\text{M}+\text{H}]^+$ 149.0961, found 149.0976. Chiral GC analysis with CYCLOSIL-B.

2-isopropyl-2-phenyloxirane



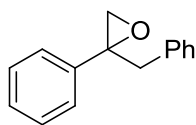
E9, colorless oil; (80% yield, 83 % ee); $^1\text{H-NMR}$ (CDCl_3 , 300 MHz, 300K) δ , ppm: 7.39 – 7.34 (s, 5H), 4.74 (d, 1H, $J = 12.2$ Hz), 4.29 (d, 1H, $J = 12.2$ Hz), 3.13 (d, 1H, $J = 5.3$ Hz), 2.83 (d, 1H, $J = 5.3$), 2.06 (s, 3H). $^{13}\text{C}\{^1\text{H}\}$ -NMR 170.6, 136.8, 128.5, 128.2, 126.1, 65.8, 58.1, 53.6, 20.8. HRMS(ESI+) m/z calculated for $\text{C}_{11}\text{H}_{13}\text{O}_3$ $[\text{M}+\text{H}]^+$ 193.0859, found 193.0863. Chiral GC analysis with CYCLOSIL-B.

(2-phenyloxiran-2-yl)methyl pivalate



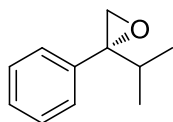
E10, colorless oil; (83% yield, 81 % ee); $^1\text{H-NMR}$ (CDCl_3 , 300 MHz, 300K) δ , ppm: 7.41 – 7.32 (s, 5H), 4.77 (d, 1H, $J = 14.7$ Hz), 4.24 (d, 1H, $J = 14.7$ Hz), 3.11 (d, 1H, $J = 5.3$), 2.84 (d, 1H, $J = 5.3$), 1.13 (s, 9H). $^{13}\text{C}\{^1\text{H}\}$ -NMR 178.0, 136.9, 128.4, 128.1, 126.2, 65.6, 58.4, 53.1, 38.8, 27.1. HRMS(ESI+) m/z calculated for $\text{C}_{14}\text{H}_{19}\text{O}_3$ $[\text{M}+\text{H}]^+$ 235.1329, found 235.1327. Chiral GC analysis with CYCLOSIL-B.

2-benzyl-2-phenyloxirane



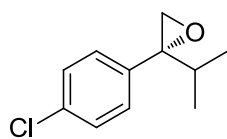
E11, white solid; (70% yield, 80 % ee); $^1\text{H-NMR}$ (CDCl_3 , 300 MHz, 300K) δ , ppm: 7.32 – 7.18 (s, 10H), 3.38 (d, 1H, $J = 12.3$ Hz), 3.23 (d, 1H, $J = 12.3$ Hz), 2.88 (d, 1H, $J = 5.3$ Hz), 2.76 (d, 1H, $J = 5.3$ Hz). $^{13}\text{C}\{^1\text{H}\}$ -NMR 140.0, 136.3, 129.9, 128.2, 128.2, 127.5, 126.6, 126.2, 60.2, 54.4, 41.5. HRMS(ESI+) m/z calculated for $\text{C}_{15}\text{H}_{14}\text{ONa}$ $[\text{M}+\text{Na}]^+$ 233.0937, found 233.0933. Chiral GC analysis with CYCLOSIL-B.

2-isopropyl-2-phenyloxirane



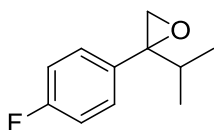
E12, colorless oil; (60% yield, 91 % ee); $^1\text{H-NMR}$ (CDCl_3 , 300 MHz, 300K) δ , ppm: 7.38 – 7.27 (m, 5H), 2.99 (d, 1H, $J = 5.2$ Hz), 2.71 (d, 1H, $J = 5.2$ Hz), 2.16 – 2.00 (m, 1H), 0.96 (d, 3H, $J = 4.0$), 0.94 (d, 3H, $J = 4.0$). $^{13}\text{C}\{^1\text{H}\}$ -NMR 139.3, 127.9, 127.4, 127.3, 64.5, 53.2, 33.1, 18.5, 17.8. HRMS(ESI+) m/z calculated for $\text{C}_{11}\text{H}_{15}\text{O}$ $[\text{M}+\text{H}]^+$ 163.1117, found 163.1131. $[\alpha]_{\text{D}}^{26}$ - 33.6 (CHCl_3 , c 1.6); Chiral GC analysis with CYCLOSIL-B.

2-(4-chlorophenyl)-2-isopropyloxirane



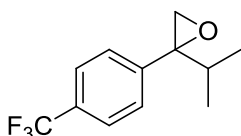
E13, yellow oil; (87% yield, 92 % ee); $^1\text{H-NMR}$ (CDCl_3 , 300 MHz, 300K) δ , ppm: 7.30 (s, 4H), 2.99 (d, 1H, $J = 5.1$ Hz), 2.67 (d, 1H, $J = 5.2$ Hz), 2.14 – 1.99 (m, 1H), 0.95 (d, 3H, $J = 4.9$), 0.92 (d, 3H, $J = 4.9$). $^{13}\text{C}\{^1\text{H}\}$ -NMR 137.9, 133.2, 128.6, 128.1, 64.0, 53.3, 32.9, 18.5, 17.7. HRMS(ESI+) m/z calculated for $\text{C}_{11}\text{H}_{13}\text{OCl}$ $[\text{M}+\text{H}]^+$ 197.0726, found 197.0710. $[\alpha]_{\text{D}}^{26}$ - 28.9 (CHCl_3 , c 1.9). Chiral GC analysis with CYCLOSIL-B.

2-(4-fluorophenyl)-2-isopropylloxirane.



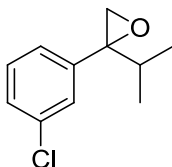
E14, colorless oil; (85% yield, 91 % ee); $^1\text{H-NMR}$ (CDCl_3 , 300 MHz, 300K) δ , ppm: 7.35 – 7.30 (m, 2H), 7.04 – 6.98 (m, 2H), 2.99 (d, 1H, $J = 5.1$ Hz), 2.69 (d, 1H, $J = 5.2$ Hz), 2.10 – 1.97 (m, 1H), 0.95 (d, 3H, $J = 4.3$), 0.92 (d, 3H, $J = 4.2$). $^{13}\text{C}\{^1\text{H}\}$ -NMR 162.0 (d, $J = 247$ Hz), 135.1 (d, $J = 3.2$ Hz), 128.9 (d, $J = 8.0$ Hz), 114.8 (d, $J = 21.4$ Hz), 64.0, 53.4, 33.2, 18.5, 17.8. HRMS(ESI+) m/z calculated for $\text{C}_{11}\text{H}_{13}\text{OF}$ $[\text{M}+\text{H}]^+$ 181.1023, found 181.1022. Chiral GC analysis with CYCLOSIL-B.

2-isopropyl-2-(4-(trifluoromethyl)phenyl)oxirane



E15, colorless oil; (77% yield, 84 % ee); $^1\text{H-NMR}$ (CDCl_3 , 300 MHz, 300K) δ , ppm: 7.60 – 7.58 (d, 2H, $J = 8.1$ Hz), 7.50 – 7.47 (d, 2H, $J = 8.1$ Hz), 3.04 (d, 1H, $J = 5.1$ Hz), 2.68 (d, 1H, $J = 5.1$ Hz), 2.19 – 2.10 (m, 1H), 0.96 (d, 3H, $J = 4.6$), 0.94 (d, 3H, $J = 4.5$). $^{13}\text{C}\{^1\text{H}\}$ -NMR 143.5, 129.6 (q, $J = 32.7$ Hz), 127.5, 124.9 (q, $J = 3.8$ Hz), 124.1 (q, $J = 274$ Hz), 64.0, 53.3, 32.6, 18.5, 17.5. HRMS(ESI+) m/z calculated for $\text{C}_{12}\text{H}_{13}\text{F}_3\text{O}$ $[\text{M}+\text{H}]^+$ 231.0991, found 231.0999. Chiral GC analysis with CYCLOSIL-B.

2-(3-chlorophenyl)-2-isopropylloxirane

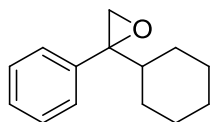


E16, yellow oil; (90% yield, 97 % ee); $^1\text{H-NMR}$ (CDCl_3 , 300 MHz, 300K) δ , ppm: 7.36 – 7.35 (m, 1H), 7.26 – 7.25 (m, 3H), 3.00 (d, 1H, $J = 5.1$ Hz), 2.68 (d, 1H, $J = 5.1$ Hz), 2.15 – 2.06 (m, 1H), 0.95 (d, 3H, $J = 5.5$), 0.93 (d, 3H, $J = 5.4$). $^{13}\text{C}\{^1\text{H}\}$ -NMR 141.6, 133.9, 129.3, 127.6, 127.3, 125.3, 63.9, 53.2, 32.7, 18.5,

EXPERIMENTAL SECTION

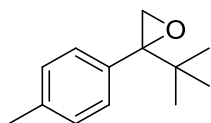
17.6. HRMS(ESI+) m/z calculated for $C_{11}H_{13}OCl$ $[M+H]^+$ 197.0728, found 197.0721. Europium tris [3-(heptafluoropropylhydroxymethylene)-(+)-camphorate] was used to determine the enantioselectivity.

2-cyclohexyl-2-phenyloxirane



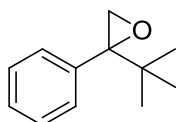
E17, colorless oil; (52% yield, 75 % ee); 1H -NMR ($CDCl_3$, 300 MHz, 300K) δ , ppm: 7.37 – 7.3 (m, 5H), 3.04 (d, 1H, $J = 5.3$ Hz), 2.72 (d, 1H, $J = 5.3$ Hz), 1.80 - 1.64.98 (m, 6H). 1.28 - 1.1 (m, 5H). $^{13}C\{^1H\}$ -NMR 139.7, 129.3, 128.9, 127.8, 127.3, 127.2, 64.2, 52.8, 43.0, 28.8, 28.2, 26.3, 26.1, 26.0. HRMS(ESI+) m/z calculated for $C_{14}H_{18}ONa$ $[M+Na]^+$ 225.1250, found 225.1243. Chiral GC analysis with astec CHIRALDEX G-TA.

2-(tert-butyl)-2-(p-tolyl)oxirane



E18, yellow oil; (79% yield, 93 % ee); 1H -NMR ($CDCl_3$, 300 MHz, 300K) δ , ppm: 7.26 – 7.22 (m, 2H), 7.11 – 7.09 (m, 2H), 3.09 (d, 1H, $J = 5.1$ Hz), 2.62 (d, 1H, $J = 5.1$ Hz), 2.33 (s, 3H), 0.97 (s, 9H). $^{13}C\{^1H\}$ -NMR 136.8, 136.5, 128.7, 127.9, 66.6, 50.9, 33.8, 26.3, 21.1. HRMS(ESI+) m/z calculated for $C_{13}H_{18}O$ $[M+H]^+$ 191.1430, found 191.1413. Chiral GC analysis with CYCLOSIL-B.

2-(tert-butyl)-2-phenyloxirane



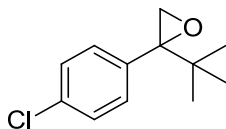
E19, yellow oil; (85% yield, 91 % ee); 1H -NMR ($CDCl_3$, 300 MHz, 300K) δ , ppm: 7.37 – 7.26 (m, 5H), 3.11 (d, 1H, $J = 5.1$ Hz), 2.65 (d, 1H, $J = 5.1$ Hz), 0.98 (s, 9H). $^{13}C\{^1H\}$ -NMR 139.5, 128.8, 127.3, 127.2, 66.8, 50.8, 33.7, 26.3.

EXPERIMENTAL SECTION

HRMS(ESI+) m/z calculated for $C_{12}H_{16}O$ $[M+H]^+$ 199.1093, found 199.1101.

Chiral GC analysis with CYCLOSIL-B.

2-(tert-butyl)-2-(4-chlorophenyl)oxirane

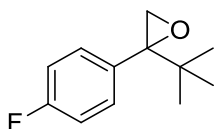


E20, yellow solid; (80% yield, 94 % ee); 1H -NMR ($CDCl_3$, 300 MHz, 300K) δ , ppm: 7.28 (s, 4H), 3.11 (d, 1H, $J = 5.1$ Hz), 2.62 (d, 1H, $J = 5.1$ Hz), 0.97 (s, 9H). $^{13}C\{^1H\}$ -NMR 138.0, 133.1, 130.1, 127.5, 66.3, 50.9, 33.7, 26.2.

HRMS(ESI+) m/z calculated for $C_{12}H_{15}OCl$ $[M+H]^+$ 211.0884, found 211.0892.

Chiral GC analysis with CYCLOSIL-B.

2-(tert-butyl)-2-(4-fluorophenyl)oxirane

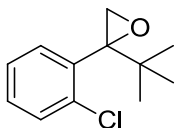


E21, yellow solid; (85% yield, 96 % ee); 1H -NMR ($CDCl_3$, 300 MHz, 300K) δ , ppm: 7.35 – 7.30 (m, 2H), 7.02 – 6.96 (m, 2H), 3.13 (d, 1H, $J = 4.9$ Hz), 2.62 (d, 1H, $J = 4.9$ Hz), 0.97 (s, 9H). $^{13}C\{^1H\}$ -NMR 161.9 (d, $J = 247$ Hz), 135.3 (d, $J = 3.2$ Hz), 130.4 (d, $J = 8.0$ Hz), 114.3 (d, $J = 21.4$ Hz), 66.3, 50.9, 33.7, 26.2.

HRMS(ESI+) m/z calculated for $C_{12}H_{15}OF$ $[M+H]^+$ 195.1180, found 195.1165.

Chiral GC analysis with CYCLOSIL-B

2-(tert-butyl)-2-(2-chlorophenyl)oxirane

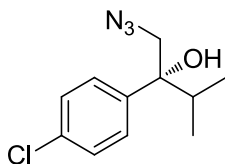


E22, white solid; (57% yield, 92 % ee); 1H -NMR ($CDCl_3$, 300 MHz, 300K) δ , ppm: 7.39 – 7.33 (m, 2H), 7.32 – 7.29 (m, 2H), 3.11 (d, 1H, $J = 5.1$ Hz), 2.67 (d, 1H, $J = 5.1$ Hz), 1.00 (s, 9H). $^{13}C\{^1H\}$ -NMR 139.5, 128.6, 127.3, 127.2, 66.8,

50.8, 33.8, 26.3 HRMS(ESI+) m/z calculated for $C_{12}H_{15}OCl$ $[M+H]^+$ 211.0884, found 211.0890 Chiral GC analysis with CYCLOSIL-B.

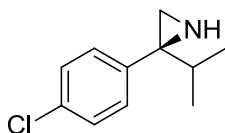
6.4) Characterization of isolated azide, aziridine and amino alcohol products

1-azido-2-(4-chlorophenyl)-3-methylbutan-2-ol



P1, orange oil; (87% yield, 92% ee); $^1\text{H-NMR}$ (CDCl_3 , 300 MHz, 300K) δ , ppm: 7.33 (s, 4H), 3.80 – 3.76 (d, 1H, $J = 12.3$ Hz), 3.71 – 3.66 (d, 1H, $J = 12.3$ Hz), 2.29 (br, 1H), 2.10 – 2.01 (m, 1H), 0.91 (d, 3H, $J = 6.7$ Hz), 0.77 (d, 3H, $J = 6.7$ Hz). $^{13}\text{C}\{^1\text{H}\}$ -NMR 141.2, 133.1, 128.3, 127.4, 78.7, 59.2, 35.9, 17.3, 16.6. HRMS(ESI+) m/z calculated for $\text{C}_{11}\text{H}_{14}\text{ClN}_3\text{ONa}$ $[\text{M}+\text{Na}]^+$ 262.0718, found 262.0699. $[\alpha]_{\text{D}}^{26}$ -2.7 (CHCl_3 , c 2.4). Chiral HPLC analysis (Chiralpack IC, n -Hex:iPrOH = 98/2, 25 °C, flow rate = 1 mL/min, $\lambda = 220$ nm), $t_{\text{minor}} = 5.9$ min, $t_{\text{major}} = 6.2$ min.

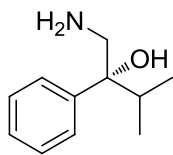
2-(4-chlorophenyl)-2-isopropylaziridine



P2, yellow oil; (80% yield, 88% ee); $^1\text{H-NMR}$ (CDCl_3 , 300 MHz, 300K) δ , ppm: 7.28 (s, 4H), 1.84 (d, 2H), 1.60 – 1.46 (m, 1H), 0.93 (d, 3H, $J = 1.7$ Hz), 0.91 (d, 3H, $J = 1.7$ Hz). $^{13}\text{C}\{^1\text{H}\}$ -NMR 139.1, 132.9, 130.8, 127.9, 46.2, 36.7, 31.7, 19.6, 18.7. HRMS(ESI+) m/z calculated for $\text{C}_{11}\text{H}_{15}\text{ClN}$ $[\text{M}+\text{H}]^+$ 196.0888, found 196.0890. $[\alpha]_{\text{D}}^{26}$ +6.5 (CHCl_3 , c 1.0). HPLC analysis (Chiralpack IC, n -Hex:iPrOH:DEA = 98/2/0.1, 25 °C, flow rate = 1 mL/min, $\lambda = 220$ nm), $t_{\text{minor}} = 13.8$ min, $t_{\text{major}} = 14.8$ min.

EXPERIMENTAL SECTION

1-amino-3-methyl-2-phenylbutan-2-ol



P3, white solid; (88% yield, 90 % ee); $^1\text{H-NMR}$ (CDCl_3 , 300 MHz, 300K) δ , ppm: 7.52 – 7.49 (m, 2H), 7.45 – 7.40 (m, 2H), 7.37 – 7.31 (m, 1H), 3.45 (d, 1H, $J = 12.8$ Hz), 3.32 (d, 1H, $J = 12.8$ Hz), 2.22 – 2.04 (m, 1H), 0.99 – 0.97 (d, 3H, $J = 6.8$ Hz) 0.77 – 0.74 (d, 3H, $J = 6.8$ Hz). $^{13}\text{C}\{^1\text{H}\}$ -NMR 140.7, 128.1, 128.1, 127.3, 126.0, 76.2, 36.3, 16.1, 15.4. HRMS(ESI+) m/z calculated for $\text{C}_{11}\text{H}_{18}\text{NO}$ $[\text{M}+\text{H}]^+$ 180.1383, found 180.1368. $[\alpha]_{\text{D}}^{26}$ -3.3 (CHCl_3 , c 0.9). HPLC analysis (Chiralpack IC, $n\text{-Hex:iPrOH:DEA} = 95/5/0.1$, 25 °C, flow rate = 1 mL/min, $\lambda = 254$ nm), $t_{\text{minor}} = 9.0$ min, $t_{\text{major}} = 8.6$ min.

References

- (1) Reitz, D.; Beak, P.; Farney, R. F.; Helmick, L. S. *J. Am. Chem. Soc.* **1978**, *100*, 5428.
- (2) Hatch, L. F.; Patton, T. L. *J. Am. Chem. Soc.* **1954**, *76*, 2705.
- (3) Baciocchi, E.; Ruzziconi, R. *J. Org. Chem.* **1991**, *56*, 4772.
- (4) Monfette, S.; Turner, Z. R.; Semproni, P. S.; Chirik, P. J. *J. Am. Chem. Soc.* **2012**, *134*, 4561.
- (5) Hoshino, Y.; Yamamoto, H.; *J. Am. Chem. Soc.* **2000**, *122*, 10452.

Experimental section: Chapter VII.3

Iron catalyzed highly enantioselective epoxidation of cyclic aliphatic enones with aqueous H₂O₂

1) Synthesis of cyclic enones

The following olefins were prepared according to the reported procedures. All the rest are commercial available. The substrate nomenclatures were exclusives for this chapter. The substrate nomenclature was exclusive for this chapter.

2- cyclooctenone (**S4**)¹

3-ethyl-2-cyclohexenone (**S10**)²

3-propyl-2-cyclohexenone (**S11**)³

3-butyl-2-cyclohexenone (**S12**)²

3-isopropyl-2-cyclohexenone (**S13**)¹

5,5-dimethylcyclohex-2-en-1-one (**S14**)⁴

6,6-dimethylcyclohex-2-en-1-one (**S15**)⁴

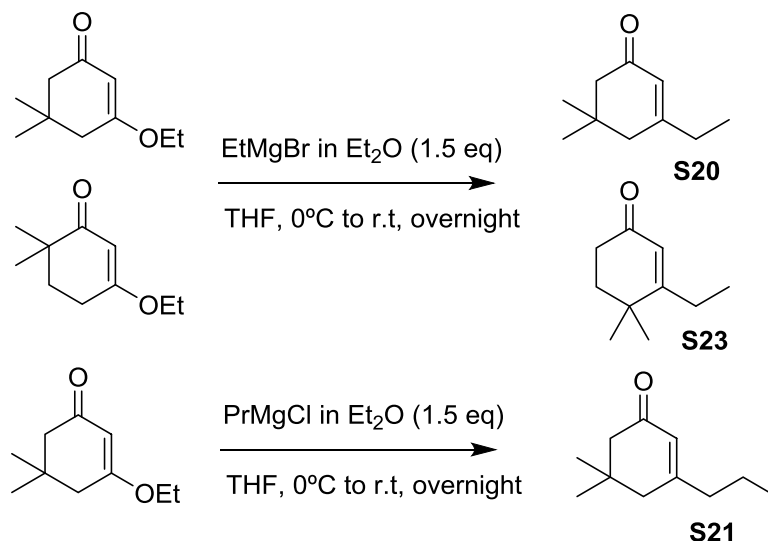
3-methyl-6,6-dimethylcyclohex-2-en-1-one (**S16**)⁵

3-ethyl-6,6-dimethylcyclohex-2-en-1-one (**S17**)⁶

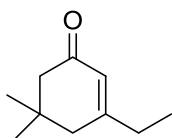
3-butyl-6,6-dimethylcyclohex-2-en-1-one (**S18**)⁷

3-ethyl-5,5-dimethylcyclohex-2-en-1-one (**S20**)⁸

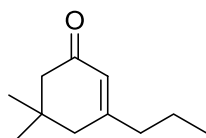
3-butyl-5,5-dimethylcyclohex-2-en-1-one (**S22**)⁹

1.1) Synthesis of cyclic enones (**S7**, **S20**, **S21** and **S23**)

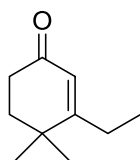
3-Ethoxycyclohexenone⁴ (6 mmols) in 10 mL THF was added dropwise to a solution of a Grignard reagent (3M in Et₂O for EtMgBr or 2M in Et₂O for PrMgBr, 9 mmols) at 0°C under nitrogen. After the addition, the resulting solution was allowed to warm to room temperature and stirred overnight. The reaction was quenched slowly with 1M HCl at 0°C. The solution was extracted three times with Et₂O (3 x 50 mL). The organic layers were washed with NaHCO₃ solution, water and brine, dried with MgSO₄, filtered and evaporated under reduced pressure. Then, the crude was purified by flash column chromatography silica gel (Hexane:ethyl acetate, 9/1) to obtain the desired olefin. The yield obtained is 55 % for **S20**, 41 % for **S21** and 38 % for **S23**



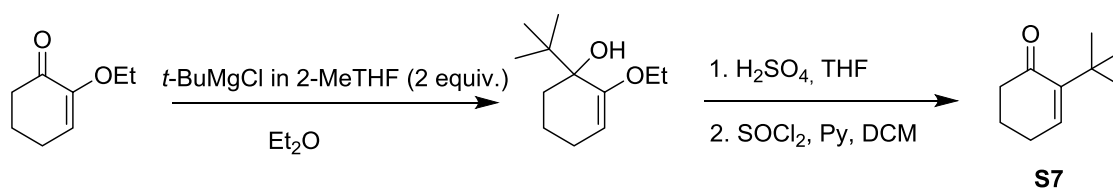
S20, Colorless oil; (3.28 mmols, 55% yield): ¹H-NMR (CDCl₃, 300 MHz, 300K) δ, ppm ¹H NMR (CDCl₃, 300 MHz, 300K) δ ppm: 5.88 (s, 1H), 2.20 (m, 6H), 1.10 (t, *J* = 7.4 Hz, 3H), 1.04 (s, 6H). ¹³C{¹H}-NMR (75 MHz, CDCl₃) δ ppm: 200.3, 165.5, 123.5, 51.1, 44., 33.6, 30.9, 28.3, 28.2, 11.3. HRMS(ESI+) *m/z* calculated for C₁₀H₁₆ONa [M+Na]⁺ 175.1093, found 175.1100.



S21, Colorless oil; (2.3 mmols, 41% yield): $^1\text{H-NMR}$ (CDCl_3 , 300 MHz, 300K) δ , ppm: 5.88 (s, 1H), 2.21 (s, 2H), 2.20 – 2.11 (m, 4H), 1.53 (m, 2H), 1.03 (s, 6H), 0.94 (t, $J = 7.4$ Hz, 3H). $^{13}\text{C}\{^1\text{H}\}$ -NMR (75 MHz, CDCl_3) δ ppm: 200.2, 164.0, 124.7, 51.1, 43.9, 40.1, 33.6, 28.3, 28.3, 20.1, 13.7. HRMS(ESI+) m/z calculated for $\text{C}_{11}\text{H}_{18}\text{ONa}$ $[\text{M}+\text{Na}]^+$ 189.1250, found 189.1256.



S23, Yellow oil; (2.3 mmols, 38% yield): $^1\text{H-NMR}$ (CDCl_3 , 300 MHz, 300K) δ , ppm: 5.80 (s, 1H), 2.54 – 2.36 (m, 2H), 2.26 (qd, $J = 7.3, 1.5$ Hz, 2H), 1.95 – 1.78 (m, 2H), 1.17 (s, 6H), 1.09 (t, $J = 7.3$ Hz, 3H). $^{13}\text{C}\{^1\text{H}\}$ -NMR (75 MHz, CDCl_3) δ ppm: 199.7, 174.1, 123.5, 38.0, 35.7, 34.3, 26.6, 26.4, 24.7, 11.7. HRMS(ESI+) m/z calculated for $\text{C}_{10}\text{H}_{16}\text{ONa}$ $[\text{M}+\text{Na}]^+$ 175.1093, found 175.1098.

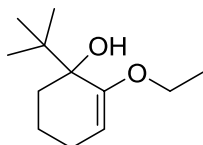


We followed the procedure described in the literature.¹⁰

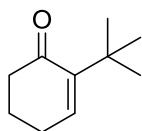
A solution of tert-butylmagnesium chloride (1 M in 2-methyltetrahydrofuran, 7.7 mL, 7.7 mmol, 2 equiv.) was added dropwise a solution of 2-ethoxycyclohexenone¹¹ (540 mg, 3.8 mmols, 1 equiv.) in 10 mL of diethyl ether. After addition, the mixture was refluxed for 1 hour. The reaction was quenched with a sat. NH_4Cl . The aqueous phase was extracted with diethyl ether and the organic phase was washed with H_2O . The organic phase was dried over MgSO_4 , filtered and evaporated under reduced pressure. The crude reaction was purified by flash chromatography silica gel (Hexane/ethyl acetate: 9/1) to

EXPERIMENTAL SECTION

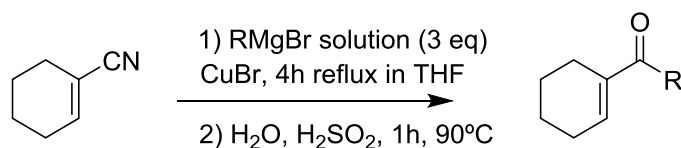
obtain a colorless oil (200 mg, 1.0 mmols, 26% yield). This product was solved in THF (5 mL) and was added conc. H_2SO_4 75 μL . After 30 minutes, the reaction was quenched slowly with sat. NaHCO_3 (7 mL). The mixture was extracted with diethyl ether (3 x 4 mL). The organic phases was dried with MgSO_4 , filtered and evaporated under reduced pressure. To this crude was solved in DCM, was added pyridine (404 μL , 5 mmols, 5 equiv.) and SOCl_2 (150 μL , 2 mmols, 2 equiv.). The mixture was stirred overnight, after which was quenched by addition of 1N HCl (4 mL). The organic phases were separated, dried over MgSO_4 , filtered and evaporated under reduced pressure. The crude was purified by flash chromatography silica column (Hexane/ethyl acetate: 98/2) to obtain a yellow oil (50 mg, 0.3 mmols, 34 %).



Yellow oil; (1.0 mmols, 26% yield): $^1\text{H-NMR}$ (CDCl_3 , 300 MHz, 300K) δ , ppm: 4.79 (dd, $J = 6.5, 2.4$ Hz, 1H), 3.67 (qd, $J = 7.0, 1.8$ Hz, 2H), 2.37 (s, 1H), 2.13 – 2.00 (m, 1H), 2.00 – 1.92 (m, 1H), 1.81 – 1.71 (m, 1H), 1.68 – 1.52 (m, 3H), 1.32 (t, $J = 7.0$ Hz, 3H), 1.02 (s, 9H). $^{13}\text{C}\{^1\text{H}\}$ -NMR (75 MHz, CDCl_3) δ ppm: 157.2, 97.9, 75.6, 61.9, 38.3, 33.6, 26.3, 24.3, 20.3, 14.7. HRMS(ESI+) m/z calculated for $\text{C}_{12}\text{H}_{22}\text{O}_2\text{Na}$ $[\text{M}+\text{Na}]^+$ 175.1512, found 221.1518.



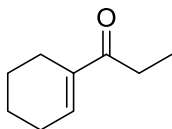
S7, yellow oil; (0.3 mmols, 34% yield): $^1\text{H-NMR}$ (CDCl_3 , 400 MHz, 300K) δ , ppm: 6.76 (t, $J = 4.3$ Hz, 1H), 2.49 – 2.32 (m, 4H), 2.02 – 1.88 (m, 2H), 1.18 (s, 9H). $^{13}\text{C}\{^1\text{H}\}$ -NMR (100 MHz, CDCl_3) δ ppm: 199.4, 146.8, 142.72, 40.6, 34.5, 29.3, 26.4, 22.9. HRMS(ESI+) m/z calculated for $\text{C}_{10}\text{H}_{16}\text{ONa}$ $[\text{M}+\text{Na}]^+$ 175.1093, found 175.1096.

1.2) Synthesis of cyclic enones (S25 – S28)

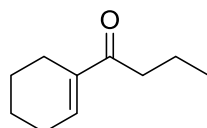
R = Et, Pr, *t*Bu and cyclopropyl

A representative procedure

A brownish solution of magnesium bromide (1 M in ether or THF, 27.9 mmol) was added into a 0°C solution of substituted cyclohexene-1-carbonitrile (9.3 mmol) dissolved in 30 mL of THF. Afterwards, copper bromide (0.1 mmol) was added under N₂ and the resulting solution was refluxed for 4 hours. The solution was then cooled to 0°C and water (10 mL) was added slowly. When the vigorous reaction ceased, a H₂SO₄ 1N solution (33 mL) was added and was refluxed during 1 hour, after that it was cooled to room temperature, basified with 2M NaOH and extracted with ethyl acetate (3 × 50 mL), dried over MgSO₄ and the solvent was removed under reduced pressure to obtain a pale yellow liquid and it was purified by flash column chromatography (hexane:EtAcO/ 9:1).



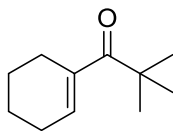
S25, Colorless oil; (5.1 mmols, 45% yield): ¹H-NMR (CDCl₃, 300 MHz, 300K) δ, ppm: 7.01 – 6.79 (m, 1H), 2.65 (q, *J* = 7.3 Hz, 2H), 2.36 – 2.14 (m, 4H), 1.76 – 1.55 (m, 4H), 1.09 (t, *J* = 7.3 Hz, 3H). ¹³C{¹H}-NMR (75 MHz, CDCl₃) δ ppm: 202.1, 139.3, 139.0, 30.1, 26.0, 23.2, 22.0, 21.6, 8.6. HRMS(ESI+) *m/z* calculated for C₉H₁₄ONa [M+Na]⁺ 161.0937, found 161.0943.



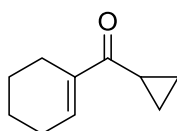
S26, Colorless oil; (3.8 mmols, 51% yield): ¹H-NMR (CDCl₃, 300 MHz, 300K) δ, ppm: 6.87 (s, 1H), 2.57 (t, *J* = 7.4 Hz, 2H), 2.26 – 2.16 (m, 4H), 1.70 – 1.52 (m, 6H), 0.90 (td, *J* = 7.4, 1.4 Hz, 3H). ¹³C{¹H}-NMR (75 MHz, CDCl₃) δ ppm: 201.5,

EXPERIMENTAL SECTION

139.4, 139.2, 38.9, 26.0, 23.1, 22.0, 21.6, 18.2, 13.9. HRMS(ESI+) m/z calculated for $C_{10}H_{16}ONa$ $[M+Na]^+$ 175.1093, found 175.1093.

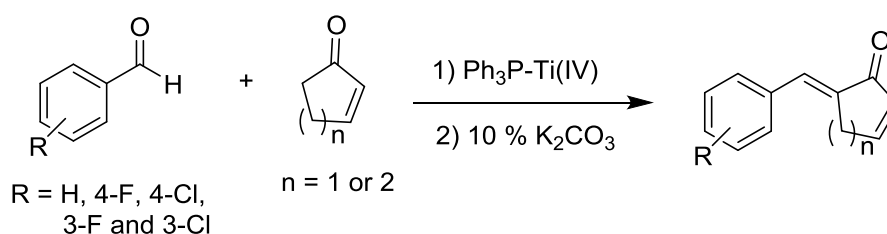


S27, Yellow oil; (4.2 mmols 54% yield): 1H -NMR ($CDCl_3$, 300 MHz, 300K) δ , ppm: 6.44 (s, 1H), 2.32 – 2.08 (m, 4H), 1.69 – 1.57 (m, 4H), 1.24 (s, 9H). $^{13}C\{^1H\}$ -NMR (75 MHz, $CDCl_3$) δ ppm: 210.2, 138.2, 133.6, 43.9, 28.3, 28.1, 25.7, 25.4, 22.3, 21.5. HRMS(ESI+) m/z calculated for $C_{11}H_{18}ONa$ $[M+Na]^+$ 189.1250, found 189.1257.



S28, Yellow oil; (3.6 mmols, 43% yield): 1H -NMR ($CDCl_3$, 300 MHz, 300K) δ , ppm: 7.04 (m, 1H), 2.42 – 2.31 (m, 1H), 2.31 – 2.19 (m, 4H), 1.73 – 1.55 (m, 4H), 1.08 – 0.99 (m, 2H), 0.89 – 0.79 (m, 2H). $^{13}C\{^1H\}$ -NMR (75 MHz, $CDCl_3$) δ ppm: 201.0, 139.9, 139.3, 26.1, 23.5, 22.0, 21.7, 15.4, 10.5. HRMS(ESI+) m/z calculated for $C_{10}H_{14}ONa$ $[M+Na]^+$ 173.0937, found 173.0934.

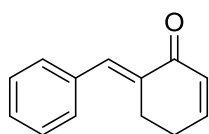
1.3) Synthesis of dienones (S32 – S39)



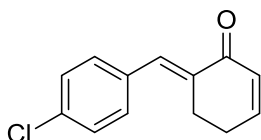
The procedure for **S29** and **S34** was reported by Takanami et.al.¹² We used the same procedure to obtain the rest of dienones.

EXPERIMENTAL SECTION

TiCl₄ was added to the solution of cyclic enone (1 equiv.) and triphenylphosphine (1 equiv.) in dry dichloromethane at -50°C. After, 15 minutes was added 2 equiv. of benzaldehyde derivative, and warmed to room temperature overnight, then the reaction was treated with 10 % of K₂CO₃ during 10 minutes. The organic layer was separated, evaporated and the residue was purified over silica gel with Hexane: Ethyl acetate (85:15) to obtain the cyclic dienone.

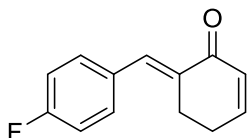


S32, Yellow solid; (4.9 mmols, 47% yield): ¹H-NMR (CDCl₃, 300 MHz, 300K) δ, ppm: 7.61 (t, *J* = 1.8 Hz, 1H), 7.42 – 7.31 (m, 5H), 7.02 (dt, *J* = 10.1, 4.2 Hz, 1H), 6.23 (dt, *J* = 10.1, 1.9 Hz, 1H), 3.01 (td, *J* = 6.4, 1.9 Hz, 2H), 2.45 – 2.37 (m, 2H). ¹³C{¹H}-NMR (75 MHz, CDCl₃) δ ppm: 188.8, 149.3, 135.7, 135.1, 135.1, 134.9, 130.8, 130.7, 129.7, 128.4, 128.3, 26.3, 25.4. HRMS(ESI+) *m/z* calculated for C₁₃H₁₂ONa [M+Na]⁺ 207.0780, found 207.0779.

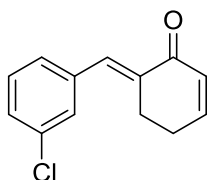


S33, Yellow solid; (4.4 mmols, 42% yield): ¹H-NMR (CDCl₃, 300 MHz, 300K) δ, ppm: 7.53 (s, 1H), 7.37 (m, 2H), 7.29 (m, 2H), 7.04 (dt, *J* = 10.1, 4.2 Hz, 1H), 6.23 (dt, *J* = 10.1, 1.9 Hz, 1H), 2.98 (td, *J* = 6.4, 1.9 Hz, 2H), 2.49 – 2.35 (m, 2H). ¹³C{¹H}-NMR (75 MHz, CDCl₃) δ ppm: 188.4, 149.4, 135.4, 134.2, 134.1, 133.69, 133.66, 131.0, 130.69, 130.66, 128.6, 26.3, 25.4. HRMS(ESI+) *m/z* calculated for C₁₃H₁₁OCINa [M+Na]⁺ 241.0391, found 241.0392.

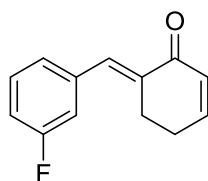
EXPERIMENTAL SECTION



S34, Yellow solid; (5.4 mmols, 52% yield): $^1\text{H-NMR}$ (CDCl_3 , 400 MHz, 300K) δ , ppm: 7.56 (s, 1H), 7.35 (m, 2H), 7.12 – 7.00 (m, 3H), 6.24 (dt, $J = 10.1, 1.9$ Hz, 1H), 2.99 (td, $J = 6.4, 1.9$ Hz, 2H), 2.44 (m, 2H). $^{13}\text{C}\{^1\text{H}\}$ -NMR (100 MHz, CDCl_3) δ ppm: 188.6, 163.7, 161.2, 149.2, 134.74, 134.72, 133.9, 131.8, 131.7, 131.6, 131.5, 130.7, 128.6, 128.5, 115.6, 115.4, 26.2, 25.4. HRMS(ESI+) m/z calculated for $\text{C}_{13}\text{H}_{11}\text{OFNa}$ $[\text{M}+\text{Na}]^+$ 225.0686, found 225.0669.



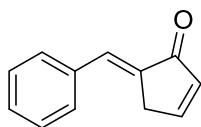
S35, Yellow solid; (2.8 mmols, 44% yield): $^1\text{H-NMR}$ (CDCl_3 , 300 MHz, 300K) δ , ppm: 7.52 (s, 1H), 7.35 – 7.29 (m, 3H), 7.22 (m, 1H), 7.05 (dt, $J = 10.1, 4.2$ Hz, 1H), 6.27 – 6.21 (m, 1H), 2.98 (td, $J = 6.3, 1.9$ Hz, 2H), 2.48 – 2.38 (m, 2H). $^{13}\text{C}\{^1\text{H}\}$ -NMR (75 MHz, CDCl_3) δ ppm: 188.4, 149.5, 137.5, 136.1, 134.3, 133.4, 130.7, 129.7, 129.3, 128.3, 127.8, 26.3, 25.4. HRMS(ESI+) m/z calculated for $\text{C}_{13}\text{H}_{11}\text{OCINa}$ $[\text{M}+\text{Na}]^+$ 241.0391, found 241.0393.



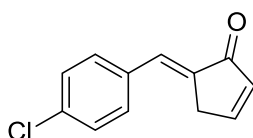
S36, Yellow solid; (2.2 mmols, 40% yield): $^1\text{H-NMR}$ (CDCl_3 , 300 MHz, 300K) δ , ppm: 7.55 (s, 1H), 7.36 (m, 1H), 7.14 (d, $J = 7.7$ Hz, 1H), 7.10 – 7.00 (m, 3H), 6.25 (dt, $J = 10.1, 1.9$ Hz, 1H), 3.00 (td, $J = 6.4, 1.9$ Hz, 2H), 2.49 – 2.39 (m, 2H). $^{13}\text{C}\{^1\text{H}\}$ -NMR (75 MHz, CDCl_3) δ ppm: 188.5, 164.2, 161.0, 149.6, 137.9, 137.8, 135.9, 133.6, 130.7, 130.0, 129.9, 125.5, 116.4, 116.1, 115.3, 115.0,

EXPERIMENTAL SECTION

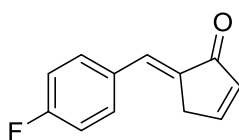
26.3, 25.4. HRMS(ESI+) m/z calculated for $C_{13}H_{11}OFNa$ $[M+Na]^+$ 225.0686, found 225.0693.



S37, Orange solid; (6.2 mmols, 72% yield): 1H -NMR ($CDCl_3$, 300 MHz, 300K) δ , ppm: 7.70 – 7.60 (m, 1H), 7.56 (dt, J = 8.5, 2.2 Hz, 2H), 7.45 – 7.35 (m, 4H), 6.45 (dt, J = 6.0, 2.2 Hz, 1H), 3.55 (q, J = 2.2 Hz, 2H). $^{13}C\{^1H\}$ -NMR (75 MHz, $CDCl_3$) δ ppm: 197.49, 157.27, 157.22, 135.45, 135.13, 132.30, 132.05, 132.03, 130.41, 129.56, 128.90, 34.32. HRMS(ESI+) m/z calculated for $C_{12}H_{10}ONa$ $[M+Na]^+$ 196.0624, found 196.0623.



S38, Yellow solid; (3.1 mmols, 51% yield): 1H -NMR ($CDCl_3$, 300 MHz, 300K) δ , ppm: 7.72 – 7.64 (m, 1H), 7.53 – 7.45 (m, 2H), 7.41 – 7.35 (m, 2H), 7.33 (s, 1H), 6.46 (dt, J = 6.0, 2.2 Hz, 1H), 3.53 (q, J = 2.2 Hz, 2H). $^{13}C\{^1H\}$ -NMR (75 MHz, $CDCl_3$) δ ppm: 197.2, 157.1, 157.1, 135.5, 135.5, 133.6, 132.7, 131.5, 130.6, 129.2, 34.2. HRMS(ESI+) m/z calculated for $C_{12}H_9OCINa$ $[M+Na]^+$ 227.0234, found 227.0236.



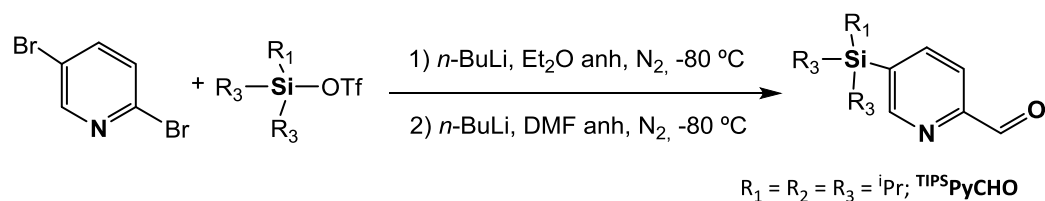
S39, Yellow solid; (3.5 mmols, 52% yield): 1H -NMR ($CDCl_3$, 300 MHz, 300K) δ , ppm: 7.73 – 7.64 (m, 1H), 7.56 (m, 2H), 7.35 (s, 1H), 7.11 (t, J = 8.7 Hz, 2H), 6.46 (dt, J = 6.0, 2.2 Hz, 1H), 3.54 (q, J = 2.1 Hz, 2H). $^{13}C\{^1H\}$ -NMR (75 MHz, $CDCl_3$) δ ppm: 197.3, 164.9, 161.6, 157.1, 135.5, 132.3, 132.2, 131.9, 131.8,

131.4, 131.4, 130.7, 116.2, 115.9, 34.1. HRMS(ESI+) m/z calculated for $C_{12}H_9OFNa$ $[M+Na]^+$ 211.0530 found 211.0526.

2) Synthesis of complexes

2.1) Synthesis of pyridine synthons.

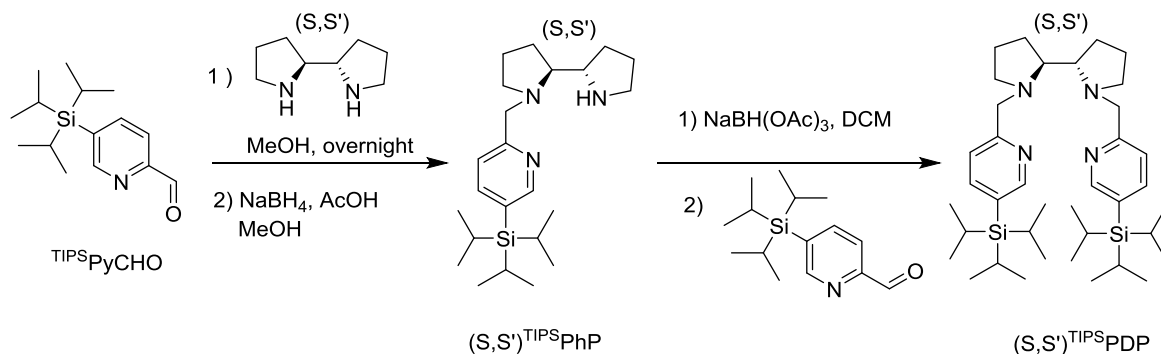
TIPSPyCHO was synthesized by reacting 2,5-dibromopyridine with the corresponding triisopropylsilyl triflate in presence of *n*-butyllithium (*n*-BuLi) and DMF at low temperature



TIPSPyCHO 2,5-dibromopyridine (2.8 g, 12 mmol) were dissolved in 30 mL of anhydrous diethyl ether under inert atmosphere at cooled to $-80\text{ }^\circ\text{C}$ in an ethyl acetate/liquid N_2 bath. Then 1 equiv. of *n*-BuLi (1.6 M in hexanes, 7.5 mL, 12 mmol) were slowly added over 10 min, and the reaction mixture was let stir for 45 min. At that point, 1.1 equiv. of triisopropylsilyl triflate (3.7 mL, 13.2 mmol) was added all at once at $-80\text{ }^\circ\text{C}$, and stirred for another hour to form the 2-bromo-5-(trimethyl)-pyridine. 1.1 equiv of *n*-BuLi (1.6 M in hexanes, 8.3 mL, 13.2 mmol) was added over 10 min to the crude reaction at $-80\text{ }^\circ\text{C}$. After 45 min, 1.6 equiv of anhydrous DMF (1.5 mL, 19.2 mmol) were slowly added. The reaction was stirred for 2h, and the temperature was raised up to $-15\text{ }^\circ\text{C}$ after that time. At this point, the reaction was quenched with 10 mL of H_2O and extracted with diethyl ether (3 x 30 mL). The combined organic layers were washed with 30 mL of brine, dried over $MgSO_4$, concentrated on a rotatory evaporator and purified by silica column chromatography eluting with hexane: ethyl acetate (10:1) to yield 2.9 g (11 mmol, 92%) of the pure product as a yellow oil. 1H -NMR ($CDCl_3$, 400 MHz, 300 K) δ , ppm: 10.10 (s, 1H), 8.86 (s, 1H), 7.95 (ddd, $J = 18.3, 7.6, 1.2$ Hz, 2H), 1.52-1.39 (m, 3H), 1.09 (d, $J = 7.5$ Hz, 18H). ^{13}C -NMR ($CDCl_3$, 100 MHz, 300 K) δ , ppm: 193.9, 155.6, 152.5, 144.0, 137.0, 120.5, 18.4, 10.6. HRMS (ESI-TOF, $[M + Na]^+$): m/z calcd for $C_{15}H_{25}NOSi$ 264.1778, found 264.1768.

2.2) Synthesis of ligands

Synthesis of (S,S') - TIP^S PDP

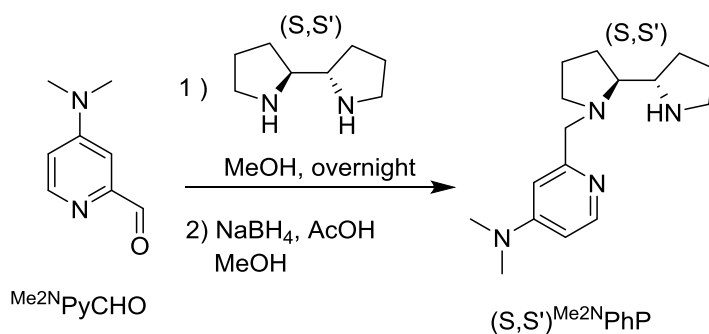


(S,S') - TIP^S PhP. To an anhydrous methanol (15 mL) solution of $(2S,2'S)$ -2,2'-bipyrrolidine (392 mg, 2.8 mmol), 3 Å molecular sieves (400 mg) were added. TIP^S PyCHO (736 mg, 2.8 mmol) was then added to this mixture and stirred overnight under inert atmosphere. At this point, the reaction was cooled to 0 °C, then 1.5 equiv of $NaBH_4$ (158 mg, 4.2 mmol) were slowly added. Afterwards, 4 equiv of AcOH (0.67 mL, 11.2 mmol) were added over 15 min. The mixture was stirred for 2 h at 0 °C, and then diluted with AcOEt (50 mL) and hydrolyzed with 15 mL of NaOH 2 M. The aqueous layer was extracted with AcOEt (2 x 30 mL) and CH_2Cl_2 (2 x 30 mL). Finally, the combined organic layers were dried over $MgSO_4$ and brought to dryness. The desired product was obtained 975 mg as a white solid (2.5 mmol, 90%). 1H -NMR ($CDCl_3$, 300 MHz, 300 K) δ , ppm: 8.57 (s, 1H), 7.75 (dd, $J = 7.7, 1.7$ Hz, 1H), 7.32 (d, $J = 7.6$ Hz, 1H), 4.22 (d, $J = 14.6$ Hz, 1H), 3.71 (d, $J = 14.7$ Hz, 1H), 3.26-3.21 (m, 1H), 3.11-2.98 (m, 3H), 2.86-2.79 (m, 1H), 2.55-2.47 (m, 1H), 2.02-1.73 (m, 7H), 1.63-1.51 (m, 1H), 1.41 (dt, $J = 14.8, 7.4$ Hz, 3H), 1.07 (d, $J = 7.4$ Hz, 18H). ^{13}C -NMR ($CDCl_3$, 75 MHz, 300 K) δ , ppm: 159.8, 154.6, 143.7, 127.9, 122.2, 67.18, 63.4, 62.2, 45.6, 28.3, 28.2, 24.6, 24.1, 18.4, 10.6. HRMS (ESI-TOF, $[M + H]^+$): m/z calcd for $C_{23}H_{41}N_3Si$ 388.3143, found 388.3162.

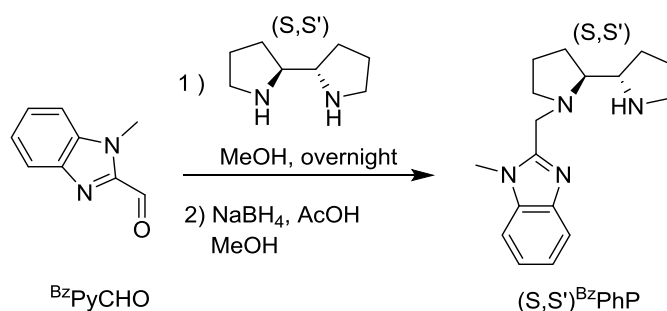
(S,S') - TIP^S PDP (S,S') - TIP^S PhP (810 mg, 3 mmol) were dissolved in CH_2Cl_2 (50 mL) and cooled to 0 °C, and 1.3 equiv of $NaB(OAc)_3$ (827 mg, 3.9 mmol) were added to the reaction mixture, which was stirred for 30 min at 0 °C. TIP^S PyCHO

(540 mg, 3.0 mmol) was added at this point, and the crude was stirred at room temperature overnight. It was then extracted with 40 mL of a NaHCO₃ aqueous saturated solution. The aqueous layer was washed with CH₂Cl₂ (2x 40 mL). The combined organic layers were dried over MgSO₄ and under vacuum. The product was purified by alumina column chromatography eluting with hexane:AcOEt (10:90) to afford 720 mg of a white solid (1.55 mmol, 52%). ¹H-NMR (CD₃OD, 400 MHz, 300 K) δ, ppm: 8.47 (s, 2H), 7.88 (dd, J = 7.8, 1.7 Hz, 2H), 7.50 (d, J = 7.8 Hz, 2H), 4.15 (d, J = 14.2 Hz, 2H), 3.54 (d, J = 14.2 Hz, 2H), 2.99-2.97 (m, 2H), 2.71-2.69 (m, 2H), 2.27-2.25 (m, 2H), 1.74-1.66 (m, 8H), 1.44 (dt, J = 14.9, 7.5 Hz, 6H), 1.09 (dd, J = 7.5, 1.7 Hz, 36H). ¹³C-NMR (CD₃OD, 100 MHz, 300 K) δ, ppm: 159.9, 15.4, 144.2, 128.0, 122.8, 65.8, 60.5, 25.9, 23.1, 17.5, 10.4. HRMS (ESI-TOF, [M + H]⁺): m/z calcd for C₃₈H₆₆N₄Si₂ 635.4904, found 635.4904.

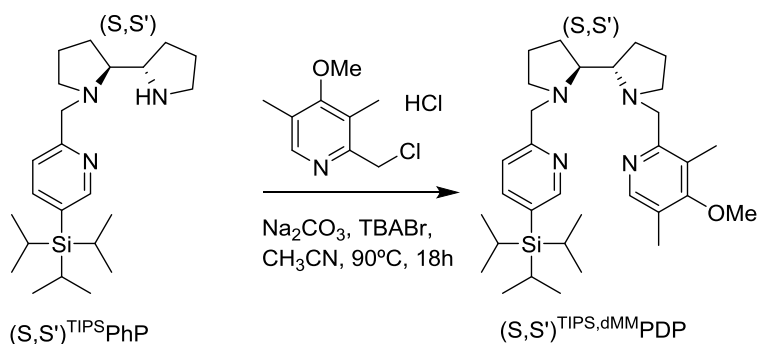
Synthesis of (S,S')^{Me2N}PhP



(S,S')^{Me2N}PhP was synthesized following a procedure analogous to (S,S')^{TIPS}PhP (1.7 mmols, 94 % yield) ¹H-NMR (CDCl₃, 400 MHz, 300K) δ, ppm: 8.17 (d, J = 5.9 Hz, 1H), 6.68 (d, J = 2.1 Hz, 1H), 6.40 (dd, J = 5.9, 2.6 Hz, 1H), 4.16 (d, J = 14.0 Hz, 1H), 3.57 (d, J = 14.0 Hz, 1H), 3.10 – 2.95 (m, 3H), 3.02 (s, 6H) 2.90 – 2.73 (m, 2H), 2.49 – 2.37 (m, 2H), 1.93 (m, 1H), 1.82 – 1.71 (m, 5H), 1.61 – 1.51 (m, 1H), 1.51 – 1.38 (m, 1H). ¹³C{¹H}-NMR (100 MHz, CDCl₃) δ ppm: 160.2, 154.9, 149.2, 105.3, 105.1, 68.0, 63.7, 62.9, 55.2, 46.4, 39.2, 28.3, 24.9, 24.0. HRMS(ESI-MS) m/z calculated for C₁₆H₂₆N₄[M+H]⁺ 275.2230, found 275.2217.

Synthesis of (S,S') ^{Bz}PhP

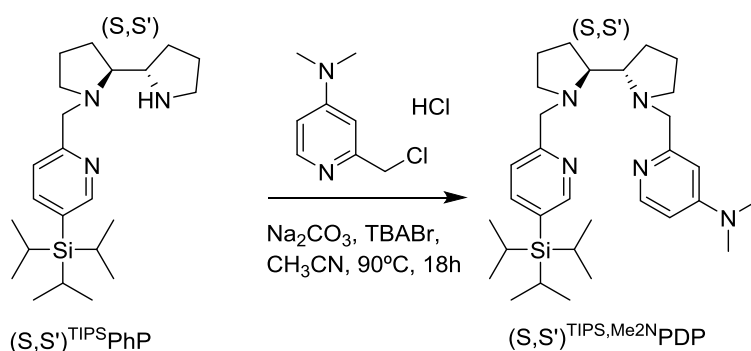
(S,S') ^{Bz}PhP was synthesized following a procedure analogous to (S,S') ^{TIPS}PhP (1.3 mmols, 84 % yield). ¹H-NMR (CDCl₃, 400 MHz, 300K) δ , ppm: 7.75 – 7.70 (m, 1H), 7.33 – 7.29 (m, 1H), 7.28 – 7.19 (m, 2H), 4.51 (d, $J = 13.6$ Hz, 1H), 3.88 (s, 3H), 3.77 (d, $J = 13.6$ Hz, 1H), 3.11 (q, $J = 7.4$ Hz, 1H), 2.97 – 2.89 (m, 1H), 2.89 – 2.77 (m, 2H), 2.71 – 2.62 (m, 1H), 2.48 (m, 1H), 1.98 – 1.88 (m, 1H), 1.79 – 1.62 (m, 5H), 1.55 (d, 1H), 1.46 – 1.33 (m, 1H). ¹³C{¹H}-NMR (100 MHz, CDCl₃) δ ppm: 153.0, 142.3, 136.2, 122.3, 121.7, 119.5, 109.0, 68.4, 63.3, 54.8, 53.3, 46.8, 30.0, 28.5, 28.0, 25.5, 23.4. HRMS(ESI-MS) m/z calculated for C₁₇H₂₄N₄[M+H]⁺ 285.2074, found 285.2072.

Synthesis of (S,S') ^{TIPS,dMM}PDP (L2).

(S,S') ^{TIPS,dMM}PDP (L2). 2-chloromethyl-4-methoxy-3,5-dimethylpyridine hydrochloride (62 mg, 0.28 mmol), (S,S) -2,2'-bipyrrrolidine (105.2 mg, 0.27 mmol) and anhydrous acetonitrile (15 mL) were mixed in a 25 mL flask. Na₂CO₃ (115 mg) and tetra-butylammonium bromide, TBABr (5 mg) were added directly as solids and the resulting mixture was heated at reflux under N₂ for 15 hours.

After cooling to room temperature, the resulting brown mixture was filtered and the filter cake was washed with CH_2Cl_2 . The combined filtrates were evaporated under reduced pressure. To the resulting residue, 1N NaOH (10 mL) was added and the mixture was extracted with CH_2Cl_2 (3 x 10 mL). The combined organic layers were dried over anhydrous MgSO_4 and the solvent was removed under reduced pressure. After, the residue was solved in *n*-hexane and stirred overnight. Finally, the solvent was decanted and removed under reduced temperature and purified by flash column chromatography to obtain 122 mg of yellow oil (0.23 mmol, yield 61 %). ^1H NMR (CDCl_3 , 400 MHz, 300K) δ , ppm: 8.58 (s, 1H), 8.16 (s, 1H), 7.73 (d, $J = 9.3$ Hz, 1H), 7.45 – 7.38 (d, $J = 7.7$ Hz, 1H), 4.15 (d, $J = 14.3$ Hz, 1H), 4.10 (d, $J = 12.0$ Hz, 1H), 3.75 (s, 3H), 3.52 – 3.40 (m, 2H), 3.07 – 2.99 (m, 1H), 2.81 – 2.73 (m, 2H), 2.27 (m, $J = 31.3$ Hz, 8H), 1.83 – 1.61 (m, 7H), 1.40 (m, 3H), 1.30 – 1.19 (m, 1H), 1.07 (d, $J = 7.1$ Hz, 18H), 0.99 – 0.78 (m, 1H). $^{13}\text{C}\{^1\text{H}\}$ -NMR (100 MHz, CDCl_3) δ ppm: 163.9, 154.5, 150.2, 148.3, 143.4, 127.5, 125.8, 125.0, 122.3, 120.5, 65.8, 65.3, 60.9, 60.3, 59.8, 55.4, 55.3, 29.7, 25.9, 23.9, 23.7, 18.48, 18.45, 18.41, 18.36, 13.3, 10.8, 10.6. HRMS(ESI-MS) m/z calculated for $\text{C}_{32}\text{H}_{52}\text{N}_4\text{OSi}[\text{M}+\text{H}]^+$ 537.3983, found 537.3980.

Synthesis of (S,S') ^{TIPS,Me2N}PDP (**L3**).

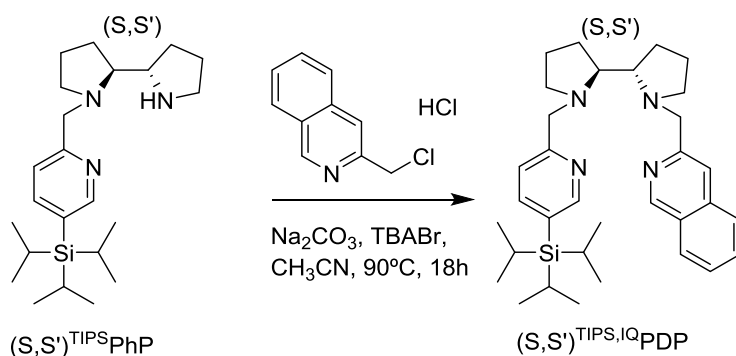


(S,S') ^{TIPS,Me2N}PDP (**L3**). It was prepared in analogous manner to (S,S') ^{TIPS,dMM}PDP to provide 91mg, (0.17 mmol, yield 59 %) of a yellow oil. ^1H -NMR (CDCl_3 , 400 MHz, 300K) δ , ppm: 8.54 (dd, $J = 1.7, 0.9$ Hz, 1H), 8.10 (d, $J = 6.1$ Hz, 1H), 7.68 (dd, $J = 7.7, 1.8$ Hz, 1H), 7.37 (d, $J = 7.7$ Hz, 1H), 6.75 – 6.59 (d, $J = 2.7$ Hz), 6.35 (dd, $J = 6.1, 2.7$ Hz, 1H), 4.24 (d, $J = 14.4$ Hz, 1H),

EXPERIMENTAL SECTION

4.13 (d, $J = 14.4$ Hz, 1H), 3.57 (d, $J = 14.5$ Hz, 1H), 3.52 (d, $J = 14.5$ Hz, 1H), 3.09 – 3.01 (m, 2H), 2.96 (s, 6H), 2.89 – 2.78 (m, 2H), 2.38 – 2.26 (m, 2H), 1.90 – 1.87 (m, 2H), 1.75 – 1.69 (m, 6H), 1.37 (dt, $J = 14.8, 7.5$ Hz, 3H), 1.05 (d, $J = 10.0$ Hz, 18H). $^{13}\text{C}\{^1\text{H}\}$ -NMR (100 MHz, CDCl_3) δ ppm: 159.9, 158.9, 155.1, 154.5, 147.9, 143.5, 129.5, 127.4, 122.2, 105.2, 105.1, 66.1, 61.5, 61.0, 55.3, 39.2, 26.4, 23.7, 23.7, 18.5, 10.6. HRMS(ESI-MS) m/z calculated for $\text{C}_{31}\text{H}_{51}\text{N}_5\text{Si}[\text{M}+\text{H}]^+$ 522.3986, found 522.4006.

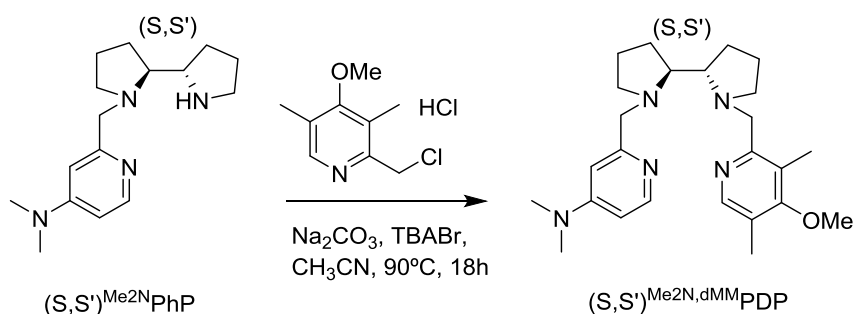
Synthesis of $(S,S)^{\text{TIPS,IQ}}\text{PDP}$ (**L4**).



$(S,S)^{\text{TIPS,IQ}}\text{PDP}$ (L4**).** It was prepared in analogous manner to **$(S,S)^{\text{dMM,TIPS}}\text{PDP}$** to provide 82.9 mg (0.16 mmol, yield 54 %) of a yellow oil. ^1H -NMR (CDCl_3 , 400 MHz, 300K) δ , ppm: 9.17 (s, 1H), 8.54 (s, 1H), 7.91 (d, $J = 8.2$ Hz, 1H), 7.76 (d, $J = 8.3$ Hz, 1H), 7.70 – 7.61 (m, 3H), 7.57 – 7.47 (m, 1H), 7.38 (d, $J = 7.7$ Hz, 1H), 4.38 (d, $J = 14.6$ Hz, 1H), 4.26 (d, $J = 14.4$ Hz, 1H), 3.69 (d, $J = 14.5$ Hz, 1H), 3.50 (d, $J = 14.3$ Hz, 1H), 3.12 (m, 1H), 3.05 (m, 1H), 2.86 (m, 2H), 2.35 – 2.20 (m, 2H), 1.88 – 1.68 (m, 9H), 1.36 (m, 4H), 1.04 (d, $J = 7.4$ Hz, 18H). $^{13}\text{C}\{^1\text{H}\}$ -NMR (100 MHz, CDCl_3) δ ppm: 160.42, 154.55, 153.57, 151.74, 143.30, 136.44, 130.14, 127.55, 127.46, 127.17, 126.49, 121.97, 118.36, 65.74, 61.43, 61.39, 61.37, 61.33, 61.11, 61.05, 60.99, 55.54, 55.39, 26.12, 23.60, 23.52, 18.44, 10.62. HRMS(ESI-MS) m/z calculated for $\text{C}_{33}\text{H}_{48}\text{N}_4\text{Si}[\text{M}+\text{H}]^+$ 529.3721, found 529.3717.

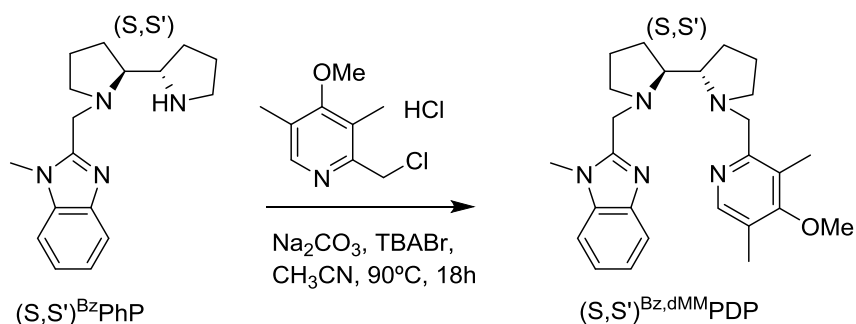
Synthesis of $(S,S)^{\text{Me}_2\text{N,DMM}}\text{PDP}$ (**L5**).

EXPERIMENTAL SECTION



$(S,S')^{\text{Me}_2\text{N,dMM}}\text{PDP}$ (L5). It was prepared in analogous manner to **$(S,S)^{\text{TIPS,dMM}}\text{PDP}$** to provide 140 mg (0.33 mmol, yield 86 %) of a yellow oil. $^1\text{H-NMR}$ (CDCl_3 , 400 MHz, 300K) δ , ppm: 8.14 (d, $J = 5.8$ Hz, 2H), 6.70 (d, $J = 2.7$ Hz, 1H), 6.37 (dd, $J = 6.0, 2.7$ Hz, 1H), 4.12 (d, $J = 12.0$ Hz, 1H), 4.00 (d, $J = 14.1$ Hz, 1H), 3.74 (s, 3H), 3.41 (d, $J = 14.2$ Hz, 1H), 3.38 (d, $J = 12.0$ Hz, 1H), 3.06 (d, $J = 17.5$ Hz, 1H), 3.00 (s, 6H), 2.79 – 2.70 (m, 3H), 2.31 (s, 3H), 2.26 (m, 2H), 2.23 (s, 3H), 1.82 – 1.61 (m, 7H). $^{13}\text{C}\{^1\text{H}\}\text{-NMR}$ (100 MHz, CDCl_3) δ ppm: 163.83, 160.21, 157.71, 154.89, 148.91, 148.25, 125.81, 124.85, 105.17, 65.63, 64.57, 61.25, 61.15, 60.53, 60.44, 59.72, 55.42, 55.35, 55.24, 39.10, 25.75, 24.04, 23.65, 13.23, 10.79. HRMS(ESI-MS) m/z calculated for $\text{C}_{25}\text{H}_{37}\text{N}_5\text{O}[\text{M}+\text{H}]^+$ 424.3071, found 424.3084.

Synthesis of **$(S,S')^{\text{Bz,dMM}}\text{PDP}$ (L6).**

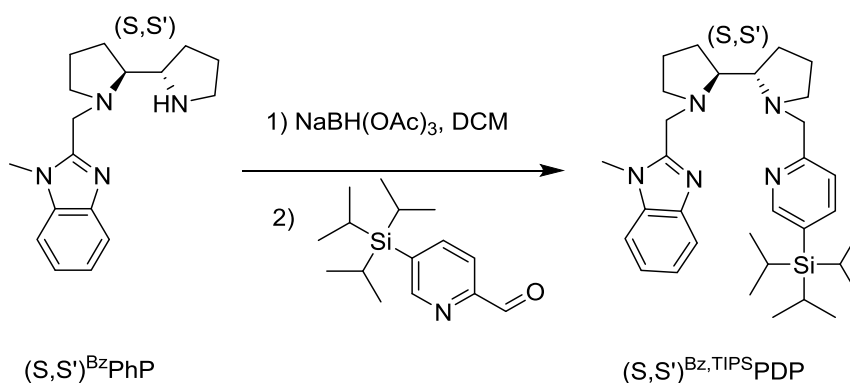


$(S,S')^{\text{Bz,dMM}}\text{PDP}$ (L6). It was prepared in analogous manner to **$(S,S)^{\text{TIPS,dMM}}\text{PDP}$** starting from **$(S,S)$ -2,2'-bipyrrrolidine** and **$^{\text{dMM}}\text{PyCH}_2\text{Cl} \cdot \text{HCl}$** to provide 84 mg (0.19 mmol, yield 77 %) of a yellow oil. Finally, the solvent was decanted and removed under reduced temperature to yield 307 mg of yellow oil (84 mg, 0.19 mmol, yield 77 %) $^1\text{H-NMR}$ (CDCl_3 , 400 MHz, 300K) δ , ppm: 8.13

EXPERIMENTAL SECTION

(s, 1H), 7.71 – 7.66 (m, 1H), 7.30 – 7.25 (m, 1H), 7.24 – 7.16 (m, 2H), 4.17 (d, $J = 13.3$ Hz, 1H), 3.99 (d, $J = 12.0$ Hz, 1H), 3.79 (s, 3H), 3.71 (s, 3H), 3.55 (d, $J = 12.0$ Hz, 1H), 3.48 (d, $J = 13.3$ Hz, 1H), 2.83 (m, 2H), 2.70 (m, 1H), 2.40 (m, 1H), 2.30 (s, 4H), 2.22 (s, 4H), 1.83 – 1.50 (m, 8H). $^{13}\text{C}\{^1\text{H}\}$ -NMR (100 MHz, CDCl_3) δ ppm: 163.9, 157.6, 152.7, 148.3, 148.3, 142.2, 136.2, 126.0, 125.1, 122.3, 121.7, 119.5, 65.5, 64.7, 60.8, 59.8, 55.7, 55.2, 52.4, 29.9, 26.3, 26.0, 24.2, 23.8, 13.2, 10.7. HRMS(ESI-MS) m/z calculated for $\text{C}_{26}\text{H}_{35}\text{N}_5\text{O}[\text{M}+\text{H}]^+$ 434.2914, found 434.2921.

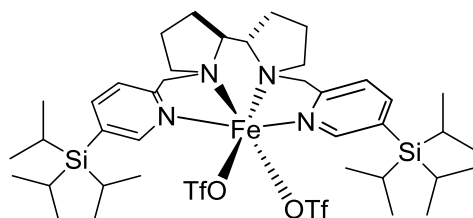
Synthesis of $(S,S')^{\text{Bz,TIPSPDP}}$ (**L7**).



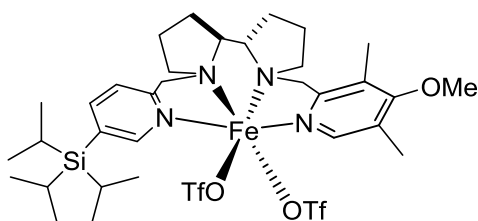
$(S,S')^{\text{Bz,TIPSPDP}}$ (L7**).** $(S,S')^{\text{BzPhP}}$ (233 mg, 0.8 mmol) were dissolved in CH_2Cl_2 (10 mL) and cooled to 0 °C, and 1.3 equiv of $\text{NaBH}(\text{AcO})_3$ (224 mg, 1.05 mmol) were added to the reaction mixture, which was stirred for 30 min at 0 °C. TIPSPyCHO (214 mg, 0.8 mmol) was added at this point, and the crude was stirred at room temperature overnight. It was then extracted with 40 mL of a NaHCO_3 aqueous saturated solution. The aqueous layer was washed with CH_2Cl_2 (2x 40 mL). The combined organic letters were dried over MgSO_4 and under vacuum. The product was purified by alumina column chromatography eluting with DCM , MeOH , NH_3 (95:4:1) to afford 250 mg of a white solid (0.47 mmol, 58%) ^1H -NMR (CDCl_3 , 400 MHz, 300K) δ , ppm: 8.57 (s, 1H), 7.71 (m, 2H), 7.37 (d, $J = 7.7$ Hz, 1H), 7.31 – 7.20 (m, 3H), 4.23 (d, $J = 13.3$ Hz, 1H), 4.13 (d, $J = 14.3$ Hz, 1H), 3.82 (s, 3H), 3.65 (d, $J = 13.3$ Hz, 1H), 3.54 (d, $J = 14.3$ Hz, 1H), 3.05 (m, 1H), 2.87 (m, 1H), 2.81 – 2.69 (m, 2H), 2.31 (m, 2H), 1.84 – 1.60 (m, 8H), 1.39 (p, $J = 7.5$ Hz, 3H), 1.06 (dd, $J = 7.5, 1.9$ Hz, 18H). $^{13}\text{C}\{^1\text{H}\}$ -NMR (100 MHz, CDCl_3) δ ppm: 160.13, 154.65, 152.56, 143.38, 142.24, 136.24, 127.48, 122.32, 122.08, 121.74, 119.60, 108.96, 65.78, 64.81,

61.08, 61.03, 60.96, 55.34, 52.59, 52.53, 52.46, 30.08, 30.00, 29.92, 29.83, 25.93, 25.88, 23.93, 23.47, 18.46, 10.63. HRMS(ESI-MS) m/z calculated for $C_{32}H_{49}N_5Si[M+H]^+$ 532.3830, found 532.3825

2.3) Synthesis of iron complexes

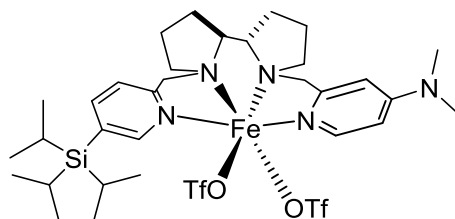


$((S,S')-[Fe(CF_3SO_3)_2(TipsPDP)] (Tips1Fe)$. A suspension of $Fe(CF_3SO_3)_2(CH_3CN)_2$ (101,8 mg, 0.23 mmol) in anhydrous THF (1 mL) was added dropwise to a vigorously stirred solution of $(S,S')^{Tips}PDP$ (150.0 mg, 0.23 mmol) in THF (1 mL). After a few seconds the solution became cloudy and a yellow precipitate appeared. After stirring for 1 hour the solution was filtered off and the resultant yellow solid dried under vacuum. This solid was solved in CH_2Cl_2 (3 mL) and the solution filtered off through celite©. Slow diethyl ether diffusion over the resultant solution afforded, in a few days, 148 mg of yellow solid (0.15 mmol, yield 64 %). Anal. Calcd. for $C_{40}H_{66}F_6FeN_4O_6S_2Si_2$ (MW = 989.11 g/mol): N, 5.66; C, 48.57; H 6.73%. Found: N, 5.64; C, 48.61; H 6.79%. 1H -NMR (400 MHz, CD_2Cl_2 , 300K) δ , ppm: 178 (s), 123 (s), 77 (s), 51 (s), 29.0 (s), 27.0 (s), 17.8-16.0 (m), 2.1-0.73 (m), -9.9 (s), -17.7 (s). HRMS (ESI-TOF, $[M - 2OTf]^+$): m/z calcd for $C_{38}H_{66}FeN_4Si_2$ 345.2088, found 345.2095.

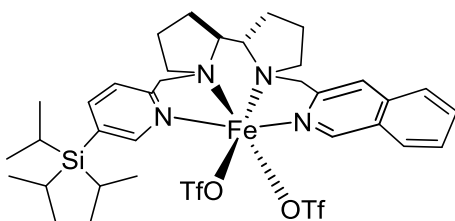


$(S,S')-[Fe(CF_3SO_3)_2(TIPS,dMM)PDP]$ (2Fe) was prepared in analogous manner to $(S,S')-[Fe(CF_3SO_3)_2(TipsPDP)]$, starting from $((S,S')^{TIPS,dMM}PDP)$ (L2) and $Fe(CF_3SO_3)_2(CH_3CN)_2$ to obtain the product as a yellow crystals (0.07 mmol,

yield 64 %). Anal. Calcd for $C_{34}H_{52}F_6FeN_4O_7S_2Si \cdot \frac{1}{2} CH_2Cl_2$: C, 44.41; H, 5.72; N, 6.00 %. Found: C, 44.71; H, 5.85; N, 6.17 %. FT-IR (ATR) ν , cm^{-1} : 2963 – 2945 (C-H) sp^3 , 2460, 2364, 1301, 1213, 1165, 1027, 635. 1H -NMR (CD_2Cl_2 , 400 MHz, 300K) δ , ppm: 177 (s), 169 (s), 126 (s), 110 (s), 85.9 (s), 67.8 (s), 46.7 (s), 32.9 (s), 29.7 (s), 22.5 (s), 9.9 (s), -7.1 (s), -9.8 (s), -18.2 (s), -21.1 (s). ESI-HRMS calcd. for $C_{33}H_{52}N_4SiFeF_3SO_4$ [M-OTf] $^+$: 741.2775, found: 741.2788.



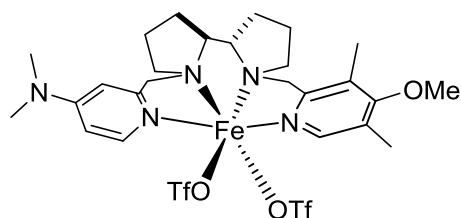
(S,S')-[Fe(CF₃SO₃)₂(^{TIPS,Me2N}PDP)] (3Fe) was prepared in analogous manner to **(S,S')-[Fe(CF₃SO₃)₂(^{TIPS}PDP)]**, starting from **((S,S')^{TIPS,Me2N}PDP) (L3)** and $Fe(CF_3SO_3)_2(CH_3CN)_2$ to obtain the product as a yellow solid (40.7 mg, 0.04 mmol, yield 39%). Anal. Calcd for $C_{33}H_{51}F_6FeN_5O_6S_2Si$: C, 45.26; H, 5.87; N, 8.00 %. Found: C, 45.35; H, 5.66; N, 7.95 %. FT-IR (ATR) ν , cm^{-1} : 2949 – 2864 (C-H) sp^3 , 2260, 2335, 1620, 1297, 1217, 1166, 1037, 882, 683. 1H -NMR (CD_2Cl_2 , 400 MHz, 300K) δ , ppm: 179.9 (s), 168.5 (s), 87.6 (s), 74.4 (s), 45.5 (s), 40.9 (s), 34.7 (s), 29.8 (s), 12.4 (s), -10.4 (s), -28.8 (s). ESI-HRMS calcd. for $C_{31}H_{51}N_5SiFeF_3SO_3$ [M-OTf] $^+$: 726.2778, found: 726.2770.



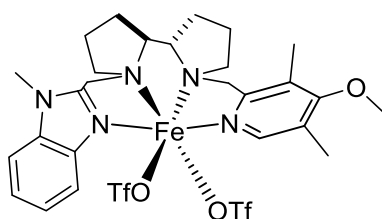
(S,S')-[Fe(CF₃SO₃)₂(^{TIPS,IQ}PDP)] (4Fe) was prepared in analogous manner to **(S,S')-[Fe(CF₃SO₃)₂(^{TIPS}PDP)]**, starting from **((S,S')^{TIPS,IQ}PDP) (L4)** and $Fe(CF_3SO_3)_2(CH_3CN)_2$ to obtain the product as a yellow solid (60.3 mg, 0.07 mmol, yield 43%). Anal. Calcd for $C_{35}H_{48}F_6FeN_4O_6S_2Si \cdot \frac{1}{2} CH_2Cl_2$: C, 46.09; H, 5.34; N, 6.06 %. Found: C, 46.35; H, 5.26; N, 6.28 %. FT-IR (ATR) ν , cm^{-1} : 2947 – 2867 (C-H) sp^3 , 2260, 2335, 1304, 12212, 1160, 1027, 696. 1H -NMR

EXPERIMENTAL SECTION

(CD₂Cl₂, 400 MHz, 300K) δ , ppm: 188.9 (s), 177.9 (s), 152.5 (s), 118.6 (s), 84.8 (s), 72.1 (s), 51.5 (s), 46.6 (s), 30.3 (s), 29.0 (s), 26.1 (s), 14.2 (s), -10. (s), -17.4 (s). ESI-HRMS calcd. for C₃₄H₄₈N₄SiFeF₃SO₃ [M-OTf]⁺: 733.2513, found: 733.2491.

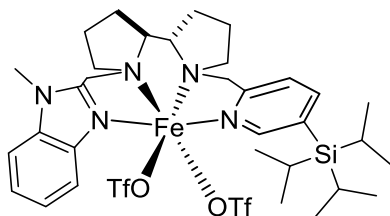


(S,S')-[Fe(CF₃SO₃)₂(^{Me2N,dMM}PDP)] (**5Fe**) was prepared in analogous manner to **(S,S')**-[Fe(CF₃SO₃)₂(^{Tips}PDP)], starting from **((S,S')**^{Me2N,dMM}PDP) (**L5**) and Fe(CF₃SO₃)₂(CH₃CN)₂ to obtain the product as a yellow solid (64.3 mg, 0.08 mmol, yield 76%). Anal. Calcd for C₂₇H₃₇F₆FeN₅O₇S₂·1/2 CH₂Cl₂: C, 40.28; H, 4.67; N, 8.54 %. Found: C, 40.21; H, 4.65; N, 8.24 %. FT-IR (ATR) ν , cm⁻¹: 2961 – 2935 (C-H)sp³, 220, 1618, 1298, 1219, 1156, 1033, 1011, 633. ¹H-NMR (CD₂Cl₂, 400 MHz, 300K) δ , ppm: 180.3 (s), 157.6 (s), 104.4 (s), 95.5 (s), 63.8 (s), 43.2 (s), 40.4 (s), 37.6 (s), 36.1 (s), 30.3 (s), -8.3 (s), -30.8 (s). ESI-HRMS calcd. for C₂₆H₃₇F₃FeN₅O₄S [M-OTf]⁺: 628.1863, found: 628.1842.



(S,S')-[Fe(CF₃SO₃)₂(^{BZ,dMM}PDP)] (**6Fe**) was prepared in analogous manner to **(S,S')**-[Fe(CF₃SO₃)₂(^{Tips}PDP)], starting from **((S,S')**^{BZ,dMM}PDP) (**L6**) and Fe(CF₃SO₃)₂(CH₃CN)₂ to obtain the product as a yellow solid (45.8 mg, 0.06 mmol, yield 64%). Anal. Calcd for C₂₈H₃₅F₆FeN₅O₇S₂·1/2 CH₂Cl₂: C, 41.24; H, 4.37; N, 8.43 %. Found: C, 41.51; H, 4.35; N, 8.6 %. FT-IR (ATR) ν , cm⁻¹: 3454, 2971 (C-H)sp³, 2360, 2334, 1458, 1300, 1219 1159, 1031, 747, 633. ¹H-NMR

(CD₂Cl₂, 400 MHz, 300K) δ , ppm: 148.9 (s), 130.8 (s), 116.3 (s), 83.0 (s), 75.4 (s), 41.8 (s), 37.1 (s), 29.0 (s), 14.6 (s), -11.2 (s), -32.3 (s). ESI-HRMS calcd. for C₂₇H₃₅N₅FeF₃SO₄ [M-OTf]⁺: 638.1706, found: 638.1719.



(S,S)-[Fe(CF₃SO₃)₂(^{Bz,TIPDS}PDP)] (7Fe) was prepared in analogous manner to **(S,S')-[Fe(CF₃SO₃)₂(^{TIPDS}PDP)]**, starting from **((S,S')^{Bz,TIPDS}PDP) (L7)** and Fe(CF₃SO₃)₂(CH₃CN)₂ to obtain the product as a yellow solid (93.8 mg, 0.1 mmol, yield 87%). Anal. Calcd for C₃₄H₄₉F₆FeN₅O₆S₂Si: C, 46.1; H, 5.58; N, 7.91 %. Found: C, 46.20; H, 5.35; N, 7.91 %. FT-IR (ATR) ν , cm⁻¹: 2946 – 2867 (C-H)sp³, 2365, 2354, 1457, 1212, 1161, 1025, 634. ¹H-NMR (CD₂Cl₂, 400 MHz, 300K) δ , ppm: 163.9 (s), 128.4 (s), 87.5 (s), 72.6 (s), 37.4 (s), 28.9 (s), 28.0 (s), 15.9 (s), -12.3 (s), -26.9 (s). ESI-HRMS calcd. for C₃₃H₄₉N₅SiFeF₃SO₃ [M-OTf]⁺: 736.2622, found: 736.2634.

3) Catalytic studies

Hydrogen peroxide solutions employed in the reactions were prepared by diluting commercially available hydrogen peroxide (32% or 50% H₂O₂ solution in water, Aldrich) in acetonitrile (1:1 v:v). Olefin substrates were purchased from Aldrich and TCl, with the maximum purity available, and used as received.

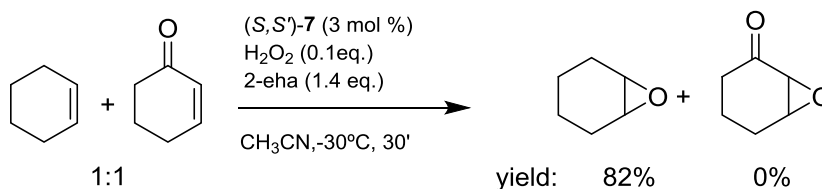
3.1) General Procedure for epoxide isolation (Figure 11, 12 and scheme 40)

An acetonitrile solution (7 mL) of an specific olefin (0.726 mmol, final reaction concentration 0.10 M) and **(S,S')-[Fe(OTf)₂(^{Bz,TIPDS}PDP)] (7Fe)** (19. mg, 21.7 μ mol, final reaction concentration 3.1 mM) was prepared in a vial (30 mL) equipped with a stir bar and cooled in an acetonitrile frozen bath. A 162 μ L of 2-ethylhexanoic acid (1 mmol, 1.4 eq.) was added directly to the solution Then, 1 mL of 9:1 v:v acetonitrile:hydrogen peroxide solution 50% (2.2 equiv.1.6 mmol) was added by syringe pump over a period of 30 min. The solution was

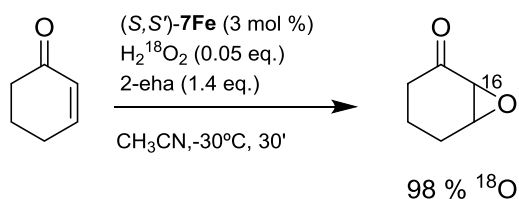
further stirred at -30 °C for 30 minutes. At this point, 30 mL of an aqueous NaHCO₃ saturated solution were added to the mixture. The resultant solution was extracted with CH₂Cl₂ (3 x 10 mL). Organic fractions were combined, dried over MgSO₄, filtered through a silica gel and alumina plugs, and the solvent was removed under reduced pressure to afford the epoxide product. This residue was purified by silica gel column to obtain the pure epoxide (Hexane/AcOEt : 96/4).

In the case of **(S,S')-[Fe(OTf)₂(^{Me2N}PDP)] (^{Me2N}1Fe)** the catalyst loading are 2 mol % (11. mg, 14.5 μmol).

4) Competition studies (Scheme 39)



An acetonitrile solution (750 μL) of 2-cyclohexenone (**S1**) (0.041 mmol), cyclohexene (**S30**) (0.041 mmol) and **(S,S')-7Fe** (1.8 mg, 2.0 μmol, final reaction concentration 2.7 mM) was prepared in a vial (10 mL) equipped with a stir bar and cooled in an acetonitrile frozen bath. A 19 μL (neat, 1.4 equiv. 0.12 mmols) of 2-ethylhexanoic acid was added directly to the solution. Then, 5 μL of 9:1 v:v acetonitrile:hydrogen peroxide solution 50% (0.1 eq.) was added by syringe pump over a period of 30 min. The solution was further stirred at -30 °C for further 30 minutes. At this point, an internal standard (biphenyl) was added and the solution was quickly filtered through a basic alumina plug, which was subsequently rinsed with 2 x 1 mL AcOEt. GC analysis of the solution provided substrate conversions and product yields relative to the internal standard integration. Products were identified by comparison to the GC retention time of authentic samples, and by their GC-MS spectrum.

5) ^{18}O labeling studies (Scheme 39)

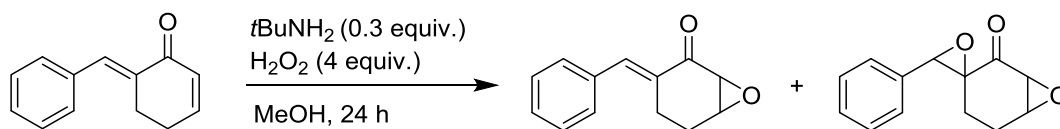
Regular epoxide

m/z	%
127.8	35.7
129.1	71.1
130.1	2963.7
131	217
132	82.3
133	6.7
133.9	3.6

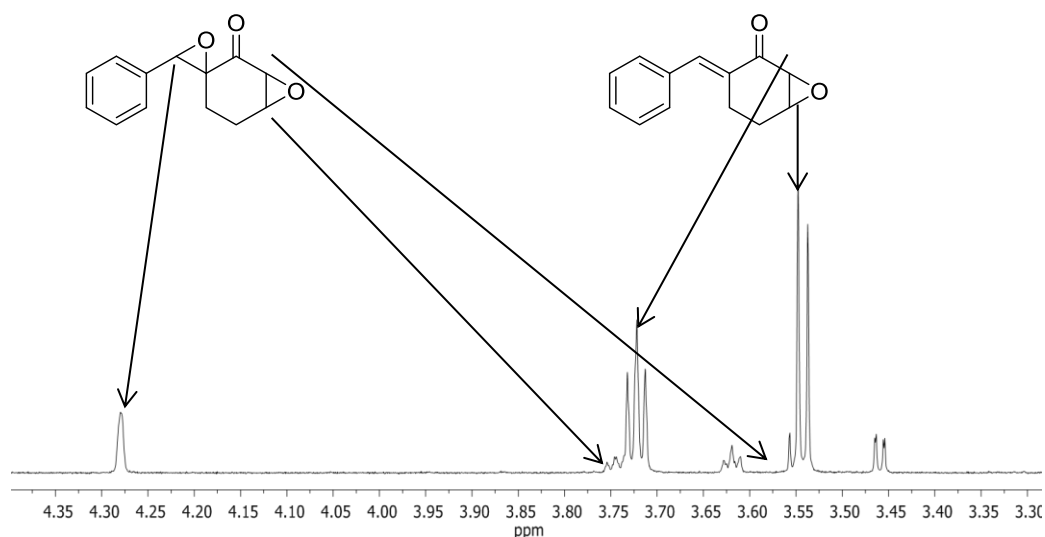
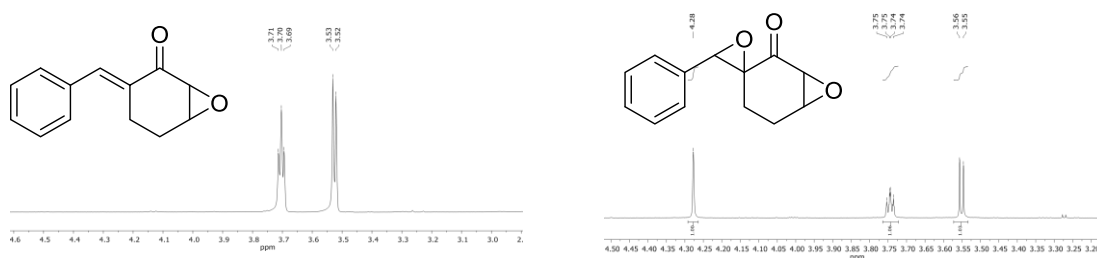
Epoxide obtained from the $\text{H}_2^{18}\text{O}_2$ experiment

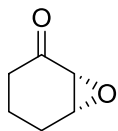
m/z	%
128	21
129	492.3
130	220.7
131	104.2
132	2147.3
133	177.8
134	83

An acetonitrile solution (0.5 mL) of 2-cyclohexenone (**S1**) (0.08 M, 0.041 mmols) and (S,S) -**7Fe** (2.5 mM, 1.25 μmol s) was prepared in a vial (10 mL) equipped with a stir bar cooled at -30°C , in an acetonitrile/ $\text{N}_2(\text{liq})$ bath. A 9.5 μL (neat, 1.4 eq. 0.06 mmols) of 2-ethylhexanoic acid was added directly to the solution. Then, 8 μL of 1:1 v:v acetonitrile:hydrogen peroxide solution 2% $\text{H}_2^{18}\text{O}_2$ (90% ^{18}O -isotopic content) in water (0.05 equiv.) was added by syringe pump over a period of 30 min. The solution was further stirred at -30°C for further 30 minutes. At this point, solution was quickly filtered through a basic alumina plug, which was subsequently rinsed with 2 x 1 mL AcOEt. At this point, the epoxide product was analyzed by GC-MS-Cl using ammonia as the ionization gas. Simulation of the isotopic pattern yields 0.4% ^{18}O -incorporation into the epoxide product.

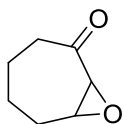
6) Catalysis with H₂O₂ and *t*BuNH₂ (Scheme 40)

The dienone **S32** (100 mg, 0.54 mmol) and *tert*-butyl amine (17 μ L, 0.016 mmol) were dissolved in methanol (2 mL) and 30% aqueous hydrogen peroxide solution (223 μ L, 2.16 mmol) was added. After stirring overnight, the reaction mixture was evaporated under reduced pressure and then we added dichloromethane (2 X 2 mL) and brine solution (1 mL) and the organic layers was separated and filtered through magnesium sulfate plug and the solvent was evaporated under reduced pressure to obtain the crude product. Purification by flash column chromatography afforded epoxide products. Total yield 71 % (59 % epoxide at cyclic aliphatic enone, 6 % of diepoxide product and 6 % of a third non identified product).

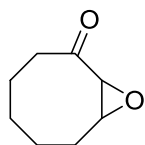
¹H-NMR of crude reaction¹H-NMR of isolated products

5) Characterization of isolated epoxide products

E2, colorless oil; (75% yield, 90% ee); $^1\text{H-NMR}$ (CDCl_3 , 300 MHz, 300K) δ , ppm: 3.62 – 3.56 (m, 1H), 3.22 (d, $J = 3.9$ Hz, 1H), 2.54 (dt, $J = 17.4, 4.9$ Hz, 1H), 2.31 – 2.22 (m, 1H), 2.08 (m, 1H), 1.99 – 1.89 (m, 2H), 1.73 – 1.63 (m, 1H). $^{13}\text{C}\{^1\text{H}\}$ -NMR (100 MHz, CDCl_3) δ ppm: 205.9, 55.9, 55.1, 36.3, 22.8, 17.0. HRMS(ESI+) m/z calculated for $\text{C}_{16}\text{H}_8\text{O}_2\text{Na}$ $[\text{M}+\text{Na}]^+$ 135.0417, found 135.0418. Chiral GC analysis with CYCLOSIL-B.

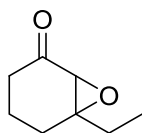


E3, colorless oil; (66% yield, 84% ee); $^1\text{H-NMR}$ (CDCl_3 , 400 MHz, 300K) δ , ppm: 3.45 – 3.32 (m, 2H), 2.72 – 2.59 (m, 1H), 2.53 – 2.40 (m, 1H), 2.38 – 2.27 (m, 1H), 1.90 – 1.68 (m, 4H), 1.07 – 0.95 (m, 2H). $^{13}\text{C}\{^1\text{H}\}$ -NMR (100 MHz, CDCl_3) δ ppm: 210.2, 59.4, 55.1, 40.5, 27.4, 23.5, 22.9. HRMS(ESI+) m/z calculated for $\text{C}_7\text{H}_{10}\text{O}_2\text{Na}$ $[\text{M}+\text{Na}]^+$ 149.0573, found 149.0573. Chiral GC analysis with CYCLOSIL-B.

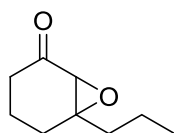


E4, white solid; (99% yield, 81% ee); $^1\text{H-NMR}$ (CDCl_3 , 400 MHz, 300K) δ , ppm: 3.77 (d, $J = 5.1$ Hz, 1H), 3.28 (ddd, $J = 9.8, 5.1, 3.7$ Hz, 1H), 2.70 (m, 1H), 2.38 (m, 1H), 2.28 – 2.17 (m, 1H), 1.94 (m, 1H), 1.81 – 1.67 (m, 2H), 1.61 – 1.43 (m, 3H), 1.09 – 0.99 (m, 1H). $^{13}\text{C}\{^1\text{H}\}$ -NMR (100 MHz, CDCl_3) δ ppm: 207.6, 58.8, 55.9, 42.8, 27.0, 24.7, 24.5, 24.5. HRMS(ESI+) m/z calculated for $\text{C}_8\text{H}_{12}\text{O}_2\text{Na}$ $[\text{M}+\text{Na}]^+$ 163.0730, found 163.0730. Chiral GC analysis with CYCLOSIL-B.

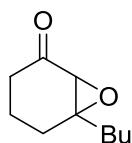
EXPERIMENTAL SECTION



E10, colorless oil; (81% yield, 70% ee); $^1\text{H-NMR}$ (CDCl_3 , 400 MHz, 300K) δ , ppm: 3.09 (s, 1H), 2.51 (dt, $J = 17.5, 4.9$ Hz, 1H), 2.18 – 1.85 (m, 4H), 1.79 – 1.64 (m, 3H), 0.98 (t, $J = 7.5$ Hz, 3H). $^{13}\text{C}\{^1\text{H}\}$ -NMR (100 MHz, CDCl_3) δ ppm: 207.0, 66.1, 60.8, 36.0, 28.8, 26.1, 17.4, 8.6. HRMS(ESI+) m/z calculated for $\text{C}_8\text{H}_{12}\text{O}_2\text{Na}$ $[\text{M}+\text{Na}]^+$ 163.0730, found 163.0732. Chiral GC analysis with CYCLOSIL-B.

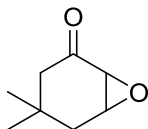


E11, colorless oil; (75% yield, 82% ee); $^1\text{H NMR}$ (CDCl_3 , 400 MHz, 300K) δ ppm 3.08 (s, 1H), 2.51 (dt, $J = 17.5, 4.7$ Hz, 1H), 2.16 – 1.84 (m, 4H), 1.73 – 1.57 (m, 3H), 1.51 – 1.39 (m, 2H), 0.94 (t, $J = 7.3$ Hz, 3H). $^{13}\text{C NMR}$ (101 MHz, CDCl_3) δ 207.0, 65.3, 61.2, 38.0, 36.0, 26.4, 18.0, 17.4, 14.0. HRMS(ESI+) m/z calculated for $\text{C}_9\text{H}_{14}\text{O}_2\text{Na}$ $[\text{M}+\text{Na}]^+$ 177.0886, found 177.0882. Chiral GC analysis with CYCLOSIL-B.

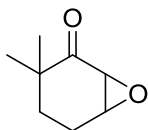


E12, colorless oil; (80% yield, 84% ee); $^1\text{H-NMR}$ (CDCl_3 , 400 MHz, 300K) δ , ppm: 3.03 (s, 1H), 2.46 (dt, $J = 16.7, 4.5$ Hz, 1H), 2.11 – 1.78 (m, 4H), 1.72 – 1.52 (m, 3H), 1.41 – 1.24 (m, 4H), 0.87 (t, $J = 7.2$ Hz, 3H). $^{13}\text{C}\{^1\text{H}\}$ -NMR (100 MHz, CDCl_3) δ ppm: 206.9, 65.4, 61.2, 35.9, 35.7, 26.7, 26.4, 22.6, 17.3, 13.9. HRMS(ESI+) m/z calculated for $\text{C}_{10}\text{H}_{16}\text{O}_2\text{Na}$ $[\text{M}+\text{Na}]^+$ 191.1043, found 191.1041. Chiral GC analysis with CYCLOSIL-B.

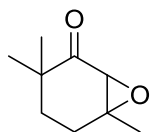
EXPERIMENTAL SECTION



E14, colorless oil; (63% yield, 90% ee); $^1\text{H-NMR}$ (CDCl_3 , 400 MHz, 300K) δ , ppm: 3.52 (t, $J = 4.2$ Hz, 1H), 3.21 (d, $J = 4.6$ Hz, 1H), 2.66 (d, $J = 13.8$ Hz, 1H), 2.04 (d, $J = 15.5$ Hz, 1H), 1.88 – 1.79 (m, 2H), 1.03 (s, 3H), 0.93 (s, 3H). $^{13}\text{C}\{^1\text{H}\}$ -NMR (100 MHz, CDCl_3) δ ppm: 207.5, 57.0, 54.6, 48.6, 37.3, 37.2, 31.0, 28.0. HRMS(ESI+) m/z calculated for $\text{C}_8\text{H}_{12}\text{O}_2\text{Na}$ $[\text{M}+\text{Na}]^+$ 163.0730., found 163.0738. Chiral GC analysis with CYCLOSIL-B.

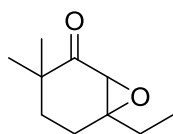


E15, colorless oil; (72% yield, 92% ee); $^1\text{H-NMR}$ (CDCl_3 , 400 MHz, 300K) δ , ppm: 3.59 – 3.51 (m, 1H), 3.19 (d, $J = 3.7$ Hz, 1H), 2.26 – 2.13 (m, 1H), 2.07 – 1.95 (m, 1H), 1.88 (td, $J = 13.2, 4.4$ Hz, 1H), 1.38 – 1.29 (m, 1H), 1.12 (s, 3H), 1.02 (s, 3H). $^{13}\text{C}\{^1\text{H}\}$ -NMR (100 MHz, CDCl_3) δ ppm: 209.5, 54.5, 53.5, 41.8, 29.2, 25.4, 25.0, 20.4. HRMS(ESI+) m/z calculated for $\text{C}_8\text{H}_{12}\text{O}_2\text{Na}$ $[\text{M}+\text{Na}]^+$ 163.0730., found 163.0739. Chiral GC analysis with astec CHIRALDEX G-TA.

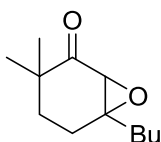


E16, colorless oil; (85% yield, 90% ee); $^1\text{H-NMR}$ (CDCl_3 , 400 MHz, 300K) δ , ppm: δ 3.00 (s, 1H), 2.03 – 1.80 (m, 3H), 1.41 (s, 3H), 1.33 – 1.25 (m, 1H), 1.07 (s, 3H), 0.97 (s, 3H). $^{13}\text{C}\{^1\text{H}\}$ -NMR (100 MHz, CDCl_3) δ ppm: 210.5, 61.0, 60.5, 41.0, 30.7, 26.0, 25.7, 25.0, 21.7. HRMS(ESI+) m/z calculated for $\text{C}_9\text{H}_{14}\text{O}_2\text{Na}$ $[\text{M}+\text{Na}]^+$ 177.0886, found 177.0881. Chiral GC analysis with astec CHIRALDEX G-TA.

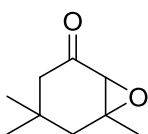
EXPERIMENTAL SECTION



E17, colorless oil; (65% yield, 95% ee); $^1\text{H-NMR}$ (CDCl_3 , 400 MHz, 300K) δ , ppm: 3.06 (s, 1H), 2.06 – 1.95 (m, 2H), 1.94 – 1.85 (m, 1H), 1.80 – 1.62 (m, 2H), 1.39 – 1.32 (m, 1H), 1.11 (s, 3H), 1.01 (s, 4H), 0.98 (d, $J = 8.8$ Hz, 2H). $^{13}\text{C}\{^1\text{H}\}$ -NMR (100 MHz, CDCl_3) δ ppm: 210.8, 64.6, 59.3, 41.4, 30.6, 28.3, 25.7, 25.1, 23.5, 8.7. HRMS(ESI+) m/z calculated for $\text{C}_{10}\text{H}_{16}\text{O}_2\text{Na}$ $[\text{M}+\text{Na}]^+$ 191.1043, found 191.1046. Chiral GC analysis with astec CHIRALDEX G-TA.



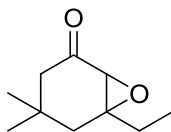
E18, colorless oil; (74% yield, 95% ee); $^1\text{H-NMR}$ (CDCl_3 , 400 MHz, 300K) δ , ppm: 3.02 (s, 1H), 2.04 – 1.82 (m, 3H), 1.75 – 1.66 (m, 1H), 1.63 – 1.53 (m, 1H), 1.41 – 1.30 (m, 5H), 1.09 (s, 3H), 0.98 (s, 3H), 0.89 (t, $J = 7.2$ Hz, 3H). $^{13}\text{C}\{^1\text{H}\}$ -NMR (100 MHz, CDCl_3) δ ppm: 210.8, 63.9, 59.8, 41.3, 35.2, 30.6, 26.8, 25.7, 25.0, 23.8, 22.6, 13.9. HRMS(ESI+) m/z calculated for $\text{C}_{12}\text{H}_{20}\text{O}_2\text{Na}$ $[\text{M}+\text{Na}]^+$ 219.1356, found 219.1354. Chiral GC analysis with CYCLOSIL-B.



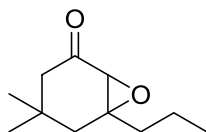
E19, colorless oil; (71% yield, 89% ee); $^1\text{H-NMR}$ (CDCl_3 , 400 MHz, 300K) δ , ppm: 3.04 (s, 1H), 2.61 (dd, $J = 13.3, 0.8$ Hz, 1H), 2.07 (dt, $J = 14.9, 0.8$ Hz, 1H), 1.80 (ddd, $J = 13.3, 2.2, 1.1$ Hz, 1H), 1.68 (dd, $J = 14.9, 2.2$ Hz, 1H), 1.41 (s, 3H), 1.01 (s, 3H), 0.90 (s, 3H). $^{13}\text{C}\{^1\text{H}\}$ -NMR (100 MHz, CDCl_3) δ ppm: 208.0, 64.3, 61.5, 48.02, 42.8, 36.2, 30.8, 27.9, 24.1. HRMS(ESI+) m/z

EXPERIMENTAL SECTION

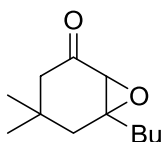
calculated for $C_9H_{14}O_2Na$ $[M+Na]^+$ 177.0886, found 177.0880. Chiral GC analysis with CYCLOSIL-B.



E20, colorless oil; (82% yield, 85% ee); 1H -NMR ($CDCl_3$, 400 MHz, 300K) δ , ppm: 3.00 (s, 1H), 2.60 (d, $J = 13.2$ Hz, 1H), 1.98 (d, $J = 14.9$ Hz, 1H), 1.76 (ddd, $J = 13.2, 2.2, 1.1$ Hz, 1H), 1.72 – 1.60 (m, 2H), 1.57 – 1.45 (m, 1H), 0.98 (s, 3H), 0.93 (t, $J = 7.5$ Hz, 3H), 0.85 (s, 3H) $^{13}C\{^1H\}$ -NMR (100 MHz, $CDCl_3$) δ ppm: 208.1, 68.0, 60.3, 48.2, 40.79, 36.2, 30.9, 30.4, 27.6, 8.9. HRMS(ESI+) m/z calculated for $C_{10}H_{16}O_2Na$ $[M+Na]^+$ 191.1043, found 191.1046. Chiral GC analysis with CYCLOSIL-B.



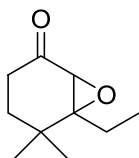
E21, colorless oil; (78% yield, 91% ee); 1H -NMR ($CDCl_3$, 400 MHz, 300K) δ , ppm: 3.01 (s, 1H), 2.61 (d, $J = 13.2$ Hz, 1H), 1.99 (d, $J = 14.9$ Hz, 1H), 1.82 – 1.68 (m, 2H), 1.67 – 1.54 (m, 1H), 1.54 – 1.36 (m, 3H), 1.00 (s, 3H), 0.92 (t, $J = 7.2$ Hz, 3H), 0.87 (s, 3H). $^{13}C\{^1H\}$ -NMR (100 MHz, $CDCl_3$) δ ppm: 208.1, 67.2, 60.6, 48.2, 41.0, 39.7, 36.2, 30.9, 27.7, 18.2, 14.03. HRMS(ESI+) m/z calculated for $C_{11}H_{18}O_2Na$ $[M+Na]^+$ 205.1199, found 205.1200. Chiral GC analysis with astec CHIRALDEX G-TA.



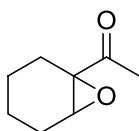
E22, colorless oil; (73% yield, 85% ee); 1H -NMR ($CDCl_3$, 400 MHz, 300K) δ , ppm: 3.02 (s, 1H), 2.66 – 2.58 (m, 1H), 2.01 (d, $J = 14.9$ Hz, 1H), 1.84 – 1.69

EXPERIMENTAL SECTION

(m, 2H), 1.65 – 1.60 (m, 1H), 1.52 – 1.46 (m, 1H), 1.41 – 1.28 (m, 4H), 1.01 (s, 3H), 0.91 – 0.88 (m, 6H). $^{13}\text{C}\{^1\text{H}\}$ -NMR (100 MHz, CDCl_3) δ ppm: 24, 67.4, 60.7, 48.3, 41.1, 37.4, 36.3, 31.0, 27.7, 27.0, 22.6, 13.9. HRMS(ESI+) m/z calculated for $\text{C}_{12}\text{H}_{20}\text{O}_2\text{Na}$ $[\text{M}+\text{Na}]^+$ 219.1356, found 219.1352. Chiral GC analysis with CYCLOSIL-B.

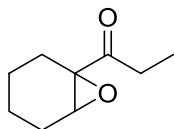


E23, colorless oil; (35% yield, 92% ee); ^1H -NMR (CDCl_3 , 400 MHz, 300K) δ , ppm: 3.22 (s, 1H), 2.41 (ddd, $J = 19.1, 7.3, 2.1$ Hz, 1H), 2.26 (m, 1H), 2.17 – 2.04 (m, 1H), 1.89 (m, 2H), 1.27 (ddd, $J = 13.5, 7.3, 2.0$ Hz, 1H), 1.16 (s, 3H), 1.06 (s, 3H), 0.81 (t, $J = 7.5$ Hz, 3H). ^{13}C NMR (101 MHz, CDCl_3) δ 208.0, 70.8, 34.7, 33.5, 31.9, 25.4, 23.5, 21.0, 7.7. HRMS(ESI+) m/z calculated for $\text{C}_{10}\text{H}_{16}\text{O}_2\text{Na}$ $[\text{M}+\text{Na}]^+$ 191.1043, found 191.1046. Chiral GC analysis with astec CHIRALDEX G-TA.

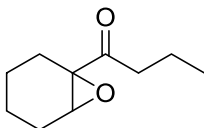


E24, colorless oil; (98% yield, 90% ee); ^1H -NMR (CDCl_3 , 400 MHz, 300K) δ , ppm: 3.31 (dt, $J = 3.3, 1.2$ Hz, 1H), 2.59 – 2.46 (m, 1H), 2.10 – 2.03 (m, 1H), 2.04 (s, 3H), 1.92 – 1.79 (m, 1H), 1.74 – 1.63 (m, 1H), 1.51 – 1.37 (m, 2H), 1.37 – 1.23 (m, 2H). $^{13}\text{C}\{^1\text{H}\}$ -NMR (100 MHz, CDCl_3) δ ppm: 208.4, 63.0, 57.0, 24.3, 23.3, 22.1, 19.4, 18.8. HRMS(ESI+) m/z calculated for $\text{C}_8\text{H}_{12}\text{O}_2\text{Na}$ $[\text{M}+\text{Na}]^+$ 163.0730, found 163.0723. Chiral GC analysis with CYCLOSIL-B.

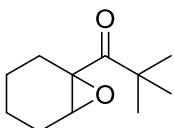
EXPERIMENTAL SECTION



E25, colorless oil; (77% yield, 87% ee); $^1\text{H-NMR}$ (CDCl_3 , 400 MHz, 300K) δ , ppm: 3.25 (dt, $J = 3.3, 1.2$ Hz, 1H), 2.60 – 2.49 (m, 1H), 2.49 – 2.40 (m, 1H), 2.30 (dq, $J = 18.3, 7.2$ Hz, 1H), 2.09 – 2.00 (m, 1H), 1.89 – 1.79 (m, 1H), 1.75 – 1.66 (m, 1H), 1.52 – 1.37 (m, 2H), 1.37 – 1.25 (m, 2H), 1.01 (t, $J = 7.3$ Hz, 3H). $^{13}\text{C}\{^1\text{H}\}$ -NMR (100 MHz, CDCl_3) δ ppm: 210.8, 63.0, 57.3, 28.7, 24.4, 22.7, 19.4, 18.9, 7.4. HRMS(ESI+) m/z calculated for $\text{C}_9\text{H}_{14}\text{O}_2\text{Na}$ $[\text{M}+\text{Na}]^+$ 177.0886, found 177.0888. Chiral GC analysis with CYCLOSIL-B.



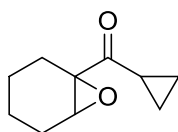
E26, colorless oil; (80% yield, 92% ee); $^1\text{H-NMR}$ (CDCl_3 , 400 MHz, 300K) δ , ppm: 3.25 (dt, $J = 3.2, 1.2$ Hz, 1H), 2.54 (dt, $J = 16.0, 6.4$ Hz, 1H), 2.48 – 2.36 (m, 1H), 2.29 – 2.18 (m, 1H), 2.11 – 1.99 (m, 1H), 1.90 – 1.79 (m, 1H), 1.75 – 1.63 (m, 1H), 1.62 – 1.51 (m, 2H), 1.42 (m, 2H), 1.27 (m, 2H), 0.89 (t, $J = 7.4$ Hz, 3H). $^{13}\text{C}\{^1\text{H}\}$ -NMR (100 MHz, CDCl_3) δ ppm: 210.3, 63.0, 57.0, 37.1, 24.4, 22.5, 19.4, 18.9, 16.8, 13.7. HRMS(ESI+) m/z calculated for $\text{C}_{10}\text{H}_{16}\text{O}_2\text{Na}$ $[\text{M}+\text{Na}]^+$ 191.1043, found 191.1059. Chiral GC analysis with CYCLOSIL-B.



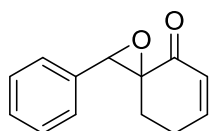
E27, colorless oil; (88% yield, 80% ee); $^1\text{H-NMR}$ (CDCl_3 , 400 MHz, 300K) δ , ppm: 3.06 (dt, $J = 3.3, 1.1$ Hz, 1H), 2.17 (dt, $J = 14.8, 6.5$ Hz, 1H), 1.91 (m, 1H), 1.86 – 1.73 (m, 2H), 1.49 – 1.34 (m, 2H), 1.28 (m, 2H), 1.14 (s, 9H). $^{13}\text{C}\{^1\text{H}\}$ -NMR (100 MHz, CDCl_3) δ ppm: 214.0, 64.7, 56.8, 44.3, 26.8, 25.7, 24.0, 19.5,

EXPERIMENTAL SECTION

18.7. HRMS(ESI+) m/z calculated for $C_{11}H_{18}O_2Na$ $[M+Na]^+$ 205.1199, found 205.1183. Chiral GC analysis with CYCLOSIL-B.

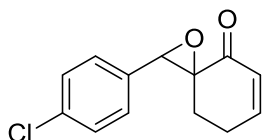


E28, colorless oil; (65% yield, 74% ee); 1H -NMR ($CDCl_3$, 400 MHz, 300K) δ , ppm: 3.42 (dt, $J = 3.2, 1.3$ Hz, 1H), 2.58 (dt, $J = 15.3, 5.9$ Hz, 1H), 2.27 – 2.15 (m, 1H), 2.15 – 2.04 (m, 1H), 1.93 – 1.82 (m, 1H), 1.76 – 1.65 (m, 1H), 1.56 – 1.38 (m, 2H), 1.38 – 1.22 (m, 2H), 1.07 – 0.98 (m, 1H), 0.98 – 0.79 (m, 3H). $^{13}C\{^1H\}$ -NMR (100 MHz, $CDCl_3$) δ ppm: 209.6, 63.0, 56.9, 24.3, 22.2, 19.5, 18.9, 13.5, 12.2, 11.2. HRMS(ESI+) m/z calculated for $C_{10}H_{14}O_2Na$ $[M+Na]^+$ 189.0886, found 189.0890. Chiral GC analysis with CYCLOSIL-B.

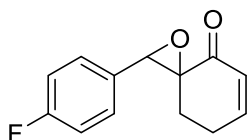


E32, Yellow solid; (92 % yield, 94 %ee); 1H -NMR ($CDCl_3$, 400 MHz, 300K) δ , ppm: 7.79 (dt, $J = 6.4, 2.7$ Hz, 1H), 7.42 – 7.33 (m, 3H), 7.31 – 7.27 (m, 2H), 6.43 (dt, $J = 6.4, 2.2$ Hz, 1H), 4.34 (s, 1H), 2.81 (dt, $J = 20.0, 2.4$ Hz, 1H), 2.48 (ddd, $J = 20.0, 2.9, 2.2$ Hz, 1H). $^{13}C\{^1H\}$ -NMR (100 MHz, $CDCl_3$) δ ppm: 201.8, 162.8, 134.5, 134.0, 128.6, 128.5, 126.3, 65.0, 62.4, 31.4. HRMS(ESI+) m/z calculated for $C_{13}H_{12}O_2Na$ $[M+Na]^+$ 223.0730, found 223.0740. HPLC-separation conditions: Chiralpack IA 25°C, 220nm, 85/15 hexane/*i*-PrOH, 1.0 mL/min; $t_{major} = 8.2$ min, $t_{minor} = 11.5$ min.

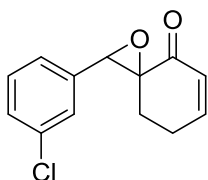
EXPERIMENTAL SECTION



E33, Yellow solid; (99 % yield, 94 %ee); $^1\text{H-NMR}$ (CDCl_3 , 300 MHz, 300K) δ , ppm: 7.39 – 7.32 (m, 2H), 7.28 (m, 2H), 7.10 – 7.01 (m, 1H), 6.21 (dd, $J = 9.5$, 2.8 Hz, 1H), 4.20 (s, 1H), 2.45 – 2.16 (m, 3H), 1.75 – 1.63 (m, 1H). $^{13}\text{C}\{^1\text{H}\}$ -NMR (75 MHz, CDCl_3) δ ppm: 194.0, 150.9, 134.2, 132.6, 130.2, 130.1, 128.6, 127.9, 63.6, 62.9, 62.8, 24.5. HRMS(ESI+) m/z calculated for $\text{C}_{13}\text{H}_{11}\text{O}_2\text{ClNa}$ $[\text{M}+\text{Na}]^+$ 257.0340, found 257.0346. Chiralpack IA 25°C, 220nm, 85/15 hexane/*i*-PrOH, 1.0 mL/min; $t_{\text{major}} = 8.4$ min, $t_{\text{minor}} = 9.4$ min.



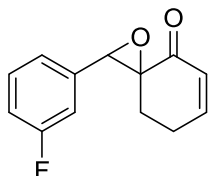
E34, Yellow solid; (93 % yield, 95 %ee); $^1\text{H-NMR}$ (CDCl_3 , 300 MHz, 300K) δ , ppm: 7.37 – 7.27 (m, 2H), 7.12 – 7.01 (m, 3H), 6.21 (dd, $J = 10.0$, 2.5 Hz, 1H), 4.21 (s, 1H), 2.46 – 2.16 (m, 3H), 1.76 – 1.63 (m, 1H). $^{13}\text{C}\{^1\text{H}\}$ -NMR (75 MHz, CDCl_3) δ ppm: 194.2, 164.3, 161.0, 150.8, 130.2, 129.8, 128.3, 128.2, 115.5, 115.2, 63.6, 62.9, 62.9, 24.4. HRMS(ESI+) m/z calculated for $\text{C}_{13}\text{H}_{11}\text{O}_2\text{FK}$ $[\text{M}+\text{K}]^+$ 241.0635, found 241.0628. HPLC-separation conditions: Chiralpack IA 25°C, 220nm, 85/15 hexane/*i*-PrOH, 1.0 mL/min; $t_{\text{major}} = 9.0$ min, $t_{\text{minor}} = 9.9$ min.



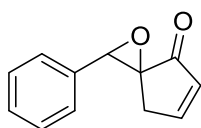
E35, Yellow solid; (45 % yield, 95 %ee); $^1\text{H-NMR}$ (CDCl_3 , 300 MHz, 300K) δ , ppm: 7.33 (m, 3H), 7.26 (m, 1H), 7.13 – 7.03 (m, 1H), 6.24 (dd, $J = 9.9$, 2.3 Hz,

EXPERIMENTAL SECTION

1H), 4.22 (s, 1H), 2.48 – 2.19 (m, 3H), 1.73 (m, 1H). $^{13}\text{C}\{^1\text{H}\}$ -NMR (75 MHz, CDCl_3) δ ppm: 193.8, 150.9, 136.2, 134.5, 130.2, 130.2, 129.7, 128.6, 126.6, 124.7, 63.6, 62.7, 62.6, 24.5. HRMS(ESI+) m/z calculated for $\text{C}_{13}\text{H}_{11}\text{O}_2\text{CINa}$ $[\text{M}+\text{Na}]^+$ 257.0340, found 257.0335. HPLC-separation conditions: Chiralpack IA 25°C, 220nm, 85/15 hexane/*i*-PrOH, 1.0 mL/min; $t_{\text{major}} = 7.5$ min, $t_{\text{minor}} = 12.3$ min.

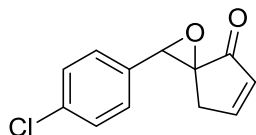


E36, Yellow solid; (80 % yield, 93 %ee); ^1H -NMR (CDCl_3 , 300 MHz, 300K) δ , ppm: 7.41 – 7.29 (m, 1H), 7.14 (d, $J = 7.4$ Hz, 1H), 7.11 – 6.98 (m, 3H), 6.23 (dd, $J = 9.9, 2.3$ Hz, 1H), 4.23 (s, 1H), 2.47 – 2.21 (m, 3H), 1.81 – 1.69 (m, 1H). $^{13}\text{C}\{^1\text{H}\}$ -NMR (75 MHz, CDCl_3) δ ppm: 193.92, 164.3, 161.1, 151.0, 136.7, 136.6, 130.2, 130.0, 122.3, 122.2, 115.5, 115.2, 113.7, 113.4, 63.6, 62.8, 62.7, 62.7, 24.5. HRMS(ESI+) m/z calculated for $\text{C}_{13}\text{H}_{11}\text{O}_2\text{FNa}$ $[\text{M}+\text{Na}]^+$ 241.0635, found 241.0637. HPLC-separation conditions: Chiralpack IC 25°C, 220nm, 85/15 hexane/*i*-PrOH, 1.0 mL/min; $t_{\text{minor}} = 28.2$ min, $t_{\text{major}} = 31.4$ min.

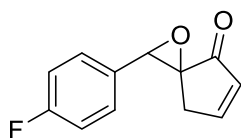


E37, Yellow solid; (82 % yield, 99 %ee); ^1H -NMR (CDCl_3 , 300 MHz, 300K) δ , ppm: 7.79 (dt, $J = 6.4, 2.7$ Hz, 1H), 7.44 – 7.34 (m, 3H), 7.30 (dd, $J = 7.5, 1.7$ Hz, 2H), 6.44 (dt, $J = 6.4, 2.2$ Hz, 1H), 4.35 (s, 1H), 2.82 (dt, $J = 20.0, 2.4$ Hz, 1H), 2.49 (ddd, $J = 20.0, 2.8, 2.2$ Hz, 1H). $^{13}\text{C}\{^1\text{H}\}$ -NMR (75 MHz, CDCl_3) δ ppm: 201.8, 162.8, 162.7, 134.5, 134.01, 126.3, 65.0, 62.5, 62.4, 31.4. HRMS(ESI+) m/z calculated for $\text{C}_{12}\text{H}_{10}\text{O}_2\text{Na}$ $[\text{M}+\text{Na}]^+$ 209.0573, found 209.0584. HPLC-separation conditions: Chiralpack IA 25°C, 220nm, 9/1 hexane/*i*-PrOH, 1.0 mL/min; $t_{\text{major}} = 10.9$ min, $t_{\text{minor}} = 14.4$ min.

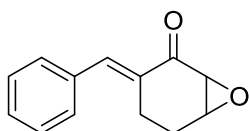
EXPERIMENTAL SECTION



E38, Yellow solid; (83 % yield, 98 %ee); $^1\text{H-NMR}$ (CDCl_3 , 300 MHz, 300K) δ , ppm: 7.80 (dt, $J = 6.4, 2.7$ Hz, 1H), 7.41 – 7.33 (m, 2H), 7.24 (m, 2H), 6.45 (dt, $J = 6.4, 2.2$ Hz, 1H), 4.33 (s, 1H), 2.80 (dt, $J = 19.9, 2.4$ Hz, 1H), 2.46 (dt, $J = 19.9, 2.5$ Hz, 1H). $^{13}\text{C}\{^1\text{H}\}$ -NMR (75 MHz, CDCl_3) δ ppm: 201.3, 162.6, 134.5, 134.08, 134.07, 133.1, 128.8, 127.6, 64.9, 61.8, 61.7, 31.3. HRMS(ESI+) m/z calculated for $\text{C}_{12}\text{H}_9\text{O}_2\text{ClNa}$ $[\text{M}+\text{Na}]^+$ 243.0183, found 243.0197. HPLC-separation conditions: Chiralpack IA 25°C, 220nm, 85/15 hexane/*i*-PrOH, 1.0 mL/min; $t_{\text{major}} = 9.0$ min, $t_{\text{minor}} = 10.0$ min.



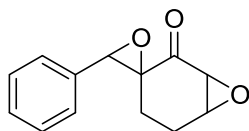
E39, Yellow solid; (93 % yield, 96 %ee); $^1\text{H-NMR}$ (CDCl_3 , 300 MHz, 300K) δ , ppm: 7.80 (dt, $J = 5.6, 2.7$ Hz, 1H), 7.27 (m, 2H), 7.08 (t, $J = 8.7$ Hz, 2H), 6.44 (m, 1H), 4.32 (s, 1H), 2.80 (dt, $J = 19.9, 2.3$ Hz, 1H), 2.46 (dt, $J = 19.9, 2.5$ Hz, 1H). $^{13}\text{C}\{^1\text{H}\}$ -NMR (75 MHz, CDCl_3) δ ppm: 201.5, 164.5, 162.7, 162.6, 161.2, 134.0, 130.32, 130.28, 128.1, 128.0, 115.8, 115.5, 64.9, 61.8, 61.8, 31.3. HRMS(ESI+) m/z calculated for $\text{C}_{12}\text{H}_9\text{O}_2\text{FNa}$ $[\text{M}+\text{Na}]^+$ 227.0479, found 227.0476. HPLC-separation conditions: Chiralpack IA 25°C, 220nm, 8/2 hexane/*i*-PrOH, 1.0 mL/min; $t_{\text{major}} = 8.9$ min, $t_{\text{minor}} = 9.7$ min.



White solid; (59 % yield); $^1\text{H-NMR}$ (CDCl_3 , 400 MHz, 300K) δ , ppm: 7.72 (s, 1H), 7.42 (d, $J = 4.4$ Hz, 4H), 7.41 – 7.34 (m, 1H), 3.72 (t, $J = 3.8$ Hz, 1H), 3.54 (d, $J = 4.2$ Hz, 1H), 2.83 (m, 2H), 2.45 – 2.36 (m, 1H), 1.96 – 1.84 (m, 1H).

EXPERIMENTAL SECTION

$^{13}\text{C}\{^1\text{H}\}$ -NMR (100 MHz, CDCl_3) δ ppm: 195.5, 137.4, 134.9, 132.5, 130.4, 129.0, 128.4, 55.4, 54.9, 22.5, 20.6. HRMS(ESI+) m/z calculated for $\text{C}_{13}\text{H}_{12}\text{O}_2\text{Na}$ $[\text{M}+\text{Na}]^+$ 223.0730, found 223.0725.



Colorless oil; (6 % yield); ^1H -NMR (CDCl_3 , 400 MHz, 300K) δ , ppm: 7.72 (s, 1H), 7.42 – 7.34 (m, 3H), 7.34 – 7.29 (m, 2H), 4.28 (s, 1H), 3.76 – 3.72 (m, 1H), 3.55 (d, $J = 4.1$ Hz, 1H), 2.33 – 2.14 (m, 2H), 2.05 – 1.93 (m, 1H), 1.51 (dddd, $J = 15.2, 5.4, 3.0, 0.7$ Hz, 1H). $^{13}\text{C}\{^1\text{H}\}$ -NMR (100 MHz, CDCl_3) δ ppm: 202.1, 133.7, 128.4, 128.3, 126.6, 63.5, 61.6, 56.5, 55.6, 21.8, 21.3. HRMS(ESI+) m/z calculated for $\text{C}_{13}\text{H}_{12}\text{O}_3\text{Na}$ $[\text{M}+\text{Na}]^+$ 239.0679, found 239.0680.

References

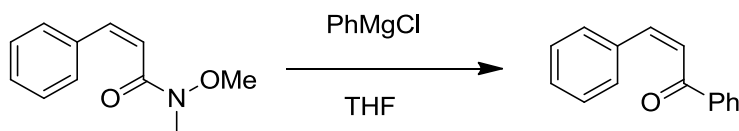
- (1) Lifchits, O.; Mahlau, M.; Reisinger, C. M.; Lee, A.; Farès, C.; Polyak, I.; Gopakumar, G.; Thiel, W.; List, B., *J. Am. Chem. Soc.* **2013**, 135, 6677.
- (2) Scheuermann née Taylor, C. J.; Jaekel, C., *Adv. Synth. & Catal.* **2008**, 350, 2708.
- (3) Shintani, R.; Takeda, M.; Nishimura, T.; Hayashi, T., *Angew. Chem. Int. Ed.* **2010**, 49, 3969.
- (4) Wińska, K.; Grudniewska, A.; Chojnacka, A.; Białońska, A.; Wawrzeńczyk, C., *Tetrahedron: Asymmetry* **2010**, 21, 670.
- (5) Vatele, J.-M., *Tetrahedron* **2010**, 66, 904.
- (6) Kraft, P.; Popaj, K., *Eur. J. Org. Chem.* **2008**, 4806..
- (7) Li, G.; Zuccaccia, C.; Tedesco, C.; D'Auria, I.; Macchioni, A.; Pellicchia, C., *Chem.-Eur. J.* **2014**, 20, 232..
- (8) Wu, Y. J.; Zhu, Y. Y.; Burnell, D. J. *J. Org. Chem.* **1994**, 59, 104.
- (9) Castelani, P.; Comasseto, J. V., *Tetrahedron* **2005**, 61, 2319.
- (10) Ebner, D. C.; Bagdanoff, J. T.; Ferreira, E. M.; McFadden, R. M.; Caspi, D. D.; Trend, R. M.; Stoltz, B. M. *Chem.-Eur. J.* **2009**, 15, 12978.
- (11) Brasca, M. G.; Amboldi, N.; Ballinari, D.; Cameron, A.; Casale, E.; Cervi, G.; Colombo, M.; Colotta, F.; Croci, V.; D'Alessio, R.; Fiorentini, F.; Isacchi, A.; Mercurio, C.; Moretti, W.; Panzeri, A.; Pastori, W.; Pevarello, P.; Quartieri, F.; Roletto, F.; Traquandi, G.; Vianello, P.; Vulpetti, A.; Ciomei, M., *J. Med. Chem.* **2009**, 52, 5152.
- (12) Takanami, T.; Suda, K.; Ohmori, H., *Tetrahedron Lett.* **1990**, 31, 677.

Experimental section: Chapter VII.4

Highly Stereoselective Epoxidation with H₂O₂ Catalyzed by Electron Rich Aminopyridine Manganese Catalysts

1) Synthesis of substrates

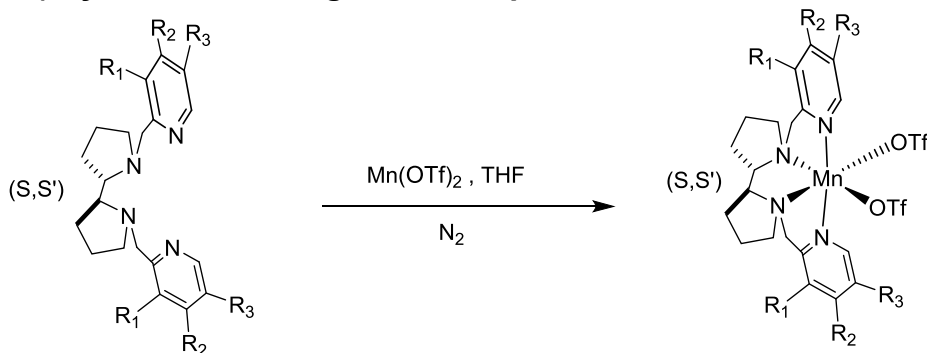
- Synthesis of *cis*-chalcone (**8**)



To a suspension of *cis*-N-methoxy-N-methylcinnamamide (4.7 mmol) in THF (15.0 mL), a solution of PhMgCl in THF (2.0 M, 7.6 mmol) was added dropwise under a nitrogen atmosphere at -30 °C. After stirring the reaction for 30 min at 0 °C, it was quenched by adding saturated aq. NH₄Cl and then diluted with 20 ml of EtOAc. The organic layer was separated and washed with brine, dried over MgSO₄ and concentrated at reduced pressure. The residue was purified by silica gel column chromatography (Hexane:ethyl acetate = 95:5) to afford the corresponding *cis*-chalcone product as a yellow solid (72 % yield). ¹H-NMR (CDCl₃, 300 MHz, 300K) δ , ppm: 8.0 - 7.97 (m, 2H), 7.52 - 7.49 (m, 1H), 7.45 - 7.40 (m, 4H), 7.26 - 7.24 (m, 3H), 7.08 (d, 1H, *J* = 12.9 Hz), 6.64 (d, 1H, *J* = 12.8 Hz). ¹³C-NMR 194.7, 139.5, 137.2, 135.2, 133.2, 129.5, 128.9, 128.6, 128.3, 126.77 HRMS(ESI+) *m/z* calculated for C₁₅H₁₂ONa [M+Na]⁺ 231.0780, found 231.0765. ¹H-NMR indicates that the product contains 15 % of *trans*-chalcone.

2) Synthesis of complexes

2.1) Synthesis of manganese complexes



(S,S')-[Mn(OTf)₂(^{Me2N}PDP)]: R₁=R₃=H, R₂= NMe₂

(S,S')-[Mn(OTf)₂(^{dMM}PDP)]: R₁=R₃=Me, R₂= OMe

(S,S')-[Mn(OTf)₂(^{MeO}PDP)]: R₁=R₃=H, R₂= OMe

(S,S')-[Mn(OTf)₂(^{Me}PDP)]: R₁=R₃=H, R₂= Me

(S,S')-[Mn(OTf)₂(^HPDP)]: R₁=R₃=R₂=H

(S,S')-[Mn(OTf)₂(^{Cl}PDP)]: R₁=R₃=H, R₂= Cl

(S,S')-[Mn(OTf)₂(^{CO2Et}PDP)]: R₁=R₃=H, R₂= CO₂Et

(S,S')-[Mn(OTf)₂(^{dMM}PDP)], ((S,S')-^{dMM}1Mn): A suspension of Mn(OTf)₂ (103.8 mg, 0.29mmol) in anhydrous THF (1 mL) was added dropwise to a vigorously stirred solution of (S,S')-^{dMM}PDP (128.9 mg, 0.29mmol) in THF (1 mL). After a few seconds the solution became cloudy and a white precipitate appeared. After stirring for 1 hour the solution was filtered off and the resultant yellow solid dried under vacuum. This solid was dissolved in CH₂Cl₂ (3 mL) and the solution filtered off through celite®. Slow diethyl ether diffusion over the resultant solution afforded, in a few days, 186.8 mg of yellow crystals (0.23 mmol, yield 80 %). Anal. Calcd for C₂₈H₃₈F₆MnN₄O₈S₂: C, 42.48; H, 4.84; N, 7.07; S, 8.10 %. Found: C, 42.46; H, 4.62; N, 7.22; S, 8.15 %. FT-IR (ATR) ν , cm⁻¹: 3485-3395, 2969, 2358, 2342, 1737, 1307, 1233, 1216, 1153, 1029, 1008, 633. HRMS (ESI-MS) calcd. for C₂₇H₃₈F₃MnN₄O₅S [M-OTf]⁺: 642.189, found: 642.190.

(S,S')-[Mn(OTf)₂(^{Me2N}PDP)], ((S,S')-^{Me2N}1Mn) was prepared in analogous manner to ((S,S')-^{dMM}1Mn) starting from ((S,S')-^{Me2N}PDP) and Mn(OTf)₂ to obtain the product as a white powder. (251.0 mg, 0.33mmol, 83%). Anal. Calcd for C₂₆H₃₆F₆MnN₆O₆S₂·1/2CH₃CN Et₂O: C, 43.49; H, 5.59; N, 10.63%. Found: C, 43.73; H, 5.34; N, 10.42 %. FT-IR (ATR) ν , cm⁻¹: 2969 – 2925 (C-H)sp³, 2358,

2333, 1738, 1614, 1306, 1233, 1215, 1157, 1010, 996, 632. HRMS (ESI-MS) calcd. for $C_{25}H_{36}F_3MnN_6O_3S$ $[M-OTf]^+$: 612.1897, found: 612.1893.

(S,S') -[Mn(OTf) $_2$ (^{MeO}PDP)], **$((S,S')$ -^{MeO}1Mn)** was prepared in analogous manner to **$((S,S')$ -^{dMM}1Mn)** starting from **$((S,S')$ -^{MeO}PDP)** and Mn(OTf) $_2$ to obtain the product as a white powder. (45.2 mg, 0.057 mmol, 56%). Anal. Calcd for $C_{24}H_{30}F_6MnN_4O_8S_2$: C, 39.19; H, 4.11; N, 7.62 %. Found: C, 39.20; H, 3.86; N, 7.52 %. FT-IR (ATR) ν , cm^{-1} : 2970 – 2975 (C-H) sp^3 , 2365, 2364, 1620, 1497, 1299, 1215, 1175, 1027, 901, 832, 625. HRMS (ESI-MS) calcd. for $C_{23}H_{30}F_3MnN_4O_5S$ $[M-OTf]^+$: 586.1264, found: 586.1274.

(S,S') -[Mn(OTf) $_2$ (^{Me}PDP)], **$((S,S')$ -^{Me}1Mn)** was prepared in analogous manner to **$((S,S')$ -^{dMM}1Mn)** starting from **$((S,S')$ -^{Me}PDP)** and Mn(OTf) $_2$ to obtain the product as a white powder. (30 mg, 0.042 mmol, 73%). Anal. Calcd for $C_{24}H_{30}F_6FeN_4O_6S_2$: C, 40.97; H, 4.30; N, 7.96 %. Found: C, 41.10; H, 4.03; N, 8.25 %. FT-IR (ATR) ν , cm^{-1} : 2975 – 2898 (C-H) sp^3 , 2181, 2009, 1620, 1305, 1235, 1209, 1161, 1035, 1015, 635. HRMS (ESI-MS) calcd. for $C_{23}H_{30}F_3MnN_4O_3S$ $[M-OTf]^+$: 554.1366, found: 554.1393.

(S,S') -[Mn(OTf) $_2$ (^{Cl}PDP)], **$((S,S')$ -^{Cl}1Mn)** was prepared in analogous manner to **$((S,S')$ -^{dMM}1Mn)** starting from **(S,S') -^{Cl}PDP** and Mn(OTf) $_2$. (87.4 mg, 0.12 mmol, 72%). Anal. Calcd for $C_{22}H_{24}Cl_2F_6MnN_4O_6S_2$: C, 35.50; H, 3.25; N, 7.53 %. Found: C, 35.63; H, 2.96; N, 7.64 %. FT-IR (ATR) ν , cm^{-1} : 2970 – 2953 (C-H) sp^3 , 2359, 2335, 1738, 1593, 1310, 1216, 1182, 1039, 635. HRMS (ESI-MS) calcd. for $C_{21}H_{24}Cl_2F_3MnN_4O_3S$ $[M-OTf]^{2+}$: 594.0273, found: 594.0291.

(S,S') -[Mn(OTf) $_2$ (^{CO₂Et}PDP)], **$((S,S')$ -^{CO₂Et}1Mn)** was prepared in analogous manner to **$((S,S')$ -^{dMM}1Mn)** starting from **(S,S') -^{CO₂Et}PDP** and Mn(OTf) $_2$. (102.2 mg, 0.12 mmol, 66%). Anal. Calcd for $C_{28}H_{34}F_6MnN_4O_{10}S_2$: C, 41.03; H, 4.18; N, 6.70 %. Found: C, 40.84; H, 3.93; N, 6.77. FT-IR (ATR) ν , cm^{-1} : 3468-3425, 2970, 2360, 1728, 1289, 1232, 1215, 1163, 1027, 635. HRMS (ESI-MS) calcd. for $C_{27}H_{34}F_3MnN_4O_7S$ $[M-OTf]^+$: 670.1475, found: 670.1481.

(S,S') -[Mn(OTf) $_2$ (^HPDP)] **$((S,S')$ -^H1Mn)** was prepared following reported procedures by Talsi and Bryliakov.¹

3) Catalytic studies

Hydrogen peroxide solutions employed in the reactions were prepared by diluting commercially available hydrogen peroxide (35% H₂O₂ solution in water, Aldrich) in acetonitrile (1:1 v:v). Commercially available glacial acetic acid (99-100%) from Riedel-de-Haën was employed. Olefin substrates were purchased from Aldrich and TCI, with the maximum purity available, and used as received. Carboxylic acids were purchased from Across and Aldrich.

3.1) Reaction conditions (Table 8 and 9)

An acetonitrile solution (7.5 mL) of *cis*- β -methylstyrene (0.83 mmol, 0.11 M) and ((*S,S*)-^{Me₂N}**1Mn**) (0.83 μ mol, 0.11 mM) was prepared in a flask bottom (25 mL) equipped with a stir bar cooled at -30 °C, in an acetonitrile/N₂(liq) bath. A 700 μ L (neat, 14 equiv.) or 17.5 μ L (0.35 equiv., Table 9) of carboxylic acid was added directly to the solution. An analogous procedure was followed when 2-eha was used instead of acetic acid. Then, 200 μ L of 1:1 v:v acetonitrile:hydrogen peroxide solution 35 % (1.2 equiv.) was added by syringe pump over a period of 30 min. The solution was further stirred at -30 °C for 30 minutes. At this point, an internal standard (biphenyl) was added and the solution was quickly filtered through a basic alumina plug, which was subsequently rinsed with 2 x 1 mL AcOEt. GC analysis of the solution provided substrate conversions and product yields relative to the internal standard integration. Products were identified by comparison to the GC retention time of authentic samples, and by their GC-MS spectrum. The epoxide product was identified by comparison to the GC retention time of racemate epoxide and by its GC-MS spectrum.

3.2) Reaction conditions (Figure 15)

An acetonitrile solution (7.5 mL) of olefin (0.52 mmol, 0.07 M) and ((*S,S'*)-^{Me₂N}**1Mn**) (2.6 μ mol, 0.34 mM) was prepared in a flask bottom (25 mL) equipped with a stir bar cooled at -30 °C, in an acetonitrile/N₂(liq) bath. A 85 μ L (neat, 1 equiv.) 2-ethylhexanoic acid was added directly to the solution. Then, 200 μ L of 1:1 v:v acetonitrile:hydrogen peroxide solution 35 % (2 equiv.) was added by syringe pump over a period of 30 min. The solution was further stirred at -30 °C

for 30 minutes. At this point, 20 mL of an aqueous NaHCO₃ saturated solution were added to the mixture. The resultant solution was extracted with CH₂Cl₂ (3 x 10 mL). Organic fractions were combined, dried over MgSO₄, and the solvent was removed under reduced pressure to afford the epoxide product. This residue was purified by flash column chromatography over silica gel (Hexane/AcOEt: 98/2) to obtain the pure epoxide. Commercially non available epoxides were identified by a combination of ¹H, ¹³C{¹H}-NMR analyses. A sample of the epoxide was dissolved in *n*-hexane/2-propanol and analyzed by HPLC.

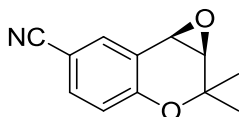
3.3) Reaction conditions (Table 10)

An ethyl acetate/acetonitrile (4:1) solution of 3 β -acetoxy- Δ^5 unsaturated steroid (0.76mmol, 0.076M) and ((**S,S**)-^{dMM}**1Mn**) (1.9 μ mols, 0.19mM) were placed in a round bottom flask, along with a stir bar at room temperature. A 2.3 g of 1:1 v:v ethylacetate/pivalic acid solution was added directly to the solution (11.4mmol), and then 894 μ L of 1.7 M H₂O₂ (35% H₂O₂ aqueous solution) solution diluted in acetonitrile was delivered by syringe pump over 30 min at room temperature. After syringe pump addition, the solution was stirred for 30 min at room temperature. At this point, the solvent was removed under reduced pressure and 40 mL of an aqueous NaHCO₃ saturated solution was added to the mixture. The resultant solution was extracted with CH₂Cl₂ (3 x 10 mL). Organic fractions were combined, dried over MgSO₄, filtered through a silica gel plug, and the solvent was removed under reduced pressure. The residue was solved in AcOEt and injected to the GC to calculate β/α ratio and then it was purified by column chromatography (Hexane/AcOEt: 98/2) over silica gel column to obtain the pure α and β epoxide products. Since the amount of α epoxide product is small, a sample was prepared from the reaction of the substrate with mCPBA/NaHCO₃ in dichloromethane according to Yang and Jiao.² Finally, epoxides were identified by a combination of ¹H, ¹³C{¹H}-NMR analyses and according to the literature.^{3,4}

4) Characterization of isolated epoxides products

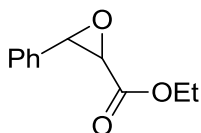
(*R,R*)-2,2-dimethyl-2,7b-dihydro-1aH-oxireno[2,3-c]chromene-6-carbonitrile.⁵

EXPERIMENTAL SECTION



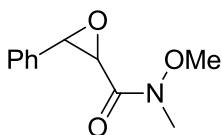
(5), white solid; (95 % yield, 97 % ee); $^1\text{H-NMR}$ (CDCl_3 , 300 MHz, 300 K) δ , ppm: 7.66 (d, 1H, $J = 2.08$ Hz), 7.53-7.51 (dd, 1H, $J = 8.46, 2.10$ Hz), 6.86 (d, 1H, $J = 8.50$ Hz), 3.91 (d, 1H, $J = 4.33$ Hz), 3.54 (d, 1H, $J = 4.35$ Hz), 1.60 (s, 3H), 1.30 (s, 3H)- $^{13}\text{C}\{^1\text{H}\}$ -NMR 156.5, 134.4, 133.8, 121.1, 119.0, 118.7, 104.3, 74.7, 62.3, 49.9, 25.5, 23.0. HRMS(ESI+) m/z calculated for $\text{C}_{12}\text{H}_{11}\text{NO}_2\text{Na}$ $[\text{M}+\text{Na}]^+$ 224.0682, found 224.0673. Chiral HPLC analysis (ChiralpackIA, n -Hex:*i*PrOH = 90/10, 25 °C, flow rate = 1.5 mL/min, $\lambda = 254$ nm), $t_{\text{minor}} = 6.3$ min, $t_{\text{major}} = 6.7$ min.

cis-Ethyl-3-phenyloxirane-2-carboxylate



(6), white solid; (77% yield, 98 % ee); $^1\text{H-NMR}$ (CDCl_3 , 300 MHz, 300 K) δ , ppm: 7.42-7.39 (m, 2H), 7.36 - 7.29 (m, 3H), 4.26 (d, 1H, $J = 4.7$ Hz), 4.05 - 3.95 (m, 2H), 3.82 (d, 1H, $J = 4.7$ Hz), 1.01 (t, 3H, $J = 7.1$). $^{13}\text{C}\{^1\text{H}\}$ -NMR 166.6, 132.9, 128.4, 128.0, 126.6, 61.2, 57.4, 55.7, 13.9. HRMS(ESI+) m/z calculated for $\text{C}_{11}\text{H}_{12}\text{O}_3\text{Na}$ $[\text{M}+\text{Na}]^+$ 215.0679, found 215.0663. Chiral GC analysis with CYCLOSIL-B

cis-*N*-methoxy-*N*-methyl-3-phenyloxirane-2-carboxamide

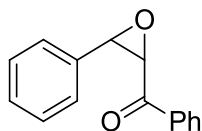


(7), yellowish oil; (90 % yield (*cis* + *trans* epoxides, *cis:trans*94:6), 96 % ee for the *cis*-epoxide and 93 for the *trans*). Characterization data only refers to the major *cis*- isomer. $^1\text{H-NMR}$ (CDCl_3 , 300 MHz, 300K) δ , ppm: 7.42-7.39 (m, 2H), 7.35 - 7.30 (m, 3H), 4.29 (d, 1H, $J = 4.7$ Hz), 4.15 (br, 2H), 3.56 (s, 3H), 3.03 (s, 3H). $^{13}\text{C}\{^1\text{H}\}$ -NMR 166.4, 133.7, 128.5, 128.2, 126.6, 61.8, 57.7, 57.6, 32.3. HRMS(ESI+) m/z calculated for $\text{C}_{11}\text{H}_{13}\text{NO}_3\text{Na}$ $[\text{M}+\text{Na}]^+$ 230.0788, found 230.0803. Chiral HPLC analysis (Chiralpack IC, n -Hex:*i*PrOH = 82/18, 25 °C,

EXPERIMENTAL SECTION

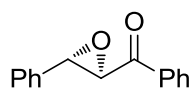
1.0ml/min, $\lambda = 220$ nm), *cis*-epoxide; $t_{minor} = 44.5$ min, $t_{major} = 49.1$ min. *trans*-epoxide; $t_{minor} = 33$ min, $t_{major} = 37$ min. The ratio *cis:trans* is identical to that of the starting olefin substrate.

cis-Epoxy-1,3-diphenyl-propan-1-one

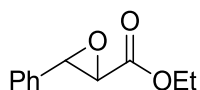


(8), yellowish oil; (65 % yield (*cis* + *trans* epoxides, *cis:trans* 85:15), 90 % ee for *cis*-epoxide and 85 % for the *trans*). Characterization data only refers to the major *cis*- isomer. $^1\text{H-NMR}$ (CDCl_3 , 400 MHz, 300K) δ , ppm: 7.88 - 7.85 (m, 2H), 7.53 (m, 1H), 7.42 - 7.40 (m, 2H), 7.34 - 7.32 (m, 2H), 7.25 - 7.21 (m, 3H), 4.51 (br, 2H). $^{13}\text{C}\{^1\text{H}\}$ -NMR 192, 135.5, 133.8, 132.9, 128.7, 128.5, 128.2, 128.1, 126.5, 60.9, 58.7. HRMS(ESI+) m/z calculated for $\text{C}_{15}\text{H}_{12}\text{ONa}$ $[\text{M}+\text{Na}]^+$ 247.0730, found 247.0733. Chiral HPLC analysis (Chiralpack IC, *n*-Hex:*i*PrOH = 90/10, 25 °C, 1.0ml/min, $\lambda = 254$ nm), $t_{major} = 16.0$ min, $t_{minor} = 22.9$ min. *trans*-epoxide; $t_{minor} = 19.3$ min, $t_{major} = 20.5$ min. The ratio *cis:trans* is identical to that of the starting olefin substrate

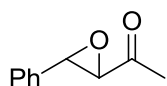
trans-(2*R*,3*S*)-Epoxy-1,3-diphenyl-propan-1-one.⁵



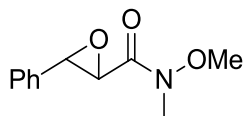
(9), white solid; (96 % yield, 96 % ee); $^1\text{H-NMR}$ (CDCl_3 , 300 MHz, 300 K) δ , ppm: 8.01 (d, 2H, $J = 8.43$ Hz), 7.62 (t 1H, $J = 7.59$ Hz), 7.49 (t, 2H, $J = 7.68$ Hz), 7.42-7.35 (m, 5H), 4.30 (d, 1H, $J = 1.91$ Hz), 4.08 (d, 1H, $J = 1.91$ Hz). $^{13}\text{C}\{^1\text{H}\}$ -NMR 193.1, 135.5, 135.5, 134.0, 129.1, 128.9, 128.8, 128.4, 125.8, 61.0, 59.41. HRMS(ESI+) m/z calculated for $\text{C}_{15}\text{H}_{12}\text{O}_2\text{Na}$ $[\text{M}+\text{Na}]^+$ 247.0730, found 247.0721. Chiral HPLC analysis (Chiralpack IA, *n*-Hex:*i*PrOH = 98/2, 25 °C, flow rate = 1.0 mL/min, $\lambda = 254$ nm), $t_{major} = 21.7$ min, $t_{minor} = 23.9$ min.

trans-Ethyl-3-phenyloxirane-2-carboxylate

(10), Colorless oil; (93 % yield, 92 % ee); $^1\text{H-NMR}$ (CDCl_3 , 300 MHz, 300 K) δ , ppm: 7.40 – 7.33 (m, 3H), 7.32-7.27 (m, 2H), 4.34 - 4.23 (dq, 2H, $J = 14.4, 7.2$ Hz), 4.09 (d, 1H, $J = 1.74$ Hz), 3.50 (d, 1H, $J = 1.75$ Hz), 1.33 (t, 3H, $J = 7.15$ Hz). $^{13}\text{C-NMR}$ 168.2, 135.0, 129.0, 128.7, 125.8, 61.8, 57.9, 56.8, 14.1. HRMS(ESI+) m/z calculated for $\text{C}_{11}\text{H}_{12}\text{O}_3\text{Na}$ $[\text{M}+\text{Na}]^+$ 215.0679, found 215.0677. ChiralHPLC analysis (Chiralpack IC, $n\text{-Hex}:\textit{iPrOH} = 85/15$, 25 °C, flow rate = 1.0 mL/min, $\lambda = 220\text{nm}$), $t_{\text{major}} = 7.1$ min, $t_{\text{minor}} = 7.7$ min.

trans-1-(3-Phenyloxiran-2-yl)ethanone

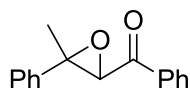
(11), colorless oil; (81 % yield, 96 % ee); $^1\text{H-NMR}$ (CDCl_3 , 300 MHz, 300 K) δ , ppm: 7.38 - 7.36 (m, 3H), 7.29 - 7.26 (m, 2H), 4.01 (d, 1H, $J = 1.89$ Hz), 3.49 (d, 1H, $J = 1.86$ Hz), 2.19 (s, 3H). $^{13}\text{C}\{^1\text{H}\}\text{-NMR}$ 204.2, 135.0, 129.0, 128.7, 125.7, 63.5, 57.8, 24.8. HRMS(ESI+) m/z calculated for $\text{C}_{10}\text{H}_{10}\text{O}_2\text{Na}$ $[\text{M}+\text{Na}]^+$ 185.0573, found 185.0588. Chiral HPLC analysis (Chiralpack IC, $n\text{-Hex}:\textit{iPrOH} = 98/2$, 25 °C, flow rate = 1.0 mL/min, $\lambda = 220$ nm), $t_{\text{minor}} = 15.1$ min, $t_{\text{major}} = 16.3$ min.

trans-*N*-Methoxy-*N*-methyl-3-phenyloxirane-2-carboxamide

(12), yellow oil; (99 % yield, 97 % ee); $^1\text{H-NMR}$ (CDCl_3 , 300 MHz, 300 K) δ , ppm: 7.39 - 7.32 (m, 5H), 4.10 (d, 1H, $J = 1.88$ Hz), 3.94 (br.s, 1H), 3.72 (s, 3H), 3.28 (s, 3H). $^{13}\text{C}\{^1\text{H}\}\text{-NMR}$ 167.5, 135.6, 128.8, 128.7, 125.8, 62.1, 57.7, 55.6, 32.6. HRMS(ESI+) m/z calculated for $\text{C}_{11}\text{H}_{13}\text{NO}_3\text{Na}$ $[\text{M}+\text{Na}]^+$ 230.0788, found 230.0780. Chiral HPLC analysis (Chiralpack IC, $n\text{-Hex}:\textit{iPrOH} = 9/1$, 25 °C, flow rate = 1.5 mL/min, $\lambda = 220$ nm), $t_{\text{minor}} = 35.9$ min, $t_{\text{major}} = 40.3$ min.

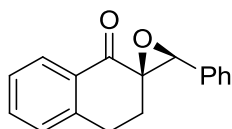
EXPERIMENTAL SECTION

(3-Methyl-3-phenyloxiran-2-yl)(phenyl)methanone

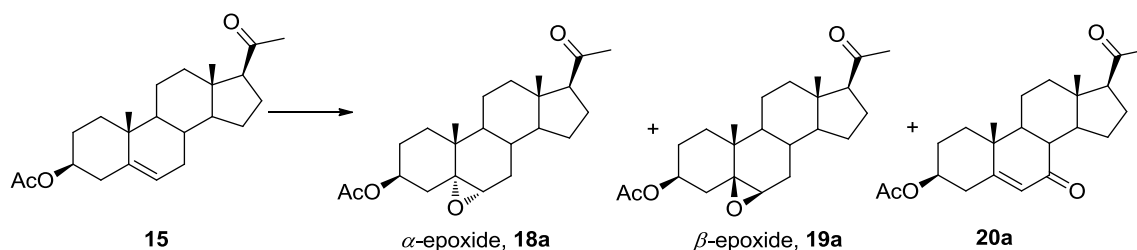


(13), white solid; (95 % yield, 57 % ee); $^1\text{H-NMR}$ (CDCl_3 , 300 MHz, 300K) δ , ppm: 7.96 (d, 2H, $J = 8.19$ Hz), 7.62 (t, 2H, $J = 7.38$ Hz), 7.52 – 7.47 (m, 4H), 7.43 (t, 2H, $J = 7.04$ Hz), 7.37 (t, 1H, $J = 7.04$ Hz), 4.16 (s, 1H), 1.64 (s, 3H). $^{13}\text{C}\{^1\text{H}\}$ -NMR 193.0, 140.4, 135.6, 134.0, 128.9, 128.8, 128.3, 125.1, 66.9, 62.8, 16.9 HRMS(ESI+) m/z calculated for $\text{C}_{16}\text{H}_{14}\text{O}_2\text{Na}$ $[\text{M}+\text{Na}]^+$ 261.0886, found 261.0881. Chiral HPLC analysis (ChiralpackIA, n -Hex: i PrOH = 98/2, 25 °C, flow rate = 1.0 mL/min, $\lambda = 254$ nm), $t_{\text{major}} = 11.1$ min, $t_{\text{minor}} = 12.6$

(2*R*,3'*S*)-3'-Phenyl-3,4-dihydro-1*H*-spiro[naphthalene-2,2'-oxiran]-1-one.⁶



(14), yellow oil; (67 % yield, 84 % ee); $^1\text{H-NMR}$ (CDCl_3 , 400 MHz, 300 K) δ , ppm: 8.14 – 8.11 (m, 1H), 7.55 – 7.50 (m, 1H), 7.43 – 7.34 (m, 6H), 7.22 (d, 1H, $J = 7.7$ Hz), 4.36 (s, 1H), 2.85 – 2.82 (dd, 2H, $J = 8.3, 4.15$ Hz), 2.49 – 2.42 (dt, 1H, $J = 13.5, 8.8$ Hz), 1.88 – 1.83 (dt, 1H, $J = 13.5, 4.3$ Hz). $^{13}\text{C}\{^1\text{H}\}$ -NMR 193.6, 143.4, 134.3, 134.1, 132.7, 128.8, 128.4, 128.3, 127.7, 127.0, 126.6, 64.3, 64.1, 27.4, 25.3. HRMS(ESI+) m/z calculated for $\text{C}_{17}\text{H}_{14}\text{O}_2\text{Na}$ $[\text{M}+\text{Na}]^+$ 273.0886, found 273.0902. Chiral HPLC analysis (Chiralpack IA, n -Hex: i PrOH = 98/2, 25 °C, flow rate = 1.0 mL/min, $\lambda = 254$ nm), $t_{\text{major}} = 22.0$ min, $t_{\text{minor}} = 25.7$ min.



β -epoxide R = COCH_3 , (**E19a**)

$^1\text{H-NMR}$ (400 MHz, CDCl_3 , 300 K) δ , ppm: 0.56 (3H, s, 18- CH_3), 0.65 (1H, m), 0.98 (3H, s, 19- CH_3), 1.02 (1H, m), 1.17-1.24 (2H, m), 1.31-1.35 (2H, m), 1.47

EXPERIMENTAL SECTION

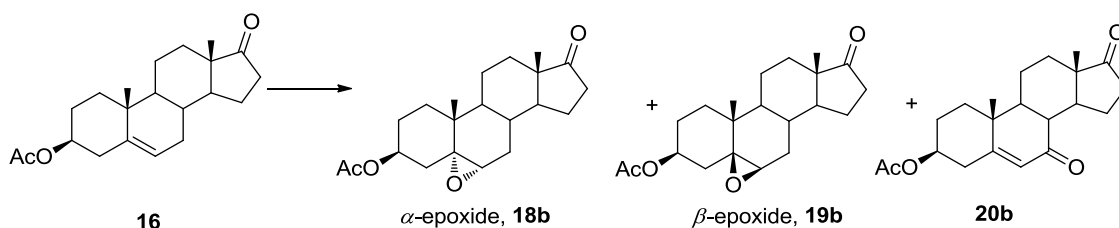
(5H, m), 1.66 (2H, m), 1.79 (1H, m), 1.96 (2H,m),2.00 (3H, s, CH₃COO), 2.06 (1H, m), 2.07 (3H, s, 21-CH₃), 2.11 (2H, m), 2.45 (1H, t,), 3.06 (1H, d, *J* = 2.0 Hz, 6 α -H), 4.74 (1H, m, 3 α -H). ¹³C-NMR (100 MHz, CDCl₃, 300 K) δ , ppm: 13.0, 17.0, 21.2, 21.8, 22.7, 24.3, 27.1, 29.7, 31.4, 32.3, 35.2, 36.6, 37.9, 38.7, 43.8, 50.8, 56.2, 62.4, 63.3, 63.6, 71.2, 170.5, 209.2. HRMS(ESI+) *m/z* calculated for C₂₃H₃₄O₄Na 397.2349, found 397.2357.

α -epoxide R = COCH₃, (**18a**)

¹H-NMR (400 MHz, CDCl₃, 300 K) δ , ppm: 0.54 (3H, s, 18-CH₃), 1.06 (3H, s, 19-CH₃), 1.12 (1H, m), 1.25 (1H, m), 1.35-1.58 (9H, m), 1.67 (4H,m),1.95 (2H,m) 1.99 (3H, s, CH₃COO), 2.09 (3H, s, 21-CH₃), 2.14 (2H, m), 2.49 (1H,m), 2.89 (1H, d, *J* = 4.3 Hz, 6 β -H), 4.93 (1H, m, 3 α -H). ¹³C-NMR (100 MHz, CDCl₃, 300 K) δ , ppm: 13.2, 15.8, 20.6, 21.3, 22.7, 24.2, 27.2, 28.6, 29.7, 31.5, 32.2, 35.0, 36.1, 38.4, 42.4, 43.9, 56.9, 58.9, 63.3, 65.2, 71.2, 170.2, 209.4. HRMS(ESI+) *m/z* calculated for C₂₃H₃₄O₄Na 397.2349, found 397.2350.

7-KO R = COCH₃, (**20a**)

¹H-NMR (400 MHz, CDCl₃, 300 K) δ , ppm: 0.66 (3H, s, 18-CH₃), 1.21 (3H, s, 19-CH₃), 2.05 (3H, s, CH₃COO), 2.13 (3H, s, 21-CH₃), 4.72 (1H, m, 3 α -H); 5.72 (1H, d, *J* = 1.6 Hz, 6-H). ¹³C-NMR (100 MHz, CDCl₃, 300 K) δ , ppm: 13.3, 17.3, 21.1, 21.3, 23.6, 26.5, 27.3, 31.6, 36.0, 37.6, 37.8, 38.4, 44.4, 45.3, 49.7, 50.0, 62.3, 72.1, 126.5, 164.2, 170.3, 201.2, 209.7. HRMS(ESI+) *m/z* calculated for C₂₃H₃₂O₄Na 395.2193, found 395.2189.



β -epoxide, (**19b**).

¹H-NMR (400 MHz, CDCl₃, 300 K) δ , ppm: 0.68 (1H, td, *J* = 11.5, 4.3 Hz) 0.83 (3H, s, 18-CH₃), 1.02 (3H, s, 19-CH₃), 1.16 (2H, m), 1.30 (2H, m), 1.35- 1.54

EXPERIMENTAL SECTION

(5H,m), 1.68 (1H,m), 1.85 (2H,m), 1.96 (2H,m), 2.02 (3H, s, CH₃COO), 2.08-2.21 (3H,m), 2.41- 2.48 (1H,dd, $J = 19.1, 8.8$ Hz), 3.12 (1H, d, $J = 2.0$ Hz, 6 α -H), 4.76 (1H, m, 3 α -H). ¹³C-NMR (100 MHz, CDCl₃, 300 K) δ , ppm: 13.5, 17.1, 21.2, 21.3, 21.7, 27.1, 29.4, 31.3, 31.4, 35.3, 35.7, 36.7, 37.9, 47.4, 51.1, 51.1, 62.6, 63.2, 71.1, 170.5, 220.7. HRMS(ESI+) m/z calculated for C₂₁H₃₀O₄Na 369.2042, found 369.2042.

α -epoxide, (**18b**).

¹H-NMR (400 MHz, CDCl₃, 300 K) δ , ppm: 0.83 (3H, s, 18-CH₃), 1.11 (3H, s, 19-CH₃), 1.27 (3H,m), 1.35-1.48 (4H, m), 1.62 (3H, m), 1.75 (3H,m), 1.92 (2H,m), 2.02 (3H, s, CH₃COO), 2.08- 2.22 (3H,m), 2.39-2.48 (dd, $J = 19.5, 8.6$ Hz) 2.94 (1H, d, $J = 2.0$ Hz, 6 β -H), 4.95 (1H, m, 3 α -H). ¹³C-NMR (100 MHz, CDCl₃, 300 K) δ , ppm: 13.5, 15.8, 19.9, 21.3, 21.7, 27.1, 27.6, 29.5, 31.1, 32.1, 35.1, 35.7, 36.0, 42.7, 47.6, 51.8, 58.6, 65.2, 71.1, 170.2, 220.5. HRMS(ESI+) m/z calculated for C₂₁H₃₀O₄Na 369.2040, found 369.2036.

7-KO R = O, (**20b**).⁷

¹H-NMR (400 MHz, CDCl₃, 300 K) δ , ppm: 0.88 (3H, s, 18-CH₃), 1.23 (3H, s, 19-CH₃), 2.04 (3H, s, CH₃COO), 4.71 (1H, m, 3 α -H); 5.75 (1H, d, $J = 1.6$ Hz, 6-H). ¹³C-NMR (100 MHz, CDCl₃, 300 K) δ , ppm: 13.8, 17.4, 20.5, 21.2, 24.2, 27.3, 30.7, 35.6, 35.9, 37.8, 38.5, 44.4, 45.7, 47.9, 50.0, 72.0, 126.5, 164.8, 170.3, 200.7, 220.2. HRMS(ESI+) m/z calculated for C₂₁H₂₈O₄Na 367.1885, found 367.1876.

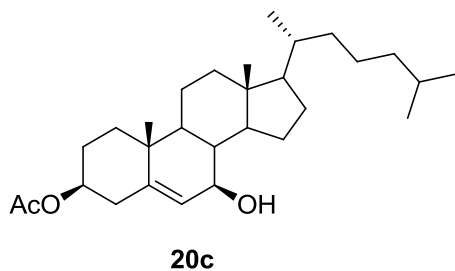
β - and α epoxides (**18c-19c**).³

β - and α epoxides could not be separated, but could be identified on the basis of the comparison of the ¹H-NMR spectra with those described in the literature.³ The integration of the two signals belonging to H-6 gave a **9.7:0.3 β / α** ratio. Spectroscopic data corresponds to the major β isomer. ¹H-NMR (400 MHz, CDCl₃, 300 K) δ , ppm: 0.63 (3H, s, 18-CH₃), 0.84-0.89 (11H, m), 0.99 (3H, s, 19-CH₃), 1.07-1.10 (6H, m), 1.20-1.36 (9H, m), 1.46-1.58 (5H,m), 1.80 (2H,m), 1.93 (2H,m), 2.02 (3H, s, CH₃COO), 2.10 (2H,m), 3.07 (1H, d, $J = 1.9$ Hz, 6 α -H), 4.76 (1H, m, 3 α -H). ¹³C-NMR (100 MHz, CDCl₃, 300 K) δ , ppm: β epoxide

EXPERIMENTAL SECTION

(major product): 11.8, 17.0, 18.7, 21.3, 21.9, 22.6, 22.8, 23.8, 24.2, 27.2, 28.0, 28.2, 29.7, 32.5, 35.0, 35.7, 36.1, 36.7, 38.0, 39.5, 39.8, 42.3, 51.0, 56.2, 56.2, 62.5, 63.6, 71.4, 170.6. HRMS(ESI+) m/z calculated for $C_{29}H_{48}O_3Na$ 467.3501, found 467.3497.

7- β -OH (**20c**).⁸



1H -NMR (300 MHz, $CDCl_3$, 300 K) δ , ppm: 0.69 (3H, s, 18- CH_3), 0.85-0.86 (each 3H, 2d, $J = 6.6$ Hz, 26- CH_3 and 27- CH_3), 0.92 (3H, d, $J = 6.6$ Hz, 21- CH_3), 1.01 (3H, s, 19- CH_3), 1.08- 1.19 (7H, m), 1.23 (3H, s), 1.27-1.36 (3H, s), 1.43-1.49 (6H, m), 1.62-1.77 (2H, m), 1.88 (3H, m), 2.04 (3H, s, 3 β - CH_3COO), 2.37 (2H, m), 3.85 (1H, m, 7 β -H), 4.65 (1H, m, 3 α -H), 5.63 (1H, d, $J = 5.01$ Hz, 6-H). ^{13}C -NMR (75 MHz, $CDCl_3$, 300 K) δ , 11.6, 18.2, 18.7, 20.7, 21.4, 21.6, 22.8, 23.7, 24.3, 27.0, 27.5, 28.0, 28.3, 35.8, 36.2, 36.7, 37.4, 37.9, 39.1, 39.5, 42.1, 42.2, 49.4, 55.8, 65.2, 73.4, 124.7, 145.2, 170.5 HRMS(ESI+) m/z calculated for $C_{29}H_{48}O_3Na$ 467.3496, found 467.3474.

References

- (1) Ottenbacher, R. V.; Bryliakov, K. P.; Talsi, E. P. *Adv. Synth. Catal.* **2011**, 353, 885.
- (2) Yang, D.; Jiao, G.-S. *Chem.-Eur. J.* **2000**, 6, 3517.
- (3) Cruz Silva, M. M.; Riva, S.; Sá e Melo, M. L. *Tetrahedron: Asymmetry*.**2004**, 15, 1173.
- (4) Carvalho, J. F. S.; Silva, M. M. C.; Sá e Melo, M. L. *Tetrahedron.* **2009**, 65, 2773.
- (5) Lyakin, O. Y.; Ottenbacher, R. V.; Bryliakov, K. P.; Talsi, E. P. *ACS Catal.* **2012**, 2, 1196.
- (6) Wang, B.; Miao, C.; Wang, S.; Xia, C.; Sun, W. *Chem.– Eur. J.* **2012**, 18, 6750.
- (7) Shing, T. K. M.; Yeung; Su, P. L. *Org. Lett.* **2006**, 8, 3149.
- (8) Poza, J. J.; Jiménez, C.; Rodríguez, J. *Eur. J. Org. Chem.* **2008**, 3960.